Applications of Lumping Kinetics Methodology to Plastic Waste Recovery via Pyrolysis

By

Haoyu Li

Submitted for the Degree of Doctor of Philosophy in Chemical Engineering

Institute of Mechanical, Process, and Energy Engineering

School of Engineering, Physical, and Sciences

Heriot-Watt University

01/2017

ABSTRACT

Plastic waste can present a huge environmental problem for conventional waste management as most plastic is not degradable in the same way as most packaging material. Plastic waste may take hundreds of years for natural degradation, and may then release some toxic chemicals simultaneously. The high cost of collection and separation occurring in the recycling and recovery stages of plastic waste conflicts with low value recyclate, contrasting with metal recycling which is cheaper and gives a much higher value product. Additionally, public opinion links waste plastic with effects on human health and wildlife. A number of technologies are being explored and deployed for the handling of plastic waste. Modelling and simulation to energy and chemicals recovery from the pyrolysis of plastic waste can be one facilitator of valorisation for the disposal of waste plastics, which furnishes a cost-effective method of process design and control of desirable product range and quality. A pyrolysis process operating in the absence or free of oxygen atmosphere permits the recovery of smaller molecular weight hydrocarbon products which can be used as fuels, or preferably chemical feedstock providing additional value. With the prospect of increasing volumes of waste and the increasing imbalance between energy demand and energy resources, modern pyrolysis techniques have recently become attractive for thermochemical conversion to mitigate adverse impacts during recycling and recovery of plastic waste. However, the installation of pyrolysis processes is always confined by location, feedstock resource, secondary pollution due to improper treatment, government policy and other extraneous factors, which leads to the pyrolysis process being costly to install and having a less beneficial social impact and awareness. This thesis is thus aimed at developing unified models to investigate predict the yields of the processes under a range of operational conditions by using the lumping methodology, at investigating the kinetic characteristics of plastic pyrolysis, to contribute a potential engineering solution in plastic waste recovery. To achieve the aim, the thesis is divided into three parts.

In the first part of the work, the optimisation of the effect of operational parameters on the yields from thermal conversion of plastic waste was studied. The individual and interaction effects of multiple operational parameters (such as temperature and feed ration

of feedstock compositions) of pyrolysis were optimised by using the design of experiments approach during the study of a thermogravimetric analyser (TGA) of plastic waste. The influence of temperature, residence time, particle size, feedstock composition and bed thickness on the conversion process of plastic waste was examined. The work has also been performed using fixed bed pyrolytic reactors (FBPR) to examine the thermal conversion behaviour and yield distribution. Waste polyethylene (PE), polypropylene (PP) and poly(ethylene phthalate) (PET) were chosen as feedstocks for the study. The thermal decomposition of plastic waste and the product distribution were experimentally investigated under inert nitrogen atmosphere over a temperature range from 400℃ to 550℃. The effect of temperature on product yields (liquid, solid and gas) within the batch reactor was discussed. Highly aliphatic nature of the pyrolysis oil and variety of C-C and C=C bonds were identified by using Fourier transform infrared spectroscopy (FTIR) coupled with the changes of wave peaks and wave range between wax (heavy oil) and oil. The experimental results indicated that temperature is a significant process parameter affecting the product distribution and reaction mechanism comparing to other parameters.

In the second part of the work, the kinetics of the chemical reactions for the primary pyrolysis of plastic waste were studied. The aim of this part work was to study the primary pyrolysis behaviour of real components of plastic waste, to examine the kinetic characteristics for the primary pyrolysis, and to evaluate the effect of lumping selection on apparent kinetic parameters during models development. A kinetic model comprising of primary and secondary reactions was formulated to describe reaction pathways of primary pyrolysis behaviour and to assess the calculation of kinetic parameters. Different lumping models were developed to explore the suitable description of possible process pathways of the pyrolysis of plastic waste, and also the effect of lumping selection on the estimation of kinetic parameters. Firstly, a three-lump model (plastic lump, volatile lump, and solid residue lump including lower molecular weight polymer, and char-like products) was introduced to predict the kinetics of plastic converted into volatile yield and solid residue; then a four-lump model (plastic, gas, oil, wax) was introduced to ascertain the effect of three phase products (gas, liquid and wax) on lumping strategy and kinetics of plastic primary pyrolysis along with secondary cracking of heavier tar component based on higher conversion of HDPE degradation at higher temperature. A five-lump (feed, gas, liquid, wax and solid char residue) model extended from the four-lump model was

proposed to define char residue as an individual lump, three secondary reaction pathways (residue to gas, oil, and wax; wax to gas and oil) were studied to determine the reaction mechanisms of the pyrolysis process of PE, PP and PE/PP mixtures. It was found that the estimation of kinetic parameters of activation energy and pre-exponential factor are affected by lump selection and temperature range. Comparison of the kinetics variation from different reaction pathways for secondary reactions suggested a five-lump model coupled with secondary of wax to oil and gas is the best reaction pathway for the pyrolysis of PE, PP, and PE/PP mixture. The model was validated against the experimental data obtained in the FBPR and showed a good agreement between the model prediction and experimental results.

In the third part of this work, a case study of the kinetic characteristic of waste HDPE pyrolysis at different bed thicknesses with a function of temperature was studied via FBPR to examine the pyrolysis kinetic characteristic. Thermal decomposition of HDPE was determined using thermal gravimetric analysis (TGA) under inert nitrogen atmosphere over a temperature range from 400℃ to 550℃. The influence of bed thickness on the products distribution was also examined over a final temperature range of 425-550℃. As a result, it was found that the main thermal decomposition of HDPE samples occurred over a temperature range of 475-510℃ corresponding to a conversion range of 10- 95%. A greater wax fraction was yielded from FBPR with a thin bed at 450℃ due to better heat transfer performance. With the temperature increase to over 500℃, more oil and wax products were generated in FBPR with thick bed, inconsistently, more gases yielded from the thin bed at the same conditions. Based on the experimental results, a discrete lumping model comprising of three primary independent parallel reactions has been developed to describe the yield distribution of gases, oil fractions, wax fractions and solid residue, coupling with secondary cracking reactions of wax fractions into lighter fractions (oil) and gases. The model result was shown to be in good agreement with the experimental data. Additionally, the kinetics of waste HDPE decomposition into gas, oil, and wax fractions were discussed, which are consistent with the measured rate constants.

ACKOLEDGEMENTS

Firstly, I would like to thank my supervisor Prof. Raffaella Ocone for her guidance, encouragement, and continuous support in this research. Her rigorous scientific attitudes have always been impressive. Special thanks to my co-supervisor Dr Ondřej Mašek for his help and support, and his professional coaching and guidance during the experimental study. Special thanks to Dr Alan Harper for his support and encouragement. Thank you to Dr Clare Peters for her advice, training and assistance during my experimental study. Special thanks to office mates Mr Maoshuai Li, Mr Adam Mustafa, and Miss Battikh Najah for their advice and assistance. A big thank you to EPS supports office and other school departments, especially Centre for Innovation in Carbon Capture and Storage, for their support.

I cannot express enough thanks to my family for their unconditional love and support through my overseas life in the UK. Lastly not means least, I will forever be indebted to my beloved wife who gives all her support and looks after our family. I could never have done this without her. Thank you

DECLARATION STATEMENT

ACADEMIC REGISTRY

Research Thesis Submission

Name*:*	Haoyu Li		
School:	IMPEE, EPS		
Version: *(i.e. First, Resubmission, Final)*	First	Degree Sought:	PhD in Chemical Engineering

Declaration

In accordance with the appropriate regulations, I hereby submit my thesis and I declare that:

1) the thesis embodies the results of my own work and has been composed by myself
2) where appropriate, I have made acknowledgement of the work of others and have made reference to work carried out in collaboration with other persons
3) the thesis is the correct version of the thesis for submission and is the same version as any electronic versions submitted*.
4) my thesis for the award referred to, deposited in the Heriot-Watt University Library, should be made available for loan or photocopying and be available via the Institutional Repository, subject to such conditions as the Librarian may require
5) I understand that as a student of the University I am required to abide by the Regulations of the University and to conform to its discipline.
6) I confirm that the thesis has been verified against plagiarism via an approved plagiarism detection application e.g. Turnitin.

* *Please note that it is the responsibility of the candidate to ensure that the correct version of the thesis is submitted.*

Signature of Candidate:		Date:	

Submission

Submitted By *(name in capitals):*	HAOYU LI
Signature of Individual Submitting:	
Date Submitted:	

For Completion in the Student Service Centre (SSC)

Received in the SSC by *(name in capitals):*			
Method of Submission *(Handed in to SSC; posted through internal/external mail):*			
E-thesis Submitted **(mandatory for final theses)**			
Signature:		Date:	

TABLE OF CONTENTS

LIST OF FIGURES

LIST OF TABLE

LIST OF NOMENCLATURE

The followings are a list of the abbreviations used throughout this thesis:

Symbols

A	Aromatic
A_0:	Pre-exponential
C:	Coke
C_n	Carbon atom
C-C	Carbon-carbon
D:	Dead chain polymer
E_a	Activation energy
G	Gas
GO	Gas olefins
GP	Gas paraffins
H:	Heavy oil fraction
K	Square matrix of rate constant
$\widehat{\boldsymbol{K}}$	Diagonal matrix with corresponding to eigenvalues of $\boldsymbol{K}$
L:	Light oil fractions
M	Lumping matrix of dimension $\hat{n} \times n$
MF	Middle fractions
N	Dimensions of reaction system n× n
O:	Oil
ODEs	Ordinary differential equations
P:	Plastic sample
R:	Gas constant and
T:	Reaction temperature
W:	Wax
X:	Matrix of eigenvectors
Y:	The yield of volatile products
$\bar{Y}$	The response of central composite dsign
C_m:	The number of monomer
N_i:	Number of bond type i
$R_{m,n,x\ and\ y}\ R'$:	The group of H atom, -OH, -COOH, CH3 and other alkyls, phenyl,

	alkenyl and so on in the polymer chain.
R_e:	Radical of end chain
$e_{f:}$	The number of bonds along a polymer chain that is excluded from this general chain fission reaction.
e_t:	The number of monomer units along a polymer chain that does not undergo this general mid-chain hydrogen abstraction reaction.
e(t)	Lumping error
f:	The vector of operation expressing the kinetics
k:	The vector of reaction rate constants
m:	Mass
n	Natural number
$\bar{n}$	Independent factor factor number
t:	Reaction time
x:	The species concentration vector with dimension of $\boldsymbol{n}$
x'	The normalized mass fraction x' from decomposed sample mass

ABBREVIATIONS

ABS	Acrylonitrile Butadiene Styrene
ANOVA:	Analysis of variance
BTX	Benzene, toluene, and xylene
CV:	Calorific value
CCD:	Central composite design
DL:	Discrete lumping
DSC	Differential scanning calorimetry
DTG:	Differential thermograme artic
EFRfW:	Energy and feedstock recovery from waste
FBPR:	Fixed bed pyrolytic reactor
FPE:	Flexible polyethylene
FTIR:	Fourier transform infrared spectroscopy
HDPE:	High density polyethylene
HPA:	Health Protection Agency
LDPE:	Low density polyethylene
MOF:	Minimizing objective function
MS:	Mass spectra
MSW:	Municipal solid waste
NO_x	Nitrogen oxide
PBE	Population balance equations
PCA :	Principle components analysis
PE:	Polyethylene
PET:	Poly (ethylene terephthalate)
PP:	Polypropylene
PS:	Polystyrene

PVC:	Polyvinyl chloride
QSSA:	Quasi-steady state approximation
RCD:	Random chain dissociation model
RDF:	Refuse derived fuel
RPE:	Rigid polyethylene
RSM:	Response surface methodology
SPI:	Society of the plastic industry
TGA:	Thermal gravimetric analysis
UKBRC:	UK Biochar Research Centre

CHAPTER 1 INTRODUCTION

Summary

This chapter presents the background and the motivation for this PhD project; a survey of plastic industry development; plastics applications in the UK and European market and the status and challenge of waste plastic recycling and recovery; the applications of lump kinetics methodology in the recovery process of plastic waste; motivation of this research, and the objectives of each chapter in this thesis.

1.1 Background

Plastic is a common term for a wide range of synthetic or semi-synthetic organic polymer with high molecular weight formed by repetition of a simple unit. The term "plastic'' is derived from the Greek word "plastikos" meaning fit for moulding, which allows it to be processed by the ways of injection, cast, press, or extrusion into diverse shapes - such as bottles, containers, films, fibres, tubes, and others. There are over thousands of groups of plastics identified on basis of their chemical structure, density, synthesis process, application, and other properties, each with numerous grades available to deliver specific properties for the individual application. Quite a few methods have been developed to identify the different plastic in the industry, especially for the handling of waste plastic. The most common types of used plastics, which account for around 75 percent of all plastics demand, is listed (Table 1.1) by the Society of the Plastic Industry to assist the recycling of plastic waste. Other solutions are also well adopted, such as floating or sinking in the water depend on their density (HDPE floats on the water while PET will sink), flaming and burning depending on the colour and smell, smelling (e.g. PET smells similar burnt sugar, PE and PP smells like candle wax, PVC burns with black smoke, and burns out once leaves ignition source). The differential scanning calorimetry (DSC) is another solution to identify and quantify various polymers in post-consumer waste plastics depend on their glass transition temperature and the melting temperature of the polymers.

In the past seventy years, plastics, as a versatile material, played a significant role in the sustainable development of environment and economy, making a real contribution to meeting the targets of resource efficiency in many areas, such as packaging, building and

construction, automotive and aeronautics; enabling the eco-efficient manufacture of products as a functional material. This is ascribed to their many attractive descriptions such as light weight, cost-effective, resource-efficient, easy processability and reusable. Plastic materials can save more than 140 times the energy needed during their production [1]. With continuously increasing demand for plastics, global production rose from approximately 1.5 million tonnes in 1950 to around 322 million tonnes in 2015 at an average rate of approximately 9 percent per annum, then a stable European market since 2000 (Figure 1-1). In the UK, there are about 2.5 and 4.8 million tonnes of plastic material produced and processed annually at present. While Europe is still the second largest zone in the world with 20 percent market share in 2015 for plastic production behind China [1]. Packaging applications are the largest customer sector for the plastic industry with 39.9 percent share in Europe, similar category applications were consumed in the UK. The details can be seen in Figure 1-2.

Table 1.1 The main plastic materials in the market

Symbol	Acronym	Formula	Applications
#1	PET(polyethylene terephthalate)	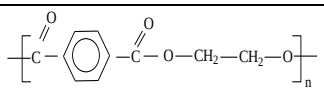	Drinking bottles etc.
#2	HDPE (high density polyethylene)	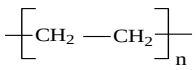	Milk and shampoo bottles, toys etc.
#3	PVC (polyvinyl chloride)	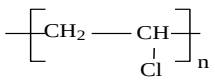	Window frame, pipe, cable insulation etc.
#4	LDPE (low density polyethylene)	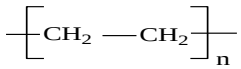	Films, bags etc.
#5	PP (polypropylene)	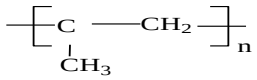	Food containers and trays, auto parts etc.
#6	PS (polystyrene)	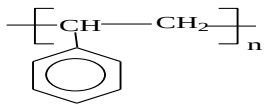	Plastic cups, building insulation (PS-E), etc.
#7	Other e.g., polycarbonate:	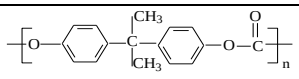	

However, a noticeable fact is that high volume consumption of plastics has had major adverse environmental implications for both industry and society at the end of its life, accompanying with millions of tonnes plastic waste injected in solid waste chain annually,

especially for disposition of mixed plastic waste contaminated by food, construction and medical residue. In the UK, around 3.7 millions of tonnes of plastic waste arisings were estimated in 2014, including that large quantity of 2.2 million tonnes of packaging waste cannot be recycled directly. Thus, plastic waste has been one of the main components of the municipal and industrial waste going into landfill in the UK. Furthermore, another severe fact is that around 8 million tonnes of plastic waste, consisting of more than 5 trillion pieces, ends up in the world's oceans each year for a longer time than in the land, causing damage throughout the food chain and ocean creatures' life [2], a samples can be seen in Figure 1-6. The environmental and ecological threats reinforce global efforts to reduce the volume of the plastic waste stream. Moreover, most plastics are derived from crude oil; roughly 5 percent of crude oil used goes to the production of plastic, which means large consumption of fossil resources. Therefore, plastic waste is not just waste but resource.

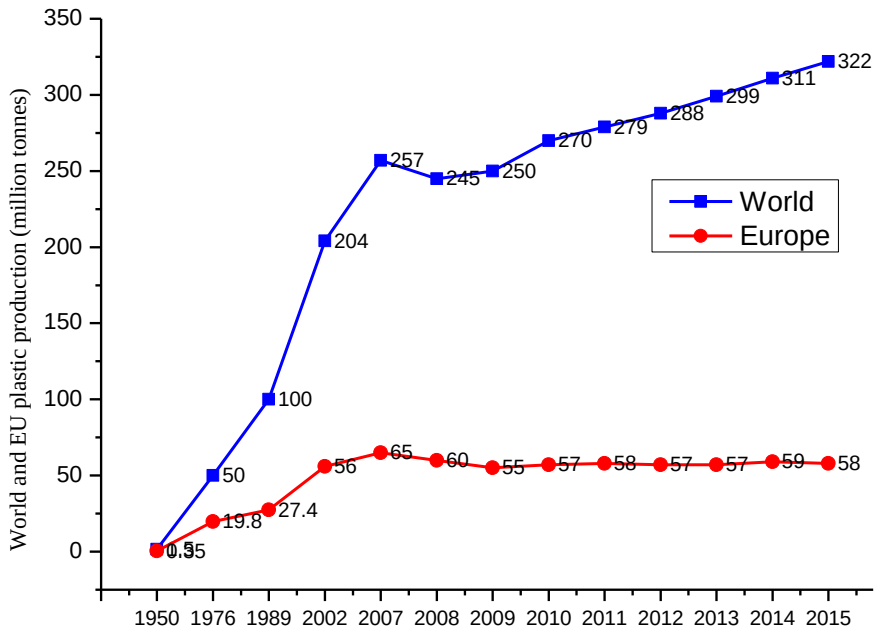

Figure 1-1 World plastic production volume since 1950 [3]

Recycling is the preferred option for plastics waste, while a large proportion of the plastic waste is not available to be handled via recycling on a large scale, due to the reduction of physicochemical properties, the presence of additives, the contamination from other materials, excessive mixtures and laminations. Numbers of technologies have being

explored and deployed for the handling of non-recycled plastic waste, such as recovery and landfilling (Figure1-3).

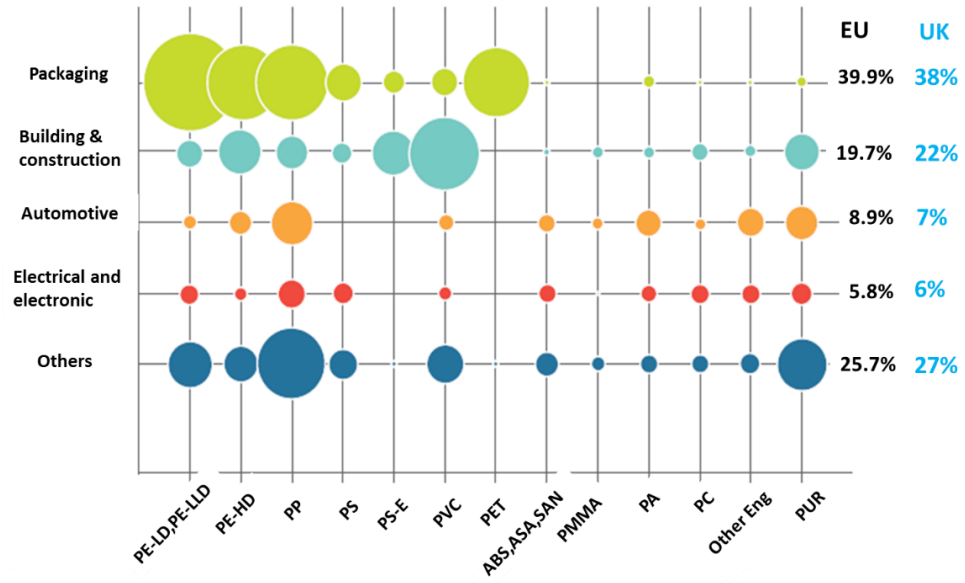

Figure 1-2 Plastic applications in European and UK market in 2015 [1]

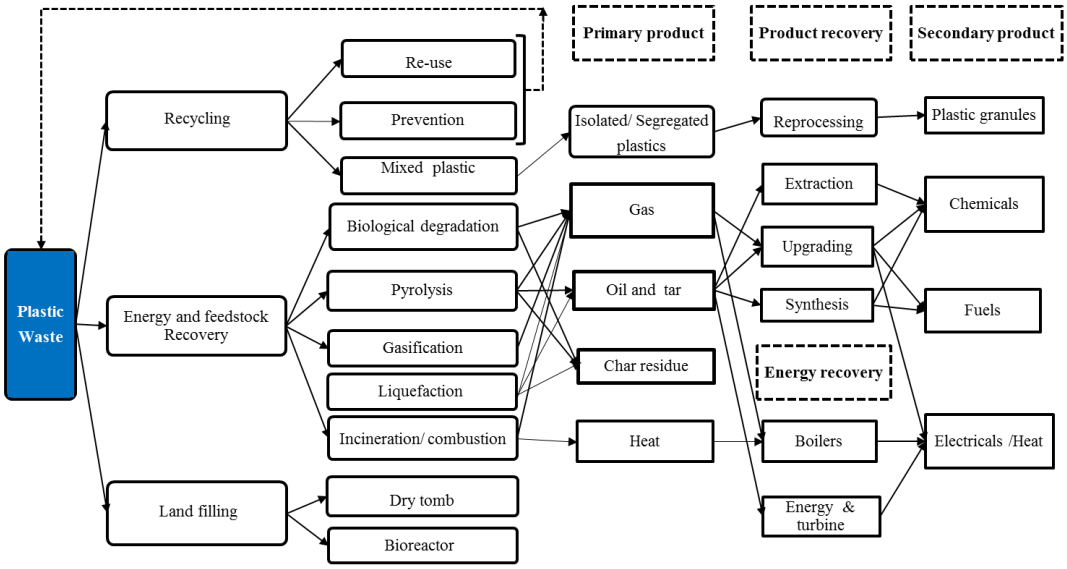

Figure 1-3 Processing technologies of plastic waste [4]

Recycling of plastic waste is usually categorised as primary, secondary and tertiary levels. Primary recycling processes waste into a product with physical and chemical characteristics close to the original product, which is realised by direct reuse (e.g. containers and trays) or prevention of the creation of plastic waste. Secondary recycling

reprocesses plastic waste with fewer properties than the original into products, which is physically released by turning waste (e.g. damaged tray) into plastic granules and then reprocessed with some additives and virgin resin. Tertiary recycling process turns waste into fuels or chemical feedstock, which is subject to waste into energy and feedstock because they are not easy to reprocessed. Landfilling is still the first option in many countries, which treats the waste physically causing a risk of further environmental burden. There were 25.8 million tonnes of plastic waste generated with only 29.7 percent recycled and 30.8 percent landfilled in the EU (Figure 1-4) in 2014 [1]. Plastics Europe singles out the UK for high landfilled plastics rate with over 40 percent sent to landfill or incinerated, ranked in 17th place in EU countries in 2015. To optimise resource allocation, the EU has already mandated the target of zero plastic to landfill by 2020, the implementation of this strategy indicates that 60 million tonnes plastic waste must be diverted from landfill, equivalent to over 750 million barrels of oil or 60 billion euros till 2037[3], as shown in Figure 1-5.

In March of 2016, the UK government just outlined the press that packaging recycling and recovery target for plastics from existing target of 52 percent for 2016 will be reduced by 57 percent till 2020, whilst also outlining plans to press ahead with changes to the Landfill Communities Fund, and to increase the landfill tax rate in line with retail price index. In Scotland, the Government issued waste regulations to achieve the target of zero waste Scotland, such as a ban on biodegradable municipal waste going to landfill from 2021. Therefore, recycling and recovery of plastic waste in the UK still have big challenges to overcome towards the reduction of the landfilling of plastic waste.

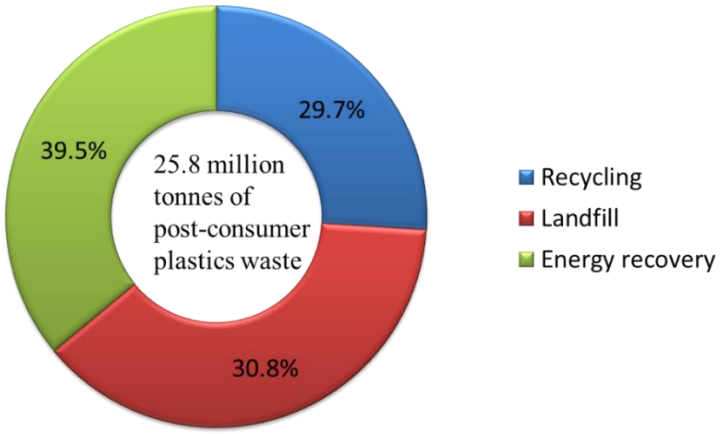

Figure 1-4 Treatment of post-consumer plastic waste in EU 27+Norway and Switzerland in 2015 [3]

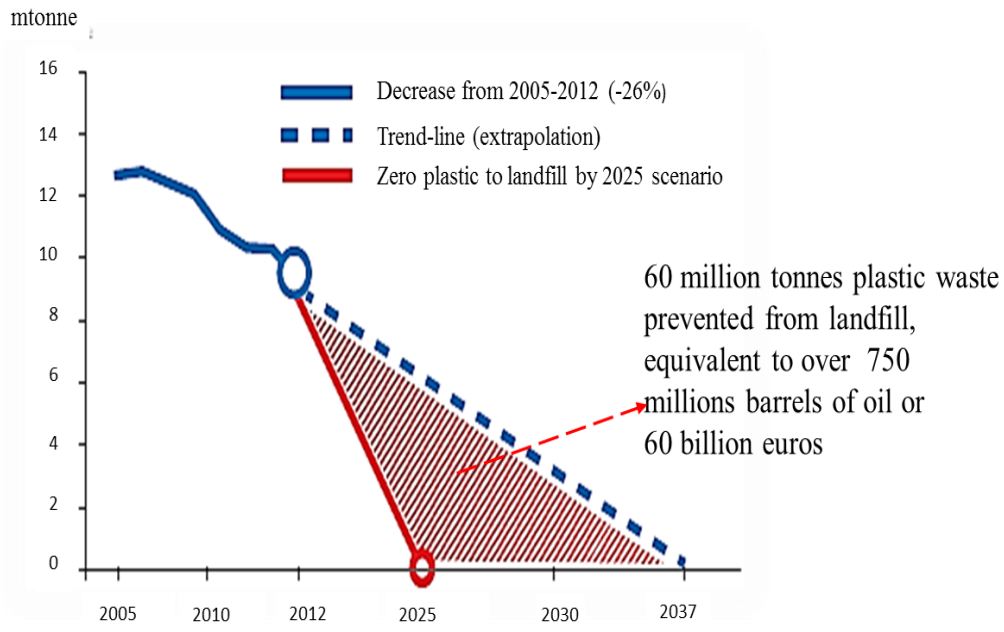

Figure1-5 Potential prevention from plastic waste ended to landfill in Europe [3]

Recovery from waste is, therefore, becoming a feasible innovative solution in waste management, including plastic waste. Management solutions for plastic recycling and recovery, especially for mixed packaging waste, have been developed using advanced thermal heat treatment methods such as gasification [5, 6] and pyrolysis [6-10]. Pyrolysis processes are being considered as promising routes for energy recovery due to simplicity, enabling conversion of the heterogeneous plastic waste into lower molecular weight hydrocarbon products, which can be used as fuel or chemical feedstock and mitigate the negative environmental impact. However, it is confused in the mind of the general public, journalists and some legislators with the mass burning of plastic wastes with its problems of excess greenhouse gas (GHG) emission, and potentially toxic by-products.

A pyrolysis process usually involves a complex reaction scheme, probably comprising of polymer decomposition, cracking, and re-polymerisation stages, with different detail reaction mechanisms from the various components in the waste and their derived fractions. The numerous unclear (and unknown sometimes) species present in pyrolysis scheme are often impossible to be precisely identified. Additionally, the kinetic parameters and reaction order may cause significant differences even for the same polymer with various operational conditions [11]. Thus, the optimisation of the pyrolysis process through mass and energy balance and product distribution needs to overcome the challenges to

accurately predict the levels of product distribution, the control of pyrolytic kinetic characteristic, and the critical design of the reactor to improve the product distribution and avoid further pollution. On the basis of this point, mathematical modelling methodology has been introduced for accounting the difference to describe reaction type and to mathematically translate reaction system into a series of rate equations [12]. The behaviour of chemical and physical properties of pyrolysis of feedstock can be expressed in a mathematical mode to mimic the processes.

As a result, mathematical modelling of thermal decomposition reaction enables to help in understanding the design control of pyrolysis process, in examining the reliability and validity of assumptions, and in deducing quantitative conclusions [13]. Reliable models for the plastic pyrolysis are powerful to predict yields of desired and undesired products, to estimate the kinetic characteristic in different operating conditions and for a given range of feedstock. The model simulation for large quantities of mixtures to know their kinetic characteristic is useful in the identification of elemental reaction and species. A proper kinetic model could avoid running expensive experiments in a laboratory or pilot plant [14]. However, a considerable fact is how to find a proper solution to describe a very complex reaction system, which involves many dimensions and multiple time scales of reactions. The number of species and reactions are possible to be explored following with more detail and accuracy of the predictions.

The application of order reduction technique to the modelling of complex chemical process benefits rigorous investigation of the detail chemistry and simplification of reaction networks. There are quite a few approaches based on such time-honoured mechanism reduction techniques, such as quasi-steady state approximation (QSSA) [15], sensitivity analysis [16-18], time scale analysis [17-19], and principal components analysis (PCA) [20, 21], which will be reviewed in Chapter 2. Apart from those model reduction techniques, lumping is also a powerful technique to describe a spatially distributed physical system in mathematic mode under some assumptions, which simplifies a state space of the system into a finite dimension system [18]. For a complex reaction system, lumping approach is introduced by grouping the reaction system into a lower order system of dimensions, which is realised by grouping components (or reactions) into substituting pseudo-components to each lump. The discrete pseudo-component lump will then represent the original group and mimicking the behaviour of the original components. The modelling reduction by lumping method is helpful to

increase the work efficiency as simplifying the complexity of mixture [22]. Therefore lumping methodology is valuable to be undertaken in the prediction of the pyrolysis process of plastic waste in a cost-effective solution, which was adopted in this PhD research.

1.2 Motivation of this research

The motivation behind this study is based on an understanding of the implication of plastic waste management to the environment and the society. With the improper propensity of increasingly over-consuming, discarding, littering of plastic waste, plastic waste has become a knotty problem in the world, which badly affects human being's health and safety, wildlife especially ocean creatures', recycling challenge etc., which can be seen in Figure 1-6. China is the largest base of plastic production and application in the world; while China also consumed around 56 percent of plastic waste from the USA and Europe and other countries in the past two decades, as well as the UK, which resulted in that large quantity of toxic plastic waste (e.g. used plastic packaging from medical and chemical) entering normal recycling processes then producing toys or bags etc. (Appendix 1) and reprocessed at low-technology with less concern for environment protection. Around 70 percent of scraped plastic waste in the UK exported to emerging market (e.g. China, India, Vietnam) since the 1990s. The Chinese government has started to implement Green Fence Policy to reduce scraped plastic waste into China directly since 2010. This will increase the threat on the handling of the capacity of UK plastic waste recycling and recovery. Turning of plastic waste into value-added products and reducing the dispose of plastic waste via landfilling in the UK are also facing the challenges to fulfill the targets from UK government and EU.

Therefore, it is global demand aggressively exploring the potential solution for recovering plastic waste into value-added products in terms of energy balance and quality of co-products demands knowledge, and control of the kinetics of pyrolysis. Pyrolysis process can be one of the advanced choices, which can tranform plastic waste into a valuable fuel source for substituting fossil fuel. Moreover, plastic has higher calorific value than biomass, municipal solid waste (MSW), or refuse derived fuel (RDF), and also lower moisture content and narrower product distribution than biomass, as shown in Table 1.2 [23]. The fuels produced from plastic waste are similar to those derived from petroleum. Particularly, pyrolytic fuel generated from polyvinyl waste has lower sulphur content than that from crude oil [10]. Therefore fuel and chemical feedstocks generated from plastic

waste can release the carbon factor within the plastic polymer life cycle to reduce the overall GHG emissions.

China	China	Brazil	United Kingdom
Philippine	Indonesia	United states	Norway
Ocean creature	India	South Africa	Ocean creature

Figure 1-6 Plastic pollution in different countries and oceans [24]

Table 1.2 Energy density of plastics, Biomass, MSW, RDF and conventional fuels [25, 26]

Plastic	Calorific value (MJ/kg)	**Fuel**	Calorific value (MJ/kg)	**Biomass** (Dry ash free)	Calorific value (MJ/kg)
PE	46.3	Coal	14.0~32.5	Wood	18.0
PP	46.4	Gasoline	46.4	Paper/cardboard	23.1
PS	41.4	Kerosene	43.4	Food	23.7
PVC	18.0	Diesel	45.6	Leaves and grass	19.6
Polyester	26.0	Crude oil	46.3	Total biomass carbon compounds	21.2
PET	23.5	Natural gas	53.6	RDF	17.4~32.9
		Biodiesel oil	42.2	MSW	18.9
				Household waste	8.0

Around 1.3 million tonnes of 3.7 million tonnes of plastic waste ended up in UK landfills representing a loss of over £500 million in value as plastics or £350 million as hydrocarbon feedstocks [3, 27]. Approximately 2.2 million tonnes packaging plastic waste arisen in the stream of plastic waste in the UK in 2014 [28]. Waste polyethylene (PE), polypropylene (PP) and polyethylene terephthalate (PET) was evaluated in this

study, as they are major components with 58 percent in the stream of plastic waste (Table 1.3).

Such a variety of feedstock can result in a wide range of products. For example, PE converts preferentially into wax and PP favours olefin, Wax and olefin are valuable in fuel and chemical chain. Indeed, the pyrolysis of waste plastic into valuable products depends on specific plastic types, and the selected technologies. Both factors depend on local economic, environmental, social and technical characteristics.

Table 1.3 Generic composition of UK domestic mixed plastic packaging materials[28]

Polymer type	**Quantity (1000 tonnes)**	**Share (wt%)**
LDPE	414	18.6
HDPE	542	24.2
PET	767	34.5
PP	266	12.1
Others	231	10.4
Total	**2220**	**100**

1.3 Aims and Objectives of the Investigation

This project aims to study the applications of lumping kinetics methodology to energy-intensive chemical feedstock recovery from post-consumer plastic waste via pyrolysis , to determine the distribution of product yield and compositions during pyrolysis process using TGA and fixed bed pyrolytic reactor (FBPR), and to analyse the kinetic characteristic of pyrolysis reaction through of lumping models.

Thus the main objectives of this study are:

1. Primary pyrolysis characteristics of plastic waste
    - To determine the thermal pyrolysis characteristics of real components of plastic waste (PE, PP, PET and their mixtures) by TGA and FBPR;
    - To study the optimisation of the process parameters;
    - To determine the process parameters for the distribution of product yield and composition and variation and sensitivity of kinetic parameters;
2. Discrete lumping kinetic model development
    - To describe the most probable reaction pathways of plastic pyrolysis;

- To develop a kinetic model based on the different reaction routes for kinetics estimation;
- To validate the developed model against experimental data;
- To assess the effect of lump selection on the variation of kinetic parameters.

3. Case Study: The effect of varying bed thickness on the kinetics, product distribution and yield of HDPE pyrolysis
    - To examine the kinetic characteristic of HDPE pyrolysis at varying bed thicknesses;
    - To evaluate the yield distribution and the change of product composition;
    - To estimate the kinetics of HDPE pyrolysis and validate the model by experimental data.

1.4 Outline of the thesis

This thesis is presented in the following chapters.

Chapter 1 Introduction

This Chapter highlights the background of plastics and its waste, kinetic modelling of energy and feedstock recovery processes via pyrolysis, and to establish the motivation and the aims of this project;

Chapter 2 Literature review

This Chapter presents a review of feedstock recovery solutions from plastic waste; a review of mechanism of pyrolysis process; a review of the effect of processing conditions on the plastic pyrolysis process; a review of pyrolysis model development for plastic waste; a review of kinetic lumping development; a review of estimation of kinetics from different models of plastic pyrolysis.

Chapter 3 Experiment and Methodology

This Chapter presents the selection of feedstock in this project; the experimental design; the experimental apparatus for fixed bed pyrolytic reactions and thermogravimetric

analysis and their experimental procedures; the analysis methods of liquid and gas products; the methodology of kinetic model development, and model solution using MATLAB software to determine model parameters.

Chapter 4 Pyrolysis of PE, PP, PET and their mixtures

This Chapter presents the thermal conversion characteristics of selected materials in this study; the effect of temperature and residence time on the product distribution.

Chapter 5 The effect of reaction pathway simulation and lump selection on the kinetics estimation of waste plastic pyrolysis

This Chapter presents the possible reaction pathways in different processing conditions; lumping scheme and their effect on the estimation of kinetic parameters; the kinetics estimation of thermal decomposition; validation of proposed kinetic lumping models.

Chapter 6 Kinetic study of the pyrolysis of HDPE waste at different bed thickness over FBPR

This Chapter presents a kinetic study of pyrolysis of high density polyethylene (HDPE) waste at varying bed thicknesses in the fixed bed reactor, the kinetic characteristics, the product distribution and composition at different temperatures.

Chapter 7 Conclusions and Future Recommendations

This Chapter concludes the research results and addresses the future work.

CHAPTER 2 LITERATURE REVIEW

Summary

This Chapter reviews the techniques of energy and feedstock recovery from plastic waste; the pyrolysis of plastic polymer and its thermal decomposition mechanism; the effect of process parameters on the pyrolysis process and product distribution; the kinetic model development of plastic pyrolysis and reduction methods of complex reaction system; lumping methodology and development of discrete lumping approach.

2.1 Energy and Feedstock Recovery from Waste (EFRfW)

EFRfW is a thermochemical process generating a useable form of energy (e.g. heat and fuels) and chemicals, coincidentally reducing the solid volume of residual waste. Residual waste is often a kind of mixed waste that cannot be usually reused or recycled directly, being too contaminated for the recycling process to be economically or practically feasible to take to the market [29]. Plastic waste subject to energy and chemical recovery process is one kind of fossil fuel based residual waste. Conversion of large-volume plastic waste into value-added products could be an environment-friendly solution. Incineration is the most well-known approach to deal with this kind of material, frequently and erroneously as the option of energy recovery from the waste process. In fact, incineration, as a specific type of combustion process, often involves the release of toxic matter (e.g.dioxin and furan) and GHGs, especially in the case of polyvinyl chloride. The generation of chlorine (e.g. CI2 or HCI) from combustion in waste-to-energy facilities presents a major operating threat as it causes significant corrosion in the reactor and boiler system [32]. The landfill is another popular solution to dispose of residual waste as shown in Chapter 1. In the Europe, the technology of emission clean-up step for EFRfW is well developed ensuring that all the waste off-gases emitted from the processes meet the very tight limits placed on them by EU legislation. These emissions have been assessed by the Health Protection Agency (HPA) which has found little effect on health [29]. These make EFRfW process flexible enough to cope with such variations or to seek out the alternative route to further process the waste stream to ensure the required environmental benefits. EFRfW closely depends on the feedstock and the efficiency with which it is pre-selected, for instance, unknown feedstock composition, may occur due to

supply chain irregularities from the local community and thus requires assessment for potential sources of pollution. As shown in Figure 1-3, around 40 percent of plastic waste was converted into value added products (e.g. fuels and chemicals) in Europe in 2015, while approximately 31 percent was still ended into landfilling. Therefore, a study of pyrolysis processes for EFRfW will be informative and beneficial.

EFRfW in the form of pyrolysis, gasification, and liquefaction with/without catalyst has significant advantages in the portfolio of sustainable waste management measures, with potential renewable energy outputs compared to landfill or combustion.

- Gasification of plastic waste operates at high temperature (>600-800℃) with the presence of air or oxygen. The desired primary product is a syngas of carbon monoxide and hydrogen, and minor percentages of carbon dioxide and gaseous hydrocarbons also formed. The syngas can be used as a substitute for natural gas or in the chemical industry as feedstock for the production of numerous chemicals. However, some challenges for gasification technology have to be considered, such as economic gas purification, uncertain compositions of plastic waste, process scale-up and emissions.

- Liquefaction of plastic waste operates at a lower temperature range (e.g. 370-420℃ for polyolefins) to decompose plastic polymer back to lower molecular weight liquid form such as paraffin, olefin, naphtha, and aromatics, it can be a special pyrolysis. Liquefaction process often takes place in the presence of te catalyst and high-pressure, targeting for maximum yield of liquid, least yield of gas and the solid residue.

- Pyrolysis involves plastic decomposition with free oxygen and temperature range of 350-800 ℃ through carbon-carbon (C-C) bond rupture depending on the feedstock composition and target products. Pyrolysis products include gas, liquid, wax, and char-like residue with the proportions of each depending on the parameters of the process and feedstock composition. Pyrolysis process often takes place at normal atmospheric pressure, which gives an advantage of cost-saving in facility establishment. The studies of pyrolysis process enable to give information on thermal stability and degradation kinetics, to operate at a flexible conditions comparing to gasification and liquefaction, and to permit identification

of pyrolysis products. Thus, pyrolysis technique is chosen to investigate the thermal conversion of plastic waste in this PhD project.

2.2 Pyrolysis of plastics

Pyrolysis techniques have been used from as early as the 1930s in Germany for the upgrading of hydrogenation residues derived from coal liquefaction. Since then, pyrolysis processes have been gradually introduced for the upgrading of solid waste and energy-dense materials to the standard of feedstock required for the chemical industry. The oxygen-free atmosphere can prevent the degradation and decomposition of organic matter into carbon oxides which lead to GHG emissions, and entails negligible production of toxic oxides species (e.g. NO_x) and less energy consumption during the core reaction at an elevated temperature [30]. Thus, pyrolysis of plastic waste into fuel and other value added chemicals is becoming a competing interest. Surely, the main concern is that the yield and quality of the products generated from plastics, which depends on the feedstock and process conditions. For most thermoplastics, Buekens et al [31] reported plastic pyrolysis process can be categorised as low ($< 400℃$), medium ($400\sim600℃$), or high temperature ($> 600℃$). Pyrolysis of plastic can be categorised as fast pyrolysis and slow pyrolysis. Fast pyrolysis (also called flash pyrolysis) of plastic occurs in less than two seconds with the temperature range of 350-600℃, slow pyrolysis may last a few hours and days, or even longer.

2.2.1 Thermal decomposition mechanism of plastics

The decomposition of plastic waste used to be understood how to control the end product distribution according to the specific mechanisms based on the molecular structure of polymers. Beyler and Hirschler [32] proposed that the chemical reactions occurring during the polymer decomposition can be divided into main chain reactions (e.g. chain scission and cross- linking) and side chain or substituent reactions (e.g. side chain elimination and side chain cyclisation). Generally, the most common reaction mechanism involves chain scissions in the main polymer chain. These chain scissions may occur at chain end or at random locations in the chain. End chain scission mostly results in the production of monomers. Random-chain scissions may result in the generation of monomers, oligomers as well as a variety of other chemical species due to the uncertainty of chain cleavage.

Decomposition by chain scission undergoes a multistep radical chain reaction (Eq. 2.1

and Eq. 2.2) comprising the steps of hydrogen transfer with the progressive breaking of the plastic backbone. The free radicals formed by the hydrogen atom transfer between intermolecular and intramolecular polymer molecules lead to the cleavage of the carbon-carbon bond by the mechanism of end chain scission or unzipping (Eq. 2.1 and Eq.2.2), random chain scission/fragmentation (Eqs. 2.4, 2.5 and 2.6), and β −scission (Eq. 2.3).

Radical chain reactions:

Initiation

$$R_n^* \longrightarrow R_{n-1}^* + R \tag{2.1}$$

$$R_{n-1}^* \longrightarrow R_{n-2}^* + R \tag{2.2}$$

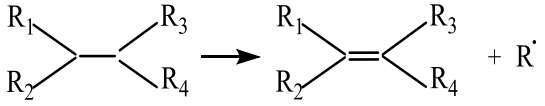

(2.3)

Propagation

$$R_n \longrightarrow R_x - R_y \xrightarrow{heat} R_x^* + {}^*R_y \tag{2.4}$$

$$R_x^* M - N \longrightarrow R_x\text{-}M + {}^*N \tag{2.5}$$

$$N^* P S \longrightarrow N\text{-}P + {}^*S \dashrightarrow \text{etc} \tag{2.6}$$

Termination (recombination and disproportionation reactions)

$$R_m \longrightarrow R'_m \tag{2-7}$$

$$R_m + R'_n \longrightarrow R_{m+n} \tag{2-8}$$

$$R_m + R'_n \longrightarrow R_n + R'_m \tag{2-9}$$

where $R_{i,j,m,n}$ and $R'_{i,j,m,n}$ stand for the functional group of H atom, -OH, -COOH, CH_3 and other alkyls, phenyl, alkenyl and so on. Cross-linking occurs after initial stripping of substituents and involves the creation of bonds between two adjacent polymer chains. In side-chain elimination reactions, side groups often react with other eliminated groups. In cyclisation reactions, two adjacent side groups form a bond between them, resulting in the production of a cyclic structure. The processes of cross-linking reaction and cyclisation reaction result in the formation of chars. The reactions of thermal pyrolysis suspend and terminate due to disproportionation (Eq. 2.9) or recombination (Eq. 2.8). The

saturated or unsaturated monomer unit is consecutively generated once the backbone bonds are weaker than the bonds of the side group. As a result, a branched product may be formed by the free radical interaction from the secondary cracking reaction and skeletal isomerisation. The secondary reactions are favour for the formation of lighter fractions (e.g. wax cracking into light oils) and char residue (e.g. aromatic cracking) during the intermediate reactions, which are shown in Eq. 2.10. Thus thermal cracking yields a range of product distribution (e.g., the carbon number of yield distribution of PE ranges of $C_{1\text{-}60}$) [10].

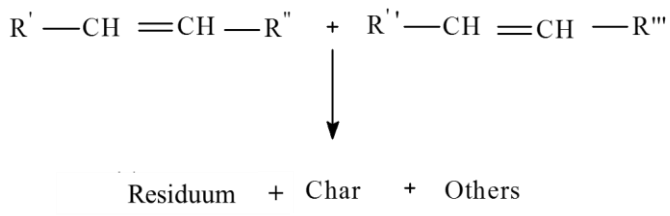

(2.10)

2.2.2 Products generation from pyrolysis

The products formed by the devolatilisation process via thermal pyrolysis, are usually divided into three phases in terms of their aggregated state at normal temperature, which is referred to the gas of gaseous phases, the oil of the liquid phase, and the solid char residue of the solid phase. The primary pyrolysis of plastic waste can generate intermediate liquids and gaseous components. Those components are possible decomposed further at some conditions to give lower molecular weight components (secondary reaction), such as olefins, alkanes, BTX (benzene, toluene and xylene, which favour the formation of char), and char.

Gas

The gas fraction is the group of species commonly consisting of the dry gases such as H_2, CO, and CO_2; the alkane and alkene whose molecule is not more than four carbon atom number in the molecular formula.

Liquid

The oil fraction in the pyrolysis process of plastic is the group of species that are liquid at normal temperature although they are gaseous at pyrolysis temperature with carbon number range of 5-21. Nevertheless, heavy tar and partially melted wax also with carbon atom numbers are over 22. Oil species are the most complex phase for plastic pyrolysis,

and difficult to determine the each component in the mixture, but liquid is most desired product in the pyrolysis process of plastic waste.

Char

Char is a porous and hard carbon structure from incomplete organic pyrolysis and usually assumed that char completely exists of carbon, but since char is often defined as the solid residue after pyrolysis, it is often polluted with other components and unreacted polymers. Char favours the condition of higher temperature and longer residence time.

2.2.3 Fuel properties of the oils/waxes from the plastic pyrolysis

Tables 2.1 and 2.2 present the properties of oils recovered from plastic waste, which show a high potential for application as fuels. Kosior [33] reported that there is a similar carbon number distribution between regular diesel and derived diesel from plastic pyrolysis process, but conveniently higher C_{8-9} hydrocarbon fraction from plastic shows better octane ratings than the petroleum is clearly observed (Figures 2-1 and 2-2).

Table 2.1 Fuel properties of oils derived from the pyrolysis of various plastics [10, 34]

Fuel property	PE	PP	PS	Nylon	PP/PE/Nylon (50/43/7: wt %)
Flash point (℃)	33.6	27.8	26.1	34.8	26.0
Pour point(℃)	2.7	-39	-67	-28	-5.0
Water content (ppm)	0.18	0.13	0.67	2500	310
Ash (wt. %)	0.03	0.010	0.006	0.018	0.001
Viscosity (cSt at 50℃)	2.190	1.9	0.0181.4	1.8	1.485
Density (g/cm^3)	0.858	0.792	0.960	0.926	0.799
Cetane rating		56.8	12.6		54.3
Sulphur (wt %)	0.01	0.01	0.01	0.01	0.013
Nitrogen (ppm)	0.2	0.2	0.2	6400	1750
Energy content (kJ/kg)	52263	53371	50365	44403	46270

Therefore, plastic waste is regarded as a potentially valuable source for pyrolysis processes for energy recovery. Vinyl polymers (e.g. PE, PP, and PS) could be the main source as they are entirely hydrocarbon.

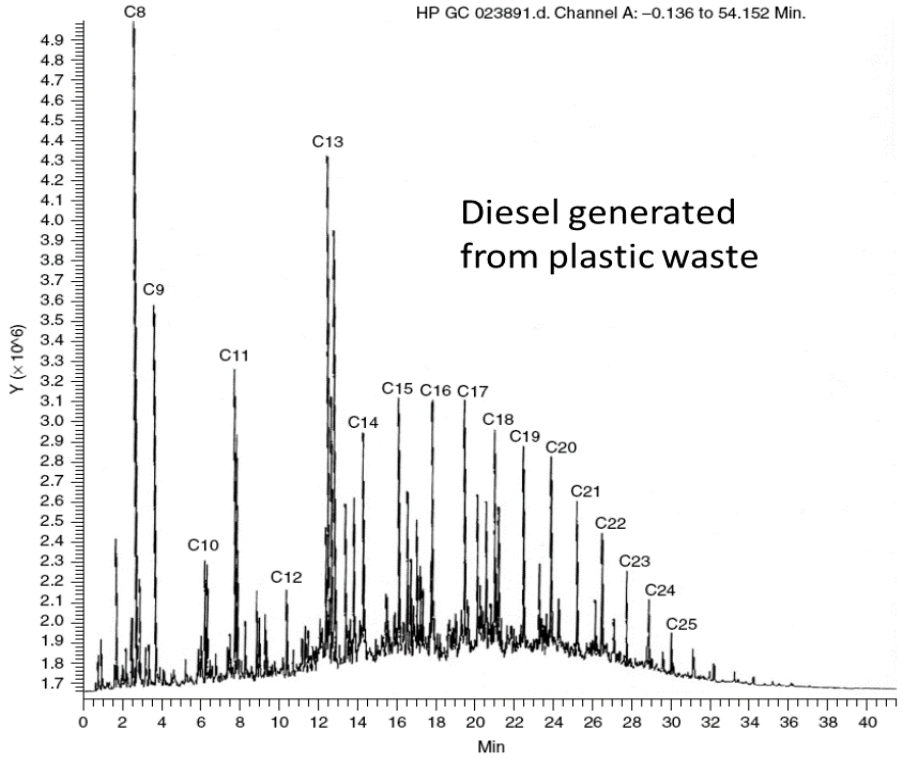

Figure 2-1 Carbon number distribution of diesel derived from plastic waste [33]

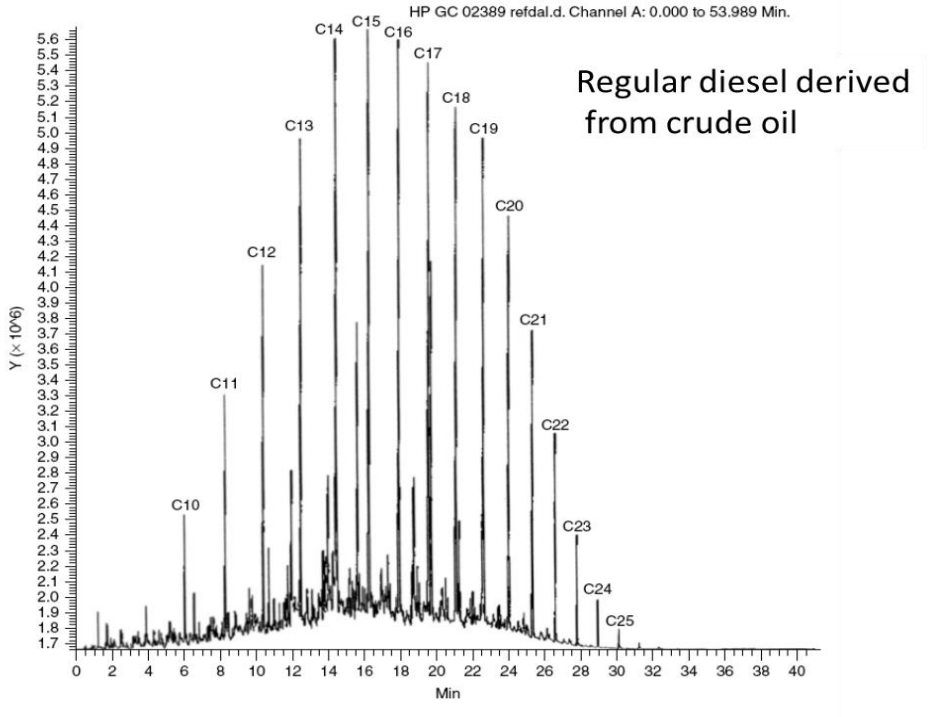

Figure 2-2 Carbon number distribution of regular diesel [33]

Table 2.2 Fuel properties of petroleum-derived fuels [35, 36]

Fuel test	Kerosene	Gas oil	Light fuel oil	Heavy fuel oil	No1-D	No2-D	No3-D
Carbon residue	9	<0.35			0.15	0.15	
Viscosity cSt at 40 ℃	1.2	3.3	21	30	1.3-2.4	1.9-4.1	5.5-24.0
Water content (wt %)		0.05	0.1		0.05	0.05	0.50
Density (kg/m^3)	0.84	0.78	0.89	0.95	0.832[a]	0.832[a]	0.832[a]
Ash content		0.01	0.02		0.01	0.01	0.10
Flash point (℃)	40	75	79	110	38	52	55
Carbon (wt%)		87.1	85.5				
Hydrogen (wt%)	13.6	12.8	12.4	11.8			
Sulphur (wt%)	0.1	0.9	1.4	2.1	0.50	0.50	2.0
Initial boiling point	140	180	200	252	180-360	180-360	180-360
10% boiling point (℃)							
50% boiling point (℃)	200	300	347				
90% boiling point (℃)	315						
CV (MJ/kg^3)	46.6	46.0	44.8	44	40	40	30

No 1-D: A volatile distillate fuel oil for engines in service requiring frequent speed and load changes

No 2-D: A distillate fuel oil of lower volatility for engines in industrial and heavy mobile service

No 3-D: A fuel oil for low and medium-speed engine

[a]: data from Wikipedia

2.3 The effect of operational parameters on pyrolysis of plastic waste

The output performance of the pyrolysis process is often determined by selected process variables that single and/or combinational influence during the process, such as temperature, residence time, pressure, catalyst. These process parameters have been widely studied in the literature.

2.3.1 Chemical composition of feedstock

The chemical composition is an intrinsic character of the feedstock and determines the product distribution through different functional groups in the polymers during the pyrolysis process. Generally, the pyrolysis yield distribution of PE favours alkane content, PS gives more aromatic component in the end product, and PP is inclined to alkene formation [37]. PET and other condensation polymers can be broken into their monomer units via depolymerisation processes [38]. Moreover, the chemical composition also influences different mechanism of chain breakage and random scission of carbon-carbon bonds of polymer with the presence of branched chain so as to increase the complexity of thermal degradation [39]. The kinetic behaviour of a plastic mixture may be influenced by each component during the pyrolysis. Faravelli et al [40] reported that the radicals formed from PS decomposition can increase the conversion of PE and PP from the same mixture under the study of the kinetic behaviour of thermal degradation of polyethylene and polystyrene mixtures.

2.3.2 Temperature and heating rate

Temperature can be the most dominant process variable influencing pyrolysis for its significant effect on both the conversion and product distribution. Higher reaction temperatures and heating rates both enhance bond cleavage and favour the production of small molecules, resulting in the increased proportion of the gas phase and the decrease of liquid phase [8, 10, 39, 41-43]. Plastic polymers start to decompose once the temperature contributes sufficient thermal energy to break the covalent bond between different functional groups in the polymer molecules. Lopez et al [41] studied the influence of temperature on plastic waste in a semi-bed reactor, and found that 500 ℃ is optimal temperature for most mixed plastic waste (40wt% PE, 35wt% PP, 18wt% PS, 4wt% PET and 3wt% PVC) pyrolysis in terms of both conversion and quality of the pyrolysis liquids.

Heating rates also have considerable influence on the pyrolysis process and product distribution. Kaminsky and co-authors [10] described that conventional pyrolysis usually takes place at moderate heating rates in the range of 10–100℃/min and at a maximum temperature of 600℃ which produces almost equal amounts of solids, liquids and gases. However, a fast or flash pyrolysis occurring at very high heating rates of about 100–1000℃/s with temperatures below 650℃ and fast quenching leads to the formation of mainly liquid product. High heating rates reduce the formation of char, and the oil products quickly break down to a favourable yield before cracking into gas products.

2.3.3 Residence time

Residence time (known as reaction time, or retention time at final peak temperature), is another key process variable for waste plastic pyrolysis. The residence time has been widely investigated in many studies [10, 41-45]. It is closely related to the pyrolysis regime and reaction temperature and other variables. In fast pyrolysis or continuous pyrolysis process, residence time refers to the contact time on the surface of the plastic throughout the reactor; it means the duration between the time of heating start to extraction in the slow pyrolysis and batch processes [10]. Longer residence time increases the thermal conversion and product yields but promotes the carbonisation process, produces more char-like residue, and increases the operation cost. In fact, residence time is impossible to measure directly in a batch reactor, it is usually controlled in terms of other parameters such as temperature, catalyst, carrier gas flow rate, and product discharge rate.

2.3.4 Catalyst

Catalysis in cracking of plastics affects kinetics, mechanism, and product distribution [20, 31]. White [46] studied the acid-catalysed cracking of polyolefin on their primary reaction mechanism, and found that the reaction pathways have numerous influences on acid-catalytic cracking; and that the catalytic reactor design can further affect relative product yields by facilitating secondary reactions. Obali, et al [47] investigated the catalytic degradation of PP over alumina loaded mesoporous catalyst and found the presence of SBA and MCM catalyst can improve the gas yield and provide better selectivity in the product distribution which favours the light olefin hydrocarbon in the carbon number range of $C_{3\text{-}7}$. Catalysts also can lead to such drawback of pyrolysis performance as the deactivation of the catalyst. Moulijn et al [48] described that the five

main deactivation factors are poisoning of the active sites, fouling, sintering or evaporation initiated from thermal degradation, mechanical damage and corrosion/leaching by the reaction mixture.

2.3.5 Other operational variables

There are some other effect factors influencing the pyrolysis process. The presence of air, oxygen, or hydrogen in the reaction is sometimes required for different purposes, such as reaction selectivity, and product quality. The presence of heterogenic atoms (i.e. chlorine, and sulphur) can reduce the quality, product yields and the progress of secondary cracking reaction [31]. The effect of reactor type for pyrolysis plastic waste mainly reflects on the heat transfer, feedstock material, the target product, residence time and the reflux level of the primary products. The pressure effect is on the conversion rate and product distribution [49]. The effect of process variables on plastic pyrolysis has been widely investigated, but effects on the pyrolysis process are not easy to evaluate experimentally, especially the impact of secondary cracking on yield distribution and product quality and the interaction effect of multi-process variables on the pyrolysis of real mixtures of plastic waste.

2.4 The modelling for thermal degradation process of plastic waste

A better understanding of the degradation behaviour is crucial for the control of pyrolysis process to achieve the desired product distribution, but it is difficult due to that there could be hundreds of inter-/intra-molecular reaction steps and species occurring simultaneously in the plastic decomposing networks, which are often impossible to precisely identify experimentally. The proportion of each fraction and its precise composition depend primarily on the nature of the polymer and on process conditions as well. The heavier fractions generated directly from the initial degradation reaction are possibly transformed into secondary light products due to the occurrence of competing reactions and proper process conditions. A key task of modelling of plastic pyrolysis is how precisely to predict the yields of the process at different processing conditions for the development and optimisation of the process, to evaluate the kinetics of plastic decomposition. The simulation and control of the kinetics of complex mixtures are feasible in the identification of elemental reactions and intermediate and terminal species in terms of simplifying the reaction system to reduce the overall dimensions. Model simplification can directly link to the identification of key reactions and species that detailed characterise

reaction network and how it may be affected [18]. Therefore, thermochemical conversions (e.g. pyrolysis) is able to be described by using the modelling approach to mimic the complex reaction systems. Theoretically, the precise kinetic studies should take all the reactions into account that all components in the feedstock can go through, but, in reality, this is a difficult task due to the complex chemistry and to the lack of kinetic data [50]. Thus, modelling pyrolysis of plastic has been widely tested in the past decades, but there are still lots of work to do.

2.4.1 Reduction for reaction system

Reliability of models for a complex reaction system is important to predict the yields of desired and undesired products for different operating conditions and given ranges of feedstock; the design of the process and selection of the appropriate catalyst. However, detailed kinetics of a complex mixture of plastic pyrolysis often requires complicated computer work in model development to restrict their potential. There may exist large quantities of uncertain or unknown kinetic parameters in the complex models, which are not easy to be determined [18]. Ho [17] presented an overview of mathematical reduction methods involving simplification and consolidation of reaction networks. As mentioned in Chapter 1, QSSA, sensitivity analysis, time scale analysis, and PCA are main techniques, which are good tools or heuristic concepts for reduction of the reaction mechanism [17]. One must determine the region of their validity within composition space when using these simplification approaches. Overall, these mathematical techniques of dimension reduction (or order reduction) concentrate on transforming the original variables of complex reaction system into a new set of pseudo-variables with more regular properties, so they can be good solutions in describing the complex reaction system. A plastic pyrolysis reaction network can thus be algebraically expressed as a set of ordinary differential equations (ODEs):

$$\frac{dx}{dt} = \bar{\mathrm{f}}\left(x; \bar{k}\right), x(t_0) = x_0 \tag{2.11}$$

where x is the species concentration vector (dimension, n), $\bar{k}$ is the vector of reaction rate constants, and $\bar{f}$ is the vector of operation expressing the kinetics. These differential equations are useful in identification of relationships among the reactants and products in terms of the model order reduction approach [51]. The model order reduction is intended to transform the system of differential equations (2.11) into one of lower order while

retaining the key kinetic information. So the reduced system can be expressed as:

$$\frac{d\hat{x}}{dt} = \hat{\hat{f}}(\hat{x}; \hat{\hat{k}}) \,,\ \hat{x}(t_0) = \hat{x}_0 \tag{2.12}$$

where $\hat{x}$ is the species vector in the reduced model (dimension $\hat{n} < n$), and is referred to as a subset of the original species or groups of original species, $\hat{\hat{k}}$ is the vector of rate constants in the reduced system, and $\hat{\hat{f}}$ is the resulting kinetics vector. The neglected species may be combined with other pseudo-species, replaced by algebraic relations, or ignored completely. The question is how to select a reaction subset to demonstrate correctly the kinetic behaviour of the reaction system.

QSSA modelling approach is often used to eliminate the highly reactive intermediate species and remove large rate constants that cannot be determined from concentration measurements of reactants and products, producing reduced model on a slower timescale [52]. Thus, its application is limited for a complex reaction system so that the accuracy of the solution is reduced. Sensitivity analysis simplifies the model in terms of identifying the effect of the model parameters or variables so they can be lumped or removed from the model in processing. This method stresses on one important variable whilst simultaneously ignoring the variance effects of other variables, which may be difficult to estimate for large variable systems. Also the selected variable need to be replicated many times. A wide span of separation of time scales describes the process scale with time dependence, and each time scale is a small subset of the entire reaction time scale spectrum. On the other hand, kinetic model usually contains a wide range of different timescales. So it can impose limitations on the size of the modelled system, which usually requires massive parallel computations to determine the chosen time span [53], and it is feasible to simplify only compact models [18]. PCA technique emphasises only on the mean vector and the covariance matrix of the data. PCA is non-parametric and agnostic to the source of the data, which means any data set can be plugged in and an answer comes out, requiring no parameters to tweak and no regard for how the data was recorded [54].

Comparing above discussed methods, the lumping approach emphasises substituting a pseudo component for the real reactants and products, and reducing a complex reaction system to a finite dimension system conveniently actualised in the computer to avoid an

excessive number of chemical species. Moreover, a lumping approach favours a global variable during reaction network generation. It is well-developed technique having been extensively applied to attack a number of problems, often in diverse fields, exploiting the common methodology of system reduction. The system reduction for reaction system via lumping approach is well adapted to modelling the pyrolysis process behaviour of polymers.

2.4.2 Species lumping scheme and lump selection

As described previously, the study of kinetics for pyrolysis process involves a series of elemental reactions (steps) that a reaction occurs before reaching the final products. The mechanisms for those complex reactions in the system should be proposed during model development, and also the reaction steps present these chemical changes that take as well [55]. The complex species in the mixture imply that high dimension numerical description is necessary for a reaction system such as polymer pyrolysis [17]. The desired solution of model reduction scheme is to reduce initial high dimension reaction systems to lower dimension pseudo-systems with similar time scales by using a proper model reduction approach. The reaction kinetics can be estimated by developed models easily. With respect to this, the lumped kinetics of pyrolysis reaction network is to be assumed as following steps: (1) let $c_i(t)(i = 1, 2, \dots, N \gg 1)$ be the concentration of reactant i with rate constant k_i and $C(t) = \sum_i c_i$ be the total concentration of total reactant at residence time t; (2) calculation of lumped kinetics with a set of reactive functionalities, and (3) coupling of lumped kinetics by updating the total composition as the reaction proceeds [17, 56]. Nevertheless, some crucial issues have to be addressed in the lumping network description (1) to determine which species are to be lumped, (2) to classify how the selected species should contribute to the lumped species, i.e. define the lumping transformation; and (3) to clarify a proper solution in estimation of kinetic parameters for lumped species [57].

Determination of lump scheme for a complex mixture involves alternative of lump selection. The reaction rate is commonly applied to justify for the identification of *redundant* species. Reactions are eliminated that are much slower than the rate-determining important steps that generate important and necessary species. Important species of the model can be any species that is important for products of the reaction and other reasons. Necessary species can be defined as those that are required to simulate the

important features to the desired degree of accuracy in the model development. The elimination of reaction also means the elimination of species. Valorani et al (2006) firstly defined important species and check in which modes they are present in the identification of redundant species using computational singular perturbation method based on the original design by Lam and Goussis[58] for the analysis of spatially homogeneous stiff systems with timescales separated by a substantial gap, offering a significant advantage in the automatic nature of the reduction strategy). Reaction steps are then identified that have a significant contribution to those modes. The reaction steps considered as necessary species, which is continuously increased using an iterative procedure until at the end of the process no more important reactions found.

2.4.3 Power law modelling

Power law modelling is popularly used for describing thermal chemical conversion by evaluating the overall rate of weight loss in thermal decomposition. The results derived correspond almost exactly to the data from TGA and differential thermogravimetric (DTG), where model equations are used to deconvolute the peaks in thermograms linking to the rate of mass loss with respect to the time or temperature [59, 60]. A first-order reaction can be, simply, introduced for describing pyrolysis process as:

$$\frac{dx}{dt} = kf(x') \tag{2.13}$$

where $f(x')$ links to the mass concentration of the reactant, k is the rate constant. To model the solution of the kinetic pyrolysis reaction, rate constant k is determined by Arrhenius law

$$k(T) = A_0 exp(\frac{-E_a}{RT}) \tag{2.14}$$

where E_a is the apparent activation energy of reaction, A_0 is the apparent pre-exponential factor, R is gas constant, and T is reaction temperature.

In isothermal condition, the reaction rate is the same as the rate of mass change of the sample, and can be expressed as a time-dependent function as:

$$\frac{dx'}{dt} = A_0 \exp\left(-\frac{E_a}{RT}\right)(1 - x') \tag{2.15}$$

The normalised mass fraction x' from decomposed sample mass obtained as:

$$x' = \frac{m_0 - m_t}{m_0 - m_\infty} \tag{2.16}$$

where $m_0, m_\infty,$ and m mean the initial sample mass, the final residual mass after pyrolysis, and the actual mass at any time t during the run.

In non-isothermal condition, the mass change function is expressed with the dependence of temperature change ratio ($\beta = \frac{dT}{dt}$) as:

$$\frac{dx'}{dT} = \frac{dx'}{dt}\frac{dt}{dT} = \frac{A_0}{\beta}\exp\left(-\frac{E_a}{RT}\right)(1 - x') \tag{2.17}$$

The power law modelling method is easy to implement by means of computation and is widely employed to determine the kinetic parameters [7, 50, 61, 62]. However, the kinetic parameters obtained from the power law model represents an apparent (measured) rather than intrinsic (bond scission) value because of the activation energy and pre-exponential factors though validated from the TGA and DTG run, are not able to describe all the phenomena observed in the experiments. The kinetic parameters could be significantly different, even if same polymer and obtained from different experimental works. The apparent pre-exponential factor spans several orders of magnitude whilst resulting that activation energy spans $\pm$50kJ/mol [62]. This may lead to a higher error of estimated kinetic parameters, even though this difference could be partially linked to either additives or weak bonds in the original polymers [63]. Also, iso-conversion pyrolysis is very sensitive in detecting pyrolysis kinetics of complex reactions, while the introduction of approximately mathematical assumptions with the extent of conversion might cause systematic errors in the value of activation energy [64]. Therefore, this model cannot clearly show a detailed kinetics for degradation process.

2.4.4 Single step model

Single step lumping models (Figure 2-3) deal the pyrolysis process using a one-step first order reaction. This model treats all decomposition products as one volatile lump and solid residue phase as another lump. Single step lumping model is suitable for predicting the pyrolysis characteristic of plastic waste in terms of TGA and DTG, where model equations are used to deconvolute the peaks in thermograms linking to the rate of mass

loss with respect to the time or temperature [59, 60]. This model has been used to describe the pyrolysis behaviour of plastics.

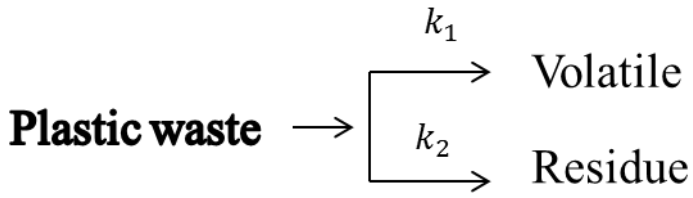

Figure 2-3 Schematic of single step lumping model of plastic waste pyrolysis

Abouklas et al [7]studied the pyrolysis kinetics of HDPE, LDPE, PP and PS during the thermal degradation via a single step global model. Yang et al [65] applied a single step lumping model to determine the kinetic parameters of thermal decomposition of polymers. Park et al [43] used a single reaction model in a study on the pyrolysis characteristics of the refused plastic fuel. However, the single step global lumping model does not represent the whole mechanism of pyrolysis process but only overall kinetic parameters instead [66], and is limited by the assumption of a fixed mass between the pyrolysis products (e.g. volatiles) which prevents the forecasting of product yields based on process conditions [67, 68]. Therefore, this model needs to be coupled with other models or analytical equipment such as gas chromatography and /or mass spectrometry.

2.4.5 Two steps model

The two steps lumping model (Figure 2-4) extends the single step lumping model to two distinct steps, with each step corresponding to two parallel reactions and is suitable for establishing the pyrolysis behaviour of two-step weight loss behaviours (e.g. PVC) and further cracking reactions in decomposing reaction system.

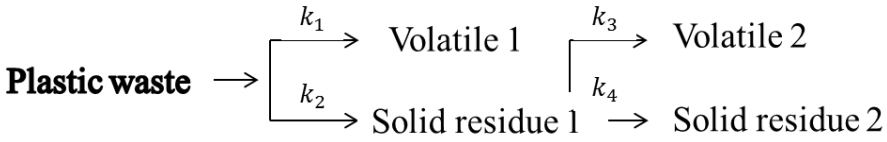

Figure 2-4 Schematic of a two steps lumping model

The two steps lumping model was employed by Mehl *et al* [69] to investigate the kinetic modelling of the thermal degradation of halogenated polymers - the first step of which corresponds to dehydrochlorination/condensation and the second to hydrocarbon

decomposition and residue char formation. While this model is still based on the prediction of overall volatile yields.

2.4.6 Primary pyrolysis model

The primary pyrolysis lumping model (Figure 2-5), also called the competing reaction model of the pyrolysis of plastic waste, applies a discrete lumping methodology to group decomposition components in three lumps formed by the gas phase, the liquid (oil) phase and the solid phase (char residue) resulting from the pyrolysis of waste. While this model has some drawback accurately to predict the product distribution [66, 68, 70]. Nevertheless, a four-lump model can be developed by specific research (e.g., wax lumped in PE pyrolysis). This technique is suitable for correlating and evaluating kinetic data from different types of plastic waste under similar operational conditions with less experimental data; however, it may not be proper for comparisons of thermal degradation data obtained from dissimilar reaction conditions [71]. This model classifies secondary reactions lumped with primary reactions within a narrow temperature range in terms of three competitive reactions, which may result in limitations in the determination of the kinetic parameters of primary reactions [72].

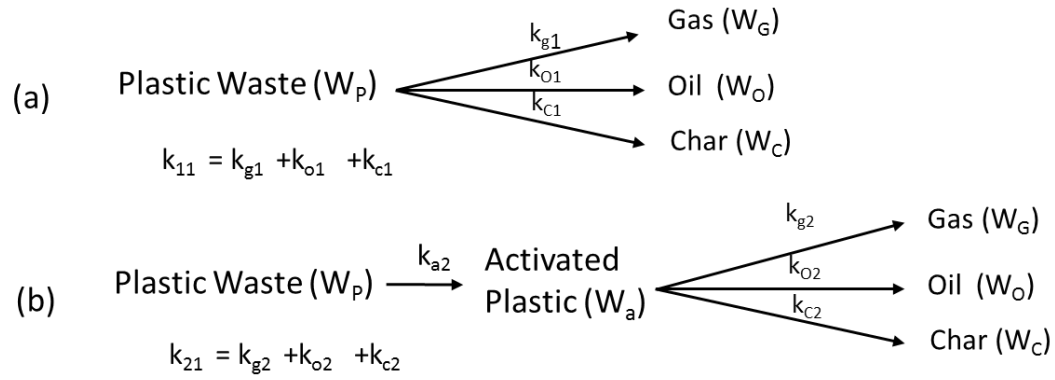

Figure 2-5 Schematic of primary lumping model of plastic waste pyrolysis

The primary pyrolysis lumping model is an empirical one and simply simulates the three phases of product from experimental data; the kinetic parameters obtained from the model may not represent the full pyrolysis characteristics of the plastic waste. Hence, the primary lumping model is rarely found in the literature since lumping models which comprise of primary and secondary cracking reactions were developed [73]. Moreover, the solid residue consists of unreacted plastic waste and char-like product, which is difficult to determine in the residue. For example, Koo and Kim [70] used the primary

model to for investigating the reaction kinetics of various input mixing ratios of plastic waste. They introduced an intermediate lump to mimic the volatile lump in several possible pathways (Figure 2-5), and reported that rate constants are affected by the mixing ratio exponentially, and plastic pyrolysis is controlled by both primary and secondary reactions in different extended competing models.

2.4.7 Primary lumping model with secondary tar cracking

A rigorous kinetic treatment of pyrolysis data must account for the formation rates of all the individual product components [68, 74]. Early models were insufficient to describe the kinetic behaviour of plastic pyrolysis, which has required modelling development to insert secondary cracking reactions, which affect the species distribution in the decomposition reaction system coupling with primary pyrolysis reaction [8, 75-78]. Westerhout et al [79] proposed a pioneering model (Figure 2-6) of the PE and PP pyrolysis in which the primary degradation mainly generates intermediate wax-like products that further crack into lighter hydrocarbon fractions in a secondary reaction. Elordi et al [75] presented some possible pathways (Figure 2-7) of primary pyrolysis coupling with secondary cracking reactions based on the Westerhout et al' model [80], and observed that Westerhout's model did not adequately predict the experimental results, especially primary products.

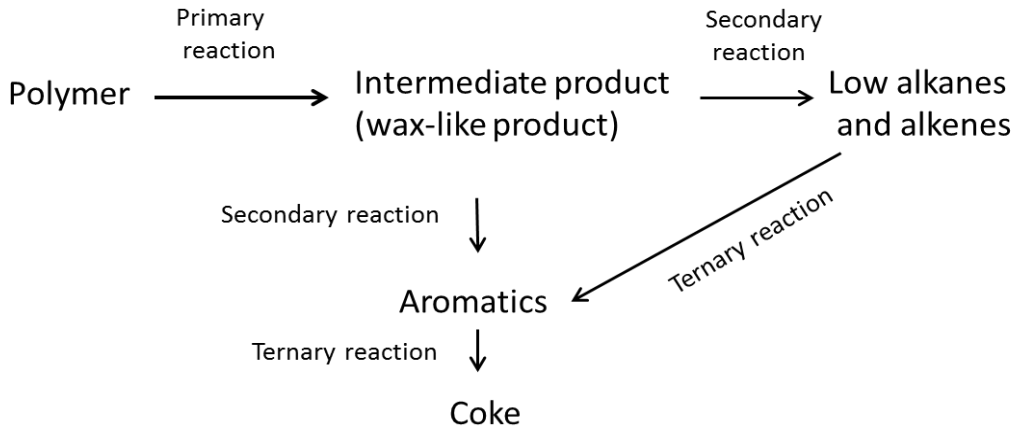

Figure 2-6 Reaction schemes of polymer pyrolysis

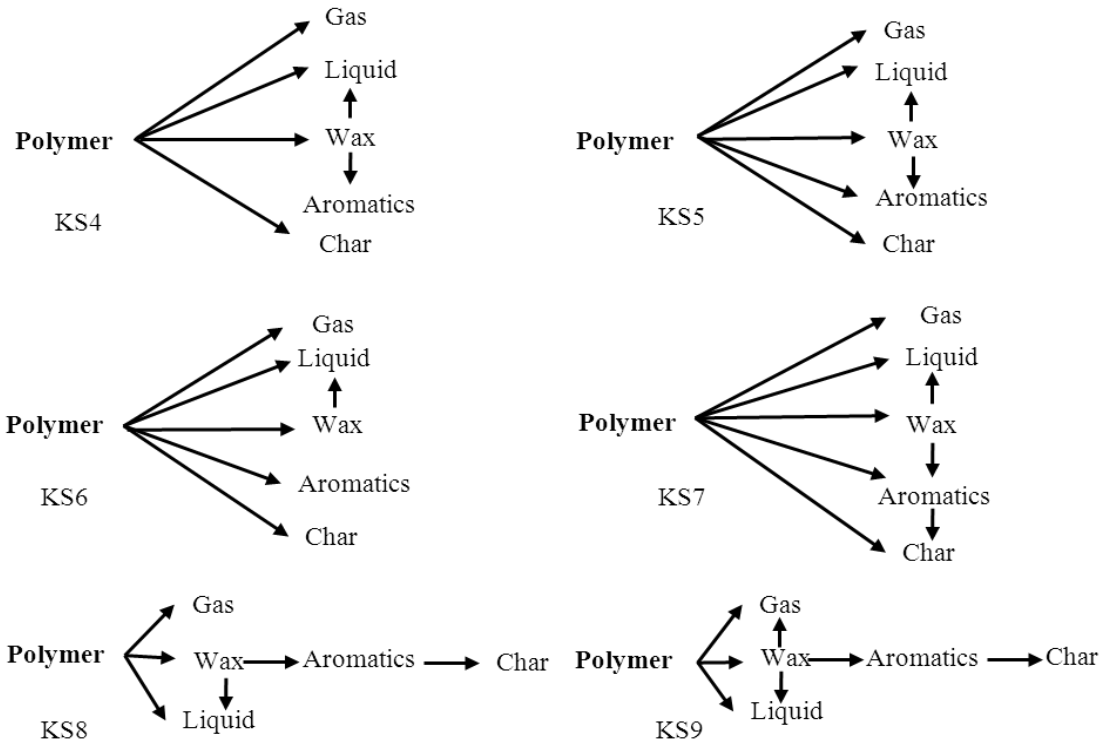

Figure 2-7 Schematic of primary pyrolysis and secondary reaction of polymer [75]

They proposed some possible reaction route schemes, which show potential primary pyrolysis route (lumped as gas, wax, liquid, and char) and secondary cracking reactions from wax, further lumped as wax gas, wax oil, wax aromatics and wax char. Al-Salem and Lettieri [8] studied the KS7 model from Elordi's model design, reported the thermal degradation behaviour of HDPE and determined the kinetic rate constant and overall activation energy.

Ding et al [42] developed a four lumped model (Figure 2-8) with the secondary reaction between light fraction, middle distillates and a heavy fraction, which resulted in a good agreement between model and experiment data obtained at a lower temperature. They did not observe the char from the reaction due to a lower reaction temperature range of 380-420℃.

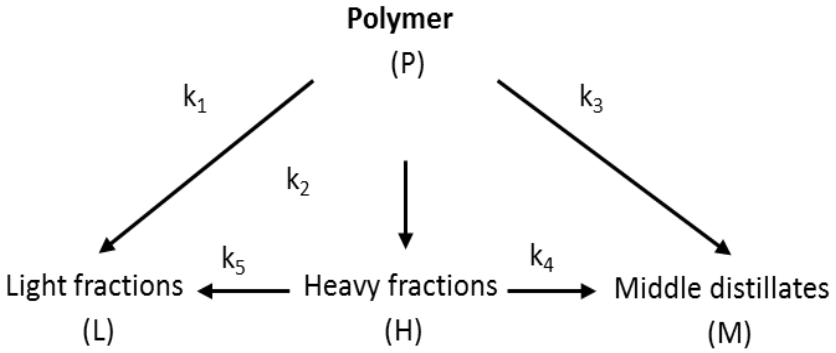

Figure 2-8 Reaction mechanism of the pyrolysis of plastic mixtures

Ramdoss and Terr et al [76] studied the kinetics of a higher temperature range (475-525℃) liquefaction of commingled postconsumer plastic using the lumping model (Figure 2-9) consisting of parallel and competing reactions, where P, H, L, G and C represents the mass fraction of un-reacted plastic sample, heavy oil, light oil, gas and coke, respectively. Further cracking from heavy oil and light oil into gas and coke was proposed. Johannes et al [81] simplified the scheme of the pathway to assume two steps PE pyrolysis behaviour of plastic destruction and oil cracking (Figure 2-10). A similar model (Figure 2-11) involving primary pyrolysis and secondary cracking via different routes was developed by Costa et al [82] to study the kinetic of pyrolysis of PE, PS and PP. They proposed different reaction pathways at different reaction temperatures.

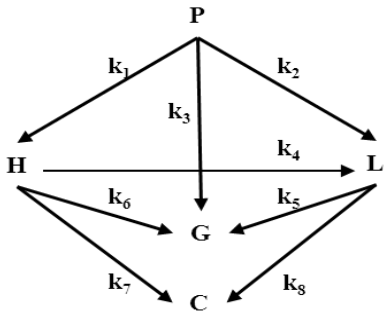

Figure 2-9 Reaction pathway of plastic liquefaction

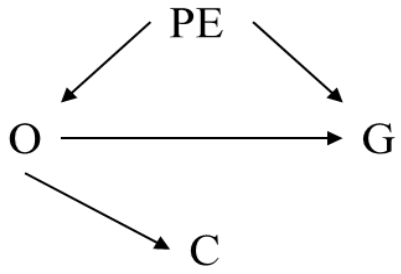

Figure 2-10 Simplified scheme of PE pyrolysis

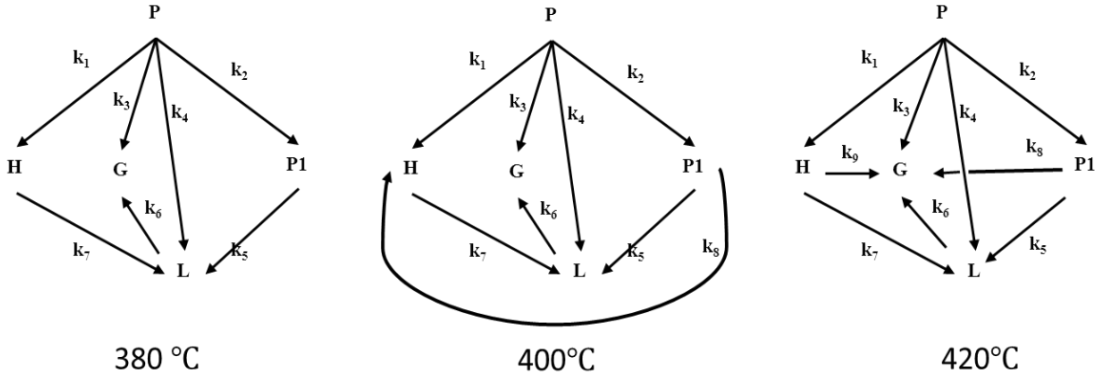

Figure 2-11 Reaction pathway of the pyrolysis of PE, PP and PS at temperature ranges of 380℃, 400℃ and 420℃ (P, plastic mixture; P1, solid lower molecular weight polymer; G, Gas; L, light liquid fraction; H, heavy liquid fraction).

Csukas et al [78] proposed a scaled-up primary lumping model with secondary reaction and simplified in four steps (Figure 2-12), found that middle complexity is a good compromise between the sophisticated detailed kinetic models and the experimentally established heuristic knowledge. Besides that, the model is in good agreement with the experimental data for the yields of the product fractions, and for the composition of the fractions, where real1, real2, real3 and real4 are four steps. *Pol*, ***G***, *GO, GP, Liq, MF, MO, MP, MA*, ***N***, *NO, NP, NA, Wax, Aro, H, HC and HO* means polymer, gas, gas olefins, gas paraffin, liquid, middle (gas oil) fraction, middle (olefins, paraffin and aromatics), naphtha, naphtha (olefins, paraffin, aromatics). Nevertheless, this model is not easy to validate by using proper experimental data.

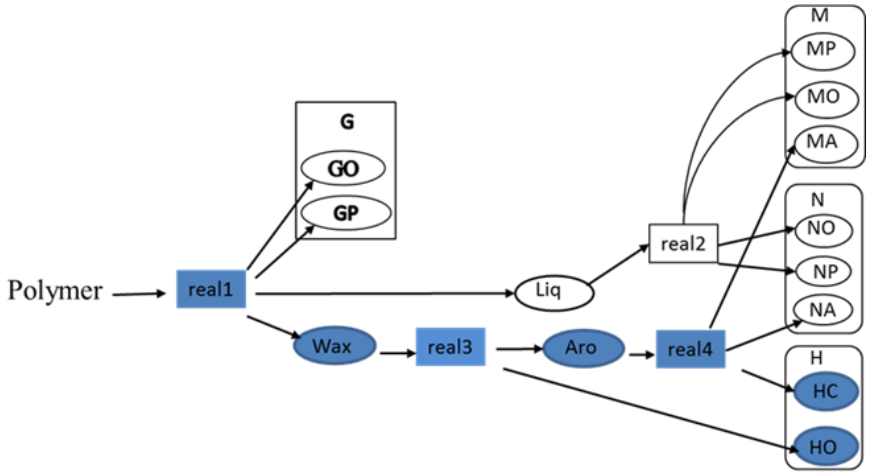

Figure 2-12 Illustration of the simplified kinetic model [78]

Additionally, primary lumping models with secondary reaction are widely used in analysing catalytic pyrolysis of plastic waste. Lin et al [83] applied the lumping model (Figure 2-13) to investigate the pyrolysis of post-consumer plastic waste (HDPE/LDPE/PP/PVC) mixture over cracking catalysts. They proposed a mechanistic scheme including the main features and kinetic reaction schemes for polymer degradation over cracking catalyst, carbenium ion in catalytic cracking chemistry was discussed. They considered lumping criteria based on the nature of chemical bonds instead of molecular weight to group the products as paraffins, olefins and aromatics.

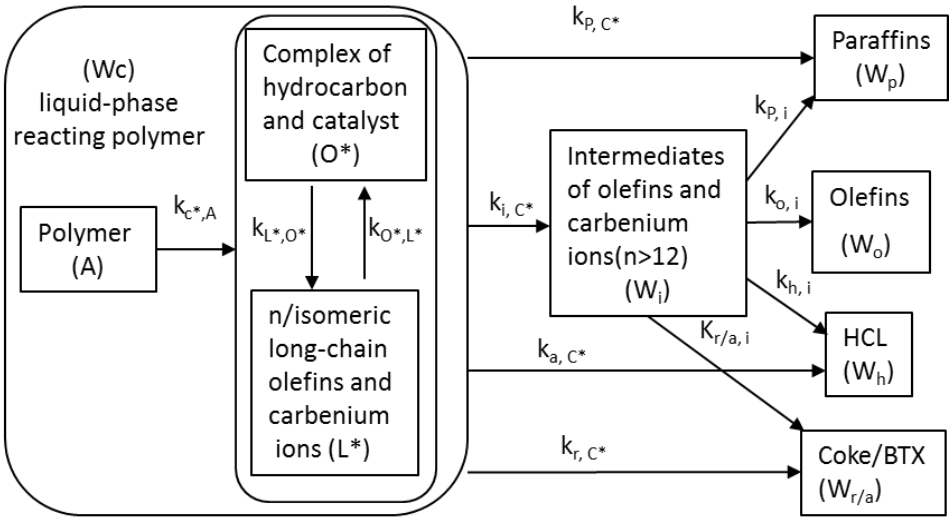

Figure 2-13 Kinetic and mechanistic reaction schemes for the mixture of PE/PP/PS/PVC plastic waste degraded over cracking catalyst

Aguado et al [20] commented that the selection of the lumping criterion that best represents the multiple cracking reactions the polymer undergoes is a key factor for examining the kinetics of polymer pyrolysis. They introduced principle component analysis as a technique to determine the selection of the criterion for the lumping scheme. They analysed the formation rate of polyolefins thermal pyrolysis products by using PCA, and proposed a kinetic scheme of thermal pyrolysis of HDPE (Figure 2-14) at a temperature range of 550-650℃.

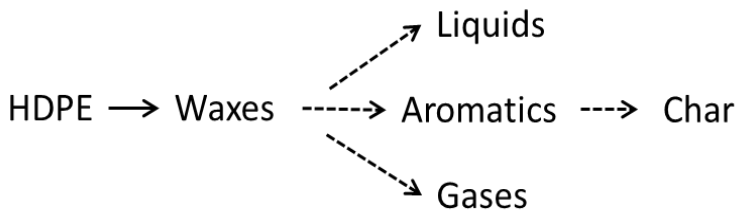

Figure 2-14 Kinetic scheme proposed for thermal pyrolysis of HDPE

2.4.8 Other model development

There are quite a few other models developed to study the decomposition characteristics of plastic, such as population balance equation, response model, and direct computer mapping model.

Population balance equation (PBE) model is based on the moment method for both "dead" and "live" polymer chains and a pseudo-steady-state hypothesis to describe the polymeric chain changes of polymer decomposition at a mechanistic level. This approach has been developed by many researchers [69, 84-89] to model the molecular weight change and small molecule evolution simultaneously. The decomposition reactions are described by the changes in chain length (typically chain-end scission, random scission), and disintegrating the explicit chain length dependence. The method of moments uses differential equations for the moments of the distribution of the mixture, which are applied to solve the molecular weight distribution as a function of time.

Kruse *et al* [90] proposed a detailed mechanistic model to predict the characteristic of PS degradation, applying the moment method to develop differential equations describing the pyrolysis kinetics based on McCoy and his co-workers' theory. They described that the terms of moment equations were derived from the following reactions: the first three terms of moments of each species, representing the birth of the particle size as a result of

the coagulation of particle size, were used to solve the associated large set of population balance equations, which reduce the computational load and stiffness of the problems; second term describes the merging of particle size with any other particles (called dead terms); then the PS degradation model can be described as:

1. Random chain fission / radical recombination

$$D_m \overset{k_f, k_c}{\longleftrightarrow} Re_i + Re_{n-j} \tag{2.18}$$

$$\frac{dD^m}{dt} = -k_f\left(2D^{m+1} - e_f D^m\right) + \frac{1}{2}k_c \sum_{j=0}^{m}\binom{m}{j} Re^j Re^{m-j} \tag{2.19}$$

$$\binom{m}{j} = \frac{m!}{j!(m-f)!} \tag{2.20}$$

$$D^3 = \frac{2D^2 D^2}{D^1} - \frac{D^2 D^1}{D^0} \tag{2.21}$$

$$\frac{dRe^m}{dt} = -2k_f C_m\left(2D^{m+1} - e_f D^m\right) - k_c Re^m Re^0 \tag{2.22}$$

$$C_m = \frac{1}{m+1} \tag{2-23}$$

2. Specific chain fission/ radical recombination

$$D_m \overset{k_{fs}, k_{cs}}{\longleftrightarrow} Re_{n-s} + r_s \tag{2.24}$$

$$\frac{dD^m}{dt} = -k_{fs} D^m + k_c \sum_{j=0}^{m}\binom{m}{j} Re^{m-j}(s)^j\,[r_s] \tag{2.25}$$

$$\frac{dRe^m}{dt} = k_{fs}\sum_{j=0}^{m}\binom{m}{j}(-s)^j (D)^{m-j} - k_c Re[r_s] \tag{2.26}$$

$$Re_n + D_i \underset{k_{tr,m}}{\overset{k_{tr,e}}{\rightleftharpoons}} D_n + Rm_j \tag{2.27}$$

$$\frac{d[r_s]}{dt} = k_{fs} D^0 - k_c Re^0 [r_s] \tag{2.28}$$

3. Hydrogen abstraction

$$Re_n + D_i \underset{k_{tr,m}}{\overset{k_{tr,e}}{\rightleftharpoons}} D_n + Rm_j \tag{2.29}$$

$$\frac{dD^m}{dt} = -N_H^m k_{tr,e} Re^0 (D^{m+1} - e_t D^m) + N_H^m k_{tr,e} Re^m \tag{2.30}$$

$$(D^1 - e_t D^0) + N_H^e k_{tr,m} Rm^m D^0 - N_H^e k_{tr,m} Rm^0 D^m \tag{2.31}$$

$$\frac{dRe^m}{dt} = -N_H^m k_{tr,e} Re^m (D^1 - e_t D^0) + N_H^e k_{tr,m} Rm^0 D^m \tag{2.32}$$

$$\frac{dRm^m}{dt} = -N_H^m k_{tr,e} Re^0 (D^{m+1} - e_t D^m) - N_H^e k_{tr,m} Rm^m D^0 \tag{2.33}$$

4. β-scission/ radical addition

$$Rm_n \underset{k_{ra}}{\overset{k_{bs}}{\leftrightarrows}} Re_j + D_{n\text{-}j} \tag{2.34}$$

$$\frac{dRm^m}{dt} = -2k_{bs}Rm^m + k_{ra}\sum_{j=0}^{m}\binom{m}{j}Re^j D^{m-j} \tag{2.35}$$

$$\frac{dRe^m}{dt} = 2k_{bs}C_m Rm^m - k_{ra}Re^m D^0 \tag{2.36}$$

$$\frac{dD^m}{dt} = 2k_{bs}C_m Rm^m - k_{ra}Re^0 D^m \tag{2.37}$$

5. Depropagation /propagation

$$Re_n \underset{k_p}{\overset{k_{dp}}{\leftrightarrows}} Re + M \tag{2.38}$$

$$\frac{dRe^m}{dt} = -k_{dp}Re^m + k_p\sum_{j=0}^{m}\binom{m}{j}Re^{m-j}[M] + k_{dp}\sum_{j=0}^{m}\binom{m}{j}(-1)^j Re^{m-j} - k_p Re^m[M] \tag{2.39}$$

$$\frac{d[M[}{dt} = k_{dp}Re^0 - k_p Re^0[M] \tag{2.40}$$

6. Backbiting, which describes intramolecular termination resulting in the formation of cyclic oligomers

$$Re_n \underset{k_{bbr}}{\overset{k_{bdr}}{\leftrightarrows}} Rm_n \tag{2.41}$$

$$\frac{dRe^m}{dt} = -k_{bbf}Re^m + k_{bbr}Rm^m \tag{2.42}$$

$$\frac{dRm^m}{dt} = k_{bbf}Re^m - k_{bbr}Rm^m \tag{2.43}$$

7. Specific β-scission/ radical addition

$$Rm_n \underset{k_{ra}}{\overset{k_{bs}}{\leftrightarrows}} Re_{n\text{-}s} + d_s \tag{2.44}$$

$$\frac{dRm^m}{dt} = -k_{bs}Rm^m + k_{ra}\sum_{j=0}^{m}\binom{m}{j}Re^{m-j}(s)^j[d_s] \tag{2.45}$$

$$\frac{dRe^m}{dt} = k_{bs}\sum_{j=0}^{m}\binom{m}{j}(-s)^j Rm^{m-j} - k_{ra}Re^m[d_s] \tag{2.46}$$

$$\frac{d[d_s]}{dt} = k_{bs}Rm^0 - k_{ra}Re^0[d_s] \tag{2.47}$$

8. Disproportionation

$$\mathrm{R}e_n + Re_i \overset{k_d}{\rightarrow} D_n + D_i \tag{2.48}$$

$$\frac{dD^m}{dt} = k_d Re^m Re^0 + k_d Re^0 Re^m \tag{2.49}$$

$$\frac{dRe^m}{dt} = -k_d Re^m Re^0 - k_d Re^0 Re^m \tag{2.50}$$

where $D, R_e, R_m, C_m, M, e_f,$ and e_t mean the dead chain polymer, the end chain radicals, the mid-chain radicals, the number of monomer, monomer, the number of bonds along a polymer chain that are excluded from this general chain fission reaction, and the number of monomer units along a polymer chain that do not undergo this general mid-chain hydrogen abstraction reaction.

Faravelli et al [40] applied the PBE model – radical chain process to study the pyrolysis kinetics of PS and PE mixture with a completely segregated and also with a completely mixed model (Figure 2-15).

$$\frac{dS_n}{dt} = -a_d K_p[R]S_n + -a_e K_p[R]\sum_{i=n+a_f}^{\infty} S_i \tag{2.51}$$

$$\frac{d[R_{PE}]}{dt} = 2k_{sPE}\text{-}2k_{tPE}[R_{PE}[^2 - k_{t\ mix}[R_{PE}][R_{PS}]=0 \tag{2.52}$$

$$\frac{d[R_{PS}]}{dt} = 2k_{sPS}\text{-}2k_{tPS}[R_{PS}[^2 - k_{t\ mix}[R_{PE}][R_{PS}]=0 \tag{2.53}$$

Marongiu et al [30] applied the PBE model combining discrete approach, moments model and QSSA model describing the statistical distribution and evolution of all the species with/without QSSA for a global propagating radical and evolution of polymer and dead species.

Westerhout et al [62] introduced a **random chain dissociation model (RCD)** based on Wagenaar's work [91] to account for the fact that both physical and chemical processes occur during the pyrolysis of polymers. The polymer chain is represented as a chain of carbon atoms with side chains (Figure 2-16). Rate constant k_i is associated with the number of each bond type *i* between the carbon atoms, expressed by N_i. Then the change rate of the number of each bond type was written as:

$$\frac{\partial N_i}{\partial t} = -k_{0i}\exp\left(\frac{-E_a}{RT}\right)N_i = -k_i N_{\ i} \tag{2.54}$$

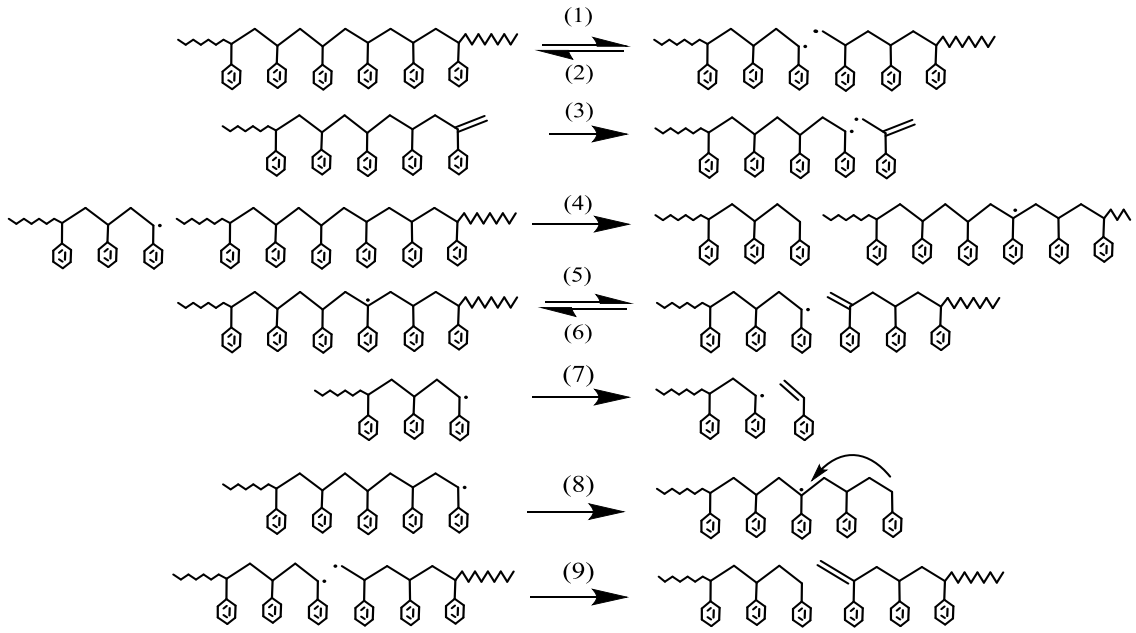

Figure 2-15 Polystyrene pyrolysis reaction incorporated in model (Reaction types are numbered in preceding text)

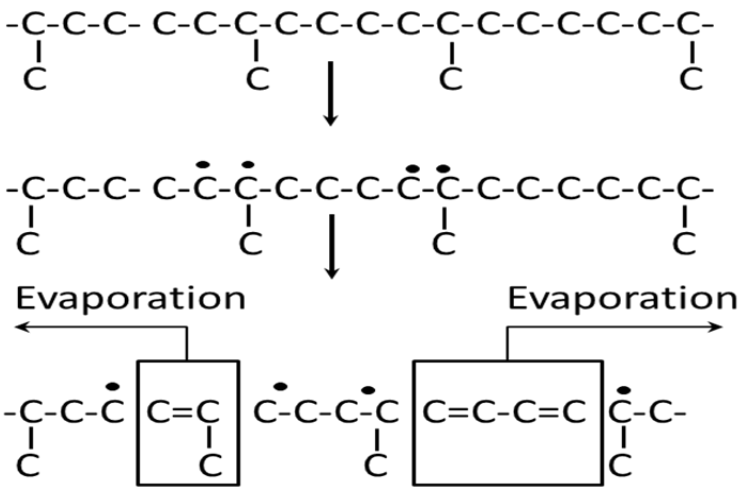

Figure 2-16 Schematic representation of process incorporated in the RCD model

Response model was developed by Wang and Frenklach [92]. They proposed that the responses are species concentrations and the model variables are the initial boundary conditions of the reacting mixture and the model parameters, such as rate constant. The solution mapping method provides a general procedure to solve model response. In this method, model responses are expressed as simple algebraic functions (usually differential polynomials) in terms of model variables. These algebraic functions are obtained by using either computer simulations or experimental data. For global solution techniques,

response modelling solutions are problem specific since they require data to build the algebraic functions [93].

Direct computer mapping model was developed by Csukas and his co-workers [78, 94]. This model is based on a generation of executable multiscale hybrid-process-frameworks to simulate the plastic waste pyrolysis. The process model produces a given set of building and connecting blocks of an elementary process, while the natural building blocks of the states, actions, and connections are mapped onto the elements of an executable code (Figure 2-17). The pyrolysis experiments were identified by a macro-granularly parallel architecture, in a cluster of 16 computers. Every identification process was built up from at least 100 generations, containing populations of 32 variants, with altogether 3200 simulations. To overcome the temperature constraint in the pyrolysis kinetic model, the incorporation of heat and mass transfer may provide combined kinetic models to describe the actual temperature of the plastics during pyrolysis [95]. Faravelli and his co-workers [96] introduced an in-depth mass transfer through bubble formation models to examine the degradation progress for a small-sized polyethylene sample; the results agreed well with the experimental evidence.

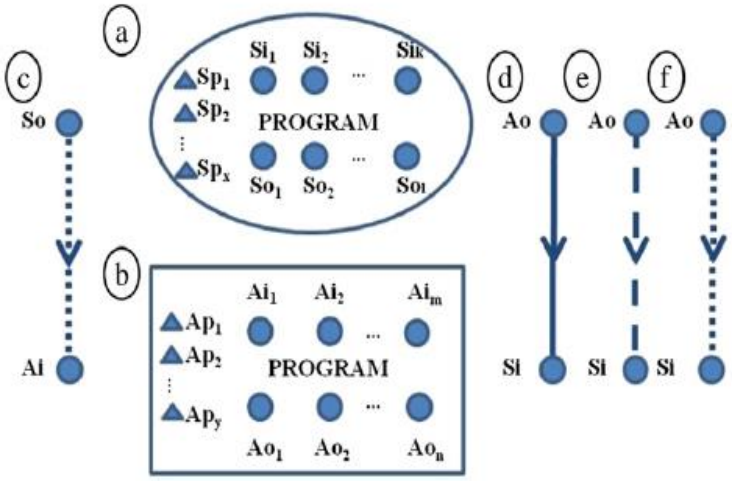

Figure 2-17 Common building elements and connections of process models [78]

2.4.9 Model selection

Overall, there were many models developed to examine the kinetic behaviour of the pyrolysis of plastic waste. For instance, the PBE is a kind of transport equations for the number density function of the particles, which depends on time, spatial location and the internal coordinates. The mathematical form of a typical PBE involves spatial transport

(e.g. convection and diffusion), derivative source terms for continuous particle size change (e.g. oxidation/dissolution and surface growth), integral terms (e.g. aggregation and breakage), and Dirac-delta-function source terms describing the formation of particles [97]. The accuracy description of population balance model using moment method could be impacted once the particle size distribution is very large due to the complexity in proper identification of system and the transition rates of reactions. RCD model is relatively higher computer load during the simulations. Response model needs more data to build model functions.

The application of lumping approach for plastic pyrolysis reactions was assumed as a series of parallel first-order irreversible reactions with a few variables. The lumping model results are often correlated with experiment data, and able to provide reasonable information of plastic pyrolysis process. However, the lumping kinetics of plastic pyrolysis is not well understood in the determination of lumping scheme, the correlation between model results and experiment results, and the existence of different composition of the same range of physical property. Especially, composition of fractioned products, prediction of light components, and their products property in the primary reaction and secondary reaction is not well developed via the mathematical model.

Table 2.3 Kinetic parameters of different models collected in the literature

Author	Reaction scheme	Sample	Kinetic model	Kinetic parameters	
				Ea (kJ/mol)	A_0 (s^{-1})
Aboulkas et al [98]	Single step lumping model	HDPE/LDPE/ PP/PS	$\ln\beta = \ln\frac{AE_a}{Rg(x)} - 5.331 - 1.052\frac{E_a}{RT}$	243, 221, 183 and 169	/
Aboulkas[7]	Power law modelling	HDPE	KAS: $\frac{dx}{f(x)} = \frac{A}{\beta}\exp(\frac{-E_a}{RT})dT$ Coats- Redfern: $\ln\frac{\beta}{T^2} = \ln\frac{AR}{E_a g(x)} - \frac{E_a}{RT}$ Flynn-Wall-Ozawa: $\ln\beta = \ln\frac{AE_a}{Rg(x)} - 5.331 - 1.052\frac{E_a}{RT}$	238±11,247±5, 243±11	/
Westerhout et al [62]	Power law modelling	HDPE		220	1.9×10^{13}
		LDPE1/LDPE2		241	1.0×10^{15}
		PP1/PP2	$\frac{\partial N_i}{\partial t} = -k_{0i}\exp\left(\frac{-E_a}{RT}\right)N_i = -k_i N_i$	201 244 188	9.8×10^{11} 3.2×10^{15} 2.2×10^{11}
		PS		204	3.3×10^{13}
Miskolczi et al [99]	Single step lumping model	LDPE	$ln(1-c) = kt$	372	/

Yang et al [100]	Single step lumping model	HDPE	$\ln({}^{dC}/_{dt}) = \ln A - \frac{E}{R}({}^{1}/_{T}) + Const$	240-265	/
Saha and Ghoshal [101]	Single step lumping model	PET	$\ln \beta \frac{dx}{dt} = \ln k_0 - \frac{E_a}{RT} + n \ln(1-x)$	322-339	/
Park et al [43]	Single step lumping model	HDPE	$\ln \beta = \ln \frac{AE_a}{Rg(x)} - 5.331 - 1.052 \frac{E_a}{RT}$	211.11	9.04×10^{13}
Park et al [43]	Parallel lumping model	PS/PP/ LDPE /PVC-1/PVC-2	$\ln \frac{\beta}{T_{p,i}^2} = \ln \frac{A_{0,i}R}{E_{a,i}} - \frac{E_{a,i}}{RT_{p,i}}$	231.83/193.55/175.92/72.26/ 164.94	2.27×10^{17} /4.49×10^{13} /7.09×10^{11}/1.24×10^{06}/2.1×10^{11}
Elordi [102]	Primary and secondary reaction model	HDPE	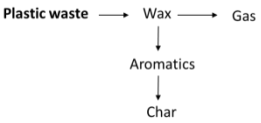	712/137/84.3/411/392/382	9.77×10^{2} /7.31×10^{6} /1.3×10^{3} /4.72×10^{22}/2.39×10^{21}/ 2.01×10^{20}
Al-Salem and Lettieri [8]	Primary and secondary reaction model	HDPE	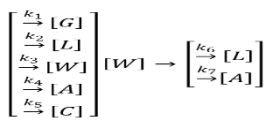	Wax/char/liquid/gas/aromatics=26.7/44.1/124.1/98.9/382.0	14.7/1.7/2.9/57.6/33.1
Ding et al [42]	Primary and secondary reaction model	HDPE/LDPE/ PP	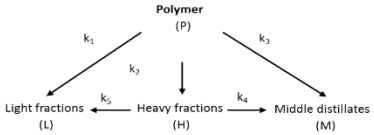	217.6/178.49	3.31×10^{15}/4.05×10^{12}

Ramdoss et al [76]	Primary and secondary reaction model	PE/PP	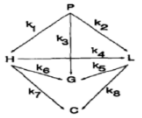	62.9/34.7/86.3/11.8/121.7/113.5/42.6/81.1	4612/30/70792/04/4.8 × 10^6 /3.5 × 10^5/1.0× 10^4/1800
	Scission of polymer chain(Population balance model)		$P(x) \xrightarrow{k_s} P(x - x_s) + P^s(x_s)$	233.2, 127.7, 193.9 and 177.8	1.79E+15, 6.35E+07, 2.86E+12 and 2.01E+11
	Global single lumping model			277.7, 172.5, 234.2 and 215.2	4.66E+18, 1.30E+11, 3.05E+15 and 1.35E+14

Based on this point, primary discrete lumping model coupling with the secondary reaction of heavier fractions is selected to study the kinetics of thermal degradation of plastic waste in this project, because this model can sufficiently describe the kinetic behaviour of plastic pyrolysis, and is widely used by many researchers in the past decades. Table 2.3 shows a brief summary of lumping application in the pyrolysis of plastic waste.

2.5 Lumping methodology

2.5.1 Lumping approach

The lumping approach seeks to transform the original variable dimensions to a lower dimensional vector based on the physical properties or on the reactivity of compounds.

$$\hat{x} = \mathrm{h(x)} \tag{2.55}$$

For a given reaction mixture as described in Eq. (2.55), it reduces an infinite complex reaction system to a finite dimension system (i.e. described in a discrete way) of dimensions N through a lower order system of dimensions $\widehat{N}$ ($N < \widehat{N}$) which can be conveniently actualised in the computer. As mentioned previously, lumping favours a global variable, which can present the characteristics of the entire variable groups in the mixture. The kinetics of global reaction system will be approximately determined in terms of fewer parameters from the defined pseudo-species (lumps), which indicate an advantage than moment method. Ocone [103] noted that the overall description of complex reactive systems can be attempted both in **discrete and continuous** descriptions of some gross overall properties such as the total concentration of all species of a certain type. Discrete description for reaction process will be reviewed at the later section.

Top-down and bottom-up approaches are commonly used methods for the lumping simplification [104]. The top-down approach involves a number of preselected, measurable kinetic lumps and determines the best reaction network and kinetics through experimental design and parameter estimation. The lumps, satisfying the conservation law and stoichiometric constraints, are usually selected based on the known chemistry, measurability, and physicochemical properties (e.g. carbon number and boiling range). This kind of kinetic models via the top-down route may have limited extrapolative power as the rate constant

relies on the feedstock, reactor hardware configuration, catalyst, and lack sufficient molecular information to predict subtle changes in product qualities and properties.

Bottom-up approaches can rectify the shortcomings of the top-down, and start by examining the kinetic reaction at the individual molecular level, then conveniently track the molecular transformation by matrix operation by computation and lump, based on a finite number of reaction families. For instance, reaction families in hydrocracking include hydrogenation, ring opening, dealkylation, hydrodenitrogenation, isomerisation, and cracking.

2.5.2 Discrete lumping

In the discrete description of a mixture, the components in a complex mixture can be described individually based on their reactivity [18]. The kinetics of a complex reaction system can be developed in the following three basic steps: a) the mixture is portioned in discrete numbers of "lumps", b) "pseudo-components" are identified, and c) the reactions among them are described [103]. This is in general obtained by grouping components (and/or other quantities such as species) and substituting pseudo-components (or pseudo-species) (e.g. isomers) to each group. Each pseudo-component will then represent the original group. A lumped pseudo-component is considered as components with similar molecular weights or true boiling points. The conversion of heavier lumps to lighter lumps is considered in terms of series and parallel reactions. Thus, the kinetics of the original reaction system can be described with lower dimensions in terms of the lumped reaction models. These kinetically consistent theories for lumping a large number of reactions in the mixture have long been the subject of many investigations (Wei and Kuo [105]; Weekman [106]; Okino et al [18], Csukás et al [78]; McCoy et al [86, 107, 108]; Ho et al [17]). Wei and Prater [109] were the first to introduce "lumping" to describe the chemical linear behaviours, and established the mathematical lumping methodology for linear systems. They proposed that the chemical transformation of a unimolecular system via linear algebraic methods which meant that a system can be "lumped" by a matrix. Later Wei and Kuo [110] considered that the unimolecular reaction systems can be transformed to lumped species with certain linear combinations of the original ones. They analysed the lumping schemes in terms of the terms "exact lumping" and "approximate lumping" to distinguish two cases of lumping corresponding to the lumped mode1 matrix either having errors or not. The linear lumping

transformation may result in either proper or improper lumping schemes, which means that one cannot always find suitable lumping schemes with a low enough dimension for them, especially under some imposed constraints. Li and Rabitz [111, 112] extended linear lumping transformations to describe arbitrary nonlinear reaction-diffusion systems. Based on Wei and Kuo's work, more applicable nonlinear transformations were developed for discrete lumping by Li and his co-workers [113]. They proposed methods of how to determine the dimension reduction for the kinetic equations of a large system, described that a theoretical basis for discrete lumping methods of unimolecular and non-molecular reactions transforming the species vector to lower dimension through matrix operations mathematically. The discrete lumping schemes are presented linearly and nonlinearly based on their works as follows:

Linear system

Linear system is a system where the state variables and output variables satisfy the superposition principle for all possible input variables and initinal state. Linear system presents a smooth response to external influence on space and time.

For a unimolecular reaction system with n species can be written by an n-dimensional first order ordinary differential equation system with timescales separation:

$$\frac{dx}{dt} = -\boldsymbol{K}\boldsymbol{x} \tag{2.56}$$

where x is a vector of the dimension of $\boldsymbol{n}$ and $\boldsymbol{K}$ is a square matrix of the rate constants. To reduce the order of the system, lumps are constructed as:

$$\hat{x} = \boldsymbol{M}x \tag{2.57}$$

where $\hat{x}$ is of dimension $\hat{n} < n$ and $\boldsymbol{M}$ is the lumping matrix of dimension $\hat{n} \times n$. This system is exactly lumpable if there exists a matrix $\widehat{\mathbf{K}}$ so that the kinetic behaviour of the lumped system can be described by:

$$\frac{d\hat{x}}{dt} = -\widehat{\mathbf{K}}\hat{x} \tag{2.58}$$

The necessary and sufficient condition for exact lumping of linear kinetic systems can be figured out as [105]:

$$\boldsymbol{M}\boldsymbol{K} = \widehat{\boldsymbol{K}}\boldsymbol{M} \tag{2.59}$$

Eq. (2.59) will always be satisfied if the left $\hat{n}$ eigenvectors of the reactivity matrix, $\boldsymbol{K}$, are chosen to compose $\boldsymbol{M}$, and $\widehat{\boldsymbol{K}}$ is a diagonal matrix with the corresponding eigenvalues of $\boldsymbol{K}$.

Order reduction is obtained once the matrix of eigenvectors $\boldsymbol{X}$, is considered as

$$\boldsymbol{MX} = \widehat{\boldsymbol{X}}\left(\hat{\boldsymbol{I}}\middle|\boldsymbol{0}\right) \tag{2.60}$$

The non-singular matrix of lumped eigenvectors is $\widehat{\boldsymbol{X}}$ ($\hat{n} \times \hat{n}$), while$\left(\hat{I}\middle|0\right)$ is a matrix whose left submatrix is $\hat{I}$ ($\hat{n} \times \hat{n}$) an identity matrix and right sub-matrix $\mathbf{0}$ is an $\hat{n} \times (\mathrm{n} - \hat{n}\ )$ null matrix. Thus, the lumping matrix $\boldsymbol{M}$ reduces the dimensionality of the system and eliminates (n -$\hat{n}$) of the eigenvectors of the reactivity matrix. The determination of the lumping matrix can be realised by transposing Eq. (2.59)

$$K^T M^T = M^T \widehat{K}^T \tag{2.61}$$

which shows that the mapping of K^T on M^T is to produce a matrix that still remains in the same vector space, so M can be constructed from any of the invariant subspace of K^T.

Wei and Kuo [114] commented that most monomolecular reaction systems are not exactly lumpable by a proper lumping matrix. Approximate lumping schemes were proposed by them to examine the magnitude of the errors that accompany lumping. It is useful to minimise some measures of inconsistencies between the lumped and full system dynamics. Initial conditions are key issues for exact lumping. Indeed, lumping error can be defined as

$$e(t) = Mx(t) - \hat{x}(t) \tag{2.62}$$

one obtains by differentiating Eq.(2.62)

$$\frac{de(t)}{dt} = \widehat{K}e - (\widehat{K}M - MK) \tag{2.63}$$

Following Eq. (2.63) of exact lumping schemes, one can find

$$\frac{de(t)}{dt} = \widehat{K}e \tag{2.64}$$

For initial condition $\hat{x}(0) = Mx(0)$, then $e(t) = 0$ for all t. The reaction trajectories for all initial conditions, upon projection onto a common subspace, are bunched together to exist within the subspace for all t. In the case of $\hat{x}(0) \neq Mx$, the lumping scheme is exact lumpable, $e(t)$ asymptotes rapidly to zero.

Actually, $\boldsymbol{MK} \neq \widehat{\boldsymbol{K}}\boldsymbol{M}$ issues from most practical applications. However, lumping is still possible and one has to define the acceptable degree of approximation to make $e(t)$ as close to 0 as possible for all t. Thus the error matrix $\boldsymbol{E}$ reflects the accuracy of a given approximate lumping scheme to determine monomolecular reaction system and is defined as.

$$\boldsymbol{E} \equiv \boldsymbol{MK} - \widehat{\boldsymbol{K}}\mathbf{M} \tag{2.65}$$

For a reaction system approximately or poorly lumpable by matrix ***M,*** matrix *E* will depend on matrix $\widehat{\boldsymbol{K}}$ and will not be unique, but its form does not influence the form of lumping equations.

Nonlinear system

The nonlinear system means a sysytem in which the output variables is not directly proportional to the input variables, no longer characterised by the superposition principle due to nonlinear resulting in irregular motions and mutations.

As described above, in consideration of the extensive applicability of discrete lumping, lumping schemes have been extended to the nonlinear reaction systems via algebraic methods by Li et al [111, 115, 116]. They started by the establishing necessary and sufficient conditions for exact nonlinear schemes x with *n*-dependent variables, which can be written as an *n*- dimensional ordinary differential equations

$$\frac{dx}{dt} = \bar{f}(x(t)) \tag{2.66}$$

Then they proposed an analysis of discrete lumping schemes to an arbitrary nonlinearities system utilising the invariant subspace of the reaction system, which assumed the equations of an exactly lumped nonlinear system could be:

$$\frac{d\hat{x}}{dt} = M\bar{f}(\bar{M}\hat{x}) \tag{2.67}$$

where $\bar{M}$ is a generalised inverse of $\boldsymbol{M}$ according with

$$M\bar{M} = I_{\hat{n}} \tag{2.68}$$

The sufficient and necessary condition for exact lumping of a nonlinear system is that the transpose of the Jacobian matrix, $\boldsymbol{J^T}$(x), of function $\boldsymbol{f}(\boldsymbol{x})$ has nontrivial fixed invariant subspaces vector $\widetilde{M}$. The basis vector $\widetilde{M}$ constructs the lumping matrix of **M**. If the system is not exactly lumpable, the error matrix $\boldsymbol{E_1(x)}$ and $\boldsymbol{E_2(x)}$ can be defined to describe the deviation from the exact lumping for given $\boldsymbol{M}$ and $\bar{M}$.

$$E_1(x) = (I_n - M^T\bar{M}^T)J^T(x)M^T \tag{2.69}$$

$$E_2(x) = M[J(x) - J(\bar{M}Mx)] \tag{2.70}$$

The lumping matrix M and generalised inverse $\bar{M}$ can be determined by minimising error matrix E_1(x) and E_2(x), an appropriate lumping matrix is defined by minimising the error Z(x), of such a lumping scheme

$$\mathrm{Z}(\mathbf{x}) = tr\,[E^T(x)\;\; E(x)] \tag{2.71}$$

tr is the trace of a matrix (the sum of the eigenvalues). The nonlinear system can therefore be analysed in terms of its instantaneous linearised versions, and the Jacobian matrix can be decomposed into a linear combination of appropriate constant matrix A_k as:

$$\boldsymbol{J^{T(x)}} = \sum_{k=1}^{m} a_k\,(x)A_k \tag{2.72}$$

The $a_k(x)$ coefficients are functions of $\boldsymbol{x}$, and the A_k matrices are constant and form a basis of $J^T(x)$. A subspace that is simultaneously invariant for all the A_k matrices is also a fixed invariant subspace of $J^T(x)$. The decompositions of Eq. (2.71) and Eq. (2.66) of the Jacobian can be treated as a linear expression, but with potential nonlinear functions of concentration $\alpha_k(x)$. Matrix M can be optimised as:

$$\min Z(x) = tr \sum_{k=1}^{m} M\,{A_k}^T(I_n - M^TM)A_kM^T \text{ subject to } MM^T = I_{\hat{n}} \tag{2.73}$$

For an exactly lumpable system, lumping matrix $\boldsymbol{M}$ could be determined based on the Eq. (2.67). Practically, most lumped models always satisfy with some restrictions, for instance, some species may be left unlumped for some purposes. The determination of the approximate lumping schemes under general constraints is an unavoidable problem. Constraints on the species can be included by specifying a part of the lumping matrix $\boldsymbol{M}$ and seeking to determine the remainder of it. Thus the lumping matrix $\boldsymbol{M}$ can be represented as

$$\mathrm{M} = \begin{pmatrix} M_G \\ M_D \end{pmatrix} \tag{2.74}$$

M_G is given with satisfying ${M_G M_G}^T = I_{\hat{n}}$ and M_D can be determined from the invariant subspace of the system. The matrix M_G is suitable for separation species, which can be tracked during the reaction.

To determine approximate nonlinear lumping schemes, Li et al [117] introduced a singular perturbation method for a chemical kinetic system described by a set of first-order ordinary differential equations with a group of small positive parameters corresponding to different time scales.

For a given $\hat{n}$ ($\hat{n} \le n$)-dimensional non-degenerate transformation

$$\hat{x} = \boldsymbol{h}(x) \tag{2.75}$$

where $\boldsymbol{h}$ is the lumping transformation operator. With $\mathbf{h}(0)=0$, one $\hat{n}$ -dimensional differential equations system can be described by

$$\frac{d\hat{x}}{dt} = \bar{f}\big(\hat{x}(t)\big) = h_x\big[\bar{h}(\hat{x})\big]\bar{f}\big[(\bar{h}(\hat{x}))\big] \tag{2.76}$$

If one defines the Jacobian of the transformation of h(x) described as $D_{h,x}(x) = \frac{\partial h}{\partial x}$, then

$$D_{h,x}\left(x\bar{f}(x)\right) = D_{h,x}\bar{h}\big(h(x)\big)\bar{f}(\bar{h}\big(h(x)\big)) \tag{2.77}$$

is a necessary and sufficient condition of exact lumping schemes.

Now the exact lumping depends on the generalisation of inverse transformation $\bar{h}$ as a high dimensional system satisfying

$$h(\bar{h}) = I_{\hat{n}} \tag{2.78}$$

To better determine the transformation h and its inverse $\bar{h}$ in the nonlinear system using a reliable method, the nonlinear lumping schemes can be transformed into a separate reaction system by time scales [118]:

$$\frac{d\theta}{d\tau} = \varphi^1(\theta, \varepsilon; k) + \epsilon\varphi^2(\theta, \varepsilon; k) \tag{2.79}$$

$$\frac{\mathrm{d}\varepsilon}{\mathrm{d}\tau} = \sigma^1(\theta, \varepsilon; \mathrm{k}) + \epsilon\sigma^2(\theta, \varepsilon; \mathrm{k}) \tag{2.80}$$

where θ and ε are vectors of concentration reacting in accordance with the slow and fast time scales, respectively. φ and σ are operator vectors, ϵ is a small parameter from the ratio of time scales and τ is the fast time variable

$$\tau = t/\epsilon \tag{2.81}$$

To understand more easily the determination of an approximate nonlinear lumping system comparing to a linear lumping case, the original reaction system can be redefined by using the linear partial differential operator Π as a series containing the small perturbation parameter $\boldsymbol{\epsilon}$.

$$\varphi_i(x) = \Pi \cdot x_i \quad i = 1, \dots, n \text{ is the reaction number} \tag{2.82}$$

$$\Pi = \sum_{i=1}^{n} \varphi_i(x) \frac{\partial}{\partial x_i} \tag{2.83}$$

The differential operator Π can also be algebraically transformed to a canonical form[119]

$$\Pi = \Pi_0 + \epsilon\Pi_1 + \epsilon^2\Pi_2 + \cdots \tag{2.84}$$

This method incorporating lumping and time-scale separation technique is useful in finding an expression for the invariant manifold for a given transformation, even though it lies in the prior need to know the relative time scales of the reactions, as it depends on the proper introduction of ϵ. Overall, these studies explicit that lumping determination scheme a prior for the exactly lumpable system and provided the foundation for the non-isothermal lumping system [120].

Overall, the lumping methodology is a useful tool in mimicking reaction systems where the individual components are numerous and are often impossible to identify precisely. Since the "lumping" model was developed, it has been cited to exploit chemical kinetic characterisation reported as early as 1953 [121]. Lumping has been extensively applied, often in diverse fields, to address a number of problems requiring a model simplification approach, exploiting the common methodology of system's reduction. The kinetics of lumped reaction schemes are estimated mathematically based on the yield of volatile products, and overall rate constants calculated, followed by the deviation of the apparent activation energy and other reaction kinetic parameters (Marcella, et al [122]; Kim, et al [70]; Pinto, et al [82, 123]; and Csukás [78]).

As described in section 2.4, some models with or without secondary reaction all use the lumping technique to address the thermal decomposition characteristic of plastics. Moreover, those models were also employed to describe the pyrolysis behaviours of biomass, rubber and other biochemical materials. An advantage of lumping is that it only needs a few parameters and simple differential equations to predict the pyrolysis characteristic compared to other methods' complex mathematical equations. However, one step lumping model and primary lumping model cannot fully mimic the pyrolysis behaviours compared to the model of primary pyrolysis reaction coupled with secondary cracking, as they cannot effectively describe more than one consecutive step in pyrolysis reactions. A model involving primary and secondary reactions is more flexible in the simulation of primary pyrolysis and secondary cracking of thermal conversion [72]. Nevertheless, a loss of inherent information about specific individual species and reactions may occur in a lumping system, resulting in lower accuracy that can be significant obstacles in its application. Moreover the obstacles in finding an appropriate lumping scheme increase dramatically for large nonlinear reaction networks [18].

2.6 Conclusions

Energy and feedstock recovery from waste via the form of pyrolysis/gasification is not just for reducing the volume of the solid waste stream but is also a potential energy and feedstock source. It contributes to sustainable environmental safety and utilisation of

natural source. The performance and outcome of complex pyrolysis process are dominated by preferred process parameters (e.g. feedstock, temperature, residence time etc.).

Modelling development is able to convert the chemical reaction data into a mathematical simulation through kinetic parameters, to provide an effective and beneficial solution for complex reaction system. Model simplification in describing the complex chemical reaction network reduces the computational costs during numerically generating solutions for the pyrolysis process. The selection of the model reduction methodology depends on the kinetic information available, composition, structure of component reaction, and the accuracy required. Kinetic parameters characterise material chemical reactivity linked to the microscopic-molecular dynamic behaviour of a reaction system, and are useful in engineering calculations in the commercial process.

The lumping approach is able to algebraically transform complex reaction system into a lower dimensional vector of pseudo-species, which may be linear or non-linear combinations of the original species. Therefore the kinetic lumping schemes can be easier to solve using a few parameters experimentally determined, although it does not furnish information on the fundamental chemistry of the process. Nevertheless, the lumping approach only performs apparent (pseudo) kinetics and treats the components of the continuous complex mixture into discrete points, ignoring the real species distribution between two points. Thus, the complex network of plastic pyrolysis results in its apparent kinetics behaviour rather than actual pyrolysis kinetics. The compositions of fractioned products in the primary reaction and secondary reaction may not be globally developed via the numerical model. So the kinetics of plastic pyrolysis must be elucidated in depth. Additionally, the fractionation of the liquid oil could present an apparent kinetics of the multi-component mixture, which is not simply explicable through the kinetics of each single reaction. Thus, there is a need to undertake further investigation to support innovation in pyrolysis processes.

CHAPTER 3 MATERIALS AND METHODOLOGY

Summary

This Chapter presents the selection of feedstock for this project; definition of conversion and yield of pyrolysis process; the experimental design in terms of response surface methodology (RSM) and the interaction effect of different ratios of plastic materials and temperature range; introduces the experimental apparatus of fixed bed pyrolytic reactor and thermogravimetric analysis and their experimental procedures; presents model development employing lumping methodology with MATLAB software to determine the optimal parameters for each model.

3.1 Feedstock for this project

As aforementioned in Chapter 1 and Chapter 2, PE, PP, PET and their mixtures are main components in plastic waste streams. They were chosen as the feedstock in this PhD study to identify the potential commercial benefits of the energy and chemical feedstock recovery from plastic waste via pyrolysis process.

Samples of waste HDPE, PE, PP (Appendix 2.1) were provided by Luxus Limited (Belvoir Way, Fairfield Industrial Estate, Louth, Lincolnshire, LN11 0LQ), a plastic recycling company in England. HDPE waste was from crates and bins, PE waste consists of flexible polyethylene (mostly LDPE) production scrap, rigid polyethylene (mostly HDPE) crates and wheelie bins, PP waste was from polypropylene trays. The samples were shredded and sifted out under 8×8 mm size. Waste PET bottles were collected from Heriot Watt University recycling centre and then cut into small pieces (approx. 10×10 mm^2) by using a scissor. The sample mixture of waste plastic was defined by the ratio of flexible PE, rigid PE at 2:1 for PE waste; flexible PE, rigid PE, and rigid PP at 10:5:9 for PEPP mixture, based on the proportion of packaging plastic waste in the UK. The sample was then weighed by electronic analytical balance (Sartorius Analytical Balance, W450E/044. IKA-Werke GmbH & Co. KG, Germany). In TGA experiments, the sample was physically processed using a milling grinder (A10, 20,000l min^{-1}, Janke & Kunkel IKA-WERK, GmbH & Co. KG, Staufen, Germany) cryogenically shredded for 5 minutes under liquid nitrogen atmosphere, then sieving the sample size to between 150 and 250 μm using stainless fine test sieves.

3.2 Definitions of conversion, yield and mass balance calculation

For a batch reactor in this PhD study, conversion and its related terms yield in the pyrolysis process are defined as:

- Conversion (X_i) describes ratios of how much of plastic waste has reacted
- Yield (Y_i) describes how much of the desired products (e.g. gas, oil and wax) is obtained from the pyrolysis process

$$X_i = \frac{n_i(t=0) - n_i(t>0)}{n_i(t=0)} \times 100\%$$

$$Y_i = \frac{product_i(t>0))}{n_i(t=0)} \times 100\%$$

- **Mass balance calculation**

The accounting of all mass in batch pyrolysis process in this PhD study is referred to as a mass balance, which is based on the fundamental "law of conservation of mass (not volume and moles)". Integral mass balances were carried out on the initial at the beginning and final states of the system at the end of a batch process. The pyrolysis process is treated as a steady-state process, there is no accumulation of mass within the process.

∑Mass in = ∑Mass out

3.3 Experimental design

As described previously in Chapter 2, the pyrolysis process involves multiple independent variables (molecular structure and chemical composition of the feedstock, temperature and heating rate, residence time, reaction system pressure, carrier gas and others), which have single and/or combinational influence on the product yield distribution. Most studies only considerd a single variable's effect on the process under experimental work, because it is not easy to evaluate the performance of combined variables in a pyrolysis process to a given product. RSM is employed in this project to optimise experimental operating parameters and to reduce the experiment numbers. This method was first introduced by Box and Wilson in 1951 and is a regression method to identify the correlation between some explanatory factors and responses [124]. The operating variables on the pyrolysis process were investigated using the standard of RSM design fitting on a second-order factorial design called central composite design (CCD). The design matrix *X* for a CCD experiment involving $\bar{\bar{k}}$ factors is derived from a matrix $\ddot{D}$ containing three different parts corresponding to the three types of

experimental runs: 1) The factorial experiment $\ddot{F}$ matrix coded factor levels as +1 and −1; 2) The centre points matrix $\ddot{C}$ denoted in coded variables as (0, 0, 0,..., 0), where there are $\bar{\bar{k}}$ zeroes; 3). An axial points matrix $\ddot{E}$ with $2^{\bar{\bar{k}}}$ rows, each factor is sequentially placed at $\pm\alpha$ and all other factors are at zero based on factorial level. The value of α is determined by the designer. The matrices can be denoted as follows

$$\ddot{\boldsymbol{D}} = \begin{bmatrix} \ddot{\boldsymbol{F}} \\ \ddot{\boldsymbol{C}} \\ \ddot{\boldsymbol{E}} \end{bmatrix}$$

$$\ddot{\boldsymbol{E}} = \begin{bmatrix} \boldsymbol{\alpha} & \mathbf{0} & \mathbf{0} & \dots & \dots & \dots & \mathbf{0} \\ -\boldsymbol{\alpha} & \mathbf{0} & \mathbf{0} & \dots & \dots & \dots & \mathbf{0} \\ \mathbf{0} & \boldsymbol{\alpha} & \mathbf{0} & \dots & \dots & \dots & \mathbf{0} \\ \mathbf{0} & -\boldsymbol{\alpha} & \mathbf{0} & \dots & \dots & \dots & \mathbf{0} \\ & & & \vdots & & & \\ \mathbf{0} & \mathbf{0} & \mathbf{0} & \mathbf{0} & \dots & \dots & \boldsymbol{\alpha} \\ \mathbf{0} & \mathbf{0} & \mathbf{0} & \mathbf{0} & \dots & \dots & -\boldsymbol{\alpha} \end{bmatrix}$$

$$\boldsymbol{X} = \left[\mathbf{1} \quad \ddot{\boldsymbol{D}} \quad \ddot{\boldsymbol{D}}(\mathbf{1}) \times \ddot{\boldsymbol{D}}(\mathbf{2}) \quad \ddot{\boldsymbol{D}}(\mathbf{1}) \times \ddot{\boldsymbol{D}}(\mathbf{3}) \dots \quad \ddot{\boldsymbol{D}}(\bar{\bar{\boldsymbol{k}}} - \mathbf{1}) \times \ddot{\boldsymbol{D}}(\bar{\bar{\boldsymbol{k}}}) \dots \dots \ddot{\boldsymbol{D}}(\bar{\bar{\boldsymbol{k}}})^{\mathbf{2}}\right]$$

CCD contains an embedded factorial or fractional factorial design with central points, 'star points' to allow estimation of curvature and axial points. Generally, each numerical code factor is varied over 5 levels: $-\partial, -1, 0, +1, +\partial$. The ∂ value depends on a number of factors in the $2^{\bar{\bar{k}}}$ factorial design (where $\bar{\bar{k}}$ is the number of factors) [124] .

In this work, RSM was used to determine the optimum experimental design matrix specified in terms of the face CCD method. The variables and levels of factorial influence in this design are specified in Table 3.1 for plastic pyrolysis process.

The production yield $\bar{Y}$ is the response in full face-CCD that was conducted. The temperature and ratio of feedstock were chosen as factors with considered 3 levels. The face CCD consists of 4 axial points, 4 fractional points and 5 replicable central points, resulting in 13 experiments in Table 3.2. A mathematical model is introduced to denote the relationship between response and the factors as shown in Eq.3.2.

Table 3.1 Specification of variables and levels of pyrolysis experiment by CCD

Factor variables	Levels and range (coded)		
	-1	0	1
A: Temperature (℃)	450	500	550
B: Ratio of flexible PE and rigid PE (%)	100:0	50:50	0:100

Table 3.2 Central composite design (CCD) matrix and yield response

		Actual variables		Coded levels		Response
Run	Type	Temperature	Ratio(Flexible: Rigid)	A	B	Volatile Yield (wt. %)
1	Centre	500	50:50	0	0	96.68
2	Axial	550	50:50	1	0	96.60
3	Factorial	550	0:100	1	-1	99.26
4	Factorial	550	100:0	1	1	93.38
5	Factorial	450	100:0	-1	1	93.23
6	Factorial	450	0:100	-1	-1	98.36
7	Axial	500	0:100	0	-1	99.22
8	Axial	500	100:0	0	1	93.24
9	Axial	450	50:50	-1	0	96.68
10	Centre	500	50:50	0	0	94.68
11	Centre	500	50:50	0	0	96.68
12	Centre	500	50:50	0	0	96.68
13	Centre	500	50:50	0	0	96.68

$$\bar{Y} = \bar{\bar{f}}(X_1, X_2, X_3 \dots X_{\bar{n}}) \quad (3.1)$$

$$\bar{Y} = \alpha_0 + \sum_{i=1}^{\bar{n}} \alpha_i \times X_i + \sum_{i=1}^{\bar{n}} \alpha_{ii} \times X_{ii} + \sum_{i=1}^{\bar{n}} \sum_{j=1}^{\bar{n}} \alpha_{ij} \times X_i X_j \quad (3.2)$$

where $\bar{Y}$ is the response, $\bar{\bar{f}}$ is the unknown function of response, $X_1, X_2, X_3, \dots X_{\bar{n}}$ are the factors and $\bar{n}$ is the number of independent factors. The independent factors are assumed to be sequential and controllable during the experiments with negligible errors; this modified quadratic response model can be written as follows to predict the dependent α and independent variables X, α_0, α_i, α_{ii}, and α_{ij} are regression coefficients for the constant,

linear, quadratic and interaction coefficients respectively. X_i, X_j are coded independent factors.

Design expert software vision 8.0.6 (Stat-Ease Inc., Minneapolis, USA) was employed in fitting the dependent variables, analysis of variance and regression. Experiments carried out by using factorial design are useful in a correct way to assess multiple variables, to evaluate the interactions between factors on the response, and to minimise the other influencing factors [125].

3.4 Experimental limitation

The experimental plan was designed to investigate the effect of temperature, composition of feedstock, and time on the pyrolysis process combining with other process parameters (e.g. heating rate, pressure, carrier gas flow rate). The investigation through this PhD project was limited by time, financial constraints and the availability of equipment. High demand for pyrolysis unit and analysis equipment (i.e. TGA and mass spectrometer (MS)) limited experiment booking for the extent of plastic pyrolysis experimentation and the test of samples and products. Also, the repair and necessary maintenance of the pyrolysis unit as TGA and MS limited the experiment progress. If more time was available then further studies on additional process parameters (i.e. catalyst) and their production optimisation would have been considered. Further analyses (i.e. MS analysis of liquid products) were not realised due to financial constraints and availability of MS unit.

3.5 Experiment setup of pyrolysis

All pyrolysis experiments within this PhD project were slow pyrolysis, and conducted by using lab-scale fixed bed pyrolytic reactor outlined in Figure 3-1 (Photographic presentation of pyrolysis unit is shown in Appendix 2.2) and thermogravimetric analysis (Figure 3-4), was carried out at the UK Biochar Research Centre (UKBRC) in the University of Edinburgh.

3.5.1 Pyrolysis conditions

As reviewed in Chapter 2, pyrolysis conditions can dramatically alter the final properties and composition of the waxes, liquids, gases and solid residue obtained from the process under the effect of a large array of process parameters. Due to time constraints of the PhD study,

temperature, residence time and feedstock were chosen as main influencing parameters to investigate the pyrolysis characterisitcs of plastic waste, since they are most important operational parameters studied in the pyrolysis process. The temperature range between 400℃ and 550℃ was studied throughout the experimental work, which covered the main regions of thermoplastic degradations associated with slow pyrolysis. Based on real-time seen in industrial sized pyrolysis units to convert plastic waste into oil, and the literature study, the residence times chosen were therefore 10, 30, 60 and 180 minutes. The chosen residence times are able to check the difference of product distribution and as a reference for a future scale-up process.

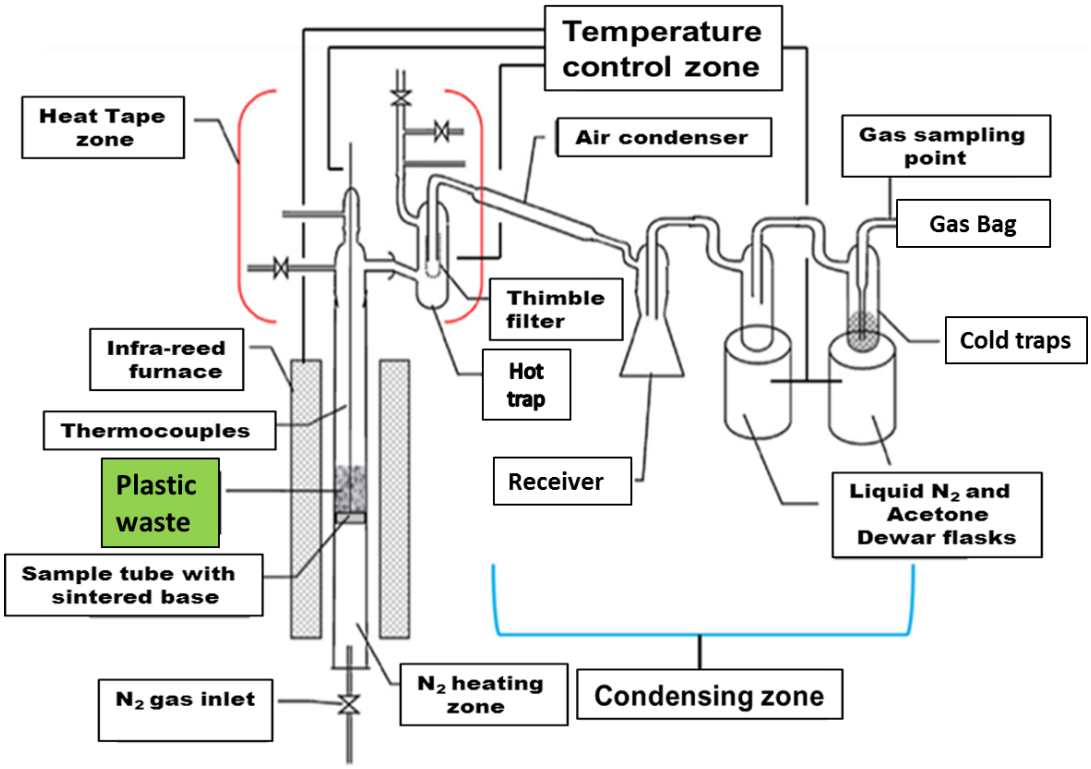

Figure 3-1 Experimental system outline

The flowing rate of nitrogen (N_2), as the carrier gas through the pyrolysis system, was 300 ± 20 ml min^{-1} at room temperature, which was initially set up by researchers at UKBRC. To fulfil a slow pyrolysis and provide a slow flow velocity to maximise vapour/solid interactions, an assumption was taken to estimate the residence time of gases in the reactor, so that the volatiles produced during pyrolysis are removed by the carrier gas at the same flow rate. The residence time (τ) of carrier gas and volatiles was calculated based on flow rate of carrier gas and reactor volume shown as following:

Quartz tube reactor specification: Inner diameter: 40 mm, Height: 300 mm

Volume of reactor $=\frac{\pi}{4} \times 0.04^2 \times 0.30 m^3 = 3.77 \times 10^{-4} m^3 = 377$ ml

For an example, the flow rate (R_f) of carrier gas and volatiles in the reactor at 500℃ can be obtained:

$R_f = (300 \pm 20) \times \frac{773}{293^*} = 795 \pm 53$ ml/min$= 13.25 \pm 0.88$ ml/s

Thus, the residence time of carrier gas and volatiles in the reactor is:

$\tau = 377 \div (13.25 \pm 0.88) = 26.68 \sim 30.48$ (s)

The reactions of thermal pyrolysis and cracking usually occur instantaneously under the reaction temperature, so this time can ensure a sufficient slow pyrolysis process.

3.5.2 Fixed bed pyrolytic reactor (FBPR) set up

The FBPR experimental study was undertaken with the designed procedures, based on the project objectives, applicable equipment, measuring tools, and the methods of product collection and analysis which shows in Figure 3-1.

The apparatus comprises a vertical quartz tube (50 mm diameter) with sintered glass plate for carrier gas distributor at the base. Around 25g of sample for each run was loaded into the reactor on a bed of tubular ceramic packing (30~40 mm height to avoid the blockage of carrier gas flow) and was heated by a 12 kW infrared gold image furnace (P610C; ULVAC-RIKO, Yokohama, Japan) with a proportional–integral–derivative (PID) controller allowing a wide range of heating rates and holding times. The thermal conversion of the plastic waste was realised in the heating zone.

1. Assembling: Samples were weighed using a four decimal place balance at the start, once the sample was loaded into the reactor and fixed in the PID furnace (Appendix 2.3), the reactor was connected with the glassware and apparatus was assembled and sealed by silica grease so as to obtain a closed loop system. The main experimental process variables (volume, time and flow rates), temperature and pressure are logged in real time before commencing the experimental runs.

2. Purging: The system was purged with nitrogen (N_2) with a controlled stable level of flow rate (300 ± 20 ml/minute) for at least 10 minutes so as to maintain an oxygen-free atmosphere before heating through the furnace. The N_2 was used to sweep the volatiles and gases away from the pyrolysis zone and into the condensation system.

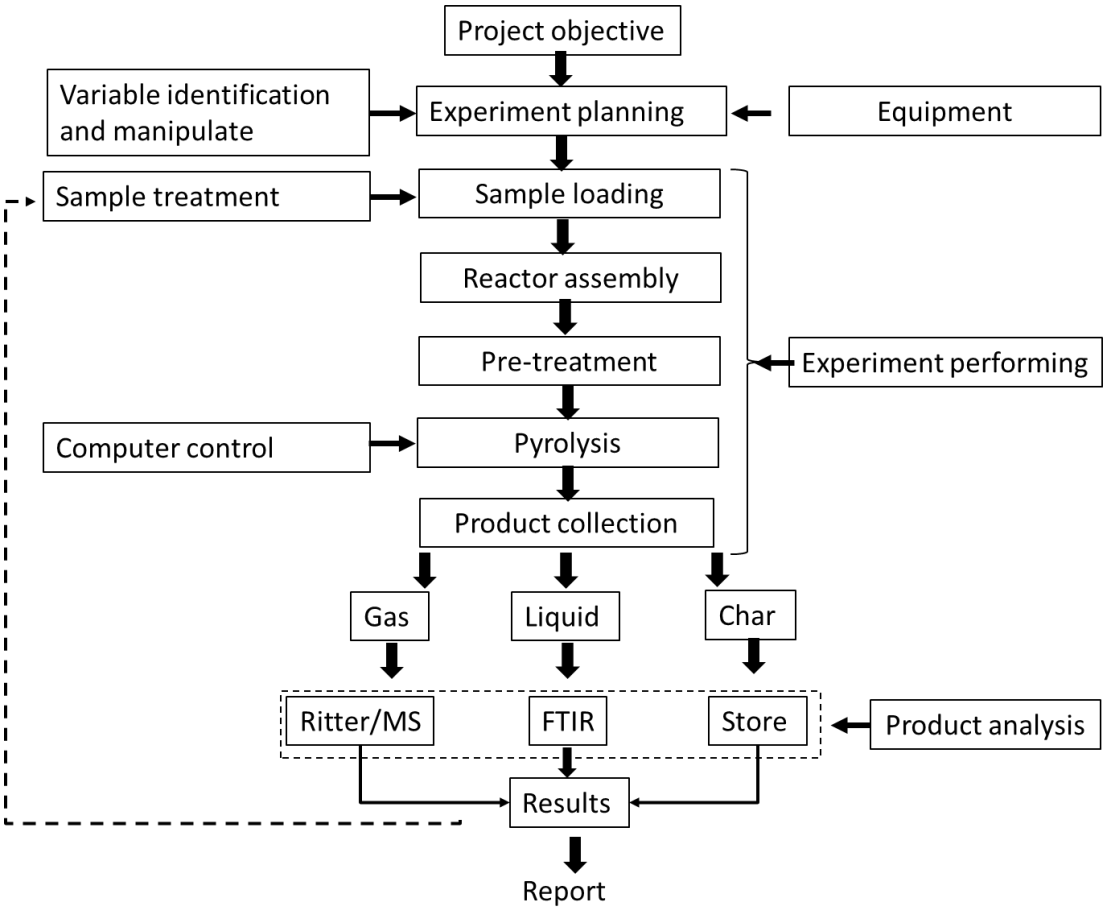

Figure 3-2 Experimental procedure to examine the pyrolysis reaction of plastic waste

3. Heating and holding: Reactor was heated from room temperature to reaction temperature at a heating rate of 25℃/min and held at this peak temperature by using ULVAC TPC-500. The temperature was monitored by automated CX-Thermo software. The reactor tube was constantly purged with N_2 to establish a balance flow rate of N_2 as carrier gas to achieve an inlet flow rate of 0.334 l/min that was monitored with RIGAMO V2.12 software (giving a linear cold flow velocity within the empty pyrolysis tube of approximately 3 mm/s at 100% N_2 composition). The heating and reaction temperatures were monitored by using three K-type thermocouples in which were located at the top, middle and bottom of the bed in the reactor. Beyond that, a heavy tar trap (160^{+20}_{-10}℃)

provided by flexible heating tape maintains the collection of heavy tar components and avoid the pipe blockage. A heated glass fibre filter (170±15℃) was adopted to confine any entrained particulates and some heavy tars in volatile products to the condenser, which was realised by using a firble beld sound the glasswares.

4. Reaction system pressure control: On-line data logging of differential pressure across the sample bed and gauge pressure in the reactor head is also monitored by PICOLOG Recorder software. Pressure sensors were zeroed and the reactor was purged with nitrogen before establishing a steady flow rate of nitrogen as carrier gas.

5. Cooling: The cooling of reaction system was realised by two stages for collection of liquid oil compounds: an ambient temperature zone, and a low temperature zone (−40±5 °C, measured by using HH12B Dual digital thermocouple thermometers, Omega Engineering Limited, 1 Northbank Ind. Park, Omega Cir, Irlam, Manchester M44 5BD, UK) realised by two cooled traps held in Dewar flask filled by cooled acetone using liquid nitrogen to avoid the entry of condensed products into the gas sample bag. The system was gradually cooled with continued N_2 flow down to 25 °C (about 30 minutes) once the designed residence time at reaction temperature had been reached.

6. The Collection of products: The reaction products of the pyrolysis of PE, PP and their mixture were lumped into groups: gases, liquid hydrocarbons, wax, and solid residue including char-like product. For the experimental study of PET pyrolysis, the products was grouped as gas, liquid, solid powder, char and solid residue, which can be seen in Appendix 2.5 and Figure 4-15. Product yields are given as recovered yields expressed as percent by weight of dry feed. Not all solid and liquid products could be recovered from the apparatus; handling losses were estimated at 3-5 per cent in total. The condensed liquid products (wax and heavier oils) were collected from hot trap and receiver, and the light oil from the cold trap (CT-1); all condensed products were stored in a refrigerator for analysis. The solid powders were collected from the glasswares in heated zone and air condensing pipe during PET pyrolysis. All the remaining non-condensable gases were collected in a 200 liter multi-layered Tedlar gas bag (JensenInert Products, Coral Springs, Florida). The part of char generated from PET waste was collected from the quartz tube and stored in 250ml glass bottles with identification labels, kept at room temperature and

retained for analysis; the rest solid residue generated from PE and PP waste was not collected instead of a burning-out procedure (Appendix 2.6).

7. Product handling: The collected non-condensed gases was analysed by MS, the gas volume was obtained using the volumetric flow meter. The apparent properties of liquid products are determined by the type of feed plastic waste, a sample is presented in Appendix 2.4. The collected tar with the presence of PE from the hot trap was grey and viscous, quickly solidifying as wax due to temperature reduction; the tar from PP waste appears grey and remains a viscous liquid. The main liquid fraction was collected from the ambient receiver for PE, PP and their mixture. Only small quantities of condensable products were collected from cold traps, which indicate small yields of light oil generated. An uncollectible and thinner layer of char formed by condensate was deposited onto the upper part of the reactor tube and the wall of glassware in heat zone. The weight of the quartz tube including plastic samples and residue was measured before and after the run, the weight difference was used for the calculation of solid residue.

3.5.3 Thermogravimetric analysis (TGA)

TGA is a powerful technique used to determine the thermal decomposition of polymers, in which the weight loss of a sample can be recorded against the temperature under specified heating rate and gas atmosphere. Mettle-Toledo TGA/DSC1 instrument (Figure 3-3) were employed; including a gas control box GC 100, sample robot, Huber chiller unit and local PC. The unit is an essentially sensitive microbalance holding a sample in a crucible, together with a reference crucible, within a programmable furnace. The weight changes of samples and heat flow into or out of the sample are under controlled temperature profiles and in a controlled nitrogen and air atmosphere.

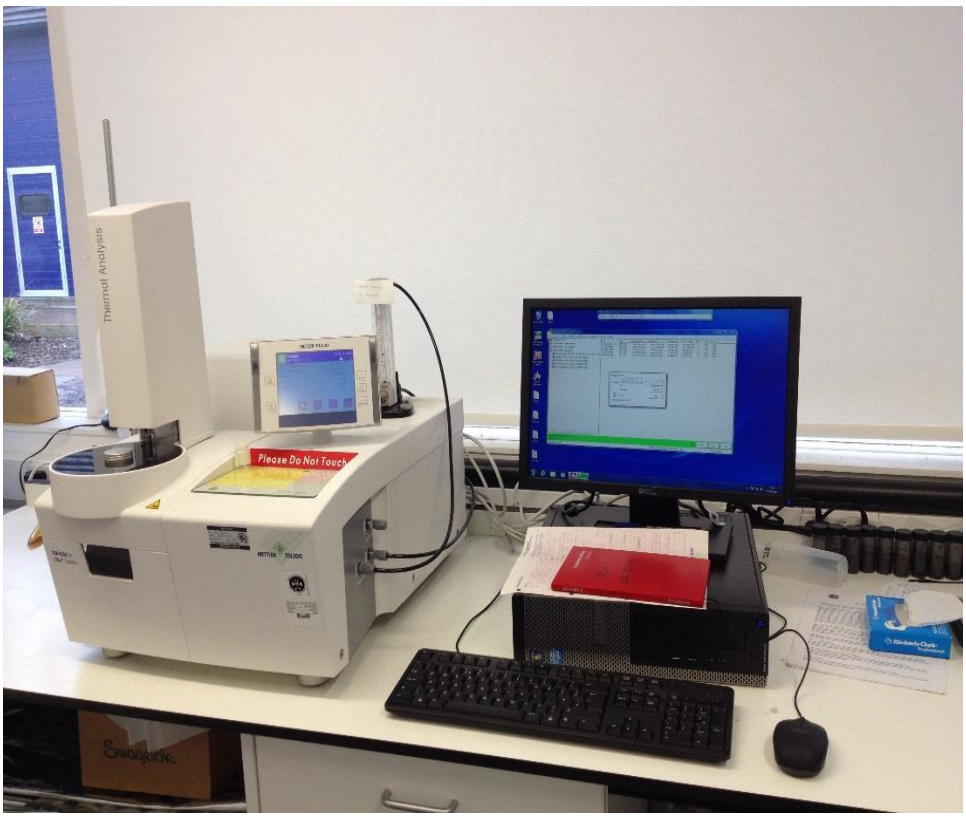

Figure 3-3 Photo of Mettle-Toledo TGA/DSC 1

The TGA procedures consist of the preparation of the instrument involving 1) nitrogen gas connection to the "balance" port and purging rate, 2) cleanness of furances and crucibles; 3) sample and crucible filling involving empty sample crucible along a pre-defined temperature program in nitrogen atmosphere etc.; 4) the setup of method and of blank experiment running, queuing sequence of experiments, and then start to run. The first series of thermogravimetric experiments were progressed to determine the accumulated weight change of the sample and heat flow into or out of the samples in a nitrogen atmosphere.

The second series of thermogravimetric experiments was with plastic waste samples under air for residue combusition and cleaning of the crucible. An outline of experiment procedures at 450℃, 500 ℃ and 550℃ is shown in Table 3.3. The disadvantage of TGA is that only volatile phase and solid residue can be quantified. It cannot show detailed information of the volatile composition, and also a limitation of specimen size may result in error on the thermal decomposition of the plastic waste mixture. Thus TGA combines with MS can be a better choice to get more information of thermal conversion, and also repeated experiments is able to reduce the experimental error.

Table 3.3 TGA plastic samples test program at 450, 500 and 550℃

Step	Description	Type	Temperature		Heating rate	Holding time	Method gas	Gas rate
			Start	End				
			℃	℃	K/min	min		ml/min
1	Equilibration/purging	Isothermal	25	25	0	2	N_2	100
2	Evaporating moisture	Dynamic	25	110	25	4.4	N2	100
		Isothermal	110	110	0	20	N2	100
	Heating	Dynamic	110	450	25	13.6		
	Holding	Isothermal			0	30		
	Cooling	Dynamic	450	25	/		N2	
3	Driving off volatiles	Dynamic	110	450	25	13.6	N2	100
		Isothermal	450	450	0	10	N2	100
4	Oxidising of fixed carbon	Dynamic	450	900	25	14	N2	100
5		Isothermal	900	900	0	10	Air	100

3.6 Sample analysis

The collected gas and liquids from each experiment were analysed by several methods to determine their composition and characterise their bond structure during the experimental study in this PhD project.

3.6.1 Gas analysis

The identification of collected gas composition was carried out by using Mass Spectrometer (HIDEN HPR QIC-20, Hiden Analytical Ltd, UK, and Figure 3-4). Before this analysis, the gas bag with collected gas, as described in section 3.4.1, was left on the plain and tidy worktop with a few times gentle pats on the bag, following with a rest for around 30 minutes to allow an equilibrated gas mixture. In the MS analysis, selected ion monitoring (SIM) programme was chosen to give potential positive detection result, which means only small

amount of mass fragments are detected during each scan by the mass spectrometer, then the overall composition of the collected gas sample was analysed for N_2, H_2, CO, CH_4, O_2, and C_2H_6. In consideration of C_2H_4, CO and N_2 all present parent peaks at mass 28, it was difficult to differentiate between them. The ratio of pure N_2 at mass 14 and 29 was determined to solve this problem, then allowing for the calculation of N_2 at mass 29 by measuring N_2 at mass 14 during the experiments. Once the amount of N_2 at mass 29 was determined it was subtracted from the remaining measurements at mass 29 leaving only CO and C_2H_4 at mass 28. To support this point, an oxygen and CO analyser (Rapidor 3100 EB Oxygen & CO Analyser, Cambridge, UK) (Figure 3-5) was introduced to detect the CO concentration in the collected gas mixture after each pyrolysis run, as well as the detected oxygen concentration will be used to identify the oxygen content in the collected gas. Thus, CO and C_2H_4 can be separated. Due to a limitation of experimental condition and time, further analysis of CO_2 and other gaseous hydrocarbons was not taken. Gas volume measurement was carried out by the volumetric flow meter (Ritter, TG5 Gas meter, Germany) (Figure 3-5). The Oxygen and CO analyser connected between the gas bag and the flow meter. Non-condensable gas volume can be directly obtained from the measurement of Ritter TG 5 gas meter. An outlet gas volume total reading was taken before and after each run to allow the produced gas volume to be estimated by subtraction of the calculated total carrier gas flow over the same period. Carrier gas (nitrogen) is not included in the composition.

3.6.2 Liquid/wax analysis

The identification of chemical compound and the functional group in the collected liquid products was analysed by using Frontier Fourier infrared/far-infrared (FT-IR/FIR) Spectrometers (PerkinElmer, UK, located at The Centre for Innovation in Carbon Capture and Storage, Heriot Watt University, Figure 3-6). Frontier FT-IR/NIR provides optimum performance in both mid-IR and near-IR regions, qualitatively and quantitatively enabling a flexible and adaptable IR solution rapidly. Additionally, FTIR is self-calibrating instrument offering an extremely accurate, reproducible and reliable service. The normal analysis process of FTIR (Figures 3-6 and 3-7) comprises of (1) the IR source: IR energy is emitted from a glowing black-body source, which satisfies the beam passes through an aperture to control the energy presented to the sample; (2) the interferometer: the beam enters the interferometer in which the "spectral encoding" takes place; (3) the sample: the beam enters the sample compartment where it is transmitted through or reflected off the surface of the

sample, depending on the type of analysis being completed; (4) the detector: the beam finally passes to the detector for final measurement; (5) the computer: the measured signal is digitised and sent to the computer where Fourier transformation takes place. Product (gas, liquid, and char residue) yields were calculated by a proportion of sample weight on a dry basis.

Figure 3-4 Photo of HIDEN HPR QIC-20

Figure 3-5 Photo of gas measurement

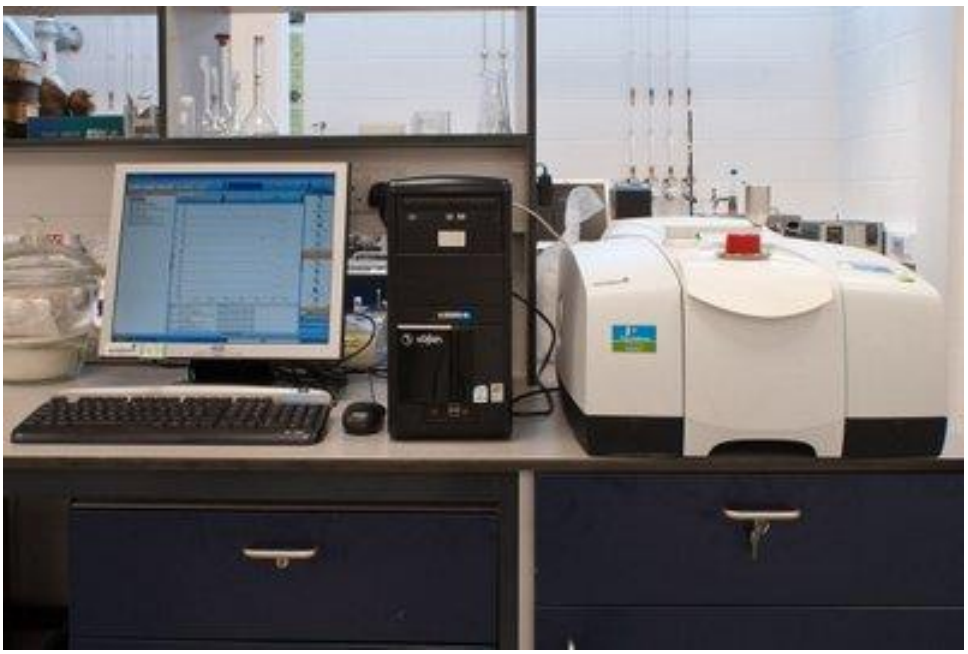

Figure 3-6 Photo of PerkinElmer FTIR

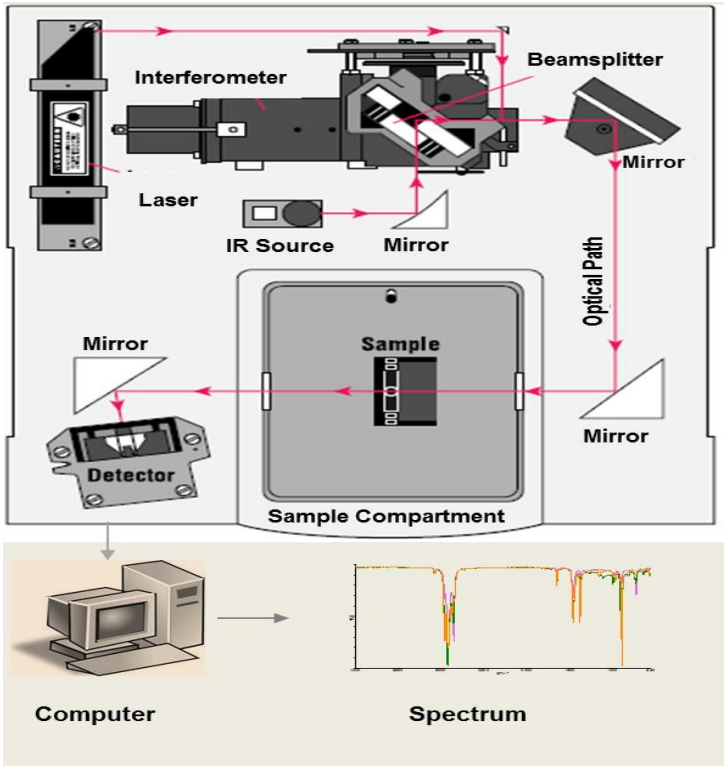

Figure 3- 7 IR spectrometer with the source, interferometer, sample, and detector [126]

3.7 Methodology of model development

To analyse the kinetic model characteristics of the pyrolysis of plastic waste, the following assumptions were made:

1) the fraction components gas (G), liquid (L), and char (C) resulting from pyrolysis of the wastes do not further decompose as they are continuously removed from the reactor;
2) all the reactions are the first-order reaction;
3) all the reactions are irreversible;
4) there are no mass transfer resistance and heat resistance limitation in the reactor;
5) the temperature dependence of rate constants is described by Arrhenius' law;
6) the pressure in the reactor is approximately 1 atmosphere absolute;
7) the evaluated predictive values of feedstock and products are assumed normalised results.

To better describe the pyrolysis process, the following kinetic pyrolysis model of plastic waste is considered with possible reaction pathway.

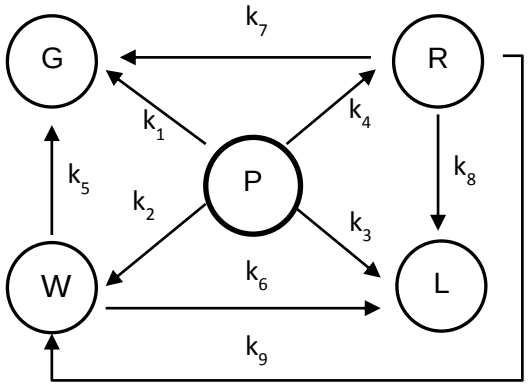

Figure 3-8 Schematic of two step pyrolysis modelling of waste polymer

The discrete lumping (DL) methodology is applied to the five lumps formed by the plastic (P), the gases phase (G), the liquid (oil) phase (L), waxes (W), and the solid residue phase (R) resulting from the pyrolysis of waste. Secondary cracking reaction pathways also occur

during the primary pyrolysis reactions. Based on the schematic pathways of Figure 3-8, the mathematical differential equation of each lump is expressed as:

$$\frac{dP}{dt} = -(k_1 + k_2 + k_3 + k_4)\,\mathrm{P} \tag{3.3}$$

$$\frac{dG}{dt} = k_1\,\mathrm{P} + k_5\,\mathrm{W} + k_7\,\mathrm{R} \tag{3.4}$$

$$\frac{dW}{dt} = k_2 P + k_8 R - (k_5 + k_6)\ \mathrm{W} \tag{3.5}$$

$$\frac{dL}{dt} = k_3 P + k_6\,\mathrm{W} + k_9 R \tag{3.6}$$

$$\frac{dR}{dt} = k_4 P - (k_7 + k_8 + k_9) R \tag{3.7}$$

The mass balance can be written as:

$$-\frac{dx_{WP}}{dt} = \frac{dx_{Gas}}{dt} + \frac{dx_{Liquid}}{dt} + \frac{dx_{Wax}}{dt}\ \frac{dx_{Char}}{dt} \tag{3.8}$$

where k_1, k_2, k_3 and k_4 represent the rate constant of the pyrolysis of plastic waste to gas phase, liquid phase, waxes and solid residue during primary reaction, and k_5, k_6 is the rate constants of wax cracking into gas and oil; k_7, k_8 and k_9 are the rate constants of solid residue cracking into gas, oil and wax.

Rate constant k is determined by Arrhenius' law

$$k(T) = A_0 exp(\frac{-E}{RT}) \tag{3.9}$$

The mass change function can be expressed with the temperature dependence as

$$\frac{dx}{dT} = \frac{A_0}{\beta} \exp\left(-\frac{E}{RT}\right)(1 - x) \tag{3.10}$$

3.8 Model Solution

To solve the ordinary differential equations (3.3-3.8), the calculated values of the evolution of mass fraction as a function of time for five lumps are obtained. The kinetic parameters in the models were determined by fitting the calculated values to the experimental data. Programmes was written in MATLAB software to determine the optimal parameters for each model. The differential equations were solved by subroutine ODE45 which implements a fourth-order Runge-Kutta method with a variable time step for efficient computation accordingly. The nonlinear least squares algorithm is employed to fit parameterised nonlinear functions by minimising the error

between the experimental and calculated values for nonlinear objective functions. Thus, the kinetic parameters of plastic pyrolysis are able to be estimated in terms of tailored experiment data based on minimising objective function (MOF) associated with each deviation as follow:

```
function  wt=curvefitPE01(k,w)
t=[0 10];
[t,w]=ode45('myfunPE01',t,w,[],k);
for i=1:4
%     i=1:5
   wt(i)=w(end,i);
end
```

$$MOF_{(x_{ij})} = \frac{\sum_{j=1}^{n_{exp}} (x_j - x_{j(cal)})^2}{n_{exp}} \tag{3.11}$$

where x_j, $x_{j(cal)}$, n_{exp} are denoted as the measured experiment values, the calculated values of modified dependent variables respectively for the mass fractions, and the number of experimental points (reaction times).

The model solution flow chart is shown in Figure 3-10, which presents the route of optimisation, validation, and modification of model solution. The detailed MATLAB programme was present in appendix 3 to solve the unconstrained nonlinear optimisation between experimental data and calculation results.

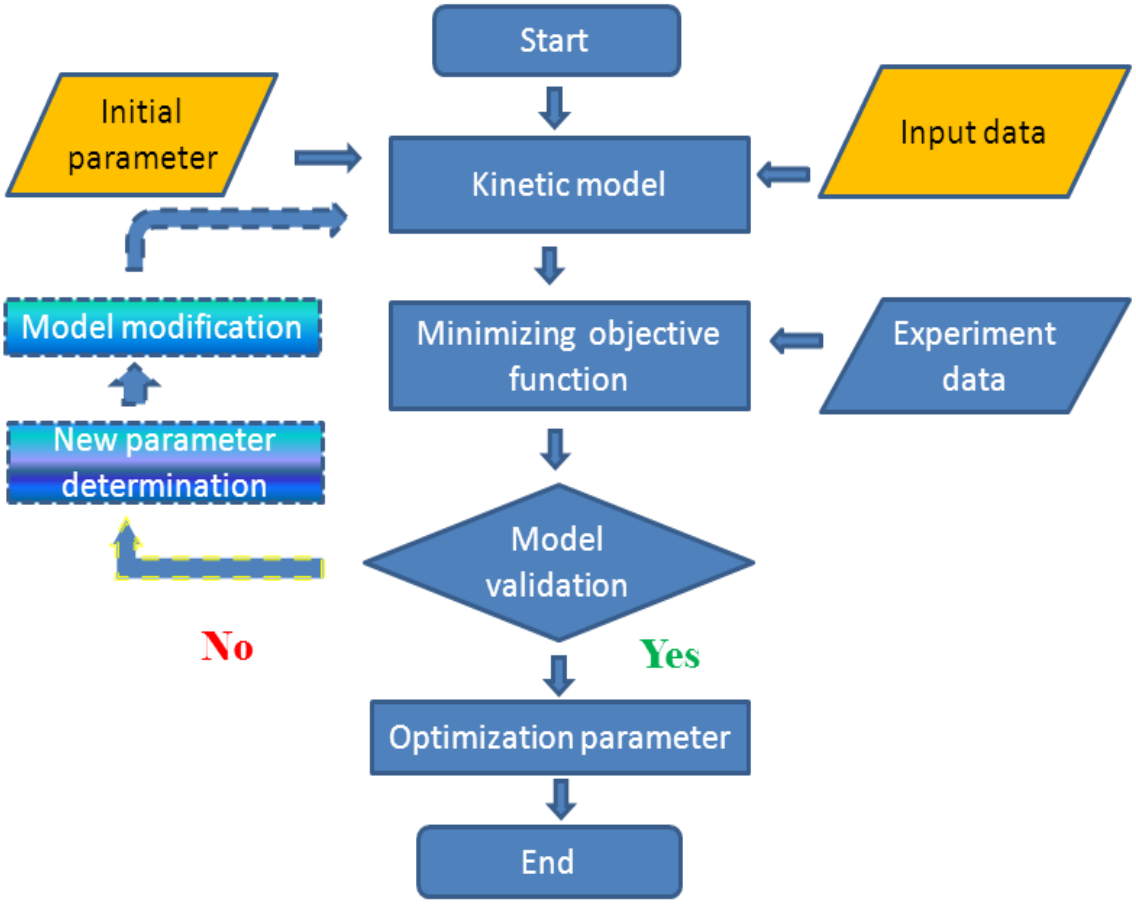

Figure 3-9 Flow chart of model solution

3.9 Conclusions

PE, PP, PET and their mixture were selected as feedstock in this PhD project, coupling with the treatment of samples in FBPR and TGA experiments. The procedure methods of FBPR and TGA were described to execute the experimental study, as well as product analysis methods. Response surface methodology is a good technique for the investigation of interactions of different process variables, and the reduction of the experimental burden. The kinetic lumping model methodology is used in this project. A unified reaction pathway was proposed comprising of primary pyrolysis and secondary cracking reactions with six discrete rate constants to solve the model development.

CHAPTER 4 PYROLYSIS OF PE, PP, PET AND THEIR MIXTURES

Summary

This Chapter presents the thermal conversion characteristic of HDPE, PE, PP, PET, and their mixtures via TGA. The optimisation and interaction effect of process parameters were studied in the experimental design by using RSM. Analysis of variance (ANVOA) corresponding to quadratic regression polynomial model was performed to study the interaction of feedstock components and temperature on the overall volatile yields distribution of the pyrolysis of flexible and rigid PE waste. Additionally, the effect of temperature and residence time (Appendix 2.10) on the yield distribution of gas, oil, wax, and solid residue were investigated via a lab scale fixed bed reactor, and the effect on the gas composition and oil property was analysed.

4.1 Thermal conversion characteristic of PE, PP, PET and their mixtures

As described in previous Chapters, waste PE, PP, and PET are the major components in plastic waste streams. PE and PP are pure hydrocarbons, so waste PE and PP can easily be a potential source for fuel generation and mitigate carbon emissions from fossil fuel. Thermal conversion of PE, PP, PET and their mixtures was carried out by using TGA in the temperature range of 450-550℃, shown in Table 4.1 and Figures 4-1 to 4-5. The degradation order of five samples at same reaction temperature is PET>PE/PP/PET >PP>PE/PP>PE. PP has the highest conversion over 99 percent in the primary pyrolysis reaction; PET pyrolysis shows the lowest volatile conversion between 80 percent and 85 percent. Nevertheless, PET pyrolysis shows the fastest pyrolysis reaction, however PE pyrolysis has slowest pyrolysis reaction. PE and PP pyrolysis did not generate clear char-like products, while over 13 percent of charring products were obtained from PET pyrolysis. A further investigation of HDPE thermal conversion was taken at the temperature range of 400-550℃. Figure 4-6 presents the yield change between 3.3 - 99.3 percent at different stages. HDPE pyrolysis shows highest degradation temperature in agreement with results in the literature [10, 127, 128]. An exceptional condition was observed that PE conversion is 95 percent at 550℃ comparing to yields of 97 percent and 98 percet at 450 and 500℃. This could be due to the presence of

carbonisation from the aromatic yield generated from branches of flexible polyethylene which mainly consists of LDPE. Figures 4-1 to 4-5 also show the main conversion temperature range, the carbon content and residue in the plastic polymer in relation to time span. The chosen samples only contain rare heteroatoms besides the intrinsic elements, which suggest that they are suitable for a pyrolysis process.

Table 4.1 Thermal conversions of PE, PP, PET and their mixtures via TGA

	Temperature (℃)	Volatile (%)	Solid residue (%)
PE	450	98.06	1.84
PE	500	98.26	1.76
PE	550	95.39	4.61
PE/PP	450	97.55	2.65
PE/PP	500	96.98	3.12
PE/PP	550	97.01	2.98
PE/PP/PET	450	93.15	6.85
PE/PP/PET	500	96.31	3.69
PE/PP/PET	550	96.14	3.86
PET	450	83.12	16.88
PET	500	86.86	13.14
PET	550	86.07	13.93
PP	450	99.33	0.71
PP	500	99.37	0.64
PP	550	99.49	0.55

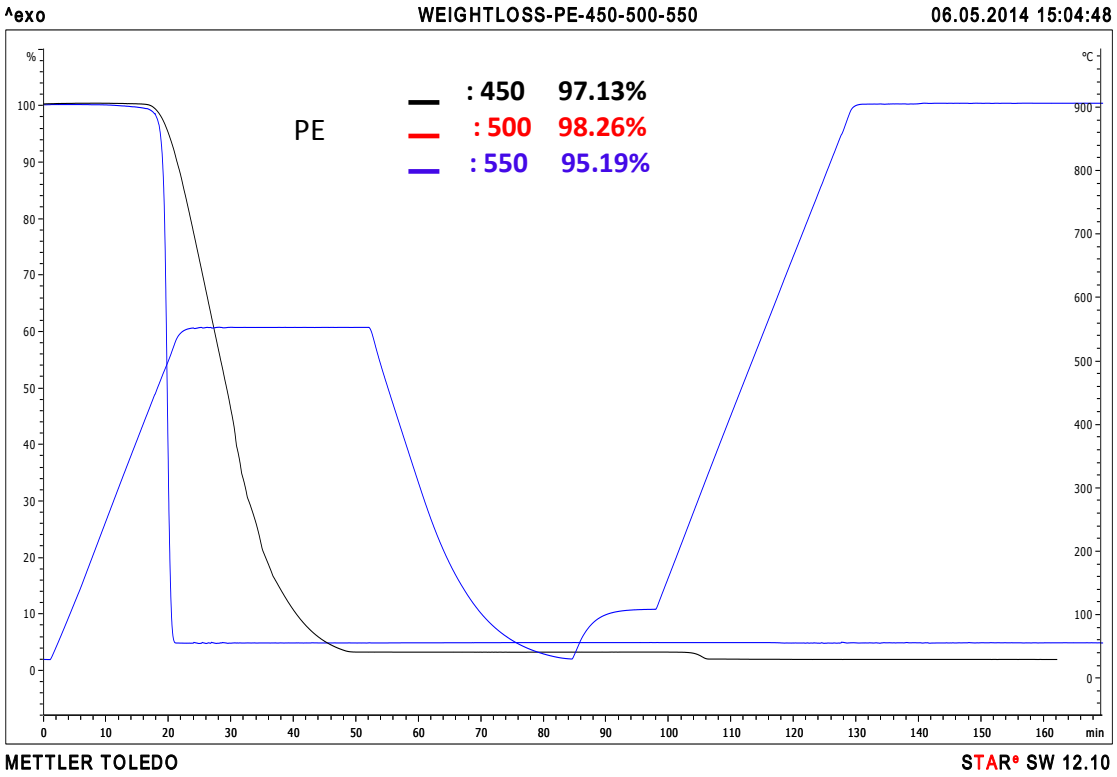

Figure 4-1 Weight loss of PE pyrolysis via TGA

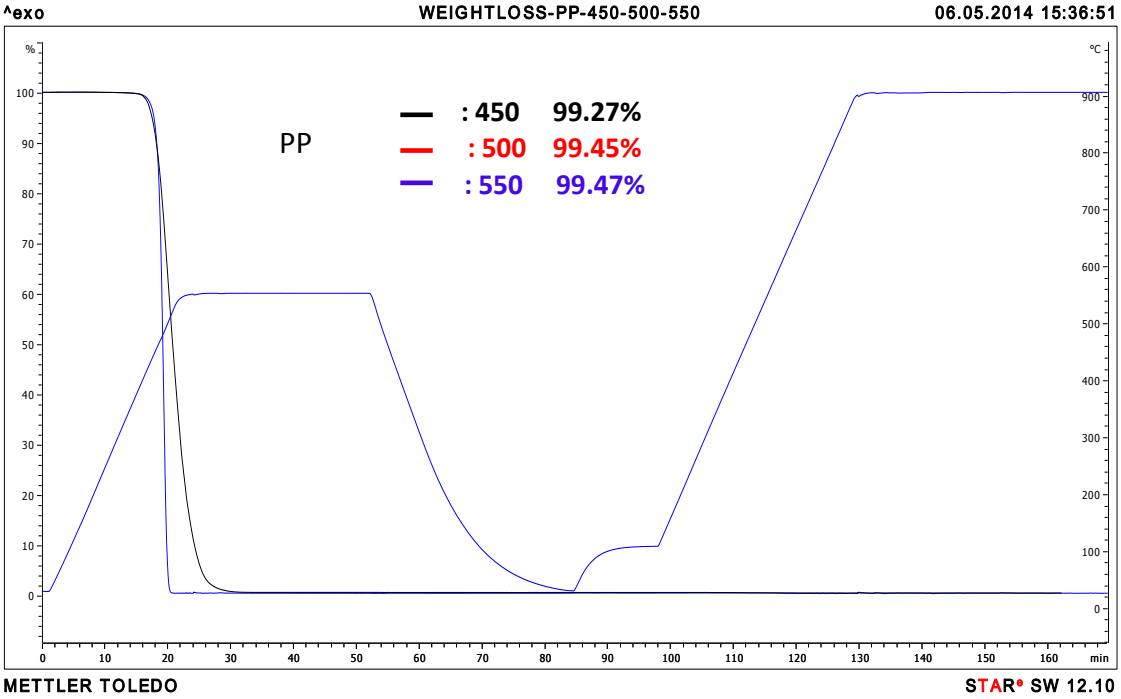

Figure 4-2 Weight loss of PP pyrolysis via TGA

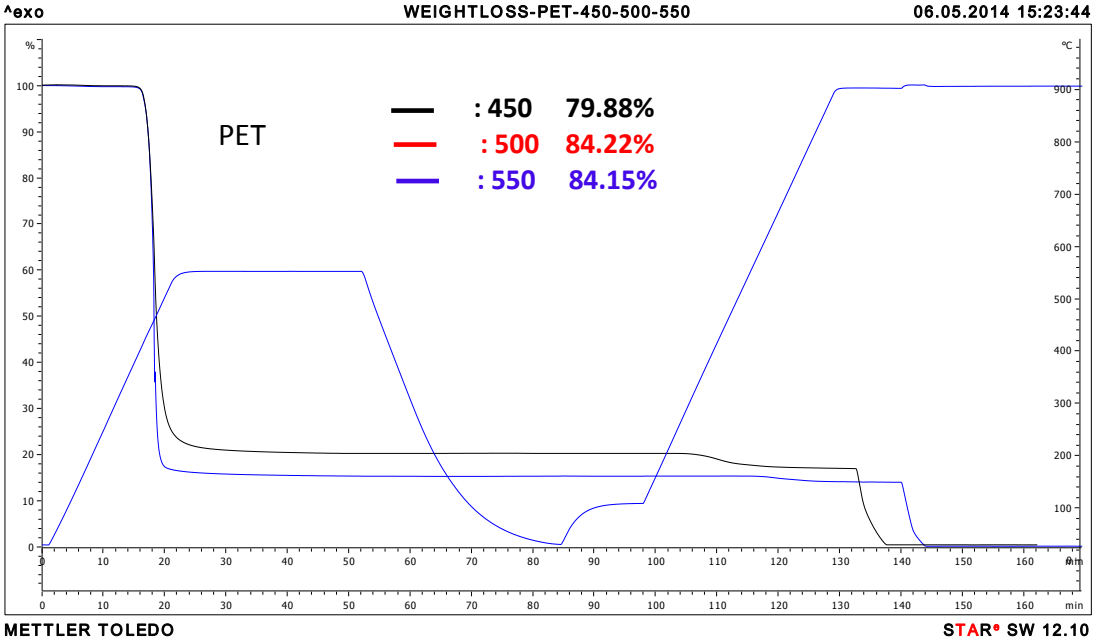

Figure 4-3 Weight loss of PET pyrolysis via TGA

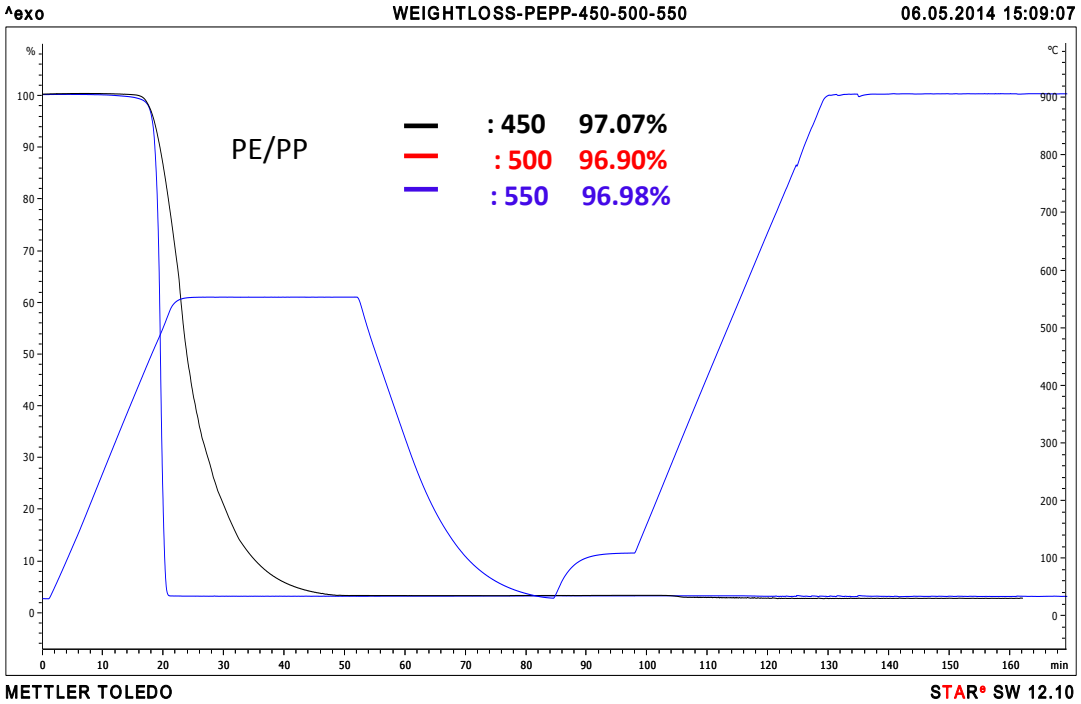

Figure 4-4 Weight loss of PE/PP pyrolysis via TGA

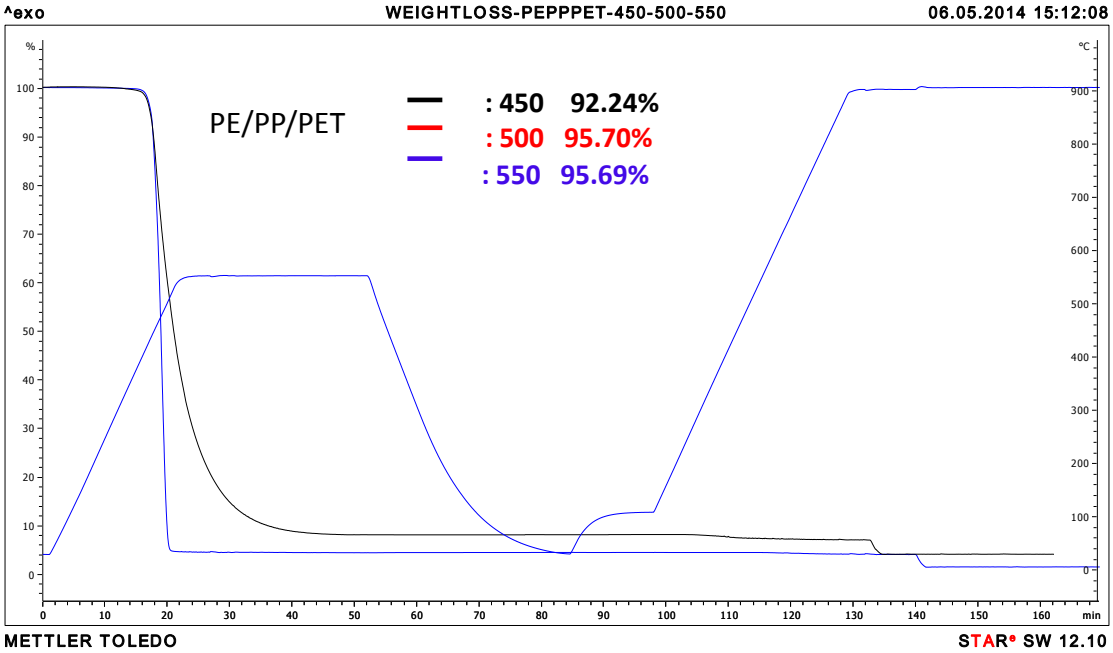

Figure 4-5 Weight loss of PE/PP/PET pyrolysis via TGA

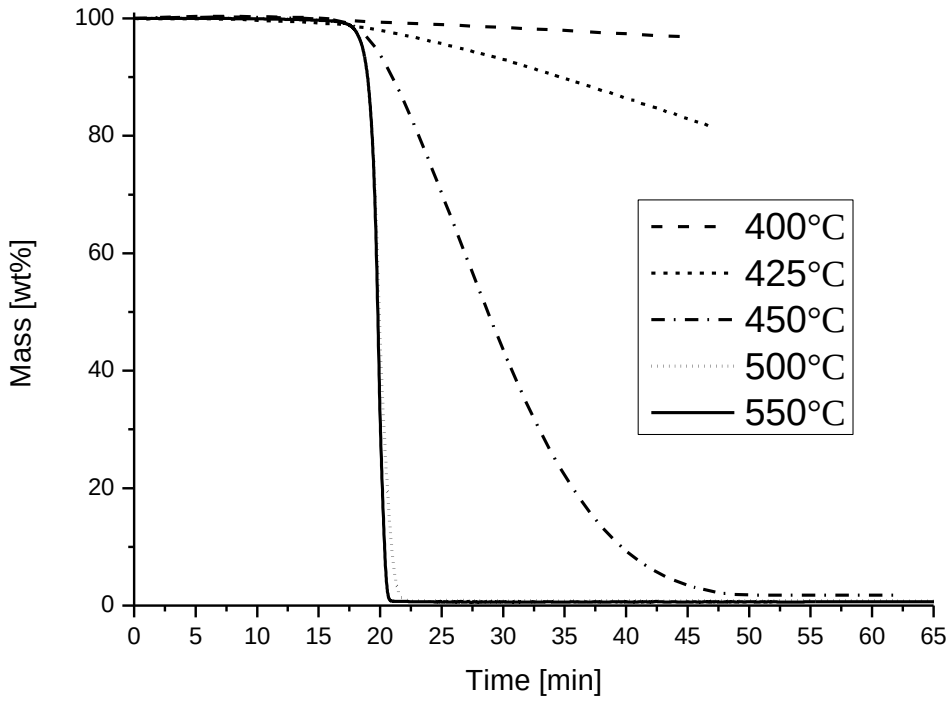

Figure 4-6 Weight loss of waste HDPE pyrolysis via TGA

4.2 Analysis and optimisation of the interaction effect of process parameters on the pyrolysis process

As mentioned in Chapter 3, RSM is a good technique in selecting optimal experimental conditions to obtain the desired product yield, and the reduction of a large number of experiments by optimising the multiple influence factors [129]. Kumar and Singh [129] used RSM to predict optimised process parameters for catalytic pyrolysis of waste HDPE into fuel to find the best conditions of temperature (450℃), the acidity of catalyst (0.341) and catalyst to feeding rate (1:4). Pinto et al [123] studied the maximisation of liquid yields from the pyrolysis of waste mixtures in the optimum of reaction temperature, time and initial pressure. In this work, pyrolysis of waste flexible and rigid polyethylene was studied to examine the optimum process conditions to obtain maximum volatile yield.

Table 4.2 Central composite design (CCD) matrix and yield response

		Actual variables		Coded levels		Response
Run	Type	Temperature (A) (℃)	Ratio(FPE: RPE) (B) (wt%)	A	B	Volatile Yield (wt. %)
1	Centre	500	50:50	0	0	96.68
2	Axial	550	50:50	1	0	96.61
3	Factorial	550	0:100	1	-1	99.25
4	Factorial	550	100:0	1	1	93.38
5	Factorial	450	100:0	-1	1	93.23
6	Factorial	450	0:100	-1	-1	98.36
7	Axial	500	0:100	0	-1	99.22
8	Axial	500	100:0	0	1	93.24
9	Axial	450	50:50	-1	0	96.68
10	Centre	500	50:50	0	0	94.68
11	Centre	500	50:50	0	0	96.68
12	Centre	500	50:50	0	0	96.683
13	Centre	500	50:50	0	0	96.6843

Additionally, the effect of multi process conditions on the product yield distribution was studied by using face central composite design (FCCD) in RSM. Temperature and feed ratio of PE waste were selected as actual variables to optimise the process parameters.

The factorial study investigation showed the volatile yields from the pyrolysis of different ratios of flexible and rigid polyethylene. The experimental results were treated as actual factors and input to *Design Expert* software to generate 13-experiment-matrix showing the variation of volatile yield from 93.2% to 99.3%. These actual factors were then developed as coded factors to fit a polynomial model using quadratic regression analysis, which is:

$$\bar{Y} = 96.58 + 0.46(A) - 2.83(B) - 0.19(A)(B) - 0.57(A^2) - 0.09(B^2) \qquad (4.1)$$

where $\bar{Y}$ is the yield of volatile products, A is the temperature, and B is the feed ratio of flexible PE and rigid PE.

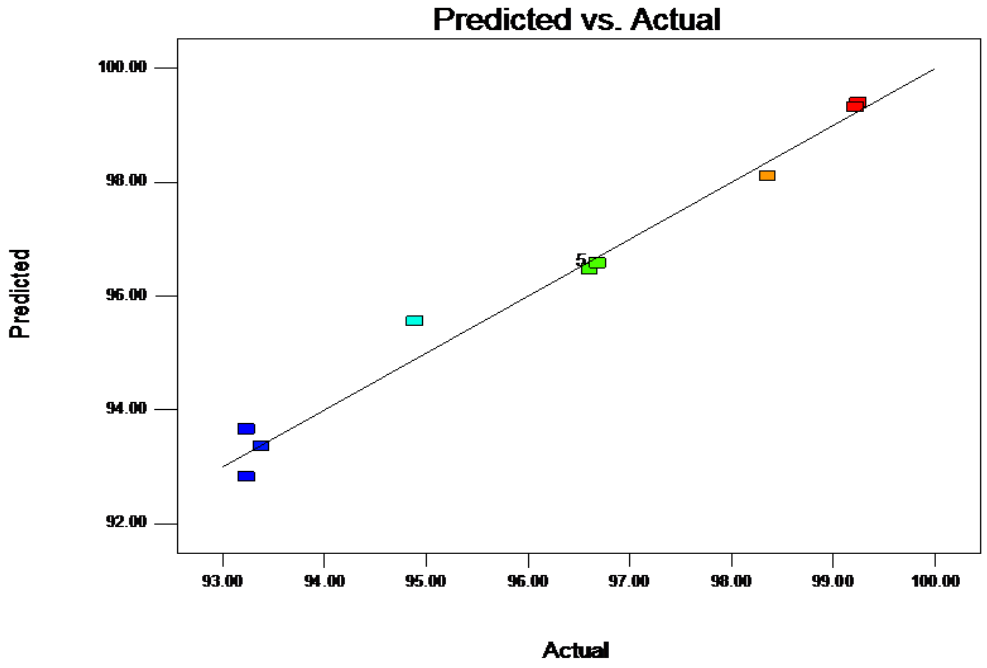

Figure 4-7 The actual and predicted plot for temperature and feed ratio during pyrolysis reaction

The analysis of variance corresponding to Eq.4.1 is reported in Table 4.3. The model f-value of 73.83 implies the model is significant with only a 0.01% chance that a "model f-value" could occur due to noise. Values of "Prob > F" less than 0.050 indicates that model terms

are significant. In this case *A, B* and A^2 are significant model terms. Values greater than 0.100 indicate the model terms are not significant. Based on the Eq.3.2 (Chapter 3), the actual and predicted plot for temperature and ratio of feed is shown in Figure 4-7. The "pred R-Squared" of 0.84 is in reasonable agreement with the "adjusted R-Squared" of 0.97. Adeq precision measures the signal to noise ratio, its value of 26.14 (greater than 4) is desirable, which indicates an adequate signal that this model could be used to navigate the design space.

Table 4.3 ANOVA for Response Surface Quadratic Model

Source	Sum of Squares	df	Mean Square	F-Value	p-value	
Model	50.6	5	10.12	73.83	< 0.0001	significant
A-Temperature	1.26	1	1.26	9.23	0.0189	
B-Ratio of feed	48	1	48	350.22	< 0.0001	
AB	0.14	1	0.14	1.01	0.3478	
A^2	0.89	1	0.89	6.48	0.0384	
B^2	0.022	1	0.022	0.16	0.6985	
Residual	0.96	7	0.14			
Lack of Fit	0.96	3	0.32			
Pure Error	0.00	4	0.00			
Cor Total	51.56	12				

R-Squared=0.9814; Adjusted R-Squared=0.9681; Pred. R-Squared=0.8366; Adeq Precision=26.142; PRESS=8.42.

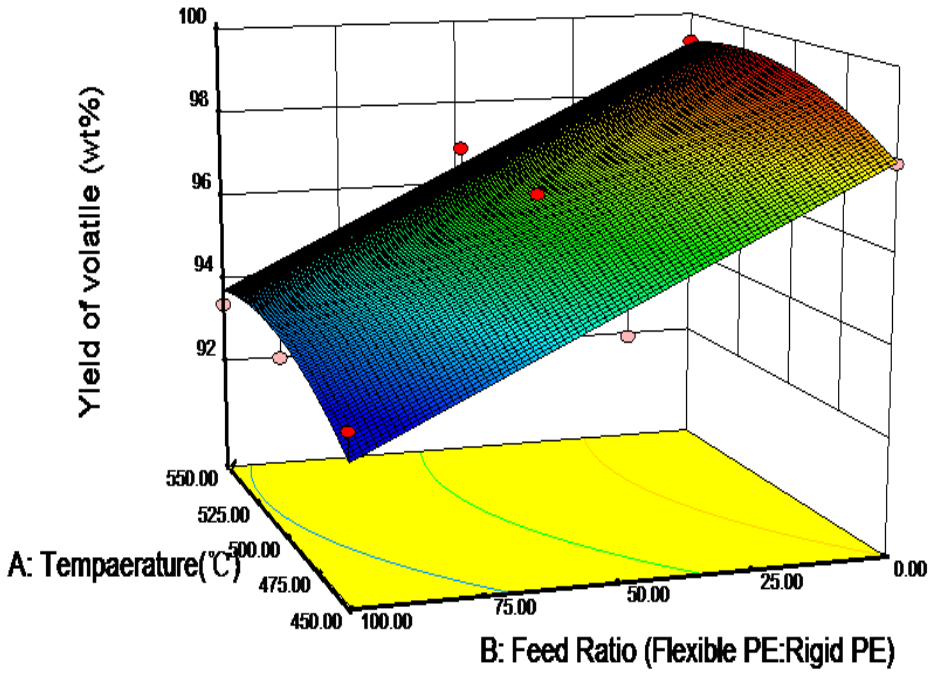

Figure 4-8 3-dimensional response surface plot of volatile yield with the combined effect of the temperature and the ratio of feed at the heating rate of 25℃/min and the residence time of 30 minutes

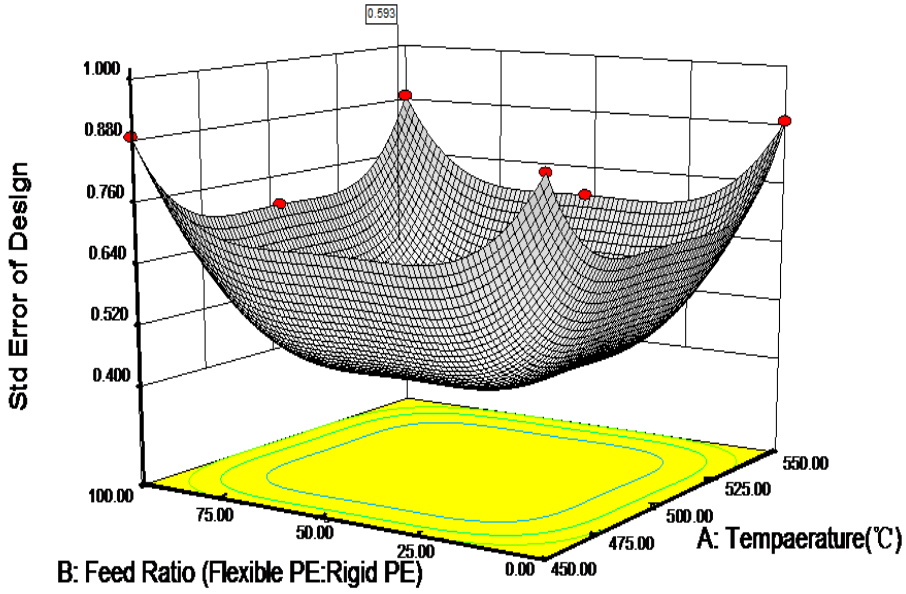

Figure 4-9 3-dimensional response surface plot of the standard error with the combined effect of temperature and ration of feed

The combined effect of temperature and feed ratio on the volatile yield is shown in Figure 4-8. The figure shows the increase both of temperature and the ratio of rigid PE improved the yield of volatile products. The highest yield occurred at 100% of rigid PE sample with the peak temperature range of 550℃ at a heating rate of 25℃/min and residence time of 30 minutes. A flat bottom (Figure 4-9) in the bowl-shaped 3-dimension surface of the standard error of 0.593 indicates a satisfactory result for RSM design for chosen plastic pyrolysis.

4.3 Degradation characteristic of flexible and rigid polyethylene at different ratios

As mentioned in section 4.2 and the calculation of mass balance (Appendix 2.11), more volatile yields can be recovered from RPE thermal degradation. It indicates that the composition of feedstock is the principal factor that determines the degradation of the polymer, unlike controllable variables such as reaction temperature, residence time etc. Figure 4-10 shows thermal degradation behaviour of flexible and rigid polyethylene at five different feed ratios, whose FPE proportion in the mixture are 100%, 33.3% (M1), 50% (M2), 66.7%(M3) and 0.0%. FPE, mainly formed by LDPE, has the lowest volatile yield, on the other hand, RPE, mainly formed by HDPE, shows the highest yield at same process condition. The volatile gradually shows a rising trend with temperature increasing at five feed ratios of FPE and RPE. However, the volatile yield of M1 decreases when the temperature increases from 500 to 550℃. The conversion of M1, M2 and M3 shows narrower gaps comparing pure FPE and RPE. The results indicate drag effect between FPE and RPE in the pyrolysis process. It is possible due to that the presence of excessive side chain and shorter chain in FPE polymer and the additives from LDPE easily lead to chain cyclisation and aromatisation during the thermal degradation, so that carbonisation can happen at a higher temperature. Mlynková et al[130] reported that aromatics content from LDPE, linear LDPE (LLDPE) and PP can reach up to 40 mass %, which indicates the presence of more short chains and branch chains in LLDPE and LDPE polymer clearly generated more aromatics than minimal branch chains in HDPE during the pyrolysis process.

4.4 Temperature effect on product distribution

Figures 4-11 to 4-14 show the yields of gases, liquids, waxes and solid residues observed from the pyrolysis runs with mass balance analysis (Appendix 2.8). The pyrolysis of PE

waste is slower than PP waste at the same reaction temperature. This could be due to the presence of methyl group in the PP molecule structure making for lower molecule thermal stability, and lower activation energy than PE molecule during the bond cleavage; additionally, methyl group becomes tertiary and chain scission occurs mainly between secondary and tertiary carbon atoms. Gao [39] proposed that temperature increase strengthens molecular vibration to overcome the Van der Waals force, once this force induced energy exceeds the bond enthalpy between atoms in the polymer molecule structure, the molecule will start to rupture. The cleavage of molecular chain starts at most unstable bonds in the molecule structure. Methyl group bonding in PP molecular chain is less stable than hydrogen. Therefore, PP polymer is easier to decompose than PE polymer. Uddin et al [131] also demonstrated that the molecular weight distribution of residue liquid obtained from LDPE is increased lower than that of HDPE, indicating that thermal degradation reaction is more difficult in HDPE than in LDPE. It is clear that polymer molecular structure affects the reaction mechanism and product distribution.

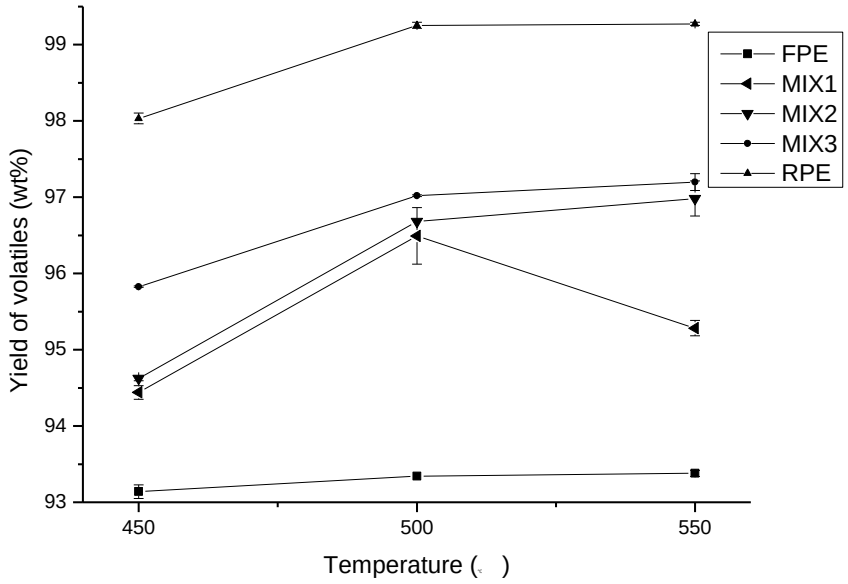

Figure 4-10 Degradation behaviours of FPE and RPE at different ratios (FPE: flexible polyethylene; RPE: rigid polyethylene; M1: FPE: RPE=2:1; M2: FPE: RPE=1:1; M3: FPE: RPE=1:2)

Nevertheless, gas and oil/wax yields of PE, PP and PE/PP mixture presented similar reaction trends, as they all followed the same decomposition mechanism--random chain scission. With temperature increase, the yields of gas, oil and wax also increase respectively. PE/PP mixtures yielded gas and oil/wax fractions between those for pure PE or PP, so the product distributions for pyrolysis of waste plastic mixtures is predictable which benefits the design of thermal degradation processes for plastic mixtures in the real world.

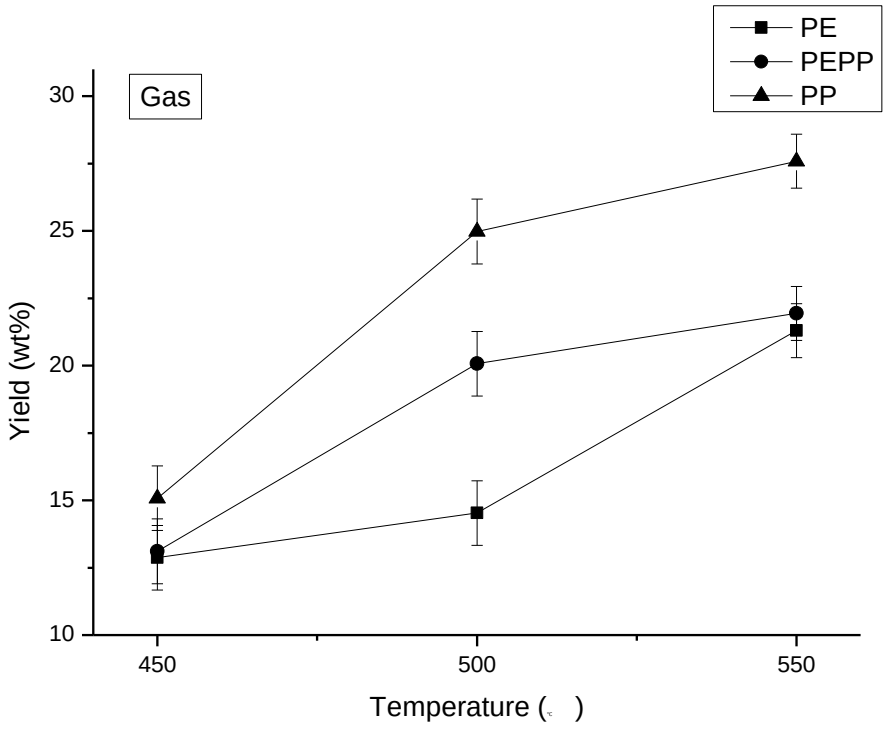

Figure 4-11 Gas yields from PE PE/PP and PP pyrolysis

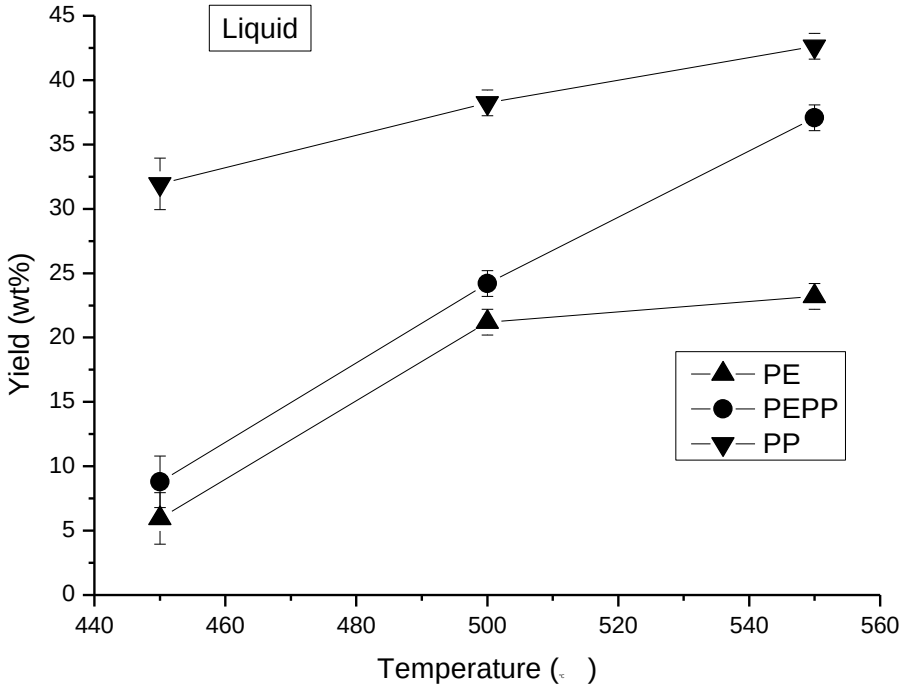

Figure 4-12 Liquids yields from PE PE/PP and PP pyrolysis

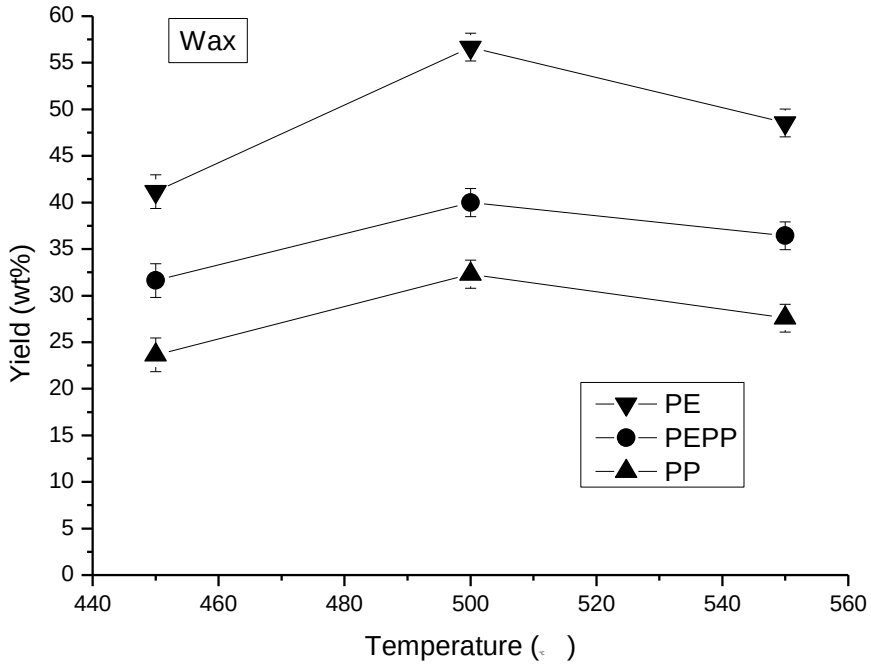

Figure 4-13 Wax yields from PE PE/PP and PP pyrolysis

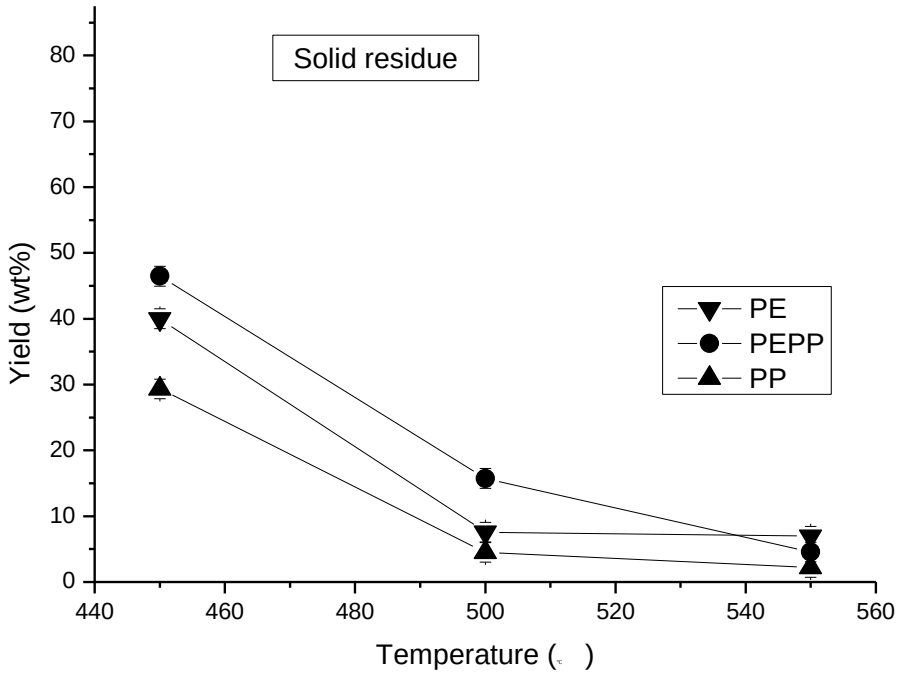

Figure 4-14 Residue yields from PE PE/PP and PP pyrolysis

Cracking reactions (secondary reactions) of heavier fractions (e.g. waxes) probably exist in the reactor in a temperature range of 450-550℃. Conesa et al [132] investigated the HDPE primary decomposition and wax cracking reactions at the temperature range from 500℃ to 900℃, and deduced that the primary pyrolysis of the HDPE in the condensed phase took place through a free radical transfer that leads to low yields of gases, and high yields of waxes. Kaminsky et al[10] also mentioned that β-scission of primary unstable molecular fragments (radicals and ions) in the plastic pyrolysis produces oligomers during the further decomposition reactions with un-cracked polymer molecules or radicals and ions, and the possibility of formation of aromatics by Diels-Alder reactions is greater at higher temperatures.

Furthermore, real plastic waste (PE and PP) from the commercial market probably contains a variety of additives (e.g. stabilisers, pigments, fillers) which have various functional groups (e.g. -OOH, -CO-, phenyls, phenols, amines, sulphur, organic metal salts). These groups readily decompose to form free radicals and affect the decomposition mechanism [133], and also modify the product distribution and selectivity. At the termination step of the cracking

mechanism, it is possible that wax generation and carbonisation occurs between primary products and radicals [134] and also leads to the presence of solid residuum [10].

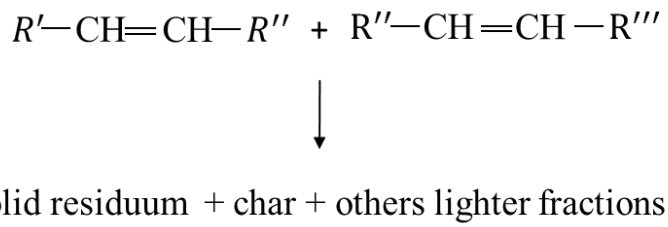

Figure 4-15 shows the pyrolysis behaviour of waste PET at different temperatures. Gases and solid powder are the main products and yields increase with temperature. Wax/oil is an insignificant fraction in the thermal conversion of PET. The presence of oxygen in the PET molecule structure dominates the product distribution; carbon dioxide was generated from the decarboxylation of the PET, also carbon monoxide may be formed via either decarboxylation or reaction between carbon dioxide and char [10, 135]. Due to the limitation of time and the availablity of analysing facility, the solid powders and char were not analysed in this study.

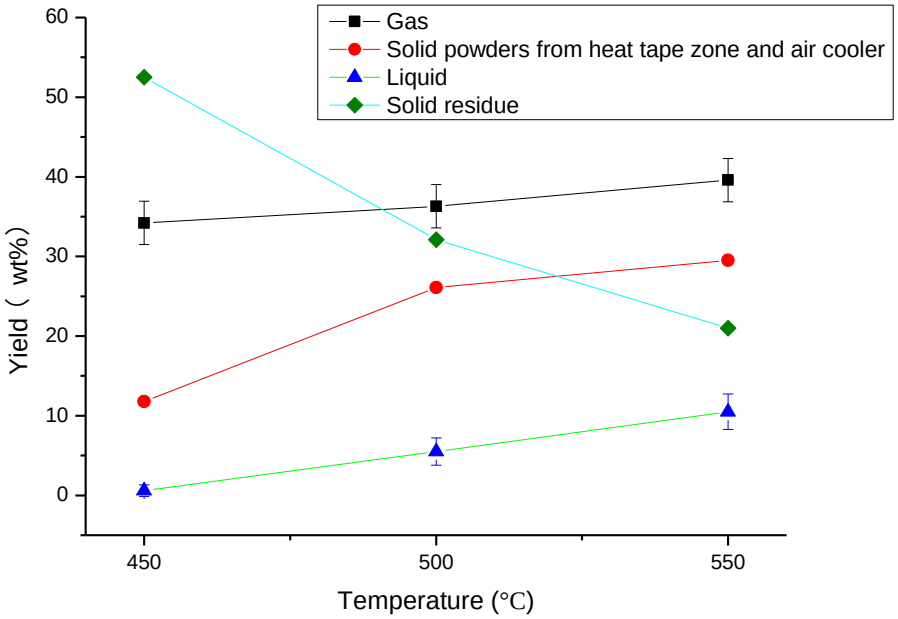

Figure 4-15 Thermal degradation of PET at 450, 500 and 550℃

To obtain a better understanding of the product distribution, oil and wax products from the pyrolysis of PE, PP and PE/PP mixture were analysed using Fourier transform infrared spectroscopy (FTIR) (Figures 4-16 & 17). The area of the spectrum band observed was at a function group region between 3100-2850 cm^{-1} and a fingerprint group region between 1600 and 550 cm^{-1}. A weak intensive peak at 3070 shows the presence of =C-H stretching vibration of the unsaturated alkene and the aromatic ring, especially in the oil/wax products of PP pyrolysis. Medium peak ranges of 2957-2952 cm^{-1}, 2872 and 2871 cm^{-1} show the presence of $-CH_3$ of the saturated alkane. The band range of sharp peaks between 2924-2914 cm^{-1}, and medium peaks of 2844-2842 cm^{-1} and 2850 cm^{-1} indicate the presence of the asymmetric and symmetric stretching vibrations of the $-CH_2$ and -C-H groups in short and long chains of alkanes. Therefore, just as other researchers reported [37, 136], the temperature is the most important process parameter influencing the thermal degradation of plastics. Product distribution and operational productivity can be modified with temperature increase during the pyrolysis process, because reaction pathways involving the free radical chain reactions (initiation, propagation, termination) can change with temperature.

At fingerprint group region, the peaks at 1650, 1649, 1642 and 1641 cm^{-1} wave numbers represent the -C=C- of alkenes stretching vibration, the wavenumbers of 1458, 1457 and 1456 cm^{-1} are assigned to the presence of asymmetric and symmetric internal C-H bending vibrations of CH_3 and $-CH_2$ groups of aromatic and alkenes. The peaks of wavenumbers at 1377 and 1376 cm^{-1} are caused by the internal bending vibration of methyl groups. The significant absorption band at 909 cm^{-1} was observed due to the =C-H external bending vibration of singly substituted alkenes.

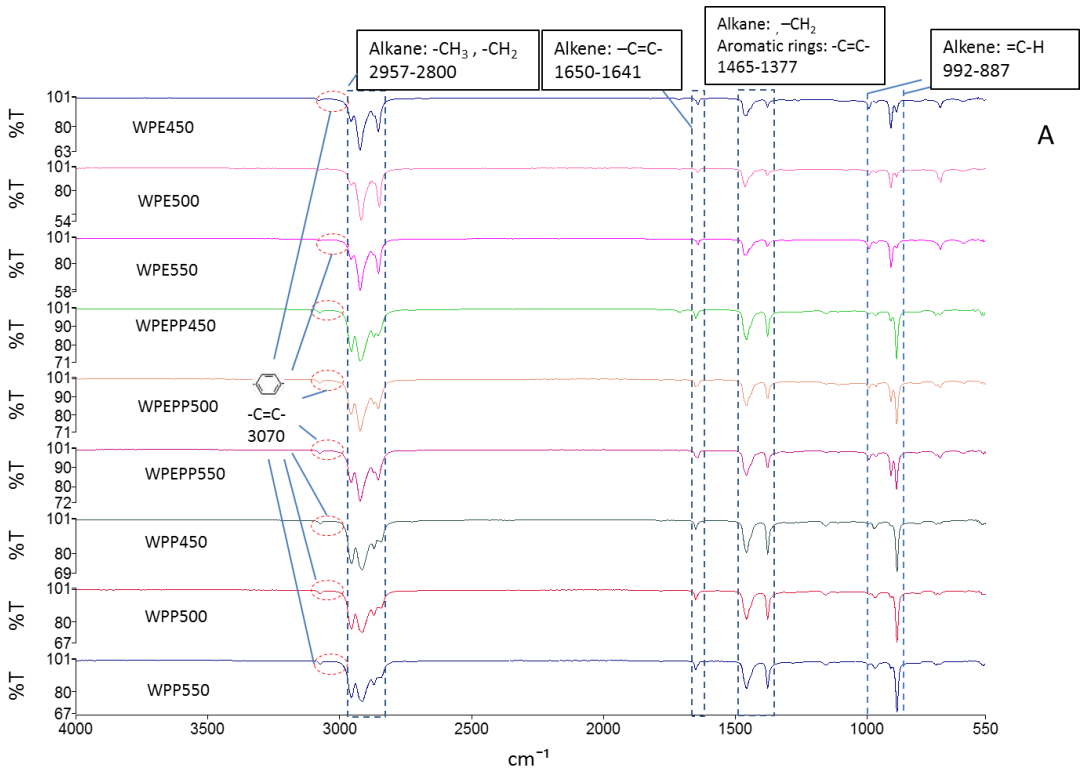

Figure 4-16 FTIR of waste PE pyrolysis light oils collected from the receiver

The peak area of 722-719 cm^{-1} was observed due to the C-H external bending vibrations of aromatics and the $–CH_2$ rocking of an alkane. Meanwhile, other significant peaks were also observed from =C-H external bending vibration absorptions, including the wavenumber range of 972–969 cm^{-1} of trans-substitute alkene, 992-991cm^{-1} of single substitute alkene and C (CH_3), $CHR=CH_2$ and CHR=CHR in the skeleton chain of the alkenes, the peaks at 888-886 cm^{-1} with the presence of carbon di-substitute group of aromatics, the peak at 738 cm^{-1} from 4,5 adjacent hydrogen atoms of aromatics, respectively. Moreover, the peak at 1156 cm^{-1} represents the C-O stretching vibrations of alcohols, ethers, carboxylic acids and esters, the peak wavenumber at 1018 cm^{-1} shows the R-O stretch of aromatic ethers. The control of gaseous product distribution and yield in relation to the temperature is an important step in thermal pyrolysis of plastic waste. Higher yields and near-ideal product distributions can gain a better financial return and enhance the public awareness of the pyrolysis process. An analysis was made to examine the gas composition distribution during the pyrolysis of PE, PP, PET, and their mixtures, which are shown in Figures 4-18 to 4-20.

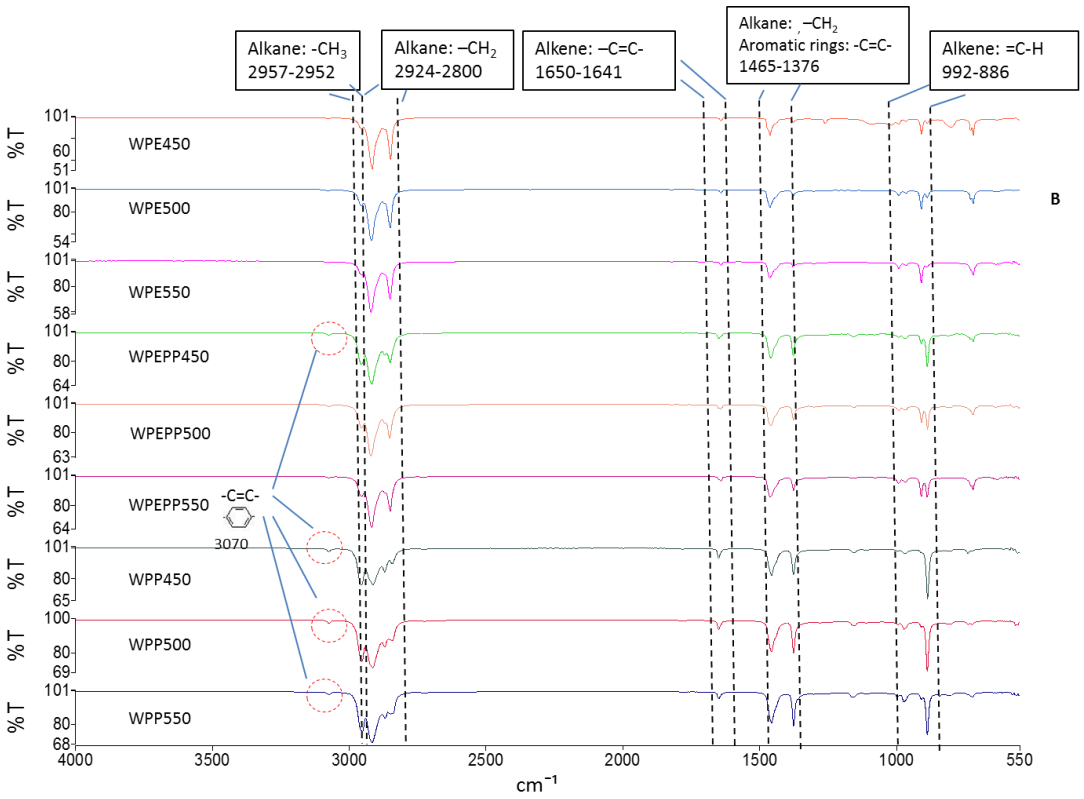

Figure 4-17 FTIR of waste PE heavier pyrolysis oils collected from hot trap

It was noticed that ethylene has a higher yield at three reaction temperatures, followed by methane during PE and PP pyrolysis. At the temperature of 450℃, ethylene generated from PE pyrolysis was clearly higher than those in PP and PEPP mixtures, the difference decreased with temperature increase. Methane, hydrogen, and carbon dioxide showed similar yield distributions at three different temperatures. Due to the limitation of calibration gas in MS analysis, only hydrogen, methane, and ethylene, were analysed in the study.

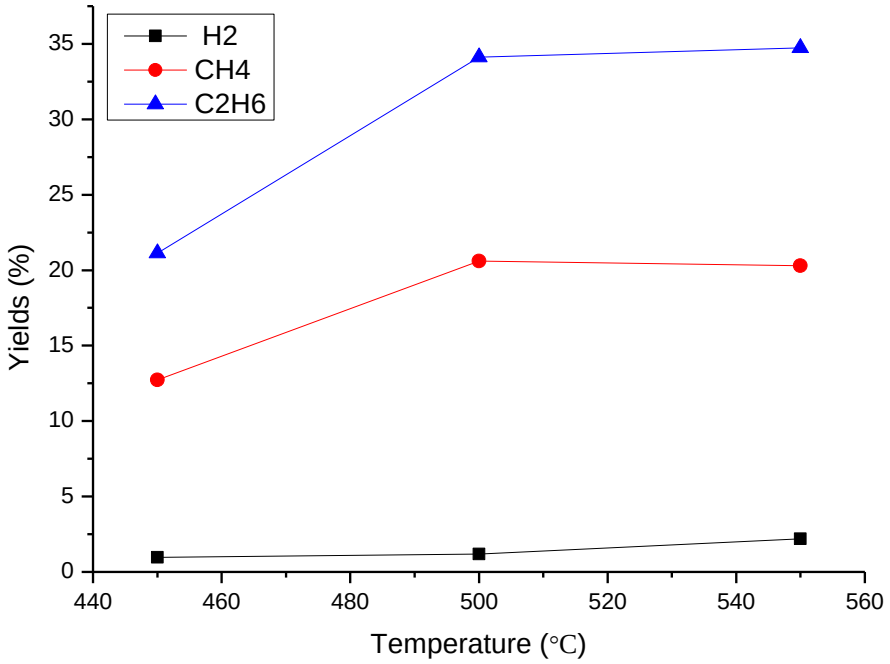

Figure 4-18 Gas composition distribution observed from waste PE pyrolysis

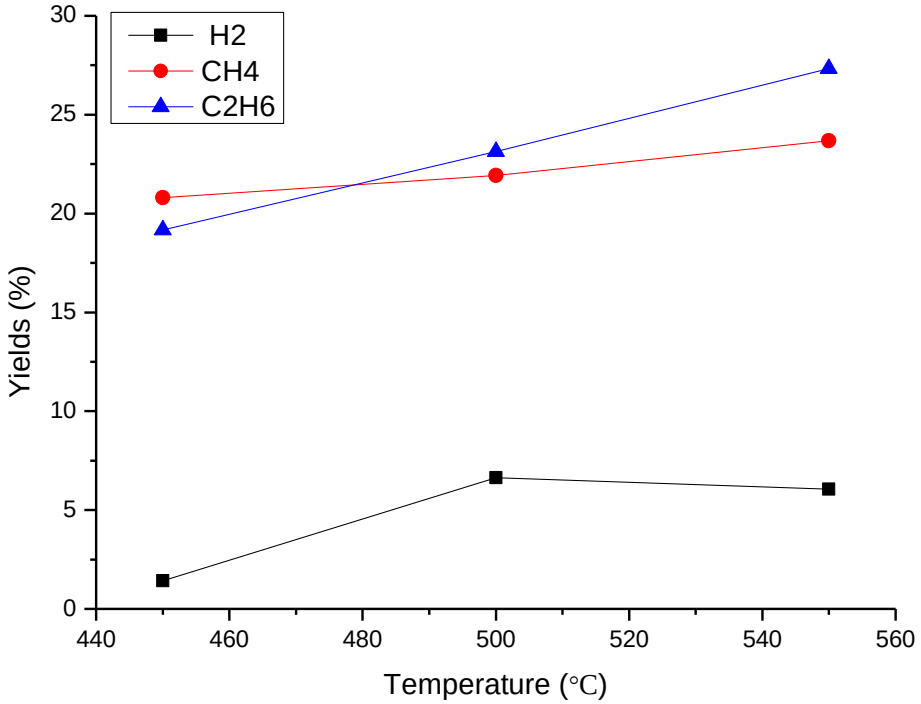

Figure 4-19 Gas composition distribution observed from waste PP pyrolysis

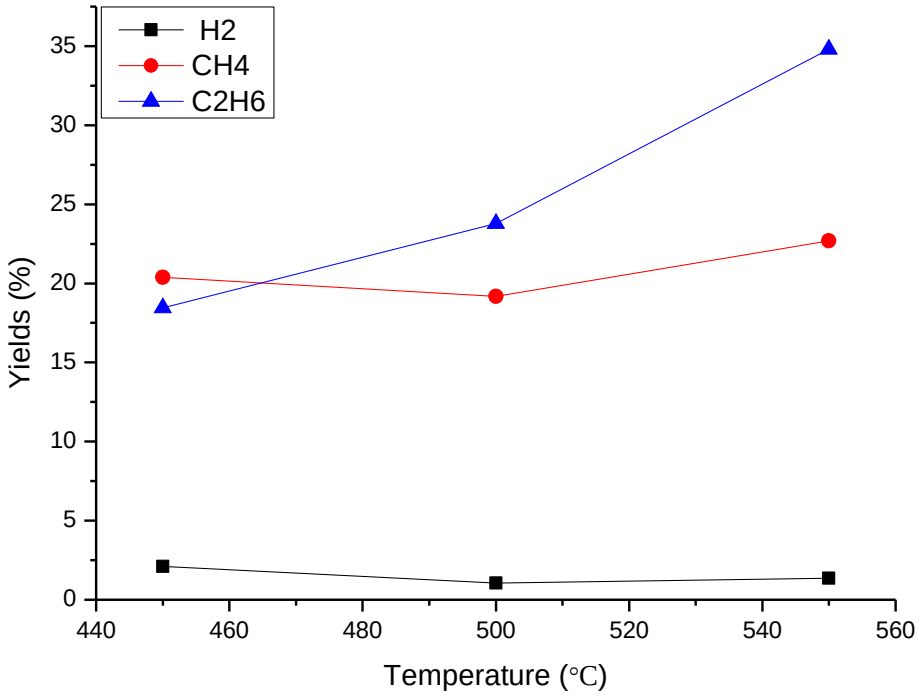

Figure 4-20 Gas composition distribution observed from the pyrolysis of PE/PP mixture

4.5 Conclusions

Response surface method is a good technique to analyse and optimise interaction effect of process parameters on the pyrolysis process to reduce the experimental numbers, resulting in the reduction of experimental numbers and the saving of operational cost and time. TGA experimental study has shown that waste PE, PP, PET are valuable material to generate hydrocarbons and other chemicals, which can be obtained with over 84% volatiles. TGA runs also provide useful information for experimental condition setup in a fixed bed pyrolytic reactor. The study of thermal conversion behaviour of PE, PP, PET and their mixtures via TGA and FBPR indicates that temperature range of 450-550℃ is a better choice to undertake their pyrolysis process. The experimental results from FBPR showed similar yields distribution obtained from TGA at same reaction conditions, which give valuable information for a scale-up process, and also indicates what the difference exists in two process devices, and provide potential solution to get better cost-effective process technology. Temperature effects on yield distribution were studied based on the gas, oil, wax and solid residue of PE,

PP PET and their mixtures, which shows that temperature dominates the product distribution in the process. Moreover, the yield difference from thermal degradation of flexible PE and rigid PE with different proportions indicates that the interaction effects between components in the plastic mixture are plausible.

CHAPTER 5 THE EFFECTS OF REACTION PATHWAY SIMULATION AND LUMP SELECTION ON THE KINETICS ESTIMATION OF WASTE PLASTIC PYROLYSIS

Summary

In this Chapter, the discrete lumping model was employed to investigate reaction kinetics of the pyrolysis of waste HDPE. A reaction network comprising a set of parallel reactions coupled with secondary reactions has been used in the model to examine the pyrolysis characteristic of HDPE decomposing into gas, liquid, wax, and solid residue. The estimation of apparent kinetic parameters was discussed, which is affected by the reaction pathways proposed and lump selection.

5.1 Introduction

Studies of chemical kinetics of pyrolysis reactions can offer the information how experimental conditions affect the thermal conversion process, determine the rates of overall and/or individual elementary reactions, and provide the evidence of reaction mechanism, as well as the construction of mathematical models to describe the characteristics of the decomposition reaction. Kinetics estimation is a complicated procedure for a complex reaction scheme, involving various effects from the nature of feedstock and process conditions. Particularly, the variety and uncertainty of the components existing in the plastic waste distinctively increases the difficulties identifying the reaction pathways of the overall pyrolysis process. Moreover, the presence of heteroatoms (i.e. chloride and sulphur) in the upgraded products is unavoidable which reduces the quality of the product properties and corrode the equipment. Those, therefore, constrain the engineering design of plastic pyrolysis processes that requires a clear comprehension of reaction kinetics in the processes. Computer simulations for the polymer pyrolysis to attack those impacts have been widely reported by many authors. The mathematical models developed in the description of chemical kinetics can also be useful in the design or modification of reactors to optimise product yield in the chemical process, as well as products separation efficiently. While kinetic modelling of the approaches to commercial refining processes is not easy tasks

because of process complexity. The simulations for pyrolysis process need to address the availability and reliability database of elementary variables involved in the chemical process. They cannot be precisely described by a one-fits-all model to predict reactions, even though it may minimise the computational costs in model simulation. Apart from this, the kinetics of pyrolysis process must be also combined with reactor hydrodynamics, mass and heat transfer, and momentum in addressing practical problems.

HDPE waste usually contains fewer additives and fillers comparing LDPE in their commercial application, and generate narrower product distribution comparing to PP at same condition because the presence of methyl group in PP molecular chain may result in more branch hydrocarbons. In this Chapter, kinetic model development of the pyrolysis of waste HDPE was selected to address kinetics variation under the selection of possible reaction pathways by using Arrhenius law. The effect of proposed reaction pathways on the estimation of kinetic parameters will also be investigated based on the lumping model.

Thermal degradation of HDPE polymer is characterised by large free radical reaction networks [137]. The determination of individual rate parameters for the elementary reactions involved in polymer pyrolysis is impossible because they are rapid and compete with numerous other reactions and process variables [138]. Lumping methodology is one of the main solutions for exploration of the mechanism of pyrolysis reactions [8, 42, 72, 138-140]. Moreover, the information of reaction pathways and kinetics can be assessed by using representative model compounds (pseudo components) based on experimental data using the lumping models.

In order to ensure the efficient control of the reaction level, and to reduce operational cost, the polymer was treated as only reactant lump in the pyrolysis process, the reaction rate being directly proportional to the concentration of the reactant. Thus, many researchers are practically inclined to assume the thermal degradation as a first–order reaction in the studies, even though most reactions do not have exact or constant reaction order as they may not obey the power-law rate equation properly [141]. Ding et al [42] studied mixed plastic waste at a lower temperature range of 380-420℃ via first order reaction to examine their kinetic parameters and reaction rates. However, Wu et al [142] investigated the pyrolysis kinetics of six principal plastic materials of municipal solid waste (MSW) and their mixtures via

reaction order of 0.5.

In chemical kinetics, reaction order commonly shows the reactant concentration effects on the reaction rate. Identification of reaction order by experiment is helpful to determine the reaction mechanism of thermal decomposition; while the real reaction order may be dominated by polymer structure, operational conditions, the presence of heteroatoms and other components in the polymer. The kinetics estimated by first-order differential reaction in the polymer pyrolysis have been successfully used in engineering designs and scale up processes [10, 38]. Therefore, an understanding of the determination of reaction order and reaction pathway of the pyrolysis helps our apprehension to cognise the kinetic characteristic of plastic degradation.

In most kinetic lumping studies, lumping methods in which grouped pseudo-species are based on their chemical structure or reactivity [57, 72, 143]; or approaches where formal rules for transformation between original and lumped variables are mathematically defined [98, 111, 144]. The lumping methods require extensive chemical expertise and more variables to explore the lumping structure [143]. There are many researchers such as Kruse et al [90], Singh et al [145] and Westorhout [62], who used the lumping methodology in their work. A transformation method was initiated by Wei and Kuo [110], later developed by Li and his co-workers to define linear and nonlinear lumping schemes [111, 116, 118], which reduce a continuous system to a finite dimension system conveniently actualised in the computer with a global variable. The criterion for the lumping approach is based on statistical information, characteristic information, or pseudo components. The lumping scheme has, therefore, been shown to be an effective approach to model reduction with intermediate time-scale separation during the process and fewer process variables. Samples of extensive lumped kinetic models can be seen in the plastic pyrolysis process as summarised in Chapter 2. Some studies are reported with only a single feed and one product lump [43], whereas numbers of lumps have been reported up to 16 [146]. In the case of the kinetic characteristics of pyrolysis of plastic polymer, the lumping selection depends on the feed material, and operational conditions, one sample of HDPE pyrolysis at different studies can be seen in Table 5.1.

Table 5.1 Lump application on predicted reaction pathway with a function of temperature

Authors	Feed	Lump selection	Conditions		
			Temperature (℃)	Time (Minute)	Reactor
Ding et al [42]	Pure PE, and PP	Four-lump of polymer, light fractions, heavy fractions and middle distillates	380-420	20-50	Autoclave reactor
Costa et al [82]	Waste PE, PP and PS	Four-lump model of polymer, gas, light liquid fractions and heavy liquid fractions	380-420	20	Autoclave reactor
Al-Salem et al [8]	Pure HDPE	six-lump model of polymer, gases, liquids, waxes, aromatics and char fractions	500-600	510-66.3 seconds	TGA
Kumar et al [147]	Pure HDPE	five-lump model of polymer, gas, liquid, wax and char	400-550	44-245	Semi-batch reactor
Elordi et al [148]	Pure HDPE	Five-lump of polymer, gas, gasoline, diesel and waxes	450-715	9-650 seconds	conical spouted bed reactor

In the chemical reaction, the products are often recognised as gases, liquids and solids based on their boiling range at atmospheric pressure. Therefore, the most popular way to explore the primary reaction pathway for a chemical process is to propose the reaction mechanism based on the observed experimental data. Kinetic study of reactive mixtures can be explored by linking kinetics to the apparent kinetics of lumped pseudo-component as reviewed in Chapter 2. The flexible kinetic model was proposed based on the earlier experimental observations to describe the pyrolysis behaviour of plastic waste. Primary reactions of pyrolysis fragments with free radicals resulting in primary products at chosen conditions were characterised to address specific processes and the desired distribution of products' composition and yields. Secondary reactions are possible if the reaction temperature is high enough. The assumption of solid char residue lump was described in two ways: 1) they are mainly unreacted HDPE polymer especially at lower temperatures and shorter residence times, the residue is the same lump with fed material; 2) at high reaction temperatures, they are lower molecular weight oligomers cracked from HDPE rather initial HDPE polymer; while the HDPE is assumed to be pyrolysed completely. Both assumptions

are used to develop two kinetic models (four-lumps, five-lumps) to simulate the thermal degradation in the pyrolysis.

5.2 Kinetic modelling

As described before, kinetic modelling of pyrolysis process can be performed mathematically by using a series of ordinary differential equations, which offer useful kinetic information of the process. This includes the establishment of a lumping model in terms of description of ODEs, and estimation of kinetic parameters of plastics in the pyrolysis process under operational conditions. The application of lumping approach has an advantage for its simplification to deal with the complex pyrolysis reaction network, which described in Chapter 2.

On the basis of the experiment result obtained from the pyrolysis of HDPE, the products formed by the devolatilisation process from HDPE decomposition were defined as four categories in terms of their aggregation state at normal atmosphere and temperature: the gas phase, the oil of the liquid phase, and the solid residue, which describe in Chapter 2. For HDPE pyrolysis, the solid residue includes unreacted polymer, the char-like products and others after devolatiliation, which was obtained at the temperature range of 400-500℃; while an assumption was taken in this study that HDPE is completely converted into gas, condensed liquid and wax components over 500℃, because over 99 percent of HDPE was decomposed between 500 and 500℃ which can be observed in Figure 4-6. The primary pyrolysis of HDPE waste generates intermediate volatile compounds, which are possible to decompose further into lower molecular weight components (secondary reaction). To simplify the pyrolysis reaction of HDPE in this project, a discrete lumping approach was employed to describe the kinetics of HDPE pyrolysis. Lump selection of HDPE polymer (P), gaseous (G), liquid oils (L), and waxes (W) and solid char residue (R) seems to be plausible for this pyrolysis process based on observed experimental data, which was obtained by the thermal pyrolysis of mixed polyethylene and polypropene at temperature range between 400-550℃.

5.2.1 Model development

The yield of the selected lumps needs to be known to determine the rate constants of the lumped reactions in the model development. The yields can be obtained experimentally by measuring the mass fraction of gases, liquid and wax, but the mass of char, un-reacted plastic

polymer, or others components grouped as solid char residue is impossible to measure separately, because they are collected together as one pseudo lump. The mass fraction of unreacted HDPE is depended on reaction conditions such as temperature. The value of the rate constants of some of the steps proposed in the reaction scheme shown in Figure 3-9 was near zero or zero, which indicated that these steps would not have taken place, and the proposed reaction scheme varies with operation conditions. Based on this point, the proposed reaction pathways for HDPE pyrolysis have been formulated as shown in Figure 3-9 at different temperature ranges and the experimental data obtained from FBPR. Four-lumps (Figure 5-1) and five-lumps (Figure 5-2) discrete kinetic models were proposed for the pyrolysis of HDPE waste in this study. Four-lump model assumes that HDPE decompose into gas, liquid, and wax at higher temperatures (e.g. 550℃), coupling with partial liquid fraction cracking into lower molecular weight hydrocarbons; and five-lump model assumes that HDPE pyrolysis into gas, liquid, wax and solid residue at lower temperature (e.g. 425℃), with secondary reaction from heavy liquid fraction decomposition. Thus, the pyrolysis reaction of HDPE is described by three/four parallel reaction for four-lump/five-lump model, respectively. Both models were validated by using the experimental data obtained from FBPR responding to the experimental conditions. The proposed four lumps model and five lumps models draw similar support in the literature on the thermal conversion of plastic waste (e.g. Ding et al [42], [62], Costa et al [82], Csukas et al [78] and Aguado et al [20]). The presence of secondary reaction of heavier fractions (e.g. wax) in the FBPR is main concern because the control is crucial for end product distribution relevant to the project proposal.

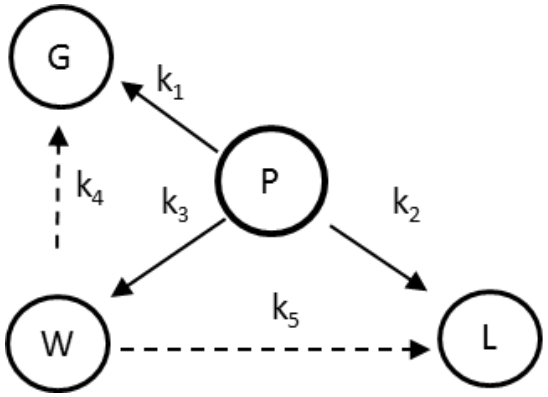

Figure 5-1 Schematic of reaction pathway for HDPE pyrolysis with four lumps (P: HDPE waste; G: Gas; W: Wax; L: Liquid)

The derivation of the four-lump kinetic model is expressed in differential equations (5.1 to 5.5) based on the mass concentrations and mass balances in the experimental study following with a first order reaction. k_1, k_2, k_3, k_4, k_5 represent the isothermal kinetic rate constant (min^{-1}) of the primary pyrolysis (solid lines) of plastic waste to gaseous, liquid fractions, wax fractions, and secondary cracking of wax fractions to gas and light liquid fractions (dash lines) during the reaction, respectively. The reaction rates were dominated by their kinetic rate constants. These kinetic rate constants can be determined by measuring the amount of each lump as a function of time.

$$\frac{dx_{Plastic}}{dt} = -(k_1 + k_2 + k_3)(1 - x) \quad (5.1)$$

$$\frac{dx_{Gas}}{dt} = k_1\,(1 - x) + \; k_4 x_{Wax} \quad (5.2)$$

$$\frac{dx_{Liquid}}{dt} = k_2(1 - x) + \; k_5 x_{Wax} \quad (5.3)$$

$$\frac{dx_{Wax}}{dt} = k_3\,(1 - x) - (k_4 + k_5)x_{Wax} \quad (5.4)$$

The mass balance can be written as:

$$-\frac{dx_{WP}}{dt} = \frac{dx_{Gas}}{dt} + \frac{dx_{Liquid}}{dt} + \frac{dx_{Wax}}{dt} \quad (5.5)$$

These equations are not related to the actual detailed mechanisms. They were considered as an objective function to minimise the margin for error between the model solution and the normalised value. The initial point (at time = 0), the fractions of the polymer and products would be described by MATLAB formula as:

w0 = $[x_{Plastic}\;\; x_{Gas}\;\; x_{Wax}\;\; x_{Liquid}\;\; (x_{Char\,residue})]$ = [100 0 0 0 (0)]

where x means decomposed mass fraction of the sample. Then reaction condition at any time = *t* (min) could be shown as follows:

t = t; $x_{Plastic} < 100$ and $[x_{Gas}\;\; x_{Wax}\;\; x_{Liquid}\;\; (x_{Char\,residue})] = f(t, x_{Plastic})$ (5.6)

The five-lump model requires that an extra char residue (R) is added into the four-lump model. The char residue lump groups unreacted plastic, lower molecular weight oligomers and char-like products together. The five-lump model, shown in Figure 5-2, can predict the new reaction pathways, which are described by different equations (5.7 to 5.12).

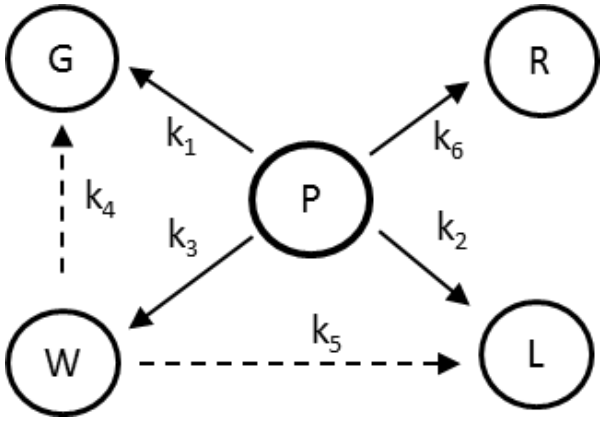

Figure 5-2 Schematic of reaction pathway for HDPE pyrolysis with five lumps (P: HDPE waste; G: Gas; W: Wax; L: Liquid; R: Char residue)

where k_1, k_2, k_3, k_4, k_5, and k_6 represent the isothermal rate constant (min^{-1}) of the primary pyrolysis of plastic waste to gaseous, liquid fractions, wax fractions, secondary cracking of wax fractions to oil phase and light liquid fractions, and solid char residue during reaction, respectively. The deferential express of HDPE pyrolysis can be written as:

$$\frac{dP}{dt} = -(k_1 + k_2 + k_3 + k_6)\mathrm{P} \tag{5.7}$$

$$\frac{dG}{dt} = k_1\,\mathrm{P} + k_4\,\mathrm{W} \tag{5.8}$$

$$\frac{dW}{dt} = k_2 P - (k_4 + k_5)\ \mathrm{W} \tag{5.9}$$

$$\frac{dL}{dt} = k_3 P + k_5 \mathrm{W} \tag{5.10}$$

$$\frac{dR}{dt} = k_6 P \tag{5.11}$$

The mass balance can be written as:

$$-\frac{dx_{WP}}{dt} = \frac{dx_{Gas}}{dt} + \frac{dx_{Liquid}}{dt} + \frac{dx_{Wax}}{dt} + \frac{dx_{Char}}{dt} \tag{5.12}$$

5.2.2 Solution for the estimation of kinetic rate constant

The lumping kinetic models were developed in this study using MATLAB software version 12.0.b to determine the optimal parameters for each model. So the value of the mass fraction

for each lump can be calculated as a function of time. The kinetic parameters (e.g. activation energy) included in the model were determined by fitting the calculated values to the experimental data with nonlinear regression equations. A fourth-order Runge-Kutta algorithm of the least square deviations is employed during numerical optimisation. Nonlinear least square (*lsqcurvefit)* was selected because it can offer a closest minimum to the initial values with an acceptable error even it does not search for the global minimum. To reduce local optimisation noise in nonlinear least–square method, a range of initial values was chosen during the calculation of rate constant in this study. Initial values and boundary values for the rate constants in the programme were selected based on the results of least squares minimisation of objective functions and in the literature. The estimated kinetic parameters are estimated in terms of experimental data based on minimising the objective function.

5.3 Result and discussion

As described above the starting material properties (e.g. molecular weight distribution, chain structure, the degree of purity) and operation variables both can lead to different reaction pathways in HDPE pyrolysis. Kinetic analysis of different reaction pathways proposed in HDPE pyrolysis has been demonstrated by many authors using different methods. This Chapter aims to examine the effects of different reaction pathways proposed for the estimation of kinetic parameters via a lumping model.

5.3.1 Kinetic study of reaction pathways of HDPE pyrolysis by lumping model

Based on the reaction routes proposed in Figures 5-1 and 5-2, kinetic models were developed. Five and six rate constants in four and five lumping models were estimated by using the experimental data observed at the temperatures of 425, 450, 475, and 500℃, respectively. Those parameters were calculated depending on systems of the differential equations (5.1 to 5.5) and (5.7 to 5.12) solved by MATLAB programmes. Tables 5.2 and 5.3 show the values of rate constants solved by using four and five lumping models, respectively. The rate constants increased with the temperature, corresponding to the same reaction direction observed in the experiments. The rate constant of k_3 is clearly higher than k_1 and k_2, which indicates that wax has a higher yield between 425℃ and 500℃. These model theoretical results are consistent with the experimental investigation, which showed the wax yielded was up from 3.7% to 61.3%, as compared to the gas yield changes from 4.3% to 14.6% and

the liquid oil yield changes from 1.5% to 22.5%. The values of the rate constants of some reaction steps in the proposed reaction schemes were less than 10^{-6}; nevertheless, the absolute function tolerance for the model solution using fourth Runge-Kutta in MATLAB is defined as 10^{-6}. Thus, those estimated rate constants of less than 10^{-6} were ignored. Some assumptions that can be considered are that the reaction would not take place once its rate constant was zero or near zero, and that secondary reaction of wax cracking was inclined to form light liquid fractions rather than gases at lower temperatures. Rate constants obtained in the four-lump model were slightly lower than those obtained from the five-lump model, which indicates that some oligomers were probably generated from HDPE pyrolysis, and combined with the char residue from HDPE pyrolysis to form char lump in the model. Selection of lumping schemes should take account of this, especially at lower temperatures (e.g. lower than 450℃ for HDPE degradation). At 425℃, both models indicate secondary reaction of wax cracking was negligible in the model development because the k_4 and k_5 were near zero. With the reaction temperature increased over 425℃, rate constant k_5 clearly increased, k_4 was still very low even though it was measurable, these findings indicate the secondary reactions of wax cracking seems mainly to convert into lighter oil fractions between 450 and 500℃, while the gas from wax cracking may not be obvious.

Table 5.2 Rate constants for the formation of gases, liquids, and waxes from HDPE pyrolysis

Temperature	Time	k_1	k_2	k_3	k_4	k_5
(℃)	(min)	(min^{-1})	(min^{-1})	(min^{-1})	(min^{-1})	(min^{-1})
425	30	2.86E-04	2.04E-04	2.03E-03	5.98E-08	7.47E-06
450	30	4.48E-03	4.67E-03	2.12E-02	1.22E-05	6.12E-04
475	30	1.06E-02	1.35E-02	4.88E-02	3.05E-05	6.11E-04
500	10	2.63E-02	3.13E-02	1.02E-01	4.89E-05	6.11E-04

5.3.2 Effect of lump selection on the determination of kinetic parameters

Based on the modified reaction pathways shown in Figures 5-3 and 5-4, kinetic parameters were re-estimated, and the rate constants are shown in Table 5.4.

Table 5.3 Rate constants for the formation of gases, liquids, and waxes from HDPE pyrolysis

Temperature (℃)	Time (min)	k_1 (min^{-1})	k_2 (min^{-1})	k_3 (min^{-1})	k_4 (min^{-1})	k_5 (min^{-1})	k_6 (min^{-1})
425	30	4.03E-03	3.63E-03	1.64E-02	2.67E-6	3.34E-5	2.63E-01
450	30	2.51E-02	2.48E-02	1.07E-01	7.65E-6	9.56E-4	1.14E-01
475	30	4.53E-02	5.79E-02	2.27E-01	3.39E-5	8.48E-4	3.19E-02
500	10	1.49E-01	1.75E-01	5.85E-01	1.85E-4	9.27E-4	2.30E-01

The kinetic parameters of activation energy (E_a) and pre-exponential factor (A_0) in the Arrhenius Law were determined using rate constants obtained from kinetic models of four lumps and five lumps and presented in Table 5.5 and Figures 5-5 to 5-12. It can be seen that different reaction pathways proposed result in a difference of kinetics during the modelling simulation for a complex reaction network. The rate constants (Table 5.4) obtained from modified models do not present any clear difference with the previous ones (Tables 5.2 and 5.3), this may be ascribed to the fact that primary reactions dominate the HDPE pyrolysis process.

Table 5.4 Rate constants for the formation of gas, liquid and wax from HDPE pyrolysis estimated by four and five lumps models

	Temperature (℃)	Time (min)	k1 (min^{-1})	k2 (min^{-1})	k3 (min^{-1})	k4 (min^{-1})	k5 (min^{-1})	k6
Five lumps	425	30	4.03E-03	3.63E-03	1.64E-02		3.34E-5	2.63E-01
	450	30	2.51E-02	2.48E-02	1.07E-01	7.65E-6	9.56E-04	1.14E-01
	475	30	4.53E-02	5.79E-02	2.27E-01	3.39E-05	8.48E-04	3.19E-02
	500	10	1.49E-01	1.75E-01	5.85E-01	1.85E-04	9.27E-04	2.30E-01
Four lumps	425	30	2.86E-04	2.04E-04	2.03E-03			
	450	30	4.48E-03	4.67E-03	2.13E-02	1.22E-05	5.41E-04	
	475	30	1.06E-02	1.35E-02	4.88E-02	3.01E-05	6.02E-04	
	500	10	2.56E-02	3.14E-02	1.02E-01	4.89E-05	6.11E-04	

Tables 5.2 and 5.3 also show the k_1 and k_2 are much higher than k_4 and k_5, which means the gas and liquid products were mainly generated from primary pyrolysis of HDPE under the

temperature range of 450-500℃. The secondary reaction was not strong at this stage due to that reaction temperature was not high enough for heavier fractions cracking in FBPR. Rate constant k_5 of the secondary reaction were almost stable between 450 and 500℃, compared to the increasing trend of k_4, which indicates wax cracking into light oil fractions was not sensitive to temperature variation unlike gases between 450 and 500℃. Based on above discussion and the values of rate constants obtained from developed models, some modifications for the pyrolysis schemes were undertaken and shown in Figures 5-3 and 5-4.

Tables 5.6 and 5.7 show the estimation of E_a and A_0 by using the kinetic lumping model scheme for the reaction pathways proposed for HDPE pyrolysis at different temperatures. The E_a values for overall HDPE conversion (HDPE→G+L+W), HDPE → Gases, HDPE→ Liquid oils, and HDPE → Waxes calculated on the basis of four lumping model are higher than the ones obtained from five lumping model, and also the values were dependent on the range of reaction temperature. As aforementioned, it is due to the hypothesis that the lump of char residue is treated as unreacted HDPE feed, even though HDPE can completely convert into gas and oil products. Higher overall E_a values were calculated at a lower start temperature (425℃), lower overall E_a values were obtained at a higher start temperature (450℃). A consideration for this may be that although the temperature was treated as constant during the determination of kinetic parameters based on the Arrhenius law; it did not take account of the effect of the start point of temperature. Higher start temperatures indicate that polymer molecules only need less free energy to become activated molecules so as to increase the efficient collisions and conversion of HDPE pyrolysis. On the other hand, higher temperature means higher conversion of HDPE degradation, Park et al [43] studied the pyrolysis characteristics of refuse plastic fuel and found a similar trend for the determination of the activation energy from 222.47 to 187.36 with the conversion from 10 per cent to 90 per cent using the integral method.

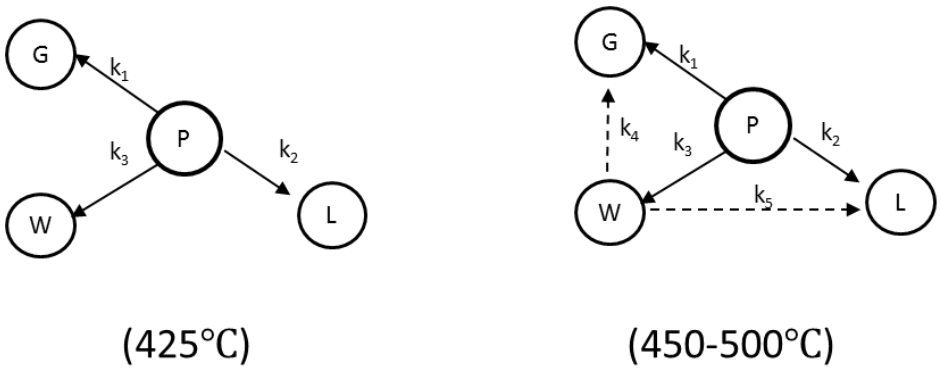

Figure 5-3 Schematic of four lumps reaction pathway for HDPE pyrolysis at the different temperatures (425, 450, 475 and 500℃) (P: HDPE waste; G: Gas; W: Wax; L: Liquid)

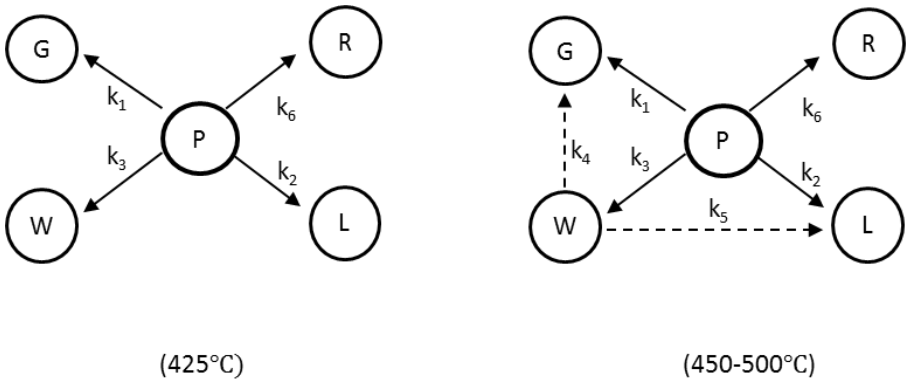

Figure 5-4 Schematic of five lumps reaction pathway for HDPE pyrolysis at the different temperatures (425, 450, 475 and 500℃) (P: HDPE waste; G: Gas; W: Wax; L: Liquid; R: Solid char residue)

The mean values of overall E_a (236.1 kJ/mol) was determined by using four lumps model based on the experimental data obtained from FBPR. The model result has matched the results obtained by other authors based on their studies of experiment and model for HDPE thermal degradation, which is shown in Table 5.5. The estimated E_a values of P-W in Tables 5.6 and 5.7 are lower than the ones of P-G and P-L which indicates that waxes are more easily transformed from HDPE degradation than smaller molecular weight gas and lighter oils, because more energy is needed to break polymer or oligomers chains into smaller molecules. The kinetic lumping modelling has been successfully employed to determine the kinetic parameters of pyrolysis behaviour of organic matters in process control and reactor design, including polymer, and biomass [42, 70, 76, 80, 82, 144]. The integral method and the differential method are popular in combining solutions with lumping modelling in numerical

descriptions of the complex pyrolysis reaction network. For instance, some authors employed lumping models to obtain kinetic parameters depending on integral methods developed by Kingsser [149, 150], Flynn-Wall-Ozawa [150-152], Friedman Method [150, 153], and Coats and Redfern [154] etc. The kinetic parameters were solved by those methods on the basis of the different conversion ratios during the thermal degradation of the polymer [43, 155, 156].

Table 5.5 Overall activation energies estimated from four /five lumping kinetic model and the experiment result from HDPE pyrolysis

		Overall activation energy (kJ/mol)	Method of activation energy calculation
This project	Four lump model	236.1	Discrete lumping model
	Five lump model	198.5	Discrete lumping model
Ballice [156]		237±4	Integral method
Flynn and Wall [151]		251-278	Integral method
Liu et al [157]		251-258.7	Integral method
Aboulkas et al[7]		247±5	Friedman method
		238±11	Kissinger-Akahira-Sunose
		243±11	Flynn-Wall-Ozawa
Kim et al[158]		190.5±10.8	Contracting cylinder model
Biswas et al[155]		171±52	Integral method

The differential method probably gives a valid result for individual reactions during estimation of kinetic parameters, so it can be a powerful tool for understanding the complex reaction network. The integral method treats a complex reaction network, which may contain multiple reaction mechanisms as a single reaction mechanism, probably providing a consistent result for the whole reaction scheme. While differential analytical method presents some limitation for the individual reactions existing in the complex reaction network, so the differential method can lead to some problems as errors are magnified from the double regression, which leads to results in which one can have little confidence. However, the integral method may not precisely present the multiple reaction mechanisms in a complex reaction system. It may be over-analysed for the kinetic parameters so that most activation

energies estimated are larger than the ones that are derived from the differential method. Moreover, during the determination of E_a by using Arrhenius law, the pre-exponential factor A_0 is treated as constant as it did not directly involve in relating to the temperature and activation energy. However, A_0 multiplies the exponential term; its value contributes to the value of the rate constant of the molecular structure and variation of collisions between molecules at different temperature in real reactions.

Tables 5.6 and 5.7 also show that estimated activation energy for the reactions of wax cracked into oil and gas is much lower than the ones for primary pyrolysis, as well as the frequency factor. On one hand, the R^2 was less than 0.80 on a linear fitting trendline, which may indicate that the wax cracking reaction is not strictly a first order reaction, indeed similar results were reported by other authors [159-161]. On the other hand, the pre-exponential factors are very small compared to the primary pyrolysis, which indicates only small fractions of the polymer molecules converted into light fractions at operational conditions (425-500℃) with limited free energy in the reaction system to overcome the activation energy for the reactions. This result accords with that rate constants of k_4 and k_5 are much lower than k_1, k_2 and k_3, which indicates the secondary reactions were weaker under such operational conditions. The presence of additives (especially those containing some metal elements) and heteroatoms (e.g. oxygen and sulphur) in the feed waste plastic may act as catalysts in the cracking reactions so that the activation energy was underestimated, and lead to multiple reaction mechanisms simultaneously. Additionally, wax into lighter gases and oils with single cracking reaction route did not represent the overall reaction of wax cracking.

From the above discussion, it can be concluded that the five lumps model for HDPE pyrolysis at a lower temperature (under 475℃) should better describe the degradation reaction of HDPE. This also corresponds to the experimental result that the degradation reaction was potentiated once the final reaction temperature was over 475℃, as presented in Chapter 4. The Four lumps model may be suitable for higher conversion at a higher temperature range (e.g. over 500℃) with complete conversion of HDPE while the precise measurement of residence time in the FBPR could be a challenge.

Table 5.6 Estimated kinetic parameters of HDPE pyrolysis on the basis of the four lumping model at different temperature ranges

Temperature range (℃)	Reaction routes	E_a (kJ/mol)	A_0 (1/min)	R^2
425-450-475-500	P-G+L+W	240.9	4.15E+15	0.94
	P-G	258.9	1.10E+16	0.92
	P-L	292.7	2.93E+18	0.97
	P-W	228	3.52E+14	0.94
	W-G	385.1	1.34E+22	0.81
	W-L	244.2	4.54E+13	0.67
425-450-475	P-G+L+W	293.9	3.11E+19	0.97
	P-G	318.9	1.65E+20	0.96
	P-L	366	6.54E+23	0.97
	P-W	277.1	1.51E+18	0.97
425-475-500	P-G+L+W	255.4	3.57E+16	0.97
	P-G	268.2	1.33E+17	0.98
	P-L	304.91	4.83E+19	0.96
	P-W	237	2.65E+15	0.99
450-475-500	P-G+L+W	154	4.05E+09	0.99
	P-G	167.2	1.70E+09	0.99
	P-L	189.1	3.07E+10	0.99
	P-W	155.7	8.10E+08	0.99
	W-G	11.4	3.68E-03	0.82
	W-L	140.7	1.73E+05	0.94
425-450-500	P-G+L+W	236.7	1.97E+15	0.96
	P-G	255.1	5.64E+15	0.95
	P-L	285.2	9.39E+17	0.92
	P-W	223.1	1.77E+14	0.94

Table 5.7 Estimated kinetic parameters of HDPE pyrolysis on the basis of the five lumping model at different temperature ranges

Temperature range (℃)	Reaction routes	E_a (kJ/mol)	A_0 (1/min)	R^2
425-450-475-500	P-G+L+W	215.9	4.11E+14	0.97
	P-G	206.2	1.32E+13	0.95
	P-L	295.9	2.56E+19	0.96
	P-W	206.1	5.40E+13	0.94
	W-G	325.2	4.99E+18	0.92
	W-L	63.0	1.86E+01	0.97
425-450-475	P-G+L+W	241.5	3.04E+16	0.94
	P-G	213.0	4.19E+13	0.93
	P-L	353.7	1.75E+24	0.94
425-475-500	P-G+L+W	227.5	2.28E+15	0.99
	P-G	215.4	5.20E+13	0.99
	P-L	315.0	4.36E+20	0.97
	P-W	217.2	2.97E+14	0.99
450-475-500	P-G+L+W	155.6	2.80E+10	0.99
	P-G	165.4	1.99E+10	0.96
	P-L	183.4	4.28E+11	0.99
	P-W	146.6	4.35E+09	0.97
	W-G	353.1	4.24E+20	0.10
	W-L	47.3	1.52E+00	0.80
425-450-500	P-G+L+W	216.7	4.69E+14	0.98
	P-G	218.4	2.64E+13	0.97
	P-L	291.3	1.14E+19	0.92
	P-W	206.8	6.49E+13	0.95

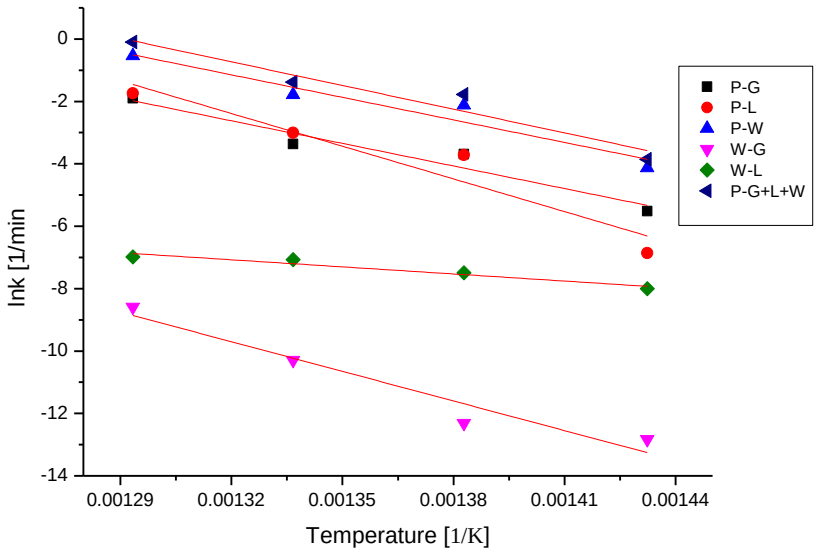

Figure 5-5 Arrhenius plot for HDPE pyrolysis at temperature range (425-450-475-500℃) with five lumps kinetic model

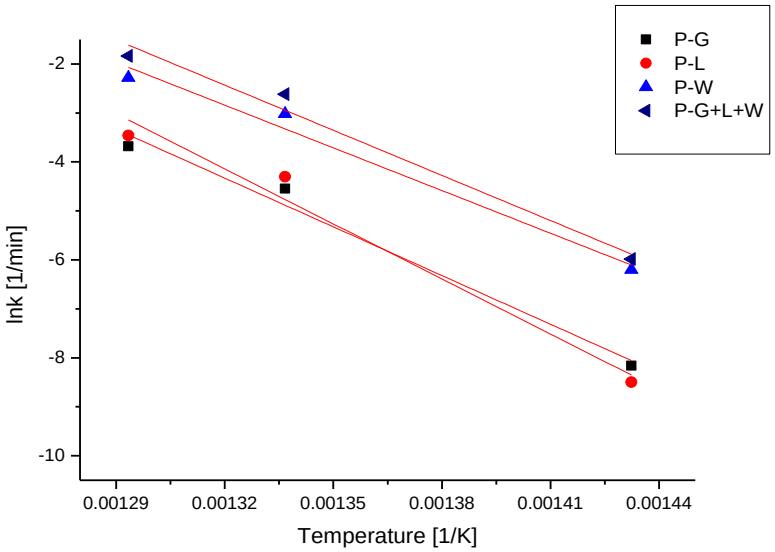

Figure 5-6 Arrhenius plot for HDPE pyrolysis at temperature range (425-450-475℃) with five lumps kinetic model

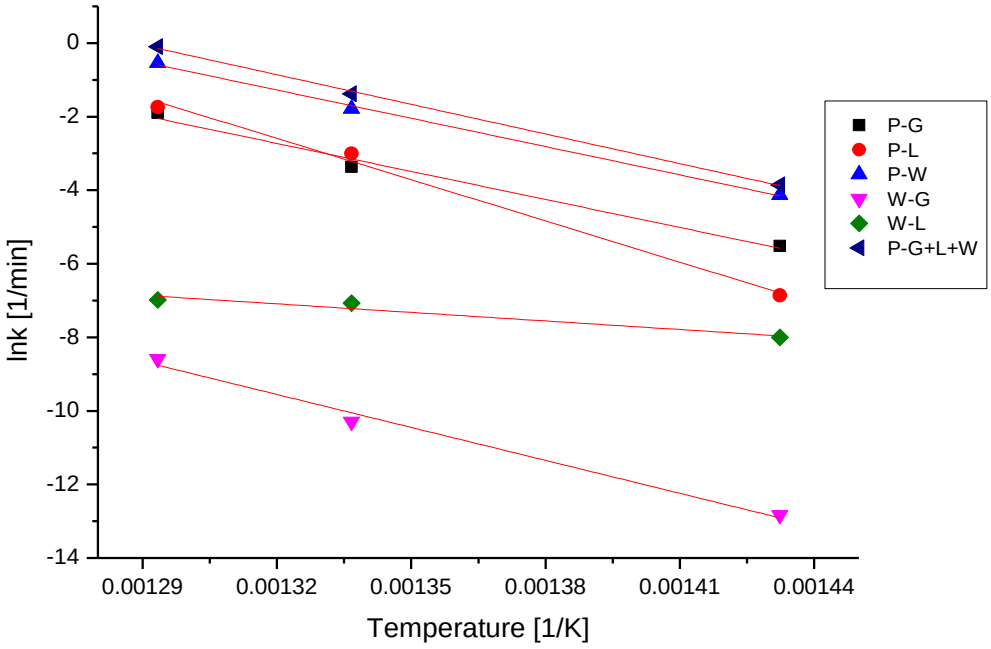

Figure 5-7 Arrhenius plot for HDPE pyrolysis at temperature range (425-475-500℃) with five lumps kinetic model

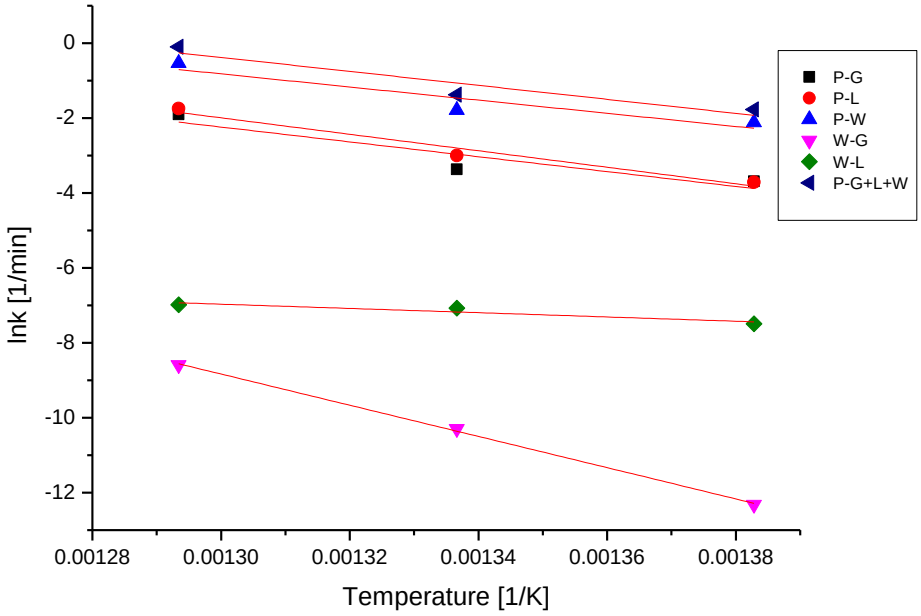

Figure 5-8 Arrhenius plot for HDPE pyrolysis at temperature range (450-475-500℃) with five lumps kinetic model

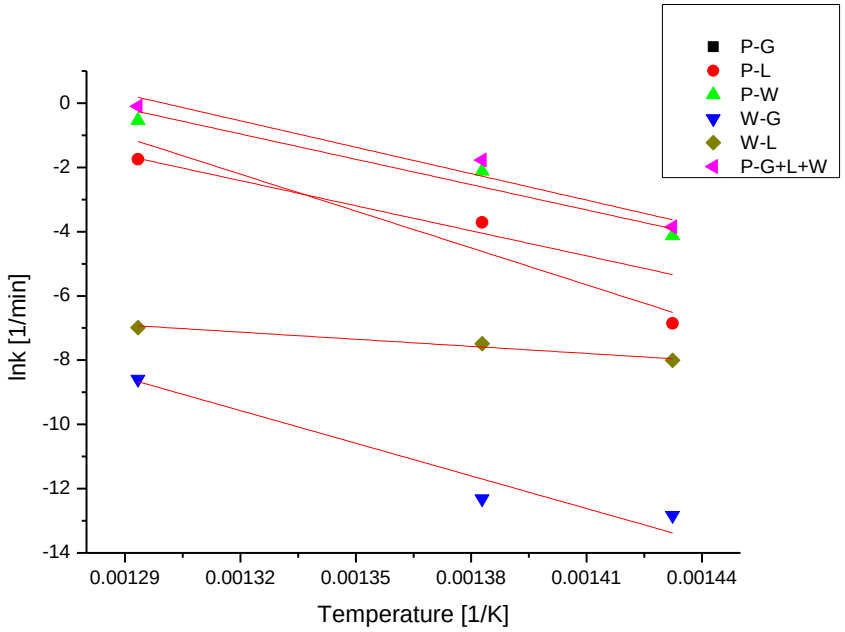

Figure 5-9 Arrhenius plot for HDPE pyrolysis at temperature range (425-450-500℃) with five lumps kinetic model

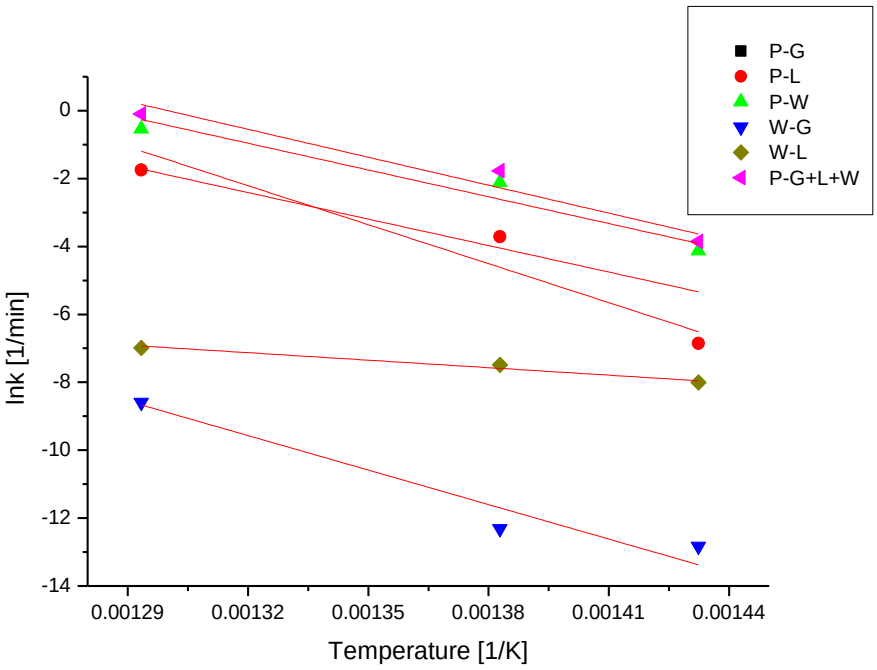

Figure 5-10 Arrhenius plot for HDPE pyrolysis at temperature range (425-450-475-500℃) with four lumps kinetic model

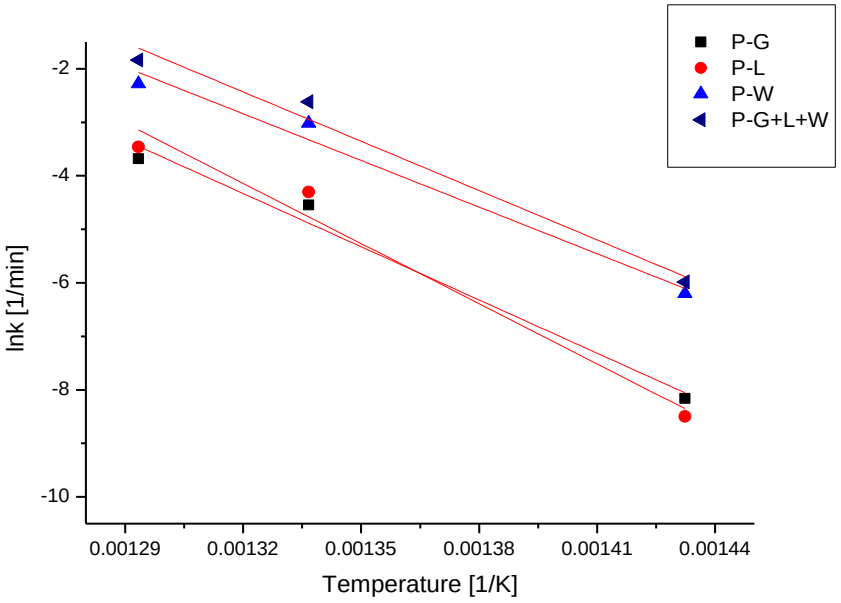

Figure 5-11 Arrhenius plot for HDPE pyrolysis at temperature range (425-475-500℃) with four lumps kinetic model

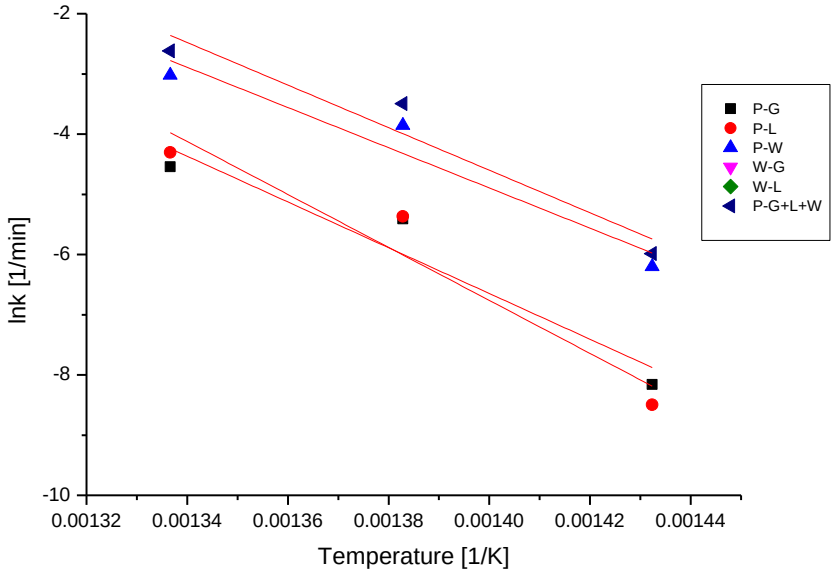

Figure 5-12 Arrhenius plot for HDPE pyrolysis at temperature range (425-450-475℃) with four lumps kinetic model

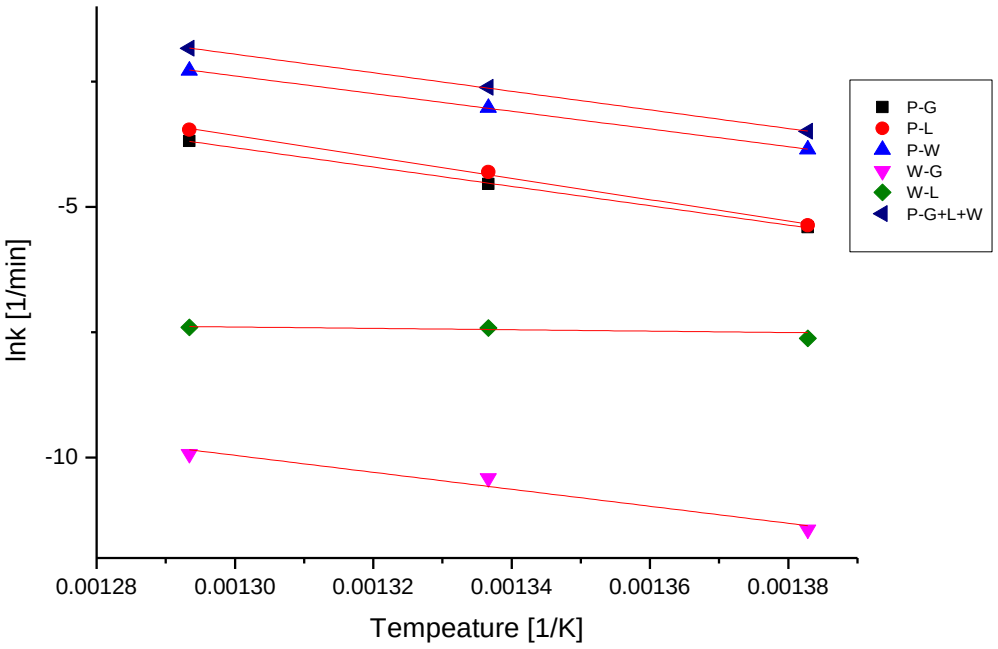

Figure 5-13 Arrhenius plot for HDPE pyrolysis at temperature range (450-475-500℃) with four lumps kinetic model

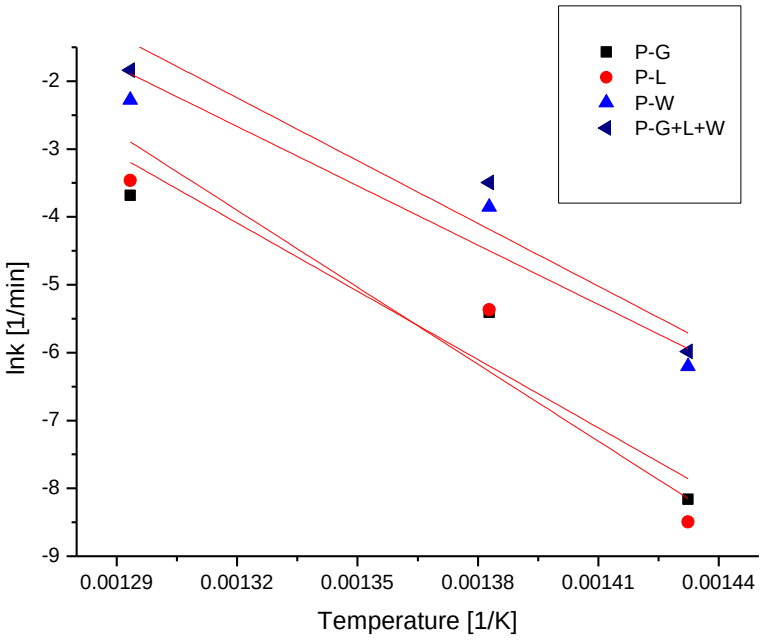

Figure 5-14 Arrhenius plot for HDPE pyrolysis at temperature range (425-450-500℃) with four lumps kinetic model

5.4 Model validation

To examine the reliability of developed models, experimental data obtained at 500 ℃ is used to validate the developed four/five lump models. The kinetic parameters were determined from the developed models by fitting the calculated values corresponding to the experimental data at 425, 450, and 475 ℃ as presented in Figures 5-15 and 5-16, which also show the flexibility of developed lumping kinetic model for the different proposal. The kinetic parameters in the models were determined.

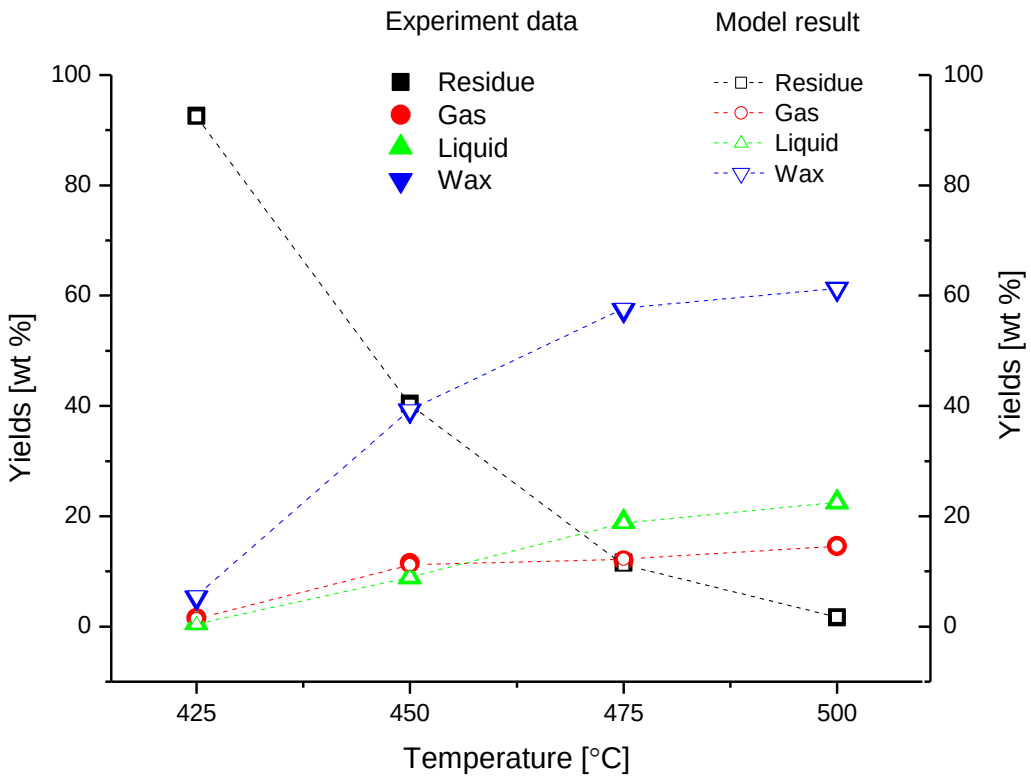

Figure 5-15 Comparison of experimental data from FBPR and model results for four lumps kinetic model

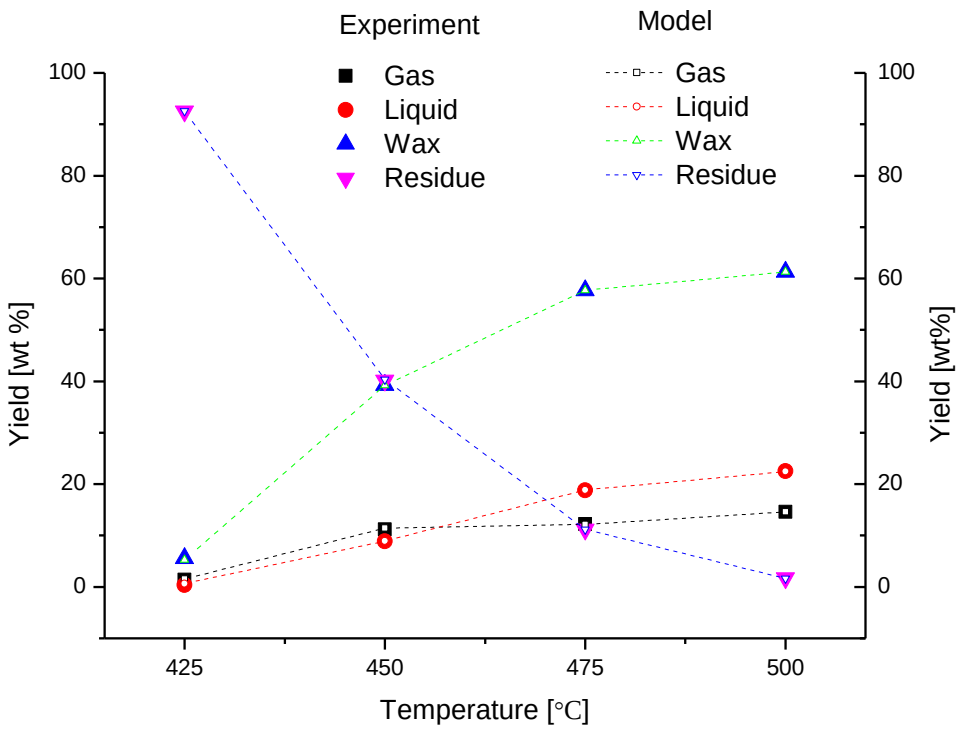

Figure 5-16 Comparison of experimental data from FBPR and model results for five-lumps kinetic model

5.5 Case study: Kinetic study of PE, PP and their mixture at higher temperature

Based on the above discussions and the assumptions of reaction networks, a four-lump model was developed to predict the mechanism of pyrolysis reaction of PE, PP, and their mixture. The proposed reaction pathway is same as the reaction schematic in Figure 5-1. In this kinetic study of pyrolysis, the activation energy (E_a) is also estimated on the basis of an Arrhenius plot of initial reactivity and first order kinetics, rate constants are obtained by fitting a model to the experimental data. As a sample, the PE waste pyrolysis results, including primary reaction and secondary cracking reaction, from the four-lump model are shown in Figure 5-17 at the end temperature of 500℃. Figure 5-17 also shows the prediction of wax cracking in the reactor within one second residence time to simulate the cracking process. The logarithmic yield of oil generated from wax cracking from 10^{-4} to 10^{-2} occurred within 0.4 seconds, and then the cracking reactions were mild. This indicates that cracking reaction occurs in a very short time at 500℃ in FBPR.

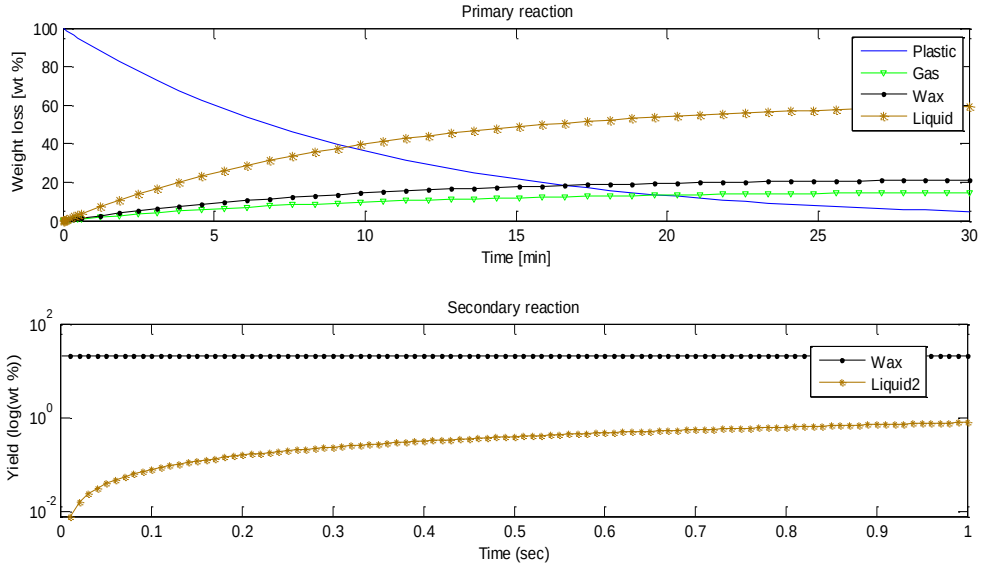

Figure 5-17 Model predictions as a function of time at 500℃ for four-lump kinetic model

Table 5.8 presents the values of rate constant obtained from the kinetic model (Figure 5-1). The rate constants were obtained by minimising the error between the model solution and the normalised value. In the primary pyrolysis step, pyrolysis rate constants of PE, PP and their mixtures ($k_p=k_1+k_2+k_3$) obviously increased with the temperature. The rate constant k_3 value of PE pyrolysis at 500℃ is higher than the value at 550℃, which indicates that more oil and gas products are generated from PE pyrolysis with the temperature change from 500 to 550℃. Secondary cracking reactions of wax into gas and liquid were faster than the rate of wax generation from PE pyrolysis at 550℃. The discrepancy of rate constants of the different samples can be observed at different temperatures. In the pyrolysis of waste PE, the rate constant k_3 is obviously larger than the values of k_2 and k_1 at three temperature ranges. The value of k_2 is higher than the values of k_1 and k_3 in PP pyrolysis. Similar values of k_2 and k_3 can be observed from the pyrolysis of PEPP mixture, which indicates the presence of interaction reaction during the thermal degradation of PEPP. At the same temperature, the value of k_1 from PP pyrolysis are higher than the values obtained PE and PEPP mixture; the rate constant of gas, liquid and wax are higher from PP pyrolysis than the ones from PE and PEPP mixture. Similar results were also reported in the literature [10, 136]. These results agree with the experimental results that PP has a higher conversion than PE at similar temperatures. As shown in Table 5.8 and Figure 5-17, all the correlation coefficients R^2 of the linear regression of rate constant data are higher than 0.96, which supports the validity of the developed four-lump kinetic model. Table 5.8 also shows that secondary reaction is

dependent on temperature, the rate constant *k* increases with temperature. The kinetic rate constants of wax cracking into oil and gas are much lower than k_2 and k_1. This indicates that the secondary cracking reaction of wax did not dominate the oil and gas yield in the temperature range between 450 and 550℃ due to that temperature is not high enough for wax cracking in the reactor. Nevertheless, both rate constants of wax cracked into gases and oils increase with temperature. Similar results were reported by Ding et al [42].

The Arrhenius plots of kinetic rate constants against temperature are shown in Figure 5-14. With an assumption of temperature–independent kinetic parameters, Arrhenius parameters via linear regression were obtained, including activation energies (E_a) and pre-exponential factors (A). The overall E_a and A of PE, PP and their mixture during thermal decomposition were estimated to be 116.7 kJ mol^{-1}, 146.4 kJ mol^{-1} and 127.5 kJ mol^{-1}; 7.99×10^6 min^{-1}. Figure 5-21 shows the correlation of simulations using the proposed model with the experimental results; the model shows a high capability for the estimation of the 3.38×10^8 min^{-1} and 5.93×10^7 min^{-1}, respectively. The values are in accordance with data in the literature (e.g. 161-172 kJ mol^{-1} for PP degradation estimated by Gao et al [162]; 147 kJ mol^{-1} for HDPE estimated by Al-Salem et al [8], 85-271kJ mol^{-1} estimated by Conesa *et al* [163]). The activation energies and pre-exponential factors for PE, PP and their mixture decomposing into gas, oil, and wax summarised in Table 5.8 were obtained from Figures 5-18 to 5-20.

It is possible that the activation energy of polymer degradation varies with conversion ratio at different temperatures, due to a change in the mechanism which can be ascribed to the presence of multiple competing reactions (steps) in the polymer degradation [133]. The evaluation of activation energy represents the kinetics of the steps (moments) estimated which dominate the kinetic process. Nevertheless, some residues from metal salts and oxidation additives added to the polymers during processing may act as catalysts to generate initiation radicals at polymer decomposition [164], the presence of heteroatom groups and their uncertain content may influence the decomposing mechanism at different temperature so as to enhance the variation of activation energy of polymer decomposition[145]. The model results are helpful to understand the kinetic characteristic for potential engineering solutions in scale-up pyrolysis process.

Table 5.8 Reaction rate constants and calculated kinetic parameters for pyrolysis kinetic model

Feed	Rate constant	Temperature (°C) and residence time (min)			Arrhenius parameters		R^2
	(min^{-1})	450, 30	500, 10	550,10	E_a (kJ mol^{-1})	A (min^{-1})	
PE	k_p	0.031	0.102	0.324	116.7	7.99×10^6	0.999
	k_1	0.006	0.02	0.059	110.7	5.58×10^5	0.98
	k_2	0.003	0.023	0.095	169.9	6.14×10^9	0.996
	k_3	0.0208	0.063	0.173	102.6	5.44×10^5	0.999
	k_4	0.00004	0.00003	0.001			
	k_5	0.000004	0.00001	0.0009			
PEPP	kp	0.010	0.061	0.152	146.4	3.38×10^8	0.974
	k_1	0.0017	0.014	0.032	146.6	1.34×10^8	0.957
	k_2	0.0030	0.021	0.059	147.4	1.50×10^8	0.983
	k_3	0.0032	0.023	0.060	146.7	1.04×10^8	0.974
	k_4	0.000001	0.00015	0.0018			
	k_5	0.000001	0.00005	0.0013			
PP	kp	0.04	0.12	0.56	127.5	5.93×10^7	0.979
	k_1	0.0078	0.025	0.1066	127.7	1.13×10^7	0.990
	k_2	0.018	0.050	0.25	127.7	2.15×10^7	0.971
	k_3	0.014	0.043	0.21	131.8	4.56×10^7	0.981
	k_4	0.0016	0.00020	0.00011			
	k_5	0.0002	0.00014	0.00008			

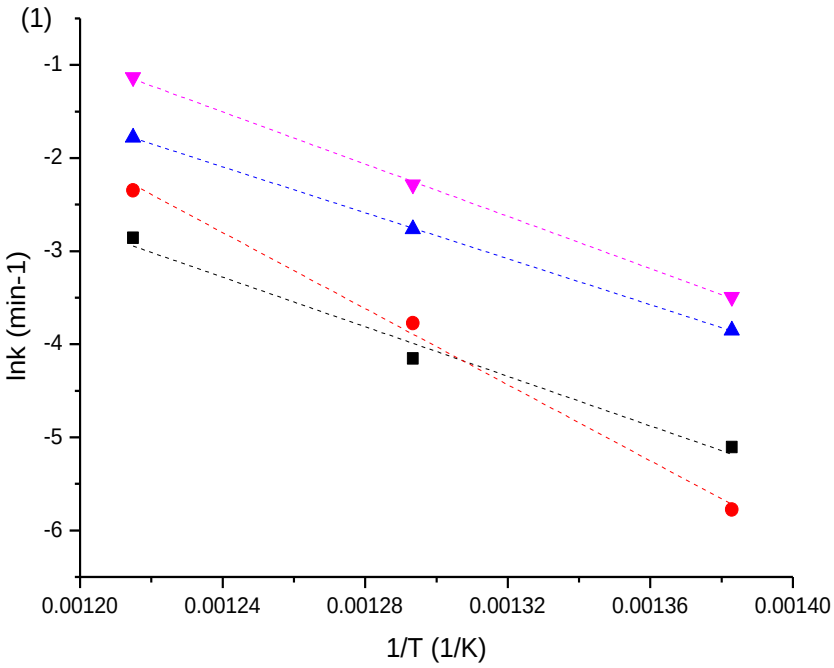

Figure 5-18 Arrhenius plots of the PE (1) pyrolysis

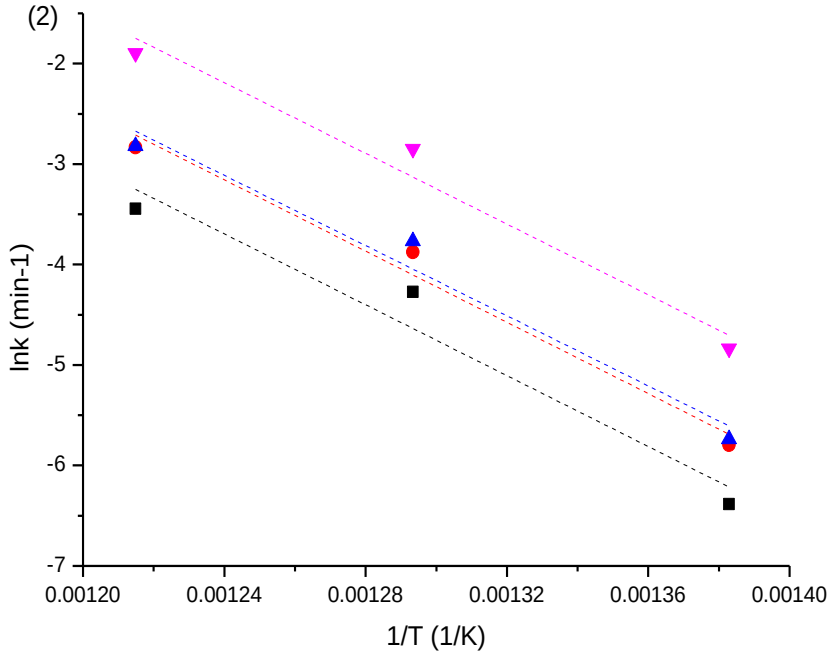

Figure 5-19 Arrhenius plots of pp (2) pyrolysis

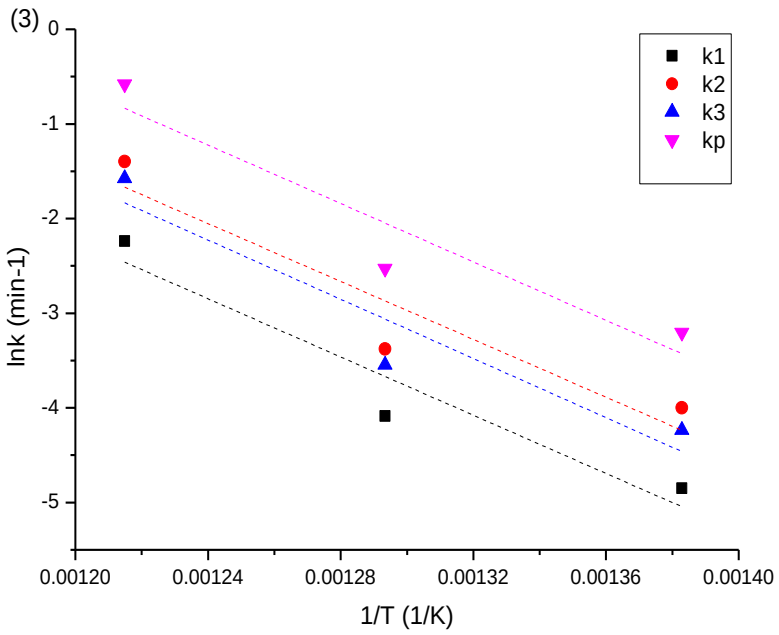

Figure 5-20 Arrhenius plots of PE/PP mixture (3) pyrolysis

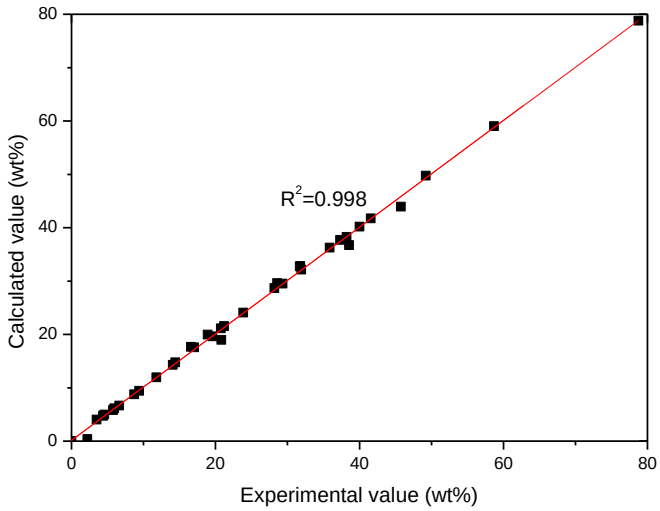

Figure 5-21 Comparison between the experimental and calculated values corresponding to all data points for four-lump model

5.6 Conclusions

Different reaction pathways of HDPE pyrolysis have been studied to better understand the reaction mechanism of complex pyrolysis reaction. Kinetic characterstics of HDPE pyrolysis was examined by using lumping approach. Parallel primary reactions and secondary

reactions proposed for HDPE pyrolysis were employed for a kinetic analysis of reaction pathways at different temperature ranges. The five lumps kinetic model is suitable to predict the pyrolysis reaction at the lower temperature (under 475℃); the four lumps model is better to mimic the pyrolysis process at a higher conversion. The uncertainty in the definition of char residue lump in the model will result in variation in the determination of kinetic parameters. Temperature ranges also deliver a difference in the estimation of kinetic parameters due to ignoring the effect of the pre-exponential factor at different temperatures. In addition, the start time of peak reaction temperature also leads to a difference in the results. A case study of the kinetic characteristic of the pyrolysis of waste PE, PP, and their mixture shows that the developed model is sufficiently flexible to predict the different pyrolysis products of different feedstocks. Estimated kinetic parameters from PE, PP, and their mixture indicate that they are temperature dependent.

CHAPTER 6 KINETIC STUDY OF PYROLYSIS OF WASTE HDPE AT DIFFERENT BED THICKNESS OVER FBPR

Summary

This chapter presents a case study on an investigation of the kinetic characteristics of HDPE pyrolysis process with different bed thicknesses and temperature, and aims to find a potential engineering solution for scale-up of the process of plastic pyrolysis. TGA and FBPR were employed for this study. The influence of bed thickness on the yield distribution and the composition of products were also examined over a final temperature range of 425-550℃. The main thermal decomposition of HDPE waste samples occurred over a temperature range of 475-510℃, corresponding to conversion between 10 percent and 95 percent. Based on the experimental results, a discrete lumping model has been developed to predict the yield distribution of gases, oil fractions, wax fractions and solid residue, coupling with secondary cracking reactions of wax fractions into lighter fractions (oil). The kinetic parameters of rigid PE waste pyrolysis were also estimated based on the model results.

6.1 Introduction

Beneficial solutions for plastic recycle and energy recovery, especially for post-consumer packaging waste have been undertaken using many techniques, such as gasification and pyrolysis [6-10]. However, full-scale energy recovery processes from waste plastic are limited in the market because they have to overcome rigorous challenges, such as raw material treatment, sourcing for product quality to meet commercial criteria, and reactor performance that requires special engineering design. Pyrolysis process may improve the carbon footprint and lifecycle impact of plastic. Moreover, pyrolysis process can offer the recycling of mixed unwashed plastic waste contaminated with soil, grease and other materials [10]. The evolving studies of upgrading of energy fuel and chemicals and the evaluation of operational factors have been most prominent in the thermal pyrolysis process, such as the effect of various process variables (e.g. residence time, temperature, catalyst, and reactor type) on product yield and distribution [10, 21, 43, 165-167], the mass change in isothermal condition [168] or non-isothermal one [42, 169]; the mechanism of thermal degradation [7, 8]; the estimation of kinetic parameters of pyrolysis process [8, 42, 43]. However, it is noted

that the effect of bed thickness is rarely referred to in the literature. This study aims to examine the effect of bed thickness of HDPE pyrolysis on its kinetics characteristics and product distribution.

Kinetics of polymer degradation are usually dependent on the conversion degree and different reaction orders, the kinetics constants are significantly different within conversion ranges [62, 161]. As described in previous chapters, kinetic parameters are usually associated with the factors such as operational condition (e.g. temperature gradient in the sample, residence time), the accuracy of model approximation, the complex of reaction mechanisms, the presence of heteroatoms in the polymer from additives and contaminants.

Thermogravimetric analysis technique enables to offer fast, quantitative methods for the examination of thermal degradation process under isothermal or non-isothermal conditions. Therefore, it can provide information on pre-exponential factors and activation energies for various decomposition reactions, and also various reaction kinetic models are available to simulate plastic degradation from experimental data [7, 8, 43, 62, 168, 170-172]. Aboulkas et al [171] applied TGA and a non-isothermal single reaction model to study the thermal decomposition of mixtures of olive residue and plastic at the temperatures range from 300K to 1273K with a nitrogen carrier gas at four heating rates of 2, 10, 20, and 50K min^{-1}. Park et al [43] studied the primary pyrolysis characteristics of refuse plastic fuel using a lab-scale fixed bed furnace and TGA. They reported the effect of temperature range (400-800℃) on the product yields of liquid, solid and gas, presented apparent activation energies and pre-exponential factors of the refuse plastic fuel by single and parallel reaction models to estimate the activate energies of PS, PP, PE and PVC to be 231.83 kJ mol^{-1}, 193.55 kJ mol^{-1}, 175.92 kJ mol^{-1}, 72.26 kJ mol^{-1} (first degradation of PVC) and 164.94kJ mol^{-1} (second degradation of PVC). AL-Salem and Lettieri [8] investigated the pyrolysis kinetics of pure HDPE under the temperatures of 500, 550 and 600℃ via an isothermal thermogravimetric condition in a micro-thermobalance reactor. They examined the thermal kinetic characteristic by a lumping modelling approach based on the thermal cracking of the polymer by primary and secondary depolymerisation reactions to form the pyrolysis product yields. However, TGA only provides meaningful data of the mass change in the thermal decomposition reactions fixed bed reactor, and has difficulty in measuring the gas and liquid fractions and the secondary

reactions of heavier fractions from primary pyrolysis. Additionally, the TGA technique provides limited information on heat transfer during the pyrolysis process. The nature of low thermal conductivity of the plastics requires a high performance of heat and mass transfer in the reactor to minimise the limitations involving the physical steps prior to devolatilisation and to ensure isothermal conditions[173]. Thus, a suitable bed thickness and position for fixed bed reactor in the furnace may allow their uniform and fast coating with fused plastic and the vigorous movement improves heat and mass transfer in the reactor, and support some potential solutions for a scale-up process.

HDPE waste is selected in this study, because HDPE, as one kind of straight-chain hydrocarbon polymers which could generate more desired oils, is the third largest component of the plastic waste stream. The product distribution of HDPE pyrolysis may be easier to be determined because HDPE waste contains fewer additives and heteroatoms comparing other plastic waste. This may increase accuracy and reliability of research output. The products of HDPE pyrolysis are mainly hydrocarbon liquids, which may be directly used as fuel or upgraded to valuable chemical feedstocks [8, 80]. Nevertheless, there exist some limitations in process scale-up and optimisation of product properties for cost effective employment. In particular, the unclear kinetics and mechanism of pyrolysis process cause a problem in the optimal design of process and reactor [167, 174]. Aguado et al [21] introduced principal component analysis method in order to recognise trends in the formation rates of a large number of components in the product stream for HDPE pyrolysis, and ignored minor components in the reaction system. Ding et al [42] only studied the kinetics of plastic mixture pyrolysis at a lower temperature (between 380℃ and 420℃) and different residence times, and developed a four-lump model to describe the product distribution and their rate constants of secondary reactions. Most works mainly studied the primary pyrolysis of pure plastics (e.g. Al-Salem et al [8]), and investigated the lower temperature lower than 420℃ (e.g. Ding et al [42] and Walendziewski [175]) and higher temperature over 600℃ (e.g. Park et al [43], Elordi et al [148]; and Conesa et al [176]). It should be an interesting investigation for cost-effective scale-up, to examine the pyrolysis characteristics of real plastic packaging waste under a middle-higher temperature range between 450℃ and 550℃.

The objective of this work is to identify the kinetic characteristics of rigid HDPE waste degradation behaviour as a function of bed thickness in fixed bed reactor based on the product

yield distribution and composition. TGA was employed to investigate the thermal degradation behaviour of HDPE at the temperature range between 400℃ and 550℃. The overall kinetic parameters of activation energy and pre-exponential factor for HDPE waste were estimated in isothermal condition with assumed first order reaction. Moreover, the TGA result was used for the design of FBPR experimental runs. The effect of bed thickness on the product yield and composition of the gas and liquid products was examined at temperatures of 425, 450, 500, and 550℃ in an FBPR. The discrete lumping model approach was developed for the estimation of various products formed during the primary pyrolysis and secondary cracking reaction of tar. The kinetic parameters obtained at different operational conditions were evaluated.

6.2 Experiment and materials

The same lab-scale pyrolysis reactor and TGA introduced in Chapter 3 were conducted for this case study. The HDPE pyrolysis of a thin bed was attempted to investigate the difference between TGA and FBPR at same conditions, corresponding a comparison to the thick bed of FBPR (Table 6.1). Samples preparation and experimental procedures of HDPE in this study follow the description in Chapter 3.

Table 6.1 The thickness of reaction bed

Bed	Description	Thickness (mm)	Particle size
Thick bed	Ceramic beads and sintered glass plate	30-50	$8\times 8mm^2$
Thin bed	Ceramic beads and sintered glass plate	2.0-3.0	150-250μm
TGA bed	TGA ceramic crucible	2.0-3.0	150-250μm

6.3 Experiment results and discussion

6.3.1 The thermal degradation behaviour of HDPE waste via TGA

The TGA experiments were undertaken at designed experimental temperatures (e.g. 400, 425, 450, 500, and 550℃) with a heating rate of 25℃/min and carrier gas (nitrogen) of 50ml/min. there is strong dependence between experimental temperature and the conversion rate, which was shown in Figure 4-6. The TGA results indicate that the reaction temperature has a

significant effect on the thermal degradation process. The lowest conversion rate was measured at 400℃ to be 3.26%; the highest conversion rate was obtained at 550℃ to be 99.4%, while 99.2% of conversion was also found at 500℃. This result indicates that a commercial cost-effective purpose can be taken for rigid PE pyrolysis at a target temperature of 500℃. The study of rigid HDPE waste pyrolysis characteristics at the temperature of 550℃ is attempted to examine the influence of higher temperature on yield distribution. The predicted kinetic parameters are estimated in terms of the conversion change linking to single step lumping model (Figure 2-3) and the Arrhenius law. The activation energy and pre-exponential factor of HDPE thermal decomposing process via TGA are 197.35 kJ mol^{-1} and 4.25×10^{13} min^{-1}.

6.3.2 Effect of the bed thickness on conversion of HDPE degradation via TGA and FBPR

Figure 6-1 shows an evaluation of the weight percentage of residue in the form of fused plastic aggregates together with some char-like residues at the plateau temperature range of 400-550℃. A clear difference of residue yields between TGA, the thin bed and the thick bed of FBPR can be observed the yield change from over 40 percent to less than 2 percent at the temperature range of 450 -500℃. While the temperature increased over 500℃, less than 5 percent residue yields were observed at three conditions. Therefore, different bed thickness and particles have an obvious effect on conversion, the difference gradually reduced with temperature increase. On one hand, less amount of sample in thin bed can have better heat transfer at low temperature than larger amount sample in thick bed. In fact, the rheological behaviour of polymer in the thin bed has better performance than in the thick bed. On another hand, the difference of reactor performance between TGA and FBPR with similar bed thickness (thin bed) showed different conversion at a lower temperature. The variation of temperature measurement between TGA and FBPR also results in the difference of conversion. Zhou et al [177] reported that the polyolefin polymers can be thermally decomposed to gaseous and liquid hydrocarbons. The part of char residue may be attributed to polymer impurities from the presence of additives in postconsumer HDPE waste.

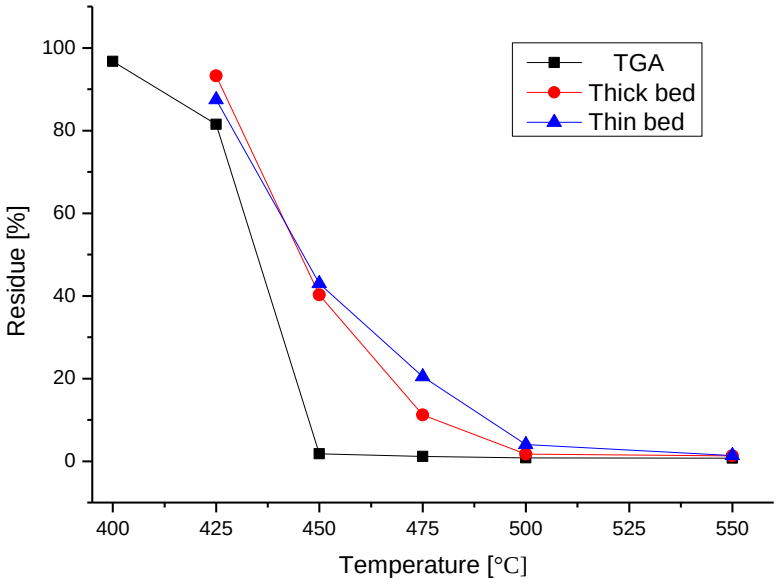

Figure 6-1 The residue yields from TGA, thin bed and thick bed at different temperature

As shown in Figure 4-6, thermal degradation of HDPE starts at the temperature of 400℃, and the conversion changes from 3.3 percent to 18.5 percent when the temperature reaches 425℃. This indicates that temperature of 400℃ provided the activation energy for bond cleavage in the HDPE hydrocarbon structure, the thermal conversion was enhanced with temperature increase. The decomposition of HDPE significantly intensified with temperature increase from 475℃ to 510℃ corresponding to the conversion from 10 percent up to 95 percent. The polyethylene decomposition initially involves scission of tertiary carbon bonds and/or ordinary carbon-carbon bonds in the beta position to tertiary carbons [178]. Higher temperature enhances the chain scission and cleavage of carbon bonds and thereby favours the production of smaller molecules.

Figure 6-2 shows that the conversion from the thick bed is higher than the one in the thin bed between 450℃ and 550℃, and lower conversion at 425℃. At lower temperature range (e.g, less than 430℃), less amount sample in thin bed can perform better in terms of heat transfer to boost the conversion of plastic waste. With temperature increase (e.g. between 450℃ and 550℃), the conversion difference between the thin bed and the thick bed is reduced, which can be seen at the temperature between 500 and 550 ℃ in Figure 6-1. Lin et al [179] also reported that high mass loading affects heat transfer and the pyrolysis outcomes in their study

of kinetics and mechanism of cellulose pyrolysis. The presence of reaction heat dominated by the secondary reactions such as cracking and re-polymerisation at a higher temperature in thick bed, gave exothermic phenomenon effects. Di Blasi et al [180] reported that exothermic effects are clearly observed at the sample centre during the pyrolysis of thick samples/beds uniformly heated along the external surface.

6.3.3 Effect of bed thickness on product yields

Figures 6-2 to 6-5, Appendices 2.9 and 2.10 also show the yield distribution of HDPE pyrolysis obtained from thin beds and thick beds between 425 and 550℃ and different residence time. At 450℃, product yields (gas, oil, and wax) obtained from thin bed was higher than the one from the thick bed. More condensed yields (oil and wax) were obtained from the thick bed at 500 ℃ and 550℃, while more gas yield was found from the thin bed reactor. The conversion difference of HDPE between the thin bed and the thick bed is narrower, down from 20 percent to 0.1 percent, with the temperature increase from 450 to 550℃. The effect of bed thickness on the product yields might be taken into account from two aspects; on the one hand is that the particles size difference, smaller particle size means larger surface area for heat transfer; on the other hand is carrier gas influence, with heated carrier gas passing through the bed via "bubble" flow, it is easier to go through thin beds, which improves heat transfer efficiency. The improvement of heat and mass transfer can result in higher conversion and more gases, especially at a lower temperature. Martínez et al [181] commented that the bed thickness increase means a growth of residence time during the study of HDPE pyrolysis process in fluidised bed reactor, which indicates thinner bed of fused plastic will result in a higher conversion than the thick bed at same residence time. Figure 6-5 also shows a clearly higher gas yield obtained from the thin bed reactor than the thick bed one.

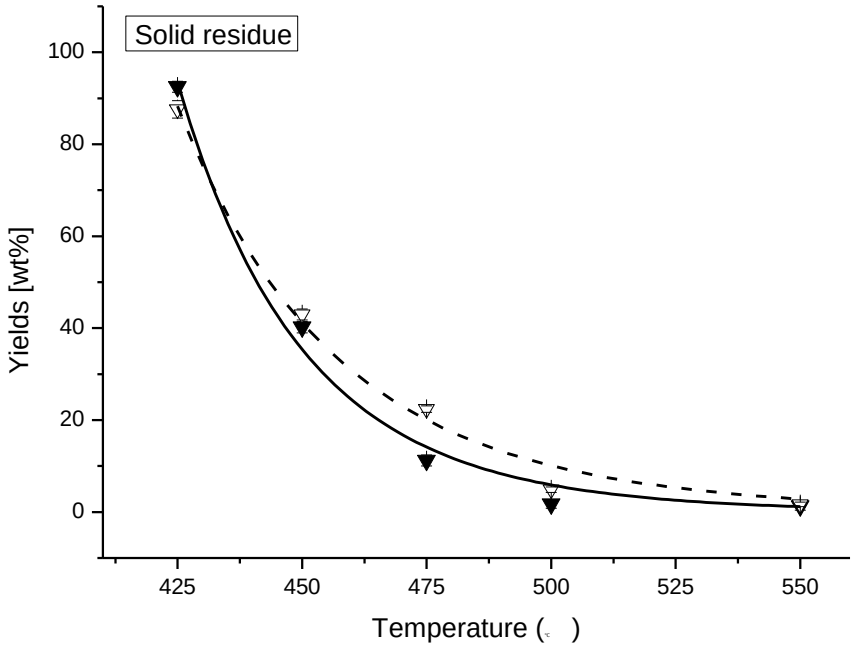

Figure 6-2 Residue yields from HDPE pyrolysis at thin bed and thick bed under different temperatures and particle sizes (Solid line: Thick bed, Dash line: Thin bed)

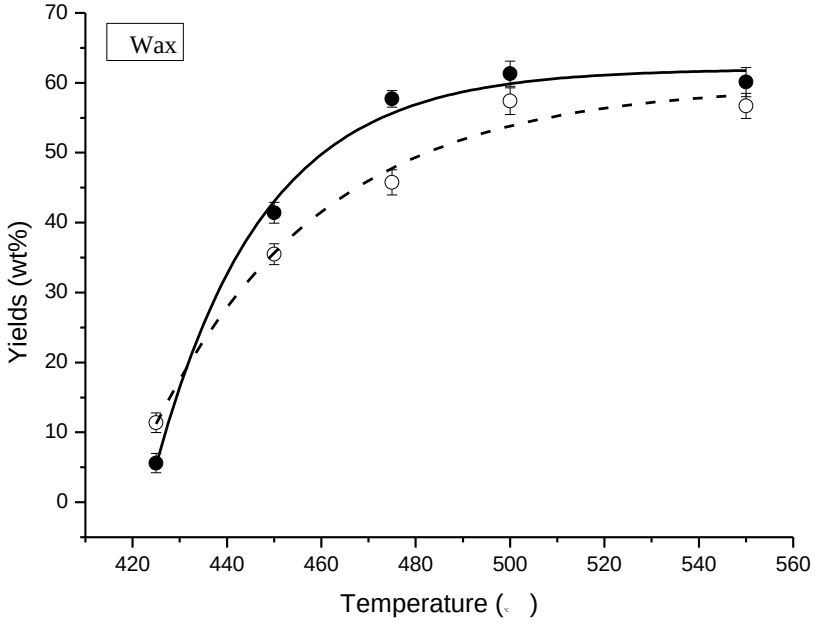

Figure 6-3 Wax yields from HDPE pyrolysis at the thin bed and the thick bed under different temperatures and particle sizes (Solid line: Thick bed, Dash line: Thin bed)

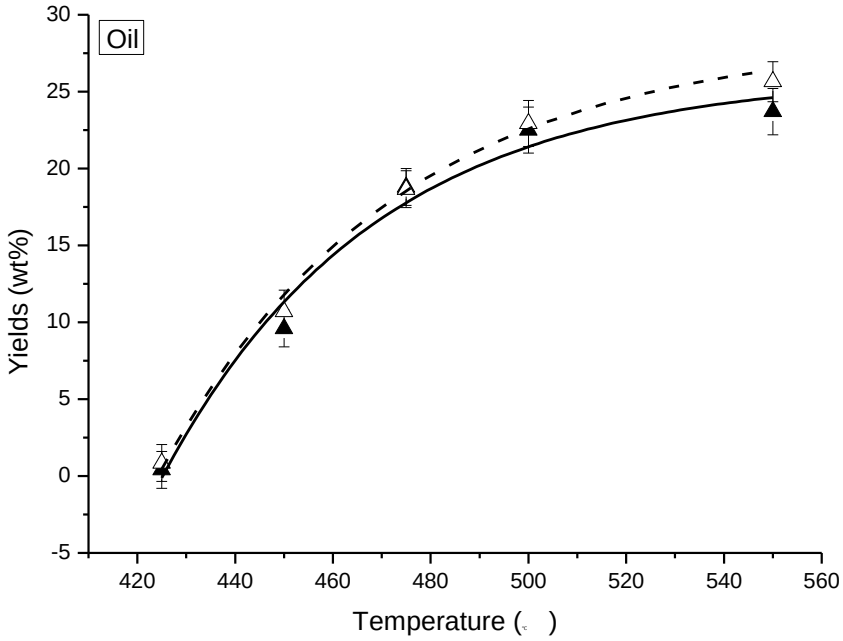

Figure 6-4 Oil yields from HDPE pyrolysis at the thin bed and the thick bed under different temperatures and particle sizes (Solid line: Thick bed, Dash line: Thin bed)

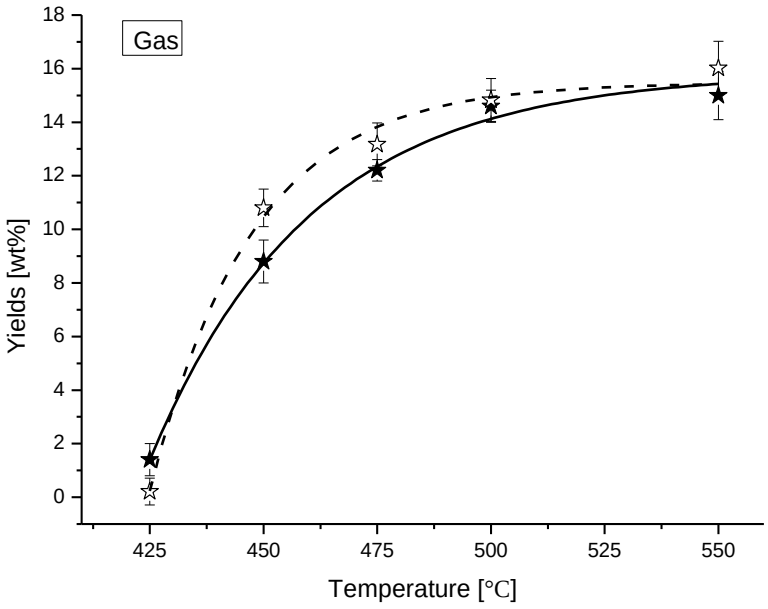

Figure 6-5 Gas yields from HDPE pyrolysis at the thin bed and the thick bed under different temperatures and particle sizes (Solid line: Thick bed, Dash line: Thin bed)

6.4 Effect of temperature on the distribution of product composition of rigid PE pyrolysis over thin bed and thick bed

As above described, the temperature is well recognised as a key variable parameter of pyrolysis process in the determination of both the rate of thermal decomposition and the stability of feedstock and reaction products [10, 136, 182, 183]. A preliminary study of HDPE pyrolysis at the temperature between 400℃ and 550℃ via TGA was conducted to investigate the impact of the pyrolysis temperature on the mass change and the thermal stability of the sample. The yields distribution was carried out via FBPR. A significant difference of product distribution at 450, 500, and 550℃ was observed in both thin bed and thick bed. The waxes were found to be the fraction of maximum yield at three temperatures. Their yield accounted for over 60 percent at 500℃ from both thin bed and thick bed reactors.

The effect of temperature on the product yields is shown in Figures 6-2 to 6-5 and Appendix 2.9. The yield of the wax, oil, and gas increased with the pyrolysis temperature from 450℃ to 500℃, a decrease of solid residue yield occurred simultaneously. The volatile compounds were condensed to the liquid phase at room temperature and below -40℃. However, the wax yield decreased when the temperature reached to 550℃ from 500℃ due to the cracking of the heavier fraction (wax and tar) in the volatilisation gases at higher temperature [8, 10, 43, 165, 182]. This also resulted in the increase of gas yield and light oil yield. Williams and Williams [136] described similarly that the cracking reaction of heavier liquid products formed caused the increase of gas evolution at a higher temperature. However, the change was slightly lower than the trend between 450℃ and 500℃, which indicates that the pyrolysis temperature of 500℃ was high enough for the primary thermal degradation of rigid PE. At 500℃, 87 percent of wax /oil was produced with 11.3 percent gas products generated.

The temperature measurement is a major concern during the pyrolysis process. Flynn [184] mentioned that temperature imprecision may be the greatest source of error in the thermal analysis experiments. Different location of temperature sensors may result in a temperature gradient along the apparatus in the same experiment and processing, where the temperature of fused plastic at a fixed-bed batch reactor is clearly lower than the temperature on the top surface of reactor [39]. The temperature measurement for thin bed reactor may cause errors in the estimation of sample temperature because small amount sample (≈1gram) in the thin

bed may displace thermocouples so that they are not in full thermal contact with samples after plastic fusion. It is considerable that there exists thermal lag of thermocouple which causes a difference between the true sample temperature and an externally measured sample temperature [185]. This temperature lag may result in noise in the temperature data so that the actual temperature controlled by software programme differs from the measured temperature (Figures (6-6 to 6-11), which would broaden the variation of yield distribution. Figures (6-6 to 6-11) show three temperatures that were monitored by three K-type thermocouples at bottom and top of reactor bed, and programme controlled by CX- thermal software. A flatter fluctuation of temperature curves in the thin bed than in the thick bed indicates thermal conversion is easier to complete in the thin bed due to less feed mass amount, and also real reactions could be more complicated than the ones from experimental observation and measurement.

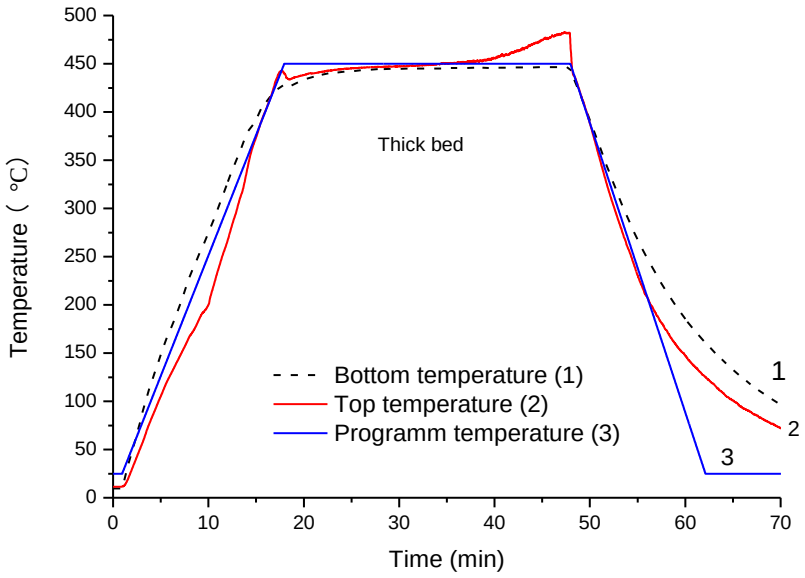

Figure 6-6 Temperature variation over thick bed at 450℃

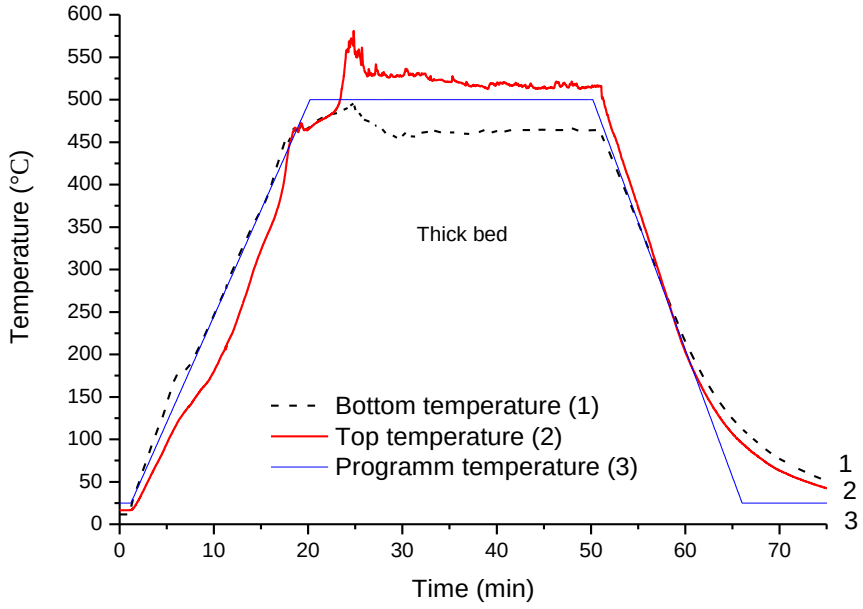

Figure 6-7 Temperature variation over thick bed at 500℃

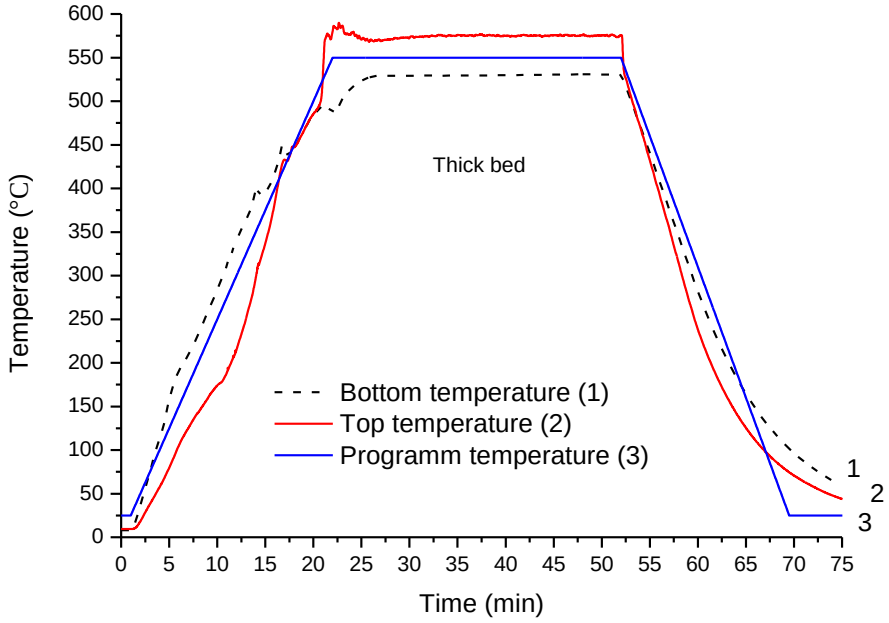

Figure 6-8 Temperature variation over thick bed at 550℃

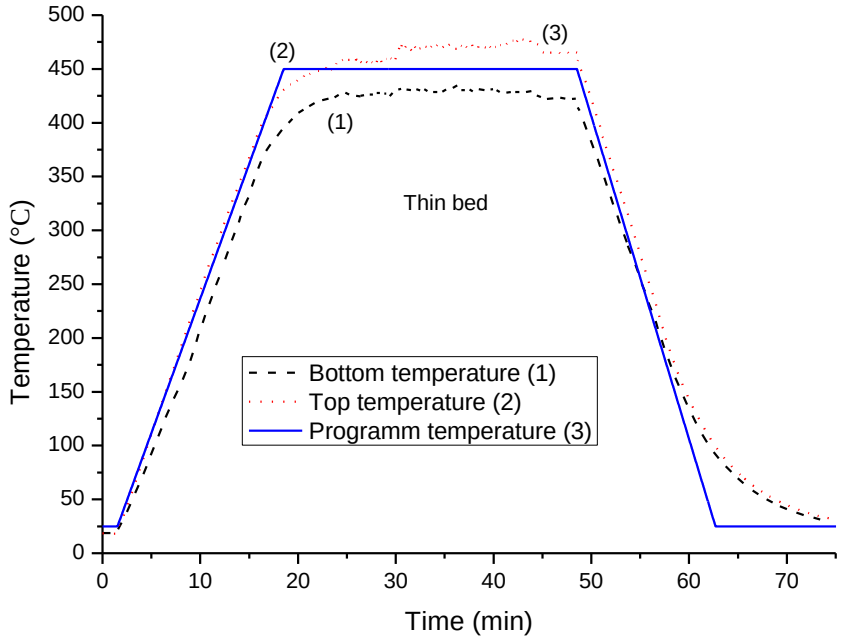

Figure 6-9 Temperature variation over thin bed at 450℃

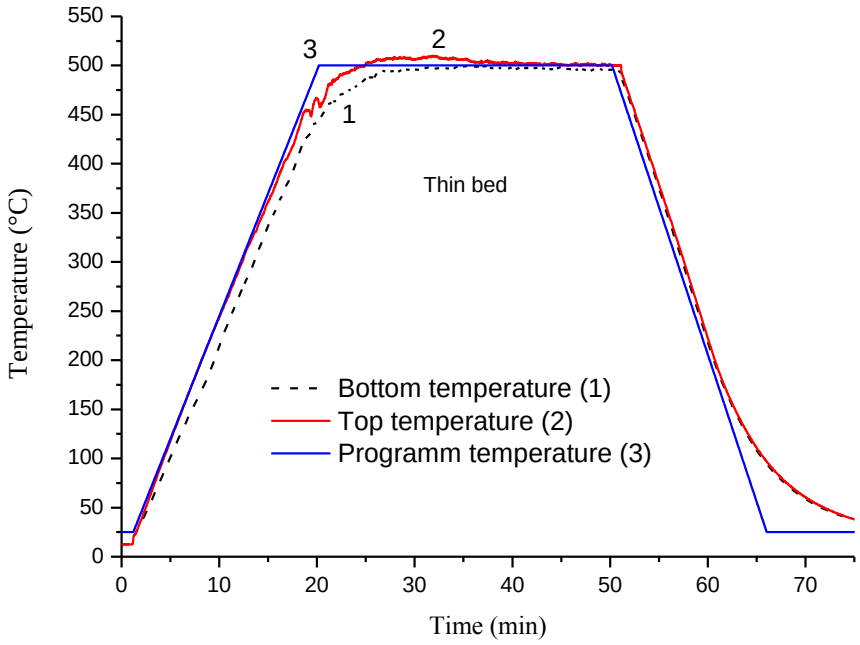

Figure 6-10 Temperature variation over thin bed at 500℃

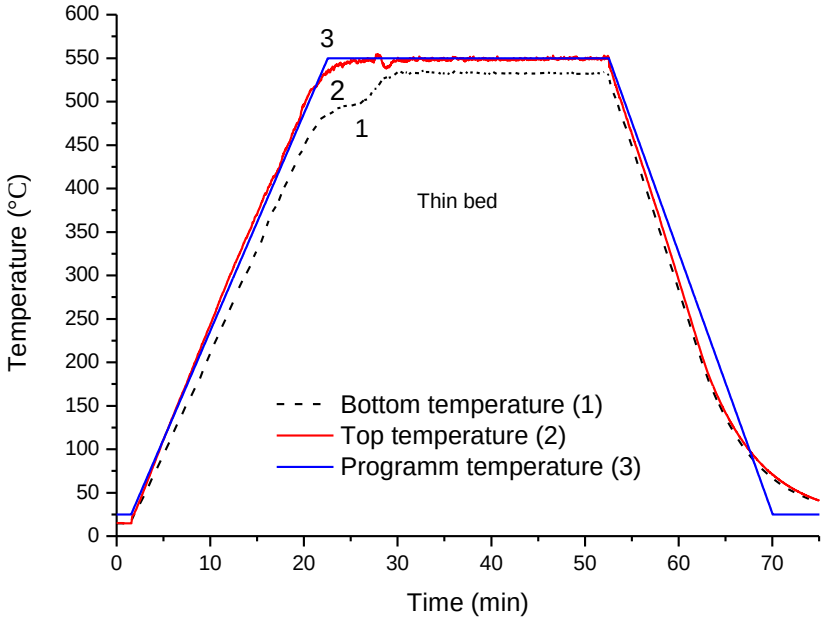

Figure 6-11 Temperature variation over thin bed at 550℃

The evolved gas compositions were established by Hiden Mass Spectrometer. The results of gas derived from the HDPE pyrolysis are given in Figures 6-12 and 6-13. H_2, CH_4, and C_2H_6 all show increased yield with temperature increase from 425℃ to 550℃, however, gases yields in thin bed were closer to each other. Higher yields of ethane observed in the thin and thick bed reactors, indicate that ethane is the main gas in HDPE pyrolysis, while higher yields of ethane from thin bed than one from thick bed indicates that bed thickness has a feasible effect on the gas composition. Hydrogen yields are not sensitive to temperature in thick bed reactors; nevertheless, they rise steadily in the thin bed reactor with temperature increase. Methane yield in both bed thickness shows steady growth, indicating that methane is not the main contributor to the increase of gas volume during rigid PE pyrolysis.

Commercial plastic waste such as HDPE often contains a variety of oxidised functionalities (e.g.-CO-, =OOR, -CHO, -OOH, etc.) due to processing and application [133, 186]. The presence of these groups may cause the generation of oxygen and carbon dioxide. Carbon monoxide was not identified from the pyrolysis of HDPE.

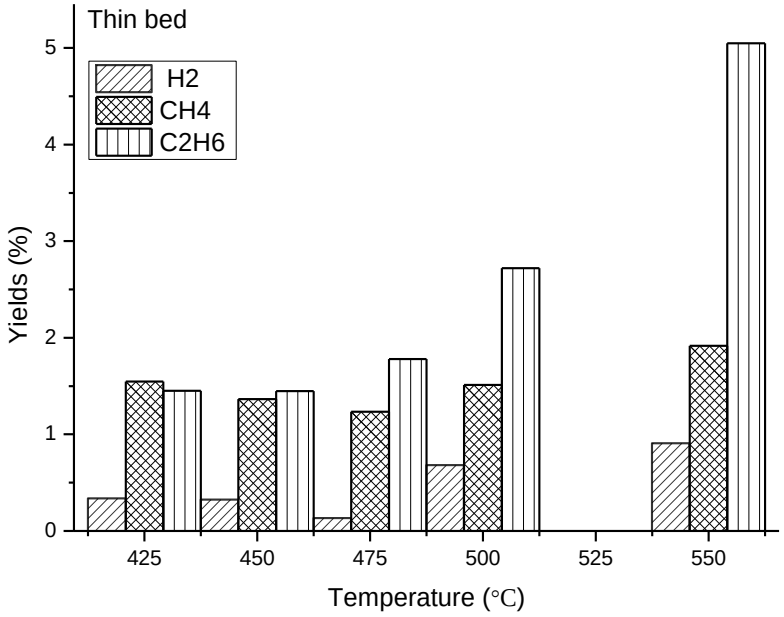

Figure 6-12 The gas composition of HDPE pyrolysis from thin bed

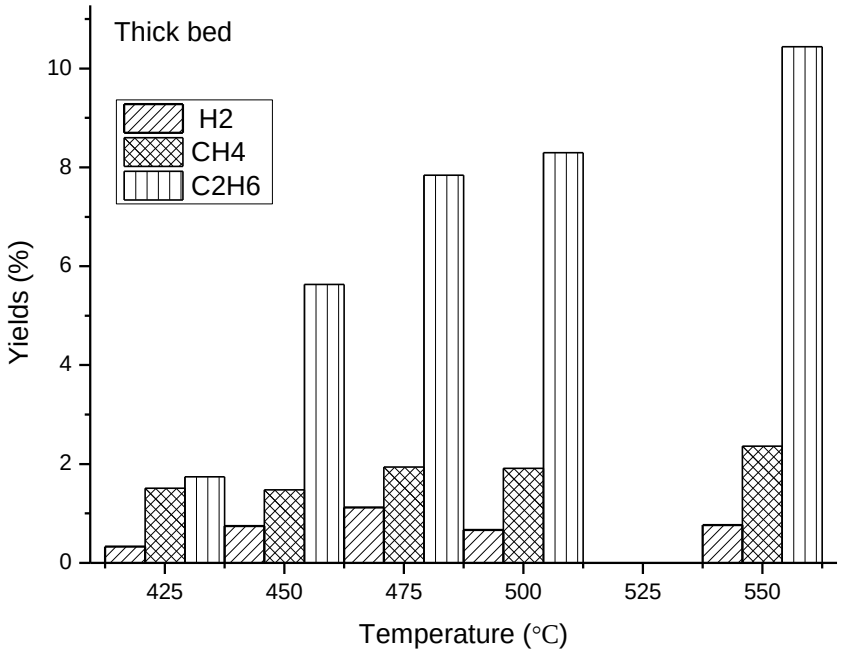

Figure 6-13 The gas composition of HDPE pyrolysis from thick bed

6.5 Kinetic analysis

The estimation of the rate constant for all reactions involved in the pyrolysis process is of crucial importance in model development [30]. In polymer degradation, pyrolysis processes usually involve a series of elementary chain reactions with different reaction mechanisms. These elementary reactions (steps) may present different kinetic parameters. In this study, the reaction pathway for rigid PE pyrolysis proposed is shown in Figure 6-14. This model contains three parallel reactions (lumps) and secondary (wax cracking) reactions when the temperature is high enough. To analyse the kinetic model characteristics of the pyrolysis of plastic waste over different bed thickness, the three parallel decompositions and secondary cracking of rigid PE pyrolysis for the four lumps scheme could be written as:

$$\frac{dx_{plastic}}{dt} = -(k_1 + k_2 + k_3 + k_4)(1 - x) \quad (6\text{-}1)$$

$$\frac{dx_{Gas}}{dt} = k_1\,(1 - x) \quad (6\text{-}2)$$

$$\frac{dx_{wax}}{dt} = k_2\,(1 - x) - k_4 x_{wax} \quad (6\text{-}3)$$

$$\frac{dx_{Liquid}}{dt} = k_3\,(1 - x) + k_5 x_{wax} \quad (6\text{-}4)$$

$$\frac{dx_{Char\ residue}}{dt} = k_4\,(1 - x) + k_5 x_{wax} \quad (6\text{-}5)$$

where $x, k_1, k_2, k_3, k_4, k_5$ represent normalised mass fraction from decomposed sample mass, the rate constant (min^{-1}) of the pyrolysis of plastic waste to gas phase, wax fractions, liquid fractions, and wax fractions to oil phase and light liquid fractions during the reaction, respectively.

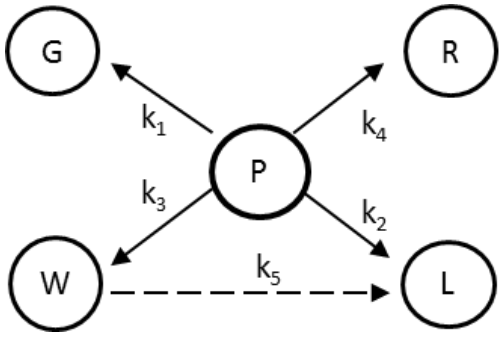

Figure 6-14 Schematic of different pathways of HDPE pyrolysis

The kinetic parameters are determined at three different temperatures by using the lumping approach based on experimental data in these models, involving five rate constants. The

numerical optimisation of a fourth-order Runge-Kutta algorithm of the least square deviations is employed using MATLAB software to determine the optimal parameters.

Table 6.2 presents the values of rate constants obtained from the kinetic model. The model results show a good agreement with experiment data (Fig. 6-12). In primary pyrolysis step, it is clear that the rate constant of rigid PE pyrolysis ($k_{HDPE} = k_1+k_2+k_3$) rises with temperature increase, along with an increase in the rate constants of gas, oil, and wax from both thin bed and thick bed. However, a discrepancy in rate constants can be seen between thin and thick beds at different temperatures. Lower overall rate constant ($k_1+k_2+k_3$) to form gas, oil, and wax was observed from thick bed at 425 and 450℃, while a slightly higher rate constant was found at 475℃. This indicates that small sample amount and particle size can enhance thermal conduction efficiency to provide better heat transfer [180], especially at lower temperatures. The limitation of heat transfer from sample amount and particle size could be ignored with increased temperature.

Table 6.2 Kinetic parameters of rigid PE pyrolysis over thin bed and thick bed at different temperatures

Bed	Temperature	Rate constant (sec^{-1})					
		$k_1+k_2+k_3$	k_1	k_2	k_3	k_4	k_5
	(℃)	(min^{-1})	(min^{-1})	(min^{-1})	(min^{-1})	(min^{-1})	(min^{-1})
Thick	425	2.40E-02	4.03E-03	3.63E-03	1.64E-02	2.60E-01	0.00061
	450	1.57E-01	2.51E-02	2.48E-02	1.07E-01	1.17E-01	0.00086
	475	3.30E-01	4.53E-02	5.79E-02	2.27E-01	4.16E-02	0.00173
Thin	425	4.61E-02	3.24E-03	4.37E-03	3.85E-02	3.59E-01	1.25E-03
	450	2.20E-01	4.11E-02	1.38E-02	1.44E-01	1.65E-01	2.02E-03
	475	3.26E-01	5.38E-02	5.36E-02	2.19E-01	4.75E-02	1.45E-03

The values of k_1 obtained from the thin bed were more than the values from the thick bed between 425 ℃ and 475℃, which may indicate the less mass amount and smaller sample size will yield more gas. The values of k_{HDPE} at 475℃ from both thin bed and thick bed are far higher than the values at 425℃. The result presents an evidence that temperature is a key parameter affecting the product distribution. The value of k_3 is obviously larger than the values of k_2 and k_1 at the same temperature. A similar result can be seen in the literature [8, 10, 42]. The kinetic constant of wax cracking into oil is much lower than k_2. This indicates that the secondary cracking reaction of wax did not dominate the oil yield variation in the temperature range between 425 and 475℃ during the pyrolysis process.

Figure 6-15 shows the model result fits well with experimental data. A prediction of wax cracking within one second residence time was simulated for the cracking process (this is a hypothetical time because it is difficult to control the residence time of volatiles in the high temperature zone in the reactor). The logarithmic yield of oil generated from wax cracking from 10^{-4} to 10^{-2} occurred within 0.3 seconds in thin bed and 0.4 seconds in thick bed. This indicates that the cracking reaction occurs in a very short time at the reaction temperature, which mentioned in Chapter 5. It also can be concluded that thinner bed thickness has more effect on wax cracking.

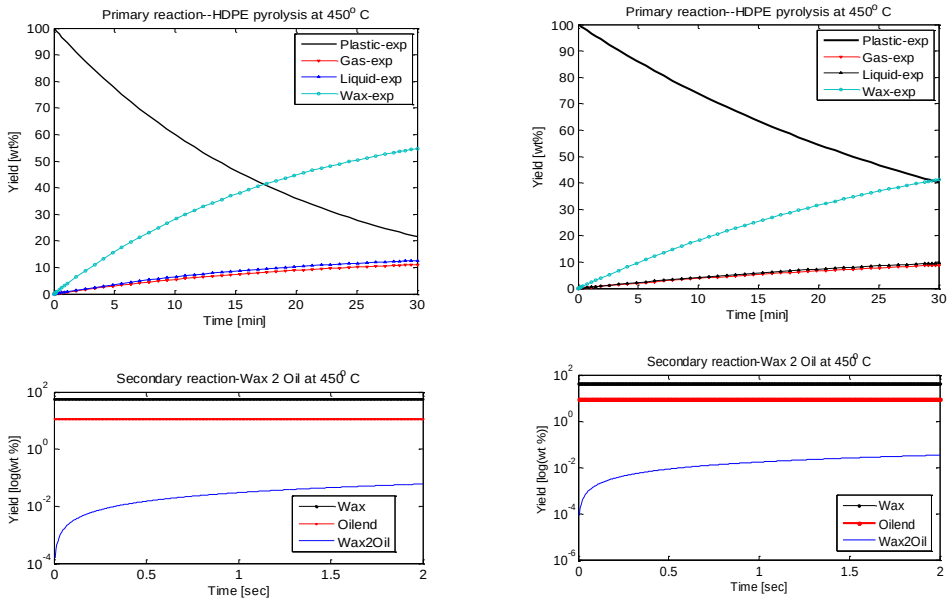

Figure 6-15 Model predictions of HDPE primary pyrolysis reactions and secondary reaction at 450℃ via (A) thin bed and (B) thick bed.

6.6 Model validation

To validate the developed kinetic model, the experimental data obtained at 550℃ was applied to validate the model, which is shown in Figure 6-16. It can be seen that the model data curves were to be consistent well with the experimental data, and the model presented a reasonable result from HDPE pyrolysis.

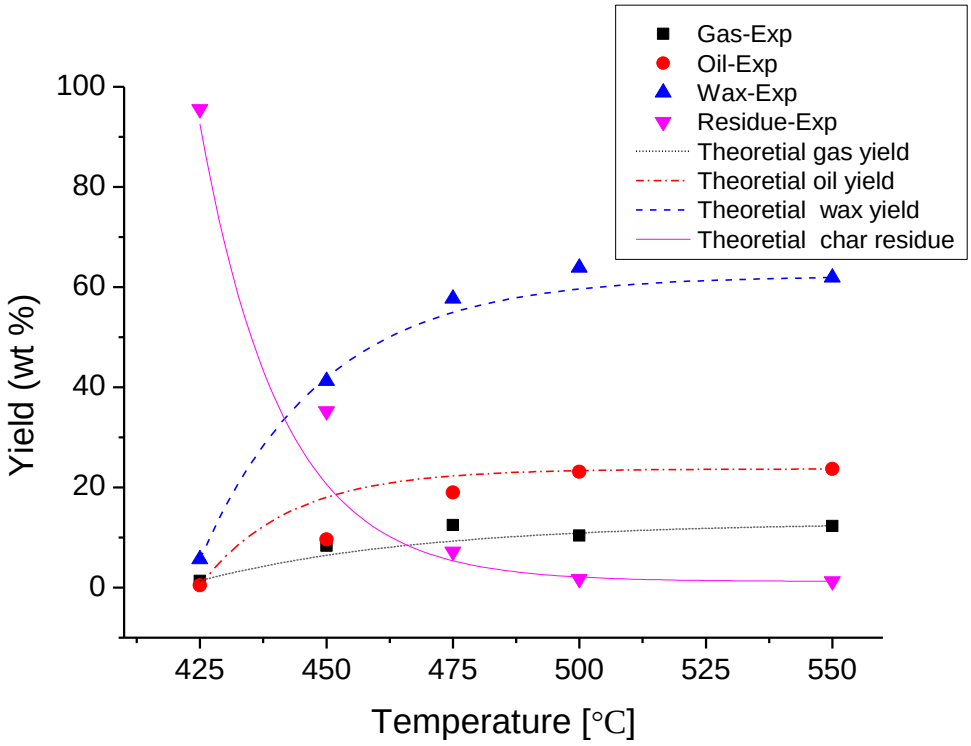

Figure 6-16 Model validation of HDPE pyrolysis

6.7 Estimation of activation energy and pre-exponential factor

Using the results obtained at 425, 450, and 475℃, the Arrhenius plots for the kinetic rate constants are shown in Figures (6-17 to 6-19) and Table 6.4. The slopes and intercepts of plots were obtained to calculate the activation energies and pre-exponential factors via linear regression. The overall activation energy of the HDPE thermal decomposition process via TGA and FRPR with thin bed and thick bed were estimated to be 197.35 kJ mol^{-1}, 171.0 kJ mol^{-1}, and 228.6 kJ mol^{-1}, respectively. The difference of estimated E_a may be ascribed to experimental data uncertainties due to reactor performance and measurement errors, as well lumping selection during model simulations. For example, the small charge in the thin bed increases the difficulty for a precise measurement of the yield of gas, liquid,

and wax, due to that measuring errors from many glasswares affects the result of mass balance calculation. Nevertheless, the calculated E_a values are in accordance with data in the literature (160-320 kJ mol^{-1} estimated by Gao et al [187]; 207-220kJ mol^{-1} estimated by Westerhout et al [62]; 185-271kJ mol^{-1} estimated by Conesa et al [163]; 147.3 kJ mol^{-1} estimated by Al-Salem and Lettieri [8]). The activation energies and pre-exponential factors for HDPE decomposition into gas, oil, and wax, and also wax cracking into oil are summarised in Table 4 obtained on the basis of Arrhenius Law presented in Figures 6-18 and 6-19.

Table 6.4 Kinetic parameters of reaction pathways of HDPE pyrolysis from different bed thickness and TGA

Reactor bed	Reaction pathways	E (kJ mol^{-1})	A (min^{-1})	R^2
Thin bed	HDPE-Gas, Oil, and Wax	171.0	3.45E+11	0.9421
	HDPE-Gas	151.8	1.00E+10	0.9127
	HDPE-Oil	229.3	2.77E+15	0.9402
	HDPE-Wax	217.4	7.69E+13	0.9457
	Wax-Oil	47.79424	5.175831	0.8474
Thick bed	HDPE-Gas, Oil and Wax	228.6	3.58E+15	0.9379
	HDPE-Gas	211.3	3.11E+13	0.9349
	HDPE-Oil	241.6	5.08E+15	0.9459
	HDPE-Wax	229.3	2.77E+15	0.9457
	Wax-Oil	125.9	1.17E+06	0.7733
TGA	HDPE-Volatile	197.35	4.26E+13	0.9667

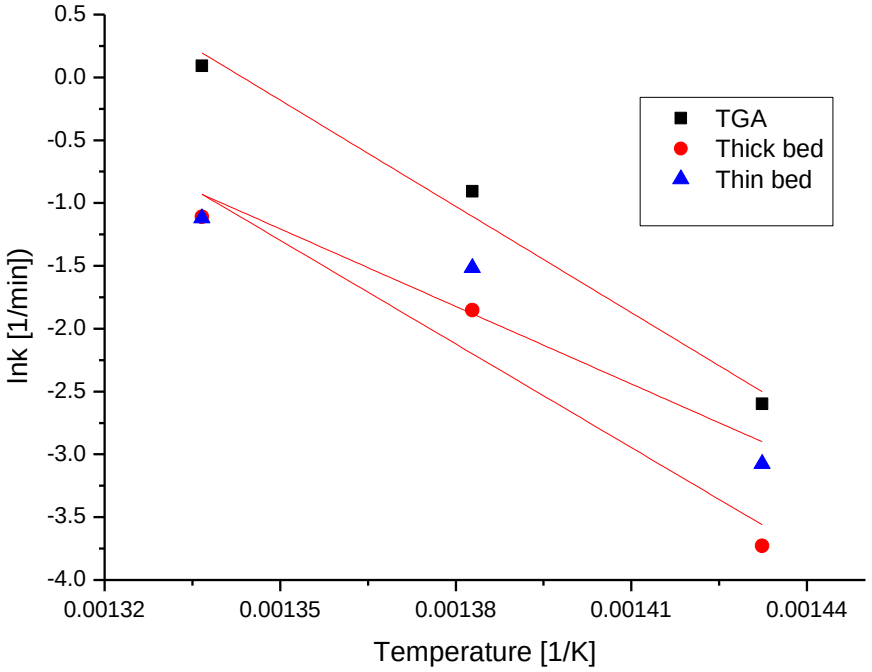

Figure 6-17 Arrhenius plot of HDPE pyrolysis

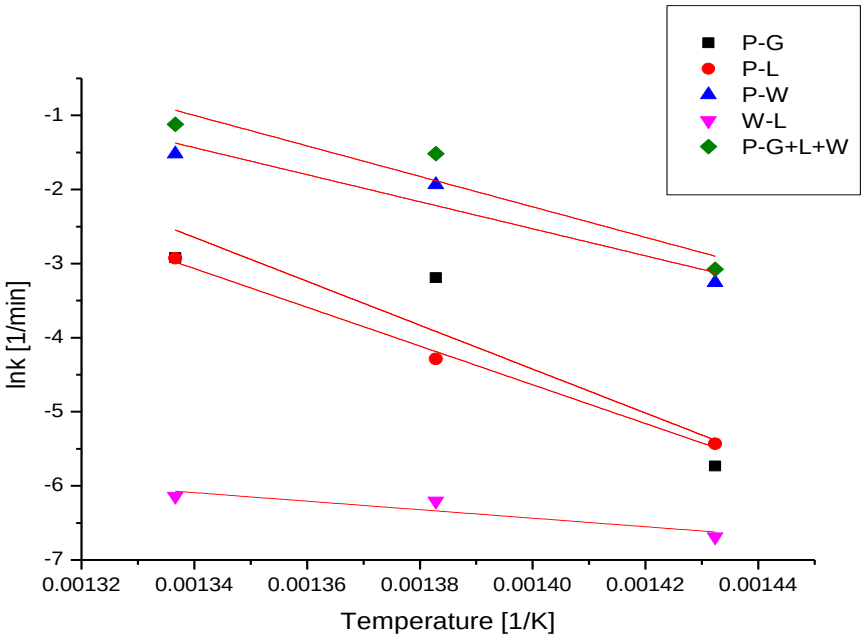

Figure 6-18 Arrhenius plot of HDPE pyrolysis into gas, oil, and wax from thin bed reactor

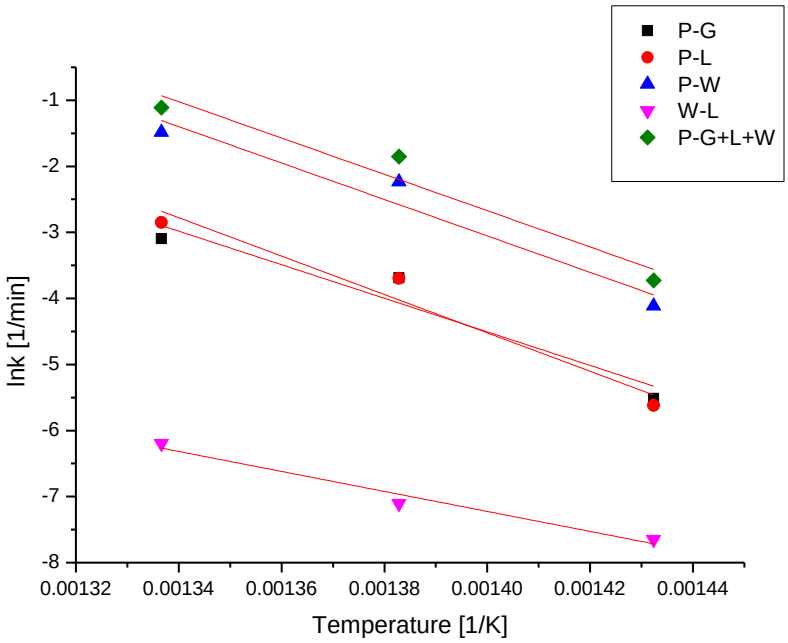

Figure 6-19 Arrhenius plot of HDPE pyrolysis into gas, oil, and wax from thick bed reactor

The activation energy variation with conversion is possible due to multiple competing reactions (steps) in HDPE degradation. The estimated activation energy may only symbolise the kinetics of the steps (element reactions) that dominate the kinetic process [133]. Nevertheless, the presence of heteroatom groups and their uncertain content may influence the decomposition mechanism of HDPE to enhance the variation of activation energy of HDPE decomposition.

6.8 Conclusion

The thermal decomposition behaviour of HDPE has been examined via TGA, and different bed thickness of FBPR. The bed thickness of TGA and FBPR affects on the product distribution, which provides the trend of production distribution with a scaled-up reactor from TGA to FBPR, and feed mass variation. The lumped kinetic model developed was validated based on experimental data, and shows a good agreement with experimental data from HDPE pyrolysis. More liquid and wax fractions were yielded from FBPR with the thin bed at the temperature range of 425-475℃, which concludes that bed thickness has a certain effect on product distribution. A slight difference in the estimation of kinetic parameters between TGA, thin bed, and thick bed was observed. This indicates that the operational variables such as

fed mass amount, particle size, and equipment have some considerable impact on the estimation of kinetic parameters.

CHAPTER 7 CONCLUSIONS AND FUTURE RECOMMENDATION

7.1 Conclusions and Scopes of the work

This PhD study was undertaken on exploring the applications of lumping kinetics methodology to energy and feedstock recovery from plastic waste via pyrolysis process. The modelling simulation was employed to identify the kinetic characteristic of primary pyrolysis of plastic waste and the reactivity in terms of their measuring property, which was realised in the experimental work. This study has also sought to know the effects of process conditions of pyrolysis on the product distribution and kinetic characteristic via thermogravimetric analysis and lab-scale fixed bed pyrolytic reactor, as well as optimisation of production conditions. The discrete lumping model approach was applied to determine the kinetic characteristic of plastic pyrolysis. Nevertheless, the development of discrete lumping models in this project involves some simplifying assumptions in the model development because of the complex pyrolysis reaction system. The model simplification approach has been employed in predicting the pyrolysis reactions with different feedstock and different decomposing mechanism. The lumped species via model reduction method are not real species in the mixture, instead of that pseudo-species defined with similar physiochemical properties (e.g. molecular weight, carbon number or boiling point). Thus, lumping methodology treats the continuous complex mixture into discrete points (nodes), there is nothing known between the nodes, because this technique only performs apparent reaction not the real reaction mechanism. While this methodology can still offer the information which ones need in practical circumstances with fewer parameters, and the boundary between nodes can be solved using lumping method mathematically. Therefore this study provides a flexible model solution to fit different proposals, and presents a considerable basic work in the optimisation of pyrolysis process.

Specifically, in the experimental study (Chapter 4), the pyrolysis behaviour of PE, PP, PET and their mixture were studied. TGA study showed that the conversion varies with function of feedstock components, time and temperature. Additionally, the interaction effect of temperature and feedstock components on the volatile yield distribution was investigated. It was found that feedstock determines the product distribution, while process parameters (e.g.

temperature and residence time) can dominate yield distribution. For instance, over 84 percent of PP waste can convert into oil/wax at 550℃, while only 60 percent of PET can convert into oil/wax products. The conversion of HDPE changed from 12.4 percent to 99 percent with the temperature increase from 425℃ to 550℃ within 30 minutes residence time. In this work, the decomposed temperature starting points of PE, PP, PET, and the mixtures of PE/PP and PE/PP/PET were observed at the temperature of 413.5℃, 407℃, 404℃, 356℃, and 270 ℃, respectively. It is slightly lower than the results reported by Scheirs et al [10], which the decomposition temperature of PE and PP, and PET started at the range of 440-490℃, 420-470℃ and 380-440℃, respectively. It maybe the sample difference, and position of the reactor in the furnace. This work also indicates the interaction effect of different sample components on the yield distribution. The investigations of the pyrolysis of different plastic waste and their mixture under TGA and FBPR indicate that combination effect of pyrolysis process parameters exist under which it is possible in the mixture of plastic waste; and also kinetic studies of plastic waste pyrolysis at different reactors and bed thickness may contribute to a potential scale-up solution of energy recovery from waste to provide potential solution to mitigate the dependence on fossil fuel.

The discrete lumping scheme is a powerful tool to describe the indefinite reactions or species of the mixture generated from the process in a definte way so that they can be predicted and modelled by only fewer numbers of parameters, even though precisely devising the exact reaction mechanism is very diffcult due to the reaction complexity in the pyrolysis reaction system. End products observed from experiments were simply selected as the basic lump to describe the kinetic pyrolysis scheme in this study.

Different reaction pathways of plastic polymer into gases, oils, waxes and/or solid residue as well as secondary reactions (residue to gases, oils, waxes, and waxes to gases and oils) were proposed. To better understand the pyrolysis process and examine the flexibility of lumping model based on the experimental data, primary pyrolysis lumping models were developed to estimate the rate constant for PE, PP and their mixture based on the experimental data obtained at different operation conditions. The developed model is flexible and suitable to describe the pyrolysis behaviour of individual and mixed plastic waste. The implementation of secondary reaction in the model development of plastic waste is shown that heavier fraction (e.g. wax) probably undergoes cracking reactions at a high reaction

temperature, which may dominate the product distribution in the waste recovery solutions. Lump selection can lead to the estimation of deviation of kinetic parameters, which is evidenced in this work. For instance, polyvinyl polymers PE and PP are almost converted into volatiles product at certain conditions (e.g. 550℃ and 30 minutes), the selection of lumped solid residue observed in the experiments at the some conditions (e.g. lower temperature and/or shorter residence time) resulted in obvious difference which is discussed in Chapter 5. The residue lumped as unreacted plastic polymer resulted in a lower value of activation energy than the one that treats residue as a new lump formed by lower molecular weight polymer. Nevertheless, residence time can also bring about less prediction accuracy. Longer residence time observed in the experiment will result that calculated rate constant from model fitting is lower than the real value so that activation energy could be lower than its real value. Besides that, other existed reactions, which are not included in the model, may cause the errors during the estimation of kinetic parameters. After the model modification and validation by using the experimental data, the proposed kinetic schemes are capable of predicting the conversion and product yields.

7.2 Recommendation for future work

1. Other process parameters, such as catalyst, are also very important variables in energy recovery from plastic waste via pyrolysis. The pyrolysis characteristic of mixed plastic waste with other organic matters such as biomass and sludge is also an attractive study to mitigate the environmental implication. Modelling development of catalyst deactivation is, therefore, valuable to study to the prediction of the catalytic pyrolysis.

2. Upgrading of higher yield and better quality oil is one of the most economical signs in energy and chemical contents recovery from plastic waste. Modelling oil yield distribution in thermal and catalytical pyrolysis via continuum lumping model deserves careful and deliberate consideration.

3. Evaluation of kinetic characteristic is a significant element in the prediction of the pyrolysis process. Modification of the estimation of deviation of kinetic parameters on the basis of operational variables and reactor performance needs further investigation.

REFERENCE

1. EPRO, P.E.P.R.E.a., *Plastics – the Facts 2016: An analysis of European plastics production, demand and waste data* 2016: PlasticsEurope.
2. Jambeck, J.R., et al., *Plastic waste inputs from land into the ocean.* Science, 2015. **347**(6223): p. 768-771.
3. EPRO, P.E.P.R.E.a., *Plastics – the Facts 2014/2015: An analysis of European latest plastics production, demand and waste data*, 2015.
4. Reinhart, D.R. and T.G. Townsend, *Landfill bioreactor design & operation*. 1997: CRC press.
5. Gershman, B.B., Inc., *Gasification of Non-Recycled Plastics From Municipal Solid Waste In the United States*. 2013.
6. Acomb, J.C., C.F. Wu, and P.T. Williams, *Control of steam input to the pyrolysis-gasification of waste plastics for improved production of hydrogen or carbon nanotubes.* Applied Catalysis B-Environmental, 2014. **147**: p. 571-584.
7. Aboulkas, A., K. El harfi, and A. El Bouadili, *Thermal degradation behaviors of polyethylene and polypropylene. Part I: Pyrolysis kinetics and mechanisms.* Energy Conversion and Management, 2010. **51**(7): p. 1363-1369.
8. Al-Salem, S.M. and P. Lettieri, *Kinetic study of high density polyethylene (HDPE) pyrolysis.* Chemical Engineering Research and Design, 2010. **88**(12): p. 1599-1606.
9. Al-Salem, S.M., P. Lettieri, and J. Baeyens, *Recycling and recovery routes of plastic solid waste (PSW): A review*. Waste Management, 2009. **29**(10): p. 2625-2643.
10. Kaminsky, J.S.a.W., *Feedstock Recycling and Pyrolysis of Waste Plastic: Converting Waste Plastics into Diesel and Other Fuels*. 2006, Wiley Series in Polymer Science. p. 1-792.
11. Flynn, J.H. and L.A. Wall, *General treatment of the thermogravimetry of polymers.*
12. Khawam, A. and D.R. Flanagan, *Solid-State Kinetic Models: Basics and Mathematical Fundamentals.* The Journal of Physical Chemistry B, 2006. **110**(35): p. 17315-17328.
13. Carrasco, F., *The Evaluation of Kinetic Parameters from Thermogrevimetric Data - Comparison between Established Methods and The Gemeral Analytical Equation.* Thermochimica Acta, 1993. **213**: p. 115-134.

14. Laxminarasimhan, C.S., R.P. Verma, and P.A. Ramachandran, *Continuous lumping model for simulation of hydrocracking.* AIChE Journal, 1996. **42**(9): p. 2645-2653.
15. Goussis, D.A. and U. Maas, *Model reduction for combustion chemistry*, in *Turbulent Combustion Modeling*. 2011, Springer. p. 193-220.
16. Saltelli, A., et al., *Sensitivity analysis for chemical models.* Chemical reviews, 2005. **105**(7): p. 2811-2828.
17. Ho, T.C., *Kinetic Modeling of Large‐Scale Reaction Systems.* Catalysis Reviews, 2008. **50**(3): p. 287-378.
18. Okino, M.S. and M.L. Mavrovouniotis, *Simplification of mathematical models of chemical reaction systems.* Chemical reviews, 1998. **98**(2): p. 391-408.
19. Lu, T. and C.K. Law, *Toward accommodating realistic fuel chemistry in large-scale computations.* Progress in Energy and Combustion Science, 2009. **35**(2): p. 192-215.
20. Aguado, R., et al., *Principal component analysis for kinetic scheme proposal in the thermal catalytic pyrolysis of waste tyres.* Chemical Engineering Science, 2014. **106**: p. 9-17.
21. Aguado, R., et al., *Principal component analysis for kinetic scheme proposal in the thermal pyrolysis of waste HDPE plastics.* Chemical Engineering Journal, 2014. **254**: p. 357-364.
22. Huang, H., et al., *A systematic lumping approach for the reduction of comprehensive kinetic models.* Proceedings of the Combustion Institute, 2005. **30**(1): p. 1309-1316.
23. United Nations Environmental Programme Division of Technology, I.a.E.I.E.T.C. and J. Osaka/Shiga, *Converting Waste Plastics into A Resource: Compendium of Technologies*. 2009.
24. Lytle, C.L.G. *WHEN THE MERMAIDS CRY: THE GREAT PLASTIC TIDE*. 2009 [cited 2015 12/07/2015]; Available from: http://coastalcare.org/2009/11/plastic-pollution/.
25. Phyllis, *Database for Biomass and Waste* 2015, Petten, Holland, Netherlands: Energy research Centre of the Netherlands.
26. Kittle, A., *Alternate daily cover materials and subtitle, the selection technique Rusmar*. Incorporated West Chester, PA, 1993.
27. Fivelman, Q. *Waste or resource? Stimulating a bioeconomy*. 2013 [cited 2015 08/07/2015]; Available from: http://www.parliament.uk/documents/lords-

committees/science-technology/wasteandbioeconomy/Wastebioeconomyevidence.pdf.

28. WRAP, *Plastics Market Situation Report*. 2016.
29. DEFRA. *Energy from waste: A guide to the debate* 2014; 74]. Available from: https://www.gov.uk/government/uploads/system/uploads/attachment_data/file/284612/pb14130-energy-waste-201402.pdf.
30. Marongiu, A., T. Faravelli, and E. Ranzi, *Detailed kinetic modeling of the thermal degradation of vinyl polymers.* Journal of Analytical and Applied Pyrolysis, 2007. **78**(2): p. 343-362.
31. Buekens, A., *Introduction to Feedstock Recycling of Plastics*, in *Feedstock Recycling and Pyrolysis of Waste Plastics*. 2006, John Wiley & Sons, Ltd. p. 1-41.
32. Hirschler, C.L.B.a.M.M., *Thermal Decomposition of Polymers*. 3rd Edition ed. National Fire Protection Association (Quincy, MA), and Society of Fire Protection Engineers (Bethesda, MD), ed. I.O.a.B.S.H.o.F.P. Engineering. 2002. Chapter 1-7.
33. Kosior, E., *Fuel from Waste Plastics*. 2012: NexTek Limited.
34. Williams, P.T. and E.A. Williams, J. Anal. Appl. Pyrolysis, 1999. **51**: p. 107.
35. Hoffman, H.L., *Petroleum (products)*. 3rd ed. Grayson, M., ed., Kirk-Othmer Encyclopedia of Chemical Technology. Vol. 17. 1982, New York: John Wiley & Sons. 257-271.
36. Harker, J.H. and J.R. Backhurst, *Fuel and energy*. London and New York, Academic Press, 1981. 373 p., 1981. **1**.
37. Williams, P.T. and E.A. Williams, *Interaction of plastics in mixed-plastics pyrolysis.* Energy & Fuels, 1999. **13**(1): p. 188-196.
38. Kaminsky, W., *Monomer Recovery of Plastic Waste in a Fluidized Bed Process*, in *Feedstock Recycling and Pyrolysis of Waste Plastics*. 2006, John Wiley & Sons, Ltd. p. 627-640.
39. Gao, F., *Pyrolysis of Waste Plastics into Fuels*, in *Chemical and Process Engineering*. 2010, University of Canterbury.
40. Faravelli, T., et al., *Kinetic modeling of the thermal degradation of polyethylene and polystyrene mixtures.* Journal of Analytical and Applied Pyrolysis, 2003. **70**(2): p. 761-777.
41. López, A., et al., *Influence of time and temperature on pyrolysis of plastic wastes in a semi-batch reactor.* Chemical Engineering Journal, 2011. **173**(1): p. 62-71.

42. Ding, F., et al., *Kinetic study of low-temperature conversion of plastic mixtures to value added products.* Journal of Analytical and Applied Pyrolysis, 2012. **94**(0): p. 83-90.
43. Park, S.S., et al., *Study on pyrolysis characteristics of refuse plastic fuel using lab-scale tube furnace and thermogravimetric analysis reactor.* Journal of Analytical and Applied Pyrolysis, 2012. **97**: p. 29-38.
44. Aguado, J., et al., *Enhanced Production of α-Olefins by Thermal Degradation of High-Density Polyethylene (HDPE) in Decalin Solvent: Effect of the Reaction Time and Temperature.* Industrial & Engineering Chemistry Research, 2007. **46**(11): p. 3497-3504.
45. Onwudili, J.A., N. Insura, and P.T. Williams, *Composition of products from the pyrolysis of polyethylene and polystyrene in a closed batch reactor: Effects of temperature and residence time.* Journal of Analytical and Applied Pyrolysis, 2009. **86**(2): p. 293-303.
46. White, R.L., *Acid-Catalyzed Cracking of Polyolefins: Primary Reaction Mechanisms*, in *Feedstock Recycling and Pyrolysis of Waste Plastics*. 2006, John Wiley & Sons, Ltd. p. 43-72.
47. Obali, Z., N.A. Sezgi, and T. Dogu, *Catalytic degradation of polypropylene over alumina loaded mesoporous catalysts.* Chemical Engineering Journal, 2012. **207**: p. 421-425.
48. Moulijn, J.A., A.E. van Diepen, and F. Kapteijn, *Catalyst deactivation: is it predictable?: What to do?* Applied Catalysis A: General, 2001. **212**(1–2): p. 3-16.
49. Murata, K., K. Sato, and Y. Sakata, *Effect of pressure on thermal degradation of polyethylene.* Journal of Analytical and Applied Pyrolysis, 2004. **71**(2): p. 569-589.
50. Pantoleontos, G., et al., *A global optimization study on the devolatilisation kinetics of coal, biomass and waste fuels.* Fuel Processing Technology, 2009. **90**(6): p. 762-769.
51. Érdi, P. and J. Tóth, *Mathematical models of chemical reactions: theory and applications of deterministic and stochastic models*. 1989: Manchester University Press.
52. Pantea, C., et al., *The QSSA in chemical kinetics: as taught and as practiced*, in *Discrete and Topological Models in Molecular Biology*. 2014, Springer. p. 419-442.

53. Vay, J.-L., *Noninvariance of space-and time-scale ranges under a Lorentz transformation and the implications for the study of relativistic interactions.* Physical review letters, 2007. **98**(13): p. 130405.
54. Shlens, J., *A Tutorial on Principal Component Analysis*. 2014.
55. Turányi, T. and A.S. Tomlin, *Analysis of Kinetic Reaction Mechanisms*. 2014: Springer.
56. Ho, T.C. and B.S. White, *Continuum approximation of large reaction mixtures in reactors with backmixing.* AIChE Journal, 2015(1): p. 159.
57. Huang, H., et al., *A systematic lumping approach for the reduction of comprehensive kinetic models.* Proceedings of the Combustion Institute, 2005. **30**(1): p. 1309-1316.
58. Lam, S. and D. Goussis. *Understanding complex chemical kinetics with computational singular perturbation*. in *Symposium (International) on Combustion*. 1989. Elsevier.
59. Mui, E.L.K., D.C.K. Ko, and G. McKay, *Production of active carbons from waste tyres—a review.* Carbon, 2004. **42**(14): p. 2789-2805.
60. Quek, A. and R. Balasubramanian, *Mathematical modeling of rubber tire pyrolysis.* Journal of Analytical and Applied Pyrolysis, 2012. **95**(0): p. 1-13.
61. Tomas-Alonso, F., L.A.A. Olmos, and M.A.M. Vidal, *Selective separation of normal paraffins from slack wax using the molecular sieve adsorption technique.* Separation Science and Technology, 2004. **39**(7): p. 1577-1593.
62. Westerhout, R.W.J., et al., *Kinetics of the Low-Temperature Pyrolysis of Polyethene, Polypropene, and Polystyrene Modeling, Experimental Determination, and Comparison with Literature Models and Data.* Ind. Eng. Chem. Res., 1997. **36**: p. 1955-1964.
63. Marin, G.B., *Advances in Chemical Engineering*. 2011: Elsevier Science.
64. Vyazovkin, S., *Modification of the integral isoconversional method to account for variation in the activation energy.* Journal of Computational Chemistry, 2001. **22**(2): p. 178-183.
65. Yang, H., et al., *Thermogravimetric Analysis−Fourier Transform Infrared Analysis of Palm Oil Waste Pyrolysis.* Energy & Fuels, 2004. **18**(6): p. 1814-1821.
66. N. Prakash, T.K., *Kinetic Modeling in Biomass Pyrolysis – A Review.* Journal of Applied Sciences Research, 2008. **4**(12): p. 1627-1636.

67. Di Blasi, C., *Comparison of semi-global mechanisms for primary pyrolysis of lignocellulosic fuels.* Journal of Analytical and Applied Pyrolysis, 1998. **47**(1): p. 43-64.

68. White, J.E., W.J. Catallo, and B.L. Legendre, *Biomass pyrolysis kinetics: A comparative critical review with relevant agricultural residue case studies.* Journal of Analytical and Applied Pyrolysis, 2011. **91**(1): p. 1-33.

69. Mehl, M., et al., *A kinetic modeling study of the thermal degradation of halogenated polymers.* Journal of Analytical and Applied Pyrolysis, 2004. **72**(2): p. 253-272.

70. Koo, J.-K. and S.-W. Kim, *Reaction Kinetic Model For Optimal Pyrolysis Of Plastic Waste Mixtures.* Waste Management & Research, 1993. **11**(6): p. 515-529.

71. Nunn, T.R., et al., *Product compositions and kinetics in the rapid pyrolysis of sweet gum hardwood.* Industrial & Engineering Chemistry Process Design and Development, 1985. **24**(3): p. 836-844.

72. Ranzi, E., et al., *Lumping procedures in detailed kinetic modeling of gasification, pyrolysis, partial oxidation and combustion of hydrocarbon mixtures.* Progress in Energy and Combustion Science, 2001. **27**(1): p. 99-139.

73. Faravelli, T., et al., *Detailed kinetic modeling of the thermal degradation of lignins.* Biomass and Bioenergy, 2010. **34**(3): p. 290-301.

74. Branca, C., A. Albano, and C. Di Blasi, *Critical evaluation of global mechanisms of wood devolatilization.* Thermochimica Acta, 2005. **429**(2): p. 133-141.

75. Sharma, K.P., S.K. Srivastava, and N.N. Singh, *THERMODYNAMICS, KINETICS, AND ENERGETICS OF CATALYTIC CRACKING OF WAX.* Industrial & Engineering Chemistry Product Research and Development, 1984. **23**(4): p. 651-656.

76. Ramdoss, P.K. and A.R. Tarrer, *High-temperature liquefaction of waste plastics.* Fuel, 1998. **77**(4): p. 293-299.

77. Costa, P., et al., *Study of the Pyrolysis Kinetics of a Mixture of Polyethylene, Polypropylene, and Polystyrene.* Energy & Fuels, 2010. **24**(12): p. 6239-6247.

78. Csukás, B., et al., *Simplified dynamic simulation model of plastic waste pyrolysis in laboratory and pilot scale tubular reactor.* Fuel Processing Technology, 2013. **106**(0): p. 186-200.

79. Westerhout, R.W.J., et al., *Recycling of polyethene and polypropene in a novel bench-scale rotating cone reactor by high-temperature pyrolysis.* Industrial & Engineering Chemistry Research, 1998. **37**(6): p. 2293-2300.

80. Westerhout, R.W.J., J.A.M. Kuipers, and W.P.M. van Swaaij, Ind. Eng. Chem. Res., 1998. **37**: p. 841.
81. Johannes, I., H. Tamvelius, and L. Tiikma, *A step-by-step model for pyrolysis kinetics of polyethylene in an autoclave under non-linear increase of temperature.* Journal of Analytical and Applied Pyrolysis, 2004. **72**(1): p. 113-119.
82. Costa, P., et al., *Study of the Pyrolysis Kinetics of a Mixture of Polyethylene, Polypropylene, and Polystyrene.* Energy & Fuels, 2010. **24**: p. 6239-6247.
83. Lin, Y.H., et al., *Acid-catalyzed conversion of chlorinated plastic waste into valuable hydrocarbons over post-use commercial FCC catalysts.* Journal of Analytical and Applied Pyrolysis, 2010. **87**(1): p. 154-162.
84. Kodera, Y. and B.J. McCoy, AIChE J., 1997. **43**: p. 3205.
85. McCoy, B.J. and G. Madras, *Oxidative degradation kinetics of polystyrene in solution.* Chemical Engineering Science, 1997. **52**: p. 2707-2713.
86. Wang, M., J.M. Smith, and B.J. McCoy, AIChE J., 1995. **41**: p. 1521.
87. Madras, G. and B. McCoy, J. Catal. Today, 1998. **40**: p. 321.
88. Sterling, W.J., K.S. Walline, and B.J. McCoy, *Experimental study of polystyrene thermolysis to moderate conversion.* Polymer Degradation and Stability, 2001. **73**(1): p. 75-82.
89. M. Kruse, T., O. Sang Woo, and L. J. Broadbelt, *Detailed mechanistic modeling of polymer degradation: application to polystyrene.* Chemical Engineering Science, 2001. **56**(3): p. 971-979.
90. Kruse, T.M., et al., *Mechanistic Modeling of Polymer Degradation: A Comprehensive Study of Polystyrene.* Macromolecules, 2002. **35**(20): p. 7830-7844.
91. Wagenaar, B.M., *The Rotating Cone Reactor for Rapid Thermal Solids Processing*. Enschede. 1994, The Netherlands: University of Twente.
92. Wang, H. and M. Frenklach, *A detailed kinetic modeling study of aromatics formation in laminar premixed acetylene and ethylene flames.* Combustion and Flame, 1997. **110**(1–2): p. 173-221.
93. Wang, H. and M. Frenklach, *Detailed reduction of reaction mechanisms for flame modeling.* Combustion and Flame, 1991. **87**(3–4): p. 365-370.
94. Csukás Béla, V.M., Balogh Sándor, *Direct computer mapping of executable multiscale hybrid process architectures*, in *Proceedings of the 2011 Summer*

Computer Simulation Conference. 2011, Society for Modeling & Simulation International: Hague, Netherlands. p. 68-75.

95. K, K., H. L, and M. H, *THERMAL PERFORMANCE OF HEAT SHIELD COMPOSITES DURING PLANETARY ENTRY*, in *Engineering Problems of Manned Interplanetary Exploration*. 1963, American Institute of Aeronautics and Astronautics.
96. Faravelli, T., et al., *Gas product distribution from polyethylene pyrolysis.* Journal of Analytical and Applied Pyrolysis, 1999. **52**(1): p. 87-103.
97. Nguyen, T.T., et al., *Solution of population balance equations in applications with fine particles: mathematical modeling and numerical schemes.* 2015.
98. Stagni, A., et al., *Lumping and Reduction of Detailed Kinetic Schemes: an Effective Coupling.* Industrial & Engineering Chemistry Research, 2014. **53**(22): p. 9004-9016.
99. Miskolczi, N., et al., *Kinetic model of the chemical recycling of waste polyethylene into fuels.* Process Safety and Environmental Protection, 2004. **82**(B3): p. 223-229.
100. Ranzi, E., et al., *Reduced Kinetic Schemes of Complex Reaction Systems: Fossil and Biomass-Derived Transportation Fuels.* International Journal of Chemical Kinetics, 2014. **46**(9): p. 512-542.
101. Wang, H. and M. Frenklach, *DETAILED REDUCTION OF REACTION-MECHANISMS FOR FLAME MODELING.* Combustion and Flame, 1991. **87**(3-4): p. 365-370.
102. Setnescu, R., S. Jipa, and Z. Osawa, *Chemiluminescence study on the oxidation of several polyolefins - I. Thermal-induced degradation of additive-free polyolefins.* Polymer Degradation and Stability, 1998. **60**(2-3): p. 377-383.
103. Ocone, R., *Continuous Lumping Kinetics of Multi-component Reactive Mixtures*. 2008: EUROKIN.
104. Ho, T.C., *MODELING OF REACTION KINETICS FOR PETROLEUM FRACTIONS* 2006: Springer.
105. Wei, J. and J.C.W. Kuo, *Lumping Analysis in Monomolecular Reaction Systems. Analysis of the Exactly Lumpable System.* Industrial & Engineering Chemistry Fundamentals, 1969. **8**(1): p. 114-123.
106. Weekman, V.W., *Lumps, Models, and Kinetics in Practice*. 1979: American Institute of Chemical Engineers.

107. McCoy, B.J., *Continuous kinetics of cracking reactions: Thermolysis and pyrolysis.* Chemical Engineering Science, 1996. **51**(11): p. 2903-2908.

108. McCoy, B.J. and G. Madras, *Discrete and continuous models for polymerization and depolymerization.* Chemical Engineering Science, 2001. **56**(8): p. 2831-2836.

109. Wei, J., Prater, C.D., *Structure and analysis of complex reaction systems*. Advances in Catalysis. Vol. 13 (203). 1962.

110. Wei, J. and J.C. Kuo, *Lumping analysis in monomolecular reaction systems. Analysis of the exactly lumpable system.* Industrial & Engineering chemistry fundamentals, 1969. **8**(1): p. 114-123.

111. Li, G. and H. Rabitz, *A general analysis of exact lumping in chemical kinetics.* Chemical engineering science, 1989. **44**(6): p. 1413-1430.

112. Li, G.Y. and H. Rabitz, *A GENERAL-ANALYSIS OF APPROXIMATE LUMPING IN CHEMICAL-KINETICS.* Chemical Engineering Science, 1990. **45**(4): p. 977-1002.

113. Li, G.Y., et al., *A GENERAL-ANALYSIS OF APPROXIMATE NONLINEAR LUMPING IN CHEMICAL-KINETICS .1. UNCONSTRAINED LUMPING.* Journal of Chemical Physics, 1994. **101**(2): p. 1172-1187.

114. Kuo, J.C. and J. Wei, *Lumping analysis in monomolecular reaction systems. Analysis of approximately lumpable system.* Industrial & Engineering chemistry fundamentals, 1969. **8**(1): p. 124-133.

115. Li, G.Y., H. Rabitz, and J. Toth, *A GENERAL-ANALYSIS OF EXACT NONLINEAR LUMPING IN CHEMICAL-KINETICS.* Chemical Engineering Science, 1994. **49**(3): p. 343-361.

116. Tomlin, A.S., et al., *A GENERAL-ANALYSIS OF APPROXIMATE NONLINEAR LUMPING IN CHEMICAL-KINETICS .2. CONSTRAINED LUMPING.* Journal of Chemical Physics, 1994. **101**(2): p. 1188-1201.

117. Li, G., et al., *Determination of approximate lumping schemes by a singular perturbation method.* The Journal of chemical physics, 1993. **99**(5): p. 3562-3574.

118. Li, G., et al., *A general analysis of approximate nonlinear lumping in chemical kinetics. I. Unconstrained lumping.* The Journal of Chemical Physics, 1994. **101**(2): p. 1172-1187.

119. Bogaevski, V.N. and A. Povzner, *Algebraic methods in nonlinear perturbation theory*. Vol. 88. 2012: Springer Science & Business Media.

120. Li, G. and H. Rabitz, *A general analysis of approximate lumping in chemical kinetics.* Chemical engineering science, 1990. **45**(4): p. 977-1002.

121. Blanding, F.H., *Reaction Rates in Catalytic Cracking of Petroleum.* Industrial & Engineering Chemistry, 1953. **45**(6): p. 1186-1197.

122. Marcilla, A., et al., *Catalytic pyrolysis of polypropylene using MCM-41: kinetic model.* Polymer Degradation and Stability, 2003. **80**(2): p. 233-240.

123. Pinto, F., et al., *Prediction of liquid yields from the pyrolysis of waste mixtures using response surface methodology.* Fuel Processing Technology, 2013. **116**(0): p. 271-283.

124. Box, G.E.P. and K.B. Wilson, *On the Experimental Attainment of Optimum Conditions.* Journal of the Royal Statistical Society, Series B, 1951. **{XIII}**(1): p. 1-45.

125. Dicholkar, D.D., et al., *Modeling and optimizing of steam pyrolysis of dimethyl formamide by using response surface methodology coupled with Box-Behnken design.* Journal of Analytical and Applied Pyrolysis, 2012. **96**(0): p. 6-15.

126. Nicolet, T., *Introduction to fourier transform infrared spectrometry.* Information booklet, 2001.

127. Sørum, L., M. Grønli, and J.E. Hustad, *Pyrolysis characteristics and kinetics of municipal solid wastes.* Fuel, 2001. **80**(9): p. 1217-1227.

128. Achilias, D.S., et al., *Chemical recycling of plastic wastes made from polyethylene (LDPE and HDPE) and polypropylene (PP).* Journal of Hazardous Materials, 2007. **149**(3): p. 536-542.

129. Kumar, S. and R. Singh, *Optimization of process parameters by response surface methodology (RSM) for catalytic pyrolysis of waste high-density polyethylene to liquid fuel.* Journal of Environmental Chemical Engineering, 2014. **2**(1): p. 115-122.

130. Mlynkova, B., et al., *Fuels obtained by thermal cracking of individual and mixed polymers.* Chemical Papers, 2010. **64**(1): p. 15-24.

131. Uddin, M.A., et al., *Thermal and catalytic degradation of structurally different types of polyethylene into fuel oil.* Polymer Degradation and Stability, 1997. **56**(1): p. 37-44.

132. Conesa, J.A., et al., *Pyrolysis of Polyethylene in a Fluidized Bed Reactor.* Energy & Fuels, 1994. **8**(6): p. 1238-1246.

133. Chan, J.H. and S.T. Balke, *The thermal degradation kinetics of polypropylene: Part III. Thermogravimetric analyses.* Polymer Degradation and Stability, 1997. **57**(2): p. 135-149.

134. B.J. Vreugdenhil, R.W.R.Z., John Neeft, *Tar formation in pyrolysis and gasification* ECN-E--08-087 June, 2009.

135. Brems, A., et al., *Polymeric Cracking of Waste Polyethylene Terephthalate to Chemicals and Energy.* Journal of the Air & Waste Management Association (1995), 2011. **61**(7): p. 721-731.

136. Williams, E.A. and P.T. Williams, *Analysis of products derived from the fast pyrolysis of plastic waste.* Journal of Analytical and Applied Pyrolysis, 1997. **40-1**: p. 347-363.

137. Levine, S.E. and L.J. Broadbelt, *Reaction pathways to dimer in polystyrene pyrolysis: a mechanistic modeling study.* Polymer Degradation and Stability, 2008. **93**(5): p. 941-951.

138. Poutsma, M.L., *Mechanistic analysis and thermochemical kinetic simulation of the pathways for volatile product formation from pyrolysis of polystyrene, especially for the dimer.* Polymer Degradation and Stability, 2006. **91**(12): p. 2979-3009.

139. Lopez, G., et al., *Kinetics of scrap tyre pyrolysis under vacuum conditions.* Waste Management, 2009. **29**(10): p. 2649-2655.

140. Amhammed, M.A., *Applications of Lumping Kinetics Methodology to Complex Reactive Mixtures*. 2013.

141. Helfferich, F.G., *Kinetics of multistep reactions*. 2004: Elsevier.

142. Chao-Hsiung, W., et al., *On the thermal treatment of plastic mixtures of MSW: Pyrolysis kinetics.* Waste Management, 1993. **13**(3): p. 221-235.

143. Jacob, S.M., et al., *A lumping and reaction scheme for catalytic cracking.* AIChE Journal, 1976. **22**(4): p. 701-713.

144. Adam, M., et al., *Kinetic Investigations of Kraft Lignin Pyrolysis.* Industrial & Engineering Chemistry Research, 2013. **52**(26): p. 8645-8654.

145. Singh, B. and N. Sharma, *Mechanistic implications of plastic degradation.* Polymer Degradation and Stability, 2008. **93**(3): p. 561-584.

146. Guoliang, W., et al., *Study on lumped kinetic reaction network of heavy oil contact cracking process.* Petrochemical Technology, 2004. **33**(2): p. 93-99.

147. Dash, A., S. Kumar, and R.K. Singh, *Thermolysis of Medical Waste (Waste Syringe) to Liquid Fuel Using Semi Batch Reactor.* Waste and Biomass Valorization, 2015(4): p. 507.

148. Elordi, G., et al., *Product Yields and Compositions in the Continuous Pyrolysis of High-Density Polyethylene in a Conical Spouted Bed Reactor.* Industrial & Engineering Chemistry Research, 2011. **50**(11): p. 6650-6659.

149. Kissinger, H.E., *Reaction Kinetics in Differential Thermal Analysis.* Analytical Chemistry, 1957. **29**(11): p. 1702-1706.

150. Starink, M.J., *The determination of activation energy from linear heating rate experiments: a comparison of the accuracy of isoconversion methods.* Thermochimica Acta, 2003. **404**(1-2): p. 163-176.

151. Flynn, J.H. and L.A. Wall, *A quick, direct method for the determination of activation energy from thermogravimetric data.* Journal of Polymer Science Part B: Polymer Letters, 1966. **4**(5): p. 323-328.

152. Ozawa, T., *A new mwthod of analyzing thermogravimetric data.* Bull. Chem. Soc. Jpn., 1965. **38**(11): p. 1881-1886.

153. Friedman, H.L., *Kinetics of thermal degradation of char-forming plastics from thermogravimetry. Application to a phenolic plastic.* Journal of Polymer Science Part C: Polymer Symposia, 1964. **6**(1): p. 183-195.

154. Coats, A.W., Redfern, J. P., *Kinetic Parameters from Thermogravimetric Data.* Nature, 1964. **201**(4914): p. 68-69.

155. Biswas, S., P. Mohanty, and D.K. Sharma, *Studies on synergism in the cracking and co-cracking of Jatropha oil, vacuum residue and high density polyethylene: Kinetic analysis.* Fuel Processing Technology, 2013. **106**: p. 673-683.

156. Ballice, L., *A kinetic approach to the temperature-programmed pyrolysis of low- and high-density polyethylene in a fixed bed reactor: determination of kinetic parameters for the evolution of n-paraffins and 1-olefins.* Fuel, 2001. **80**(13): p. 1923-1935.

157. Liu, X., et al., *Study of high density polyethylene (HDPE) pyrolysis with reactive molecular dynamics.* Polymer Degradation and Stability, 2014. **104**: p. 62-70.

158. Kim, S., Y.-C. Kim, and E.-S. Jang, *Identification of Reaction Model of Pyrolysis Reaction of HDPE.* Chemistry Letters, 2004. **33**(10): p. 1310-1311.

159. Gao, Z., I. Amasaki, and M. Nakada, J. Anal. Appl. Pyrolysis, 2003. **67**: p. 1.

160. Bockhorn, H., et al., *Kinetic study on the thermal degradation of polypropylene and polyethylene.* Journal of Analytical and Applied Pyrolysis, 1999. **48**(2): p. 93-109.

161. Costa, P.A., et al., *Kinetic Evaluation of the Pyrolysis of Polyethylene Waste.* Energy & Fuels, 2007. **21**(5): p. 2489-2498.

162. Gao, Z., et al., *A kinetic study of thermal degradation of polypropylene.* Polymer Degradation and Stability, 2003. **80**(2): p. 269-274.

163. Conesa, J.A., et al., *Thermogravimetric studies on the thermal decomposition of polyethylene.* Journal of Analytical and Applied Pyrolysis, 1996. **36**(1): p. 1-15.

164. F., G., H. Zweifel, and S.E. Amos, *Plastics additives handbook*. 5th ed. 2001, Cincinnati: Hanser Cincinnati.

165. Önal, E., B.B. Uzun, and A.E. Pütün, *An experimental study on bio-oil production from co-pyrolysis with potato skin and high-density polyethylene (HDPE).* Fuel Processing Technology, 2012. **104**: p. 365-370.

166. Yin, L.J., et al., *Simulation of an innovative reactor for waste plastics pyrolysis.* Chemical Engineering Journal, 2014. **237**(0): p. 229-235.

167. Levine, S.E. and L.J. Broadbelt, *Detailed mechanistic modeling of high-density polyethylene pyrolysis: Low molecular weight product evolution.* Polymer Degradation and Stability, 2009. **94**(5): p. 810-822.

168. Singh, S., C. Wu, and P.T. Williams, *Pyrolysis of waste materials using TGA-MS and TGA-FTIR as complementary characterisation techniques.* Journal of Analytical and Applied Pyrolysis, 2012. **94**(0): p. 99-107.

169. Saha, B. and A.K. Ghoshal, *Thermal degradation kinetics of poly(ethylene terephthalate) from waste soft drinks bottles.* Chemical Engineering Journal, 2005. **111**(1): p. 39-43.

170. Dou, B., et al., *Pyrolysis Characteristics of Refuse Derived Fuel in a Pilot-Scale Unit.* Energy & Fuels, 2007. **21**(6): p. 3730-3734.

171. Aboulkas, A., et al., *Pyrolysis kinetics of olive residue/plastic mixtures by non-isothermal thermogravimetry.* Fuel Processing Technology, 2009. **90**(5): p. 722-728.

172. Doyle, C.D., *Kinetic analysis of thermogravimetric data.* Journal of Applied Polymer Science, 1962. **6**(19): p. 120-120.

173. Artetxe, M., et al., *Kinetic modelling of the cracking of HDPE pyrolysis volatiles on a HZSM-5 zeolite based catalyst.* Chemical Engineering Science, 2014. **116**(0): p. 635-644.

174. Kumar, S., A.K. Panda, and R.K. Singh, *A review on tertiary recycling of high-density polyethylene to fuel.* Resources, Conservation and Recycling, 2011. **55**(11): p. 893-910.

175. Walendziewski, J., *Thermal and Catalytic Conversion of Polyolefins*, in *Feedstock Recycling and Pyrolysis of Waste Plastics*. 2006, John Wiley & Sons, Ltd. p. 111-127.

176. Conesa, J.A., et al., Energy Fuels, 1994. **8**: p. 1238.

177. Zhou, L., et al., *Thermogravimetric characteristics and kinetic of plastic and biomass blends co-pyrolysis.* Fuel Processing Technology, 2006. **87**(11): p. 963-969.

178. Sørum, L., M.G. Grønli, and J.E. Hustad, *Pyrolysis characteristics and kinetics of municipal solid wastes.* Fuel, 2001. **80**(9): p. 1217-1227.

179. Lin, Y.-C., et al., *Kinetics and Mechanism of Cellulose Pyrolysis.* The Journal of Physical Chemistry C, 2009. **113**(46): p. 20097-20107.

180. Di Blasi, C., et al., *Experimental Analysis of Reaction Heat Effects during Beech Wood Pyrolysis.* Energy & Fuels, 2013. **27**(5): p. 2665-2674.

181. Martínez, L., et al., *Fluidized bed pyrolysis of HDPE: A study of the influence of operating variables and the main fluidynamic parameters on the composition and production of gases.* Fuel Processing Technology, 2011. **92**(2): p. 221-228.

182. Williams, P.T., *Yield and Composition of Gases and Oils/Waxes from the Feedstock Recycling of Waste Plastic*, in *Feedstock Recycling and Pyrolysis of Waste Plastics*. 2006, John Wiley & Sons, Ltd. p. 285-313.

183. Williams, E.A. and P.T. Williams, *The pyrolysis of individual plastics and a plastic mixture in a fixed bed reactor.* Journal of Chemical Technology and Biotechnology, 1997. **70**(1): p. 9-20.

184. Flynn, J.H., *TEMPERATURE-DEPENDENCE OF THE RATE OF REACTION IN THERMAL-ANALYSIS - THE ARRHENIUS EQUATION IN CONDENSED PHASE KINETICS.* Journal of Thermal Analysis, 1990. **36**(4): p. 1579-1593.

185. White, J.E., W.J. Catallo, and B.L. Legendre, J. Anal. Appl. Pyrolysis, 2011. **91**: p. 1.

186. Elordi, G., et al., *Product distribution modelling in the thermal pyrolysis of high density polyethylene.* Journal of Hazardous Materials, 2007. **144**(3): p. 708-714.

187. Gao, Z., I. Amasaki, and M. Nakada, *A thermogravimetric study on thermal degradation of polyethylene.* Journal of Analytical and Applied Pyrolysis, 2003. **67**(1): p. 1-9.

188. *Front Matter*, in *Feedstock Recycling and Pyrolysis of Waste Plastics*. 2006, John Wiley & Sons, Ltd. p. i-xxix.

Bibliography

1. Pielichowski, K., J. Njuguna, and R.T. Limited, *Thermal Degradation of Polymeric Materials*. 2005: Rapra Technology.
2. Wang, L., *Model predictive control system design and implementation using MATLAB®*. 2009: Springer Science & Business Media
3. Houston, P.L., *Chemical kinetics and reaction dynamics*. 2012: Courier Corporation
4. Dewulf, J. and H. Van Langenhove, Renewables-based technology: sustainability assessment. 2006: John Wiley & Sons.
5. Attaway, S., *Matlab: a practical introduction to programming and problem solving*. 2013: Butterworth-Heinemann.

Appendix 1 Illegal use of medical plastic packaging waste in China

Appendix 2 Experiment study

Appendix 2.1 Photograph of feedstock

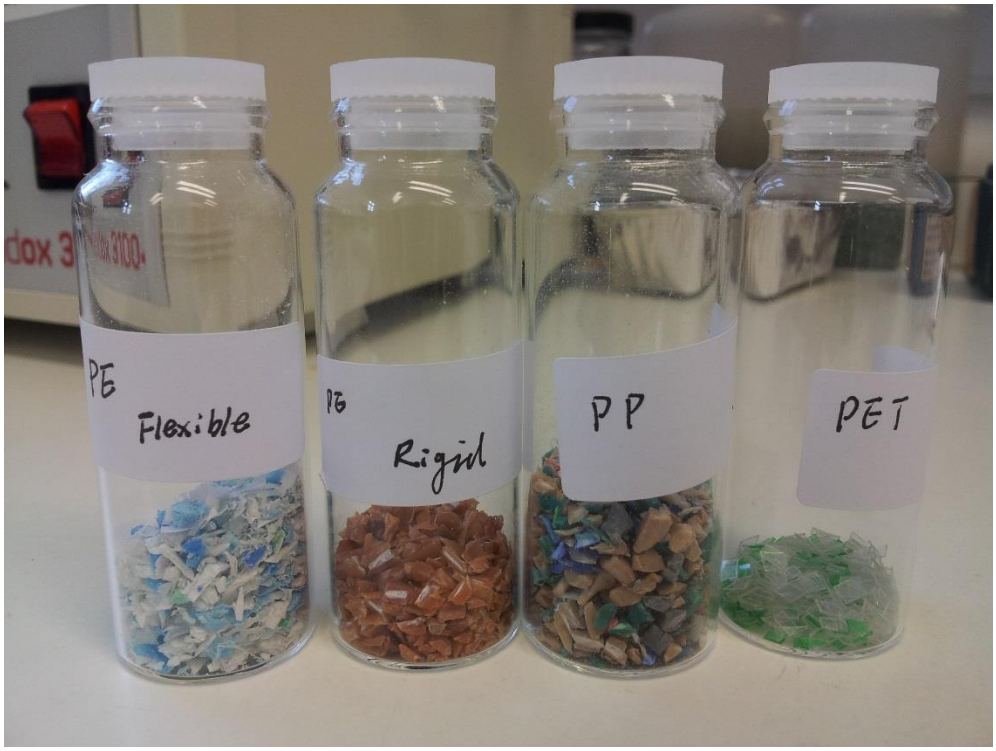

Appendix 2.2 Photographic representations of lab-scale fixed bed batch pyrolysis unit schematic presented Figure 3-1 (glassware connection set and closed system set)

Appendix 2.3 Sample loading and positioning within reactor tube and demonstrating the positioning of the feed bed in the furnace

Appendix 2.4 Collection of wax and liquid samples from hot trap (left) and receiver trap (middle) and cold traps (right) for pyrolysis of PE, PE/PP and PP at 500℃

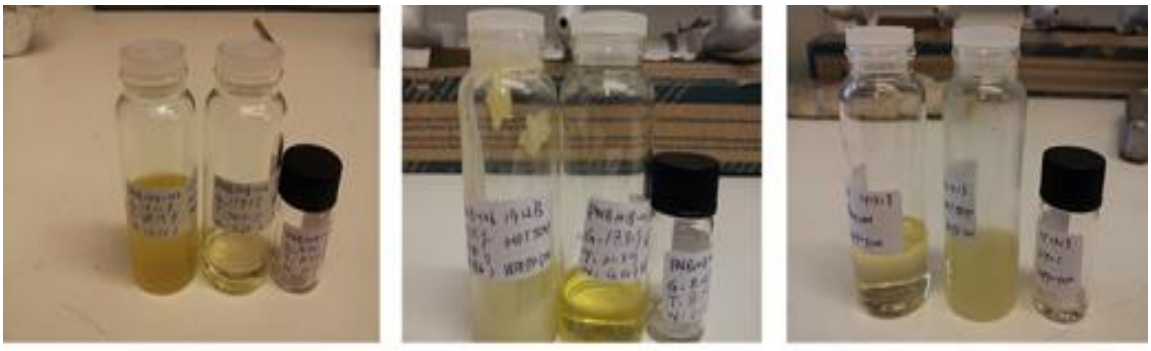

Appendix 2.5 Collection of product samples from PET pyrolysis (samples of char, yellow powder, light yellow and liquids collected from reactor, heated zone glassware, air condenser pipe, and receiver) at 550℃

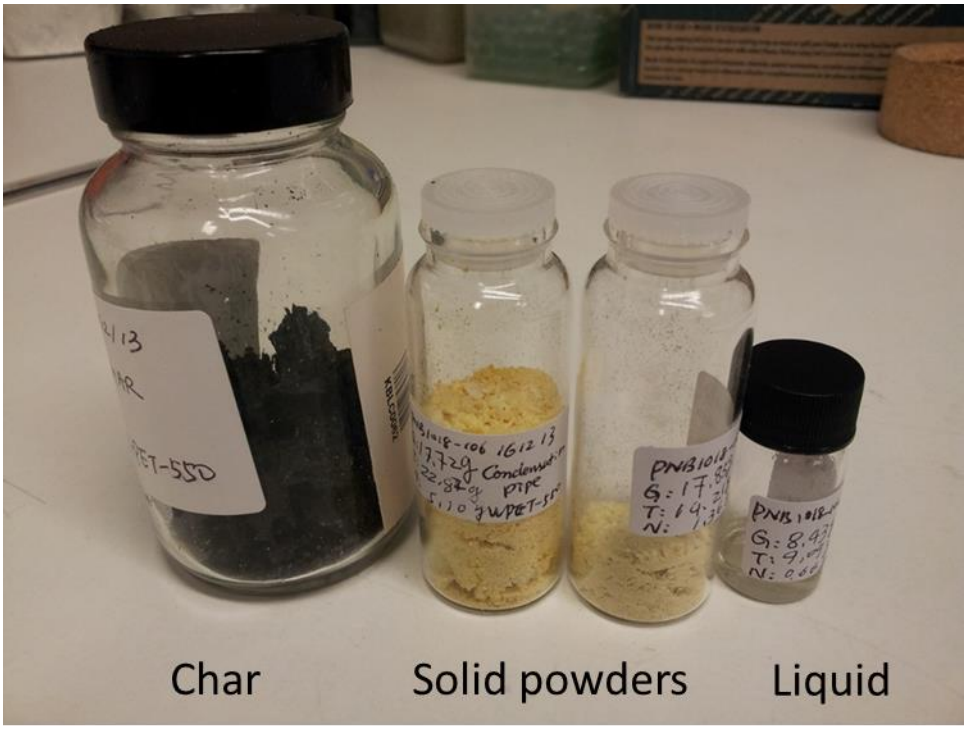

Appendix 2.6 Solid residues presented in the reactor at 450℃

Appendix 2.7 Residue of HDPE pyrolysis over thin bed reactor

HDPE pyrolysis via thin bed			
Items	450°C	500°C	550°C
Feed (g)	1.21	1.07	1.07
Bed thickness (mm)			
Thermocouple position			
Wax like product attached on the wall			
Residue of thin bed	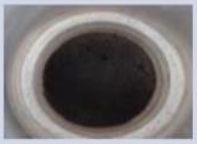	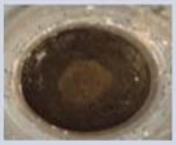	
Collected wax-like products	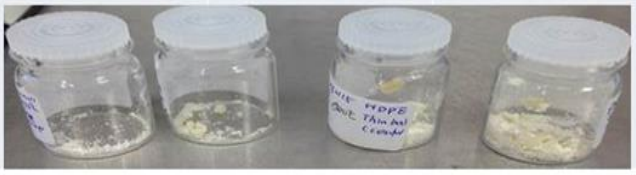		

Appendix 2.8 Production distribution and mass balance of plastic waste pyrolysis

Sample	Temperature °C	Liquid wt%	Wax wt%	Gas wt%	Residue wt%
PE	450	5.96	41.17	12.87	40.00
	500	21.21	56.68	14.53	7.58
	550	23.19	48.55	21.30	6.96
PE/PP	450	8.80	31.62	13.11	46.47
	500	24.20	39.99	20.07	15.74
	550	37.08	36.43	21.94	4.55
PP	450	31.93	23.64	15.08	29.34
	500	38.23	32.29	24.98	4.50
	550	42.63	27.58	27.59	2.20
PET	450	0.64	11.83	34.22	52.54
	500	5.49	26.09	36.31	32.12
	550	10.50	29.48	39.34	20.68

Appendix 2.9 The yields distribution and mass balances of waste HDPE pyrolysis over thin bed and thick bed at different temperatures and 30 minutes residence time

Bed	Temperature	Residue	SD*	Wax	SD	Oil	SD	Gas	SD
	℃	%		%		%		%	
Thick bed	425	92.50	0.03	5.60	0.03	0.40	0.03	1.40	0.03
	450	40.20	0.01	41.40	1.14	9.60	0.52	8.80	0.54
	475	11.20	0.02	57.70	0.03	18.80	0.62	12.20	1.08
	500	1.70	0.03	61.30	0.05	22.50	1.12	14.60	0.64
	550	1.30	0.05	60.10	0.06	23.70	1.08	15.00	0.98
Thin bed	425	87.58	0.04	11.37	0.02	0.84	0.09	0.21	0.02
	450	43.00	1.25	35.50	1.50	10.70	1.40	10.80	0.70
	475	22.40	1.36	45.77	1.80	18.65	1.20	13.17	0.80
	500	4.86	0.68	57.38	1.90	22.93	1.50	14.83	0.80
	550	1.68	0.50	56.70	1.80	25.65	1.30	16.02	1.00

Standard deviation (SD*) is a measure of how spread out numbers are. It is calculated as the square root of variance by determining the variation between each data point relative to the mean, and shown as:

$$\sigma = \sqrt{\frac{1}{\omega - 1}\sum_{i=1}^{N}(x_i - \bar{x})^2}$$

σ is standard deviation, ω is sample size, x-bar is mean of sample size.

Appendix 2.10 The yields distribution and mass balances of waste HDPE pyrolysis at 475℃

Time (Min)	Liquid wt%	Wax wt%	Gas wt%	Residue wt%
30	18.8	57.7	12.20	11.20
60	20.61	59.97	14.90	5.52
180	21.3	62.70	15.15	0.95

Appendix 2.11 The yields distribution and mass balances of flexible and rigid PE pyrolysis from TGA

Feed	Temperature (℃)	Volatiles (wt %)	Residue (wt %)
FPE	450	93.05	6.95
RPE	450	97.93	2.07
MIX1	450	94.31	5.69
MIX2	450	94.62	5.38
MIX3	450	95.79	4.21
FPE	500	93.31	6.69
RPE	500	99.16	0.84
MIX1	500	95.79	4.21
MIX2	500	96.67	3.33
MIX3	500	96.95	3.05
FPE	550	93.36	6.64
RPE	550	99.30	0.70
MIX1	550	95.31	4.69
MIX2	550	96.88	3.12
MIX3	550	97.19	2.81

Appendix 3 Discrete lumping model performed by using MATLAB programmer

1. Main programme

```
% The developed MATLAB code for determination the optimal kinetic parameters for discrete lumping model
%%%%%%%%%%%%%%%%%%%%%%%%%%%%%%%%%%%%%%%%%%%%%%%%%%%%%%%%%%%%%%%%%%%%
 clc
clear

close all

warning off
% define parameters
yelp= [0 14.6 22.5 61.3 1.7];   % Experimental value of components HDPE500
%%%%%%%%%%%%%%%%%%%%%%%%%%%%%%%%%%%%%%%%%%%%%%%%%%%%%%%%%%%%%%%%%%%%
w0= [100 0 0 0 0];             % Initial value of each component
%%%%%%%%%%%%%%%%%%%%%%%%%%%%%%%%%%%%%%%%%%%%%%%%%%%%%%%%%%%%%%%%%%%%
algorithm Opt=1;               % 1 when lower and upper boundary is needed, or 0
Numara=5;                   % parameter number =3, 4, 5, 6
if Algorithm Opt
lb. = zeros (1, NumPara);         % Lower boundary
up=lb+100;                   % Upper boundary
Options=optimset ('Algorithm','trust-region-reflective','Display','off','MaxFunEvals', 10000,'MaxIter', 50000);
else
   Lb. = [];
   Up= [];
   Options=optimset ('Algorithm','levenberg-marquardt','Display','off','MaxFunEvals', 10000,'MaxIter', 50000);
end
% Assumption of the initial values of rate constants
X01=0.0005;
% x01=0.025;%pp550
 Output=[];
k0arr=[];
for Y=-9:1:9;
   switch NumPara
      case 6
              k0=[x01*(10+Y)/10 x01*(20+Y)/20 x01*(30+Y)/30 x01*(40+Y)/40 x01*(50+Y)/50 x01*(60+Y)/60];
      case 5
             k0=[x01*(10+Y)/10 x01*(20+Y)/20 x01*(30+Y)/30 x01*(40+Y)/40 x01*(50+Y)/50];
      case  4
          k0=[x01*(10+Y)/10 x01*(20+Y)/20 x01*(30+Y)/30 x01*(40+Y)/40];
      case 3
```

```
        k0=[x01*(10+Y)/10 x01*(20+Y)/20 x01*(30+Y)/30];
    end
    k0arr=[k0arr;k0];
    [k,resnorm,residual]=lsqcurvefit(@curvefitPE02,k0,w0,yexp,lb,ub,options);
 tempoutput=[k resnorm];
 Output=[Output; tempoutput];
 end
 [m,n]=size(Output);
 %%%%%%%%%%%%%%%%%%%%%%%%%%%% Making new list because k cannot be less than zero.
Output_new=Output;
Output_new(Output<0)=0;
%%%%%%%%%%%%%%%%%% Searching minimum residues
% The smallest residue is searched and this line is listed in the output file.
temp=Output_new(:,end);
idx=find(temp==min(temp));
values=Output_new(idx,:);
 %%%%%%%%%%%%%%%%% %%%%%%%%%%%%%%%%%%%%%%%%%%%%%%%% End values
t=[0 10];
 [t,wa]=ode45('myfunPE02',t,w0,[],values);
 X=wa(:);
 T=t(:);
 wm=wa(end,:);  %last state of wa
plot (t,wa);
plot (t,wa);
 legend('Plastic','Gas','Wax','Liquid');
%  hold on
%  kk=[0.116814          0.421821     0.638192     0.000208     0.001304];% T=773
%  [t,wb]=ode45('myfunPE02',t,w0,[],kk);
%  plot(t,wb,'b*');%Making plots
 hold on
 set(gca,'FontSize',12);
 legend('Plastic-cal','Gas-cal','Liquid-cal','Char');
 xlabel('Time [min]');
 ylabel('Weight[%]');
 hold on
%plot exp and model
  Figure

 plot(1:4, wm,'o-')
 hold on
%  plot(1:4,yexp,'*-')
%  legend('Model','Exp')
```

```
hold off
```

2. Kinetic model for plastic pyrolysis reactions

```
% Ordinary differential function for plastic primary pyrolysis
%%%%%%%%%%%%%%%%%%%%%%%%%%%%%%%%%%%%%%%%%%%%%%%%%%%%%%%%%%%%%%%%%%%%%%%%%%%%%%%%%%%
```

```
function dw_dt=myfunPE01(t,w,flag,k)
dw_dt=zeros(size(w));
P=w(1);
G=w(2);
L=w(3);
W=w(4);
dw_dt(1)=-(k(1)+k(2)+k(3)).*P;
dw_dt(2)=k(1).*P+k(4).*W;
dw_dt(3)=k(2).*P+k(5).*W;
dw_dt(4)=k(3).*P-(k(4)+k(5)).*W;
end
```

3. Main file for optimisation

```
% Optimisation function

function wt=curvefitPE01(k,w)
t=[0 10];
[t,w]=ode45('myfunPE01',t,w,[],k);
for i=1:4
%     i=1:5
   wt(i)=w(end,i);
end
```

4. MATLAB Code for Mass loss

```
%%%%%%%%%%%%%%%%%%%%%%%%%%%%%%%%%%%%%%%%%%%%%%%%%%%%%%%%%%%%%%%%%%%%%%%%%%%%%%

4.1 Mass loss against Temperature
% Mass loss depend on temperature
clc
clear
```

```
close all
B=10;% B is heating rate
R=8.3145; % R is Ideal gas constant
T=273:823; % T is Absloute temperature
t=T';
A=8.2E+7; % A is Pre-exponential factor
Eng=142; % Eng is Activation energy
w=[];
for i=1:length(T)-1;
  T1=273;
T2=T(i+1);
%%%%%%%%%%%%%%%%%%%%%%%%%%%%%%%%%%%%%%%%%%%%%%%%%
h=@(T)(1-exp(-(A*R*T.^2)./(B.*(1000*Eng+2*R.*T)).*exp(-1000*Eng./(R.*T))));
w1=quadl(h,T1,T2);
w=[w; w1];
end
W11=exp(-w);
W1=((A/B).*exp(-1000*Eng./(R.*T)).*exp(-(A*R*T.^2)./(B.*(1000*Eng+2*R.*T)).*exp(-1000*Eng./(R.*T))));
%%%%%%%%%%%%%%%%%%%%%%%%%%%%%%%%%%%%%%%%%%%%%%%%%%%%%%%%%%%%
figure
 plot(T(2:end)-273,W11,'b-',T(2:end)-273,W12,'r-',T(2:end)-273,W13,'black-',T(2:end)-273,W111,'b.',T(2:end)-
273,W112,'r.',T(2:end)-273,W113,'black.');
 legend('PP','HDPE','PET')
%  legend('HDPE only','HDPE with CAT1','HDPE with CAT2');
%  legend('beta=10[^[188]C/min]','beta=20[^[188]C.min]',
   'beta=30[^{0}C/min]','   beta=40[^{0}C/min]');
xlabel('Temperature ^{0}C');
ylabel('Fraction weight loss (wt %)')
hold off
```

4.2 Mass loss against Reaction time

```
clear

close all
A=2.64E+12; % HDPE kinetic parameters data from First Year Report
B=25;
Eng=132.24;% HDPE kinetic parameters data from First Year Report
R=8.3145;
t=0:50;
w=[];
for i=1:length(t);
t1=0;
t2=t(i);
h=@ (t)(A./B).*exp(-1000*Eng./(R*B*t));
```

```
w1=quadgk(h,t1,t2);
w=[w; w1];
 end
W1=exp(-w);
W11=A.*exp(-1000*Eng./(B*R.*t)).*exp(-(A*B*R.*t.^2./(1000*Eng).*exp(-1000*Eng./(B*R*t).*(1-
2*R*B*t/(1000*Eng)))));
%%%%%%%%%%%%%%%%%%%%%%%%%%%%%%%%%%%%%%%%%%%%%%%%%%%%%%%%%%%%%%%%%%%%%%%%%%%%%%%%%%%%%%%%
w=[];
A=4.49E+13;% PP kinetic parameters data from First Year Report
Eng=138.55;% PP kinetic parameters data from First Year Report
for i=1:length(t);
t1=0;
t2=t(i);
h=@ (t)(A./B).*exp(-1000*Eng./(R*B*t));
w1=quadgk(h,t1,t2);
w=[w; w1];
 end
W2=exp(-w);
W21=A.*exp(-1000*Eng./(B*R.*t)).*exp(-(A*B*R.*t.^2./(1000*Eng).*exp(-1000*Eng./(B*R*t).*(1-
2*R*B*t/(1000*Eng)))));
%%%%%%%%%%%%%%%%%%%%%%%%%%%%%%%%%%%%%%%%%%%%%%%%%%%%%%%%%%%%%%%%%%%%%%%%%%%%%%%%%%%%%%%%
w=[];
A=7.09E+11;%LDPE kinetic parameters data from First Year Report
Eng=118.92;%LDPE kinetic parameters data from First Year Report
for i=1:length(t);
t1=0;
t2=t(i);
h=@ (t)(A./B).*exp(-1000*Eng./(R*B*t));
w1=quadgk(h,t1,t2);
w=[w; w1];
 end
W3=exp(-w);

W31=A.*exp(-1000*Eng./(B*R.*t)).*exp(-(A*B*R.*t.^2./(1000*Eng).*exp(-1000*Eng./(B*R*t).*(1-
2*R*B*t/(1000*Eng)))));
%%%%%%%%%%%%%%%%%%%%%%%%%%%%%%%%%%%%%%%%%%%%%%%%%%%%%%%%%%%%%%%%%%%%%%%%%%%%%%%%%%%%%%%%
w=[];
 A=6.21E+16;% PET kinetic parameters data from First Year Report
Eng=166.40; % PET PP kinetic parameters data from First Year Report
for i=1:length(t);
t1=0;
t2=t(i);
h=@ (t)(A./B).*exp(-1000*Eng./(R*B*t));
w1=quadgk(h,t1,t2);
```

```
w=[w; w1];
  end
W4=exp(-w);
W41=A.*exp(-1000*Eng./(B*R.*t)).*exp(-(A*B*R.*t.^2./(1000*Eng).*exp(-1000*Eng./(B*R*t).*(1-
2*R*B*t/(1000*Eng)))));
%%%%%%%%%%%%%%%%%%%%%%%%%%%%%%%%%%%%%%%%%%%%%%%%%%%%%%%%%%%%%%%%%%%%%%%%%%%%%%%%%%%%%%%%
 figure
 plot(t-1,W1,'b-',t-1,W2,'y-',t-1,W3,'black-',t-1,W4,'r-')
  legend('PE','PP','PEPP','PET');
xlabel('Time [min]');
ylabel('Fraction (wt %)')
 hold on;
 figure
 plot(t,W11,'b-',t,W21,'y-',t,W31,'black-',t,W41,'r-')
legend('PE','PP','PEPP','PET');
xlabel('Time [min]');
ylabel('Weight loss rate (dw/dt %)')
```

4.3 Mass loss against Feedstock

```
clear
close all
clc
B=[5 10 20 25 50];
A=[2.65E+12 4.49E+13 7.09E+11 6.21e+16]; % Kinetic parameters data from Chan et al(1996)
Eng=[185.24 193.55 170.92 232.4];
R=8.3145;
T=273:1000;
%%%%%%%%%%%%%%%%%%%% Kinetic parameters data from by Coats and Redfern(1964)
W1=(A(1)./B).*exp(-1000.*Eng(1)./(R.*T)).*exp(-(A(1).*R.*T.^2)./(B.*(1000.*Eng(1)).^2).*(1000.*Eng(1)-
2*R.*T).*exp(-1000.*Eng(1)./(R.*T)));
W2=(A(2)./B).*exp(-1000.*Eng(2)./(R.*T)).*exp(-(A(2).*R.*T.^2)./(B.*(1000.*Eng(2)).^2).*(1000.*Eng(2)-
2*R.*T).*exp(-1000.*Eng(2)./(R.*T)));

W3=(A(3)./B).*exp(-1000.*Eng(3)./(R.*T)).*exp(-(A(3).*R.*T.^2)./(B.*(1000.*Eng(3)).^2).*(1000.*Eng(3)-
2*R.*T).*exp(-1000.*Eng(3)./(R.*T)));
W4=(A(4)./B).*exp(-1000.*Eng(4)./(R.*T)).*exp(-(A(4).*R.*T.^2)./(B.*(1000.*Eng(4)).^2).*(1000.*Eng(4)-
2*R.*T).*exp(-1000.*Eng(4)./(R.*T)));
figure
plot(T-273,W1,'mo', T-273,W2,'g*',T-273,W3,'b.',T-273,W4,'r*');
hold on;
legend('PE','PP','PE/PP','PET');
xlabel('Temperature ^{0}C');
ylabel('Mass loss rate (wt %)')
```

4.4 Mass loss with Heating rate

```
clear
close all
A=6.21E+16;%PET FROM I.MARTIN-GALLON, PONT(2001)
B=10;
%  B=[10 20 30 40];
% Eng=217.66;
% Eng=202.24;%HDPE FROM FIRST YEAR REPORT
% Eng=193.55;%PP FROM S.S.PARK(2012)
% Eng=175.92;%LDPE FROM S.S.PARK(2012)
Eng=256.40;% PET kinetic parameters data from First Year Report
R=8.3145;
T=273:1073;
w=[];
for i=1:length(T)-1;
T1=273;
T2=T(i+1);
h=@ (T)(A./B).*exp(-1000*Eng./(R*T));
w1=quadl(h,T1,T2);
w=[w; w1];
end
W10=exp(-w);
W1=A./B.*exp(-1000*Eng./(R.*T)).*exp(-(A*R*T.^2)./(B.*(1000*Eng+2*R.*T)).*exp(-1000*Eng./(R.*T)));
%%%%%%%%%%%%%%%%%%%%%%%%%%%%%%%%%%%%%%%%%%%%%%%%%%%%%%%%%%%%%%%%%%%%%%%%%%%%%%%%%%%%%%%%%%%%%%%%%%%%%%%%%%%%%%%%%%%%%%
%%%%%%%%%%%%%%%%%%%%%%%%%%%%%%%%%% Kinetic parameters data from First Year Report

% A=3.31E+15;
% A=2.64E+12;%HDPE
% A=4.49E+13;%PP
% A=7.09E+11;%LDPE
A=6.21E+16;%PET

B=20;
% Eng=202.24;%HDPE
% Eng=193.55;%PP
% Eng=175.92;%LDPE
Eng=156.40;%PET
R=8.3145;
T=273:1073;
w=[];
M=1;
for i=1:length(T)-1;
T1=273;
T2=T(i+1);
```

```
%B1=B(j);
h=@ (T)(A./B).*exp(-1000*Eng./(R*T));
w1=quadl(h,T1,T2);
w=[w; w1];
end
W20=exp(-w);
W2=A./B.*exp(-1000*Eng./(R.*T)).*exp(-(A*R*T.^2)./(B.*(1000*Eng+2*R.*T)).*exp(-1000*Eng./(R.*T)));
%%%%%%%%%%%%%%%%%%%%%%%%%%%%%%%%%%%%%%%%%%%%%%%%%%%%%%%%%%%%%%%%
% A=3.31E+15;
% A=2.64E+12;%HDPE FROM FIRST YEAR REPORT
% A=4.49E+13;%PP FROM S.S.PARK(2012)
% A=7.09E+11;%LDPE FROM S.S.PARK(2012)
A=6.21E+16;%PET FROM I.MARTIN-GALLON, PONT(2001)
B=30;
 %B=[5 10 20 25 35];
% Eng=217.66;
% Eng=202.24;%HDPE FROM FIRST YEAR REPORT
% Eng=193.55;%PP FROM S.S.PARK(2012)
% Eng=175.92;%LDPE FROM S.S.PARK(2012)
Eng=256.40;%PET FROM I.MARTIN-GALLON, PONT(2001)
%  B=[10:10:40];
R=8.3145;
T=273:1073;
w=[];
M=1;
for i=1:length(T)-1;
T1=273;
T2=T(i+1);
%B1=B(j);
h=@ (T)(A./B).*exp(-1000*Eng./(R*T));
w1=quadl(h,T1,T2);
w=[w; w1];
end
W30=exp(-w);
W3=A./B.*exp(-1000*Eng./(R.*T)).*exp(-(A*R*T.^2)./(B.*(1000*Eng+2*R.*T)).*exp(-1000*Eng./(R.*T)));
%%%%%%%%%%%%%%%%%%%%%%%%%%%%%%%%%%%%%%%%%%%%%%%%%%%%%%%%%%%%%%%
% A=3.31E+15;
% A=2.64E+12;%HDPE FROM FIRST YEAR REPORT
% A=4.49E+13;%PP FROM S.S.PARK(2012)
% A=7.09E+11;%LDPE FROM S.S.PARK(2012)
A=6.21E+16;%PET FROM I.MARTIN-GALLON, PONT(2001)
B=40;
 %B=[5 10 20 25 35];
% Eng=217.66;
```

```
% Eng=202.24;%HDPE FROM FIRST YEAR REPORT
% Eng=193.55;%PP FROM S.S.PARK(2012)
% Eng=175.92;%LDPE FROM S.S.PARK(2012)
Eng=256.40;%PET FROM I.MARTIN-GALLON, PONT(2001)
%  B=[10:10:40];
R=8.3145;
T=273:1073;
w=[];
% M=1;
for i=1:length(T)-1;
T1=273;
T2=T(i+1);
%B1=B(j);
h=@ (T)(A./B).*exp(-1000*Eng./(R*T));
w1=quadl(h,T1,T2);
w=[w; w1];
end
W40=exp(-w);
W4=A./B.*exp(-1000*Eng./(R.*T)).*exp(-(A*R*T.^2)./(B.*(1000*Eng+2*R.*T)).*exp(-1000*Eng./(R.*T)));
%%%%%%%%%%%%%%%%%%%%%%%%%%%%%%%%%%%%%%%%%%%%%%%%%%%%%
 figure
plot(T(2:end)-273,W10,'g.',T(2:end)-273,W20,'b.',T(2:end)-273,W30,'r.',T(2:end)-273,W40,'y.')
legend('beta=10[C/min]','beta=20[C.min]','beta=30[C/min]','beta=40[C/min]');
xlabel('Temperature ^{0}C');
ylabel('Fraction (wt %)')
 hold on;
figure
plot(T-273,W1,'g.',T-273,W2,'b.',T-273,W3,'r.',T-273,W4,'y.')
legend('beta=10[^{0}C/min]','beta=20[^{0}C/min]','beta=30[^{0}C/min]','beta=40[^{0}C/min]');
xlabel('Temperature ^{0}C');
ylabel('Weight loss rate (dw/dT %)')
hold off
```